SHRINK-FIT STRESS SYSTEMS

in

BUILT CRANKSHAFTS

A Thesis submitted to the University of Glasgow

for the Degree of Ph.D.

by

WILLIAM R.S. DAVIDSON, B.Sc.

March 1951.

To

H.A.M.

LIST OF CONTENTS.

---------- oOo ----------

DETAIL OF CONTENTS.

Page No.

PART II - THEORETICAL WORK.

Page No.

Page No.

INDEX OF PHOTOGRAPHS.

NOTATION.

Principal or Normal Stress and Strain.

p = stress

e = strain

Suffices:

1,2,3 = principal directions.

x,y,z = co-ordinate directions (Cartesian).

r,θ,z = co-ordinate directions (Cylindrical).

e.g., p_θ = circumferential (hoop) stress.

$p_{\theta)k}$ = circumferential stress at outside radius.

p_e = Elastic Limit stress in tensile test-piece.

Shear Stress.

p_{xy} = shear stress in the y direction, on a plane normal to the x direction.

Elastic Constants.

E = Young's Modulus.

σ = Poisson's Ratio.

$s = \frac{1}{2} p_e$ = Elastic Limit shear stress.

Cylinder Radii.

r = cylinder radius.

Suffices:

1 = inner.

n = outside of overstrained region.

k = outside of cylinder.

$k = \frac{r_k}{r_1}$; $y = \frac{r}{r_1}$; $n = \frac{r_n}{r_1}$

Miscellaneous.

Δ = fractional fit allowance (inches per inch of fit diameter).

P = internal pressure in a cylinder, or interface pressure in a shrink-fit.

u = radial displacement of element of cylinder, e.g., circumferential strain = $\frac{u}{r}$

δ = diametral deflection, e.g., δ_R = change in size of outside diameter

also

= finite increment operator, e.g., δ_x

d, ∂ = differential operators.

ABSTRACT.

Among applications of the well-known practice of shrink-fitting, the assembly of large marine crankshafts from relatively small forgings is perhaps the most outstanding example, having regard to the stringent operating conditions in which the component must function satisfactorily. Variations in shrink-fitting practice and failures attributable to slipping of the grip have directed attention to the lack of information on crankshaft assemblies and instigated an investigation, the results of which are presented in this thesis.

A major part of the investigation comprises a survey of published literature relevant to the subject. It has been found that little is yet known about stress or grip conditions at the shrink-fit, and that the rules for sizes and proportions have evidently no theoretical foundation. The scope of the survey has therefore been extended to include work on all types of interference fits, from which it is evident that, while a useful amount of empirical data on factors affecting grip strength exists, treatment of interface pressure and stress has been limited to the application of elastic thick cylinder theory. With a view to analysing stress conditions in assemblies overstrained by fit allowances which cause permanent enlargement of the hollow element, a part of the survey is devoted to examining work on thick cylinders subjected to in-

ternal fluid pressure.

A number of features of shrink-fitting, such as prevention of free axial shrinkage, overstrain of the hollow element, and the influence of temperature on the elastic constants of the material, have been analysed as part of the theoretical work of the present investigation. On the basis of certain reasonable assumptions, a solution for the stress in a representative crank web shape has been obtained, using Relaxation Methods of analysis. Stress concentration and radial stiffness values, which correlate the complex shape to the rotationally-symmetrical, follow readily from the solution.

The experimental investigations comprise tests on rings-and-plugs, on model crank webs, and on large crank webs removed from a vessel which had been scrapped. The results indicate that prevention of free axial shrinkage does, in fact, occur to a marked degree. Furthermore, the presence of axial grip has been detected in large crank webs which had suffered extensive cold-working due to pulsating bending actions during service. Model experiments have demonstrated the influence of surface finish on the grip strength to be quite unimportant. Friction values in the large crankshaft, on the mating surfaces of which tool-marks were clearly visible, were comparable with those in model webs with near-perfect honed surfaces. Interface pressure and stress values predicted

from theoretical considerations were in sound agreement with values measured by electrical strain gauges and inferred from deformations.

A list of design formulae and data, and recommendations for improvements to shrink-fitting practice, based on the results of the investigation, are presented.

INTRODUCTION.

The larger sizes of marine engine crankshafts are nearly always manufactured in parts, in contrast to automobile and aircraft crankshafts, which are invariably of solid-forged integral construction. Consistent quality and close grain structure, necessary for high fatigue resistance, are difficult to attain with large forgings which inevitably have a slow cooling rate, the difficulty increasing with the ingot size. Even in medium-sized marine engines, a fabricated shaft is sometimes preferred to the solid-forged type. The parts may consist of sections of shafting, or of crank throws consisting of two webs and connecting crank pin, or of individual webs, crank and journal pins. In the first two cases the shaft is termed part-built and semi-built; the third type is referred to as a fully-built, or simple 'built', crankshaft. It is with this latter type that the following investigation is concerned.

Built crankshafts are invariably assembled by fitting the crank and journal pins into slightly smaller holes in the webs, which have been expanded by heating to allow the pins to enter freely. On cooling, the shrinkage of the web is partly prevented by the pins, heavy pressure being imposed on the mating surfaces, thus inhibiting further relative movement and resulting in a rigid assembly.

Shrink-fitting, as this process is called, is commonplace in engineering practice, being simple and economical for permanent and semi-permanent assemblies of suitably-shaped parts. In spite of this, however, little general agreement has been reached on important features of the design of shirnk-fitted crank assemblies. This is not surprising. The force and stress actions in the simpler case of a ring element shrink-fitted on a shaft are not yet perfectly understood in spite of much experimental investigation. The lack of rotational symmetry in the case of the crank web provides additional complex features which have been subjected to surprisingly little experimental examination.

Among numerous factors influencing the strength of an assembly, the following are clearly important: dimensions of the grip; dimensions of the scantlings; surface finish and film condition of the mating surfaces; shrink-fit allowance; tolerances of roundness, straightness, parallelism; elastic properties of the material used; workshop fitting practice; the effect of superposed force actions. Some of these have been investigated, but no general correlation, which would provide a reliable basis for design data, has been advanced

Marine engineering practice is governed to some extent by the recommendations of Lloyd's Register of Shipping. The recommended scantling sizes result in a satisfactory, though not necessarily economical, design, and variations from Lloyd's

proportions are generally slight. The requirements of cylinder spacing, bearing area, and other considerations affecting crankshaft dimensions, preclude any wide variation of scantlings.

No general agreement exists about surface finish and condition, either with regard to the final machining process or to the quality of the finish obtained. In some quarters a rough finish is thought to improve the friction grip,,while in others the opposite view is held. The film condition of the mating surfaces is also subject to important variations; some builders advocate dry surfaces, others use a lubricant to prevent seizure during assembly. A radically different technique is the introduction of carborundum powder between the mating elements.

Moderate shrink-fit allowances of between 1.5/1000 and 1.67/1000 inch per inch of pin diameter are normally used. It is recognised that with 28/32 ton mild steel webs, local overstrain occurs with this allowance, and the resulting stress condition is somewhat uncertain, but experience has shown the assembly to be, in general, satisfactory. Tolerances of roundness, straightness and parallelism are not generally specified for the mating parts, the normal standard of workmanship being accepted.

The manner in which the fitting process is carried out varies to an important degree. Both pins may or may not

be fitted at the initial heating of the web. Sometimes the second bore is trued to circular shape after the first pin is fitted. The webs may be heated in a furnace, by gas-coils in the bores, or by oil blow-lamps. The pins may be fitted in either the horizontal or vertical position. The mating surfaces may or may not be specially cleaned before assembly. Dowel pins may be fitted in the journal fit or in both fits as a precautionary measure.

The above considerations indicate a disturbing variation of design and workshop practice, due to lack of precise knowledge of the stress and grip conditions resulting from any particular combination of variables. In view of the stringent service conditions of a crankshaft, in which steady and pulsating forces of considerable magnitude are imposed on the shrink-fit, this knowledge is of paramount importance for two reasons; the residual stress system of the built shaft has a deleterious effect on the resistance to fatigue; shaft failure is possible due to slip of the fitted surfaces if the limiting friction of the grip is exceeded.

Crankshaft fractures have occurred due to fatigue cracks starting at discontinuities such as oil-holes and fillets, where high local stresses occur, and extending throughout the entire body of material. It is well known that the presence of a static stress system diminishes the fatigue resistance, and undoubtedly fractures of the webs have been aggravated by the

static stress system resulting from shrink-fits. Recent work by Gough (12)* indicates that for a particular type of stress system in which both cyclic and static combined bending and twisting are present, the influence of static stress is less than had been believed. The type of steel investigated was a 65 ton alloy steel (BSS S65A) with a high ratio of yield to ultimate tensile strength, and Gough's experiments showed a maximum reduction in fatigue stress of about 23%. It should not be assumed, however, that the comparatively small reduction would not be greater for different steels under different conditions of loading: also, since little is known about the size effect in fatigue testing, caution is necessary when applying the results of experiments carried out on small specimens to full scale work. It must still be assumed that the fatigue strength of built shafting is adversely affected by the shrink-fit residual stress system.

The more obvious weakness inherent in built crankshafts results from the discontinuity of the material at the mating parts, and structural failure due to stripping of the grip, axially or circumferentially, is clearly possible. Axial forces of high magnitude are unlikely since none are produced by the primary force actions on a crankshaft. Axial vibrations have been observed, but are comparatively uncommon in marine installations, and the amplitudes are such

* Numbers in parenthesis refer to the Bibliography at the end of the thesis.

that forces of the order necessary to strip the shrink-fit by axial displacement are extremely unlikely.

Failure by torque action, however, is a definite possibility. In a marine installation the aft journal fit is required to transmit the total developed engine torque, together with variations due to primary force actions, shock loading in heavy weather, and probably vibration torque of considerable magnitude. The relatively low torsional stiffness of the shaft together with the substantial intrinsic and associated mass can result in a vibration system with a frequency at which considerable engine forcing exists. Large amplitudes may be maintained due to absence of damping generally, and the node of the lowest order is usually in the vicinity of the aft end of the crankshaft where the engine torque is greatest.

Slip at a crankpin fit is less likely than at a journal fit, since the crankpin is not subjected to the same torque as the adjacent journals. The multithrow crankshaft under pure torque is statically indeterminate due to the main bearing constraints, and the crank pins are subject to a combination of shearing, bending and twisting effects. If, however, the main bearings are misaligned due to distortion of the hull and engine bed-plate in a seaway, or due to wear-down of the bearings, excessive torque may be imposed on a crank pin,

and failure may be incorrectly attributed to the shrink-fit.

Neither grip strength nor stress conditions have hitherto been thoroughly investigated in any type of shrink-fitted assembly. It has been customary to class shrink fits with force and expansion fits, as presenting the same problem, but there are important differences consequent on the method of assembly, and experimental data obtained with one type of interference assembly should not be too readily applied in other cases. Some experiments of a comparative nature have been carried out, but at present it is still impossible to predict the grip or the stress conditions in a particular assembly. Furthermore, as mentioned previously, experiments have been mainly confined to the simple ring-and-plug type of assembly, and no extension or modification of elastic thick cylinder theory has yet been attempted.

The industrial importance of the application of shrink-fitting to crankshaft building demands that this particular case should receive direct attention, instead of relying on data adapted from simple rings and plugs. The simpler assemblies, however, provide a more convenient means of examining effects common to all shrink fits.

A co-ordinated programme of research into both types of assemblies is at present being conducted in the Royal Technical College, Glasgow. The experimental and analytical work

presented in this thesis is mainly confined to the problem of the crank web stress system, but a limited amount of relevant work on simple shrink-fits is necessarily included, because investigation of the latter has recently disclosed some important features which cannot be ignored in the crankshaft problem, and which have not yet appeared in published literature. The minimum amount of data on rotationally-symmetrical assemblies is presented, but it will be appreciated that the additional complex features of the crank web cannot be satisfactorily resolved until the stress conditions in simple assemblies has been established beyond reasonable doubt.

From an academic view-point, the results are of value in affording experimental evidence of the stress distribution in a multiply-connected elastic body, all dimensions of which are of the same order, a type of problem very resistant to exact theoretical treatment.

The practical value requires no emphasis. Many of the measurements were made on crank webs taken from a large marine engine crankshaft which had been in service for some years, and the ideal conditions usually associated with research specimens were not present. These results may therefore be accepted by the marine engineering industry, as evidence of the stress and pressure conditions to be expected in assemblies which have been constructed in accordance with workshop practice,

and which have been subjected to normal conditions of service.

PART I

REVIEW OF PREVIOUS INVESTIGATIONS.

1. SCOPE OF THE REVIEW.

(a) Crankshafts.

A survey of publications on built crankshafts revealed that, with the exception of a photo-elastic analysis, no theoretical or experimental investigations of the stress system due to shrink-fitting have hitherto been made.

It was therefore necessary to examine the basis of Lloyd's recommendations for the design of built shafting. Two papers by Dorey (9) (10) contain surprisingly little information on aspect of the shrink-fitting process and it is evident from the discussion of one of these papers, that marine engineers are fully aware of the present unsatisfactory position.

(b) Interference Fits.

The above papers do not provide sufficient foundation for further work on the special application of shrink-fitting. It was necessary to widen the scope of the review to include all previous work concerned with shrink-fits, and, since a brief scrutiny of such papers showed that no significant difference between force -, shrink - and expansion-fits have hitherto been envisaged, to include also these other classes of interference fits.

(c) Thick Cylinders under Fluid Pressure.

The use of fit allowances which overstrain the hollow element is neither unusual nor apparently deleterious to the

assembly. Previous work has not dealt with the post-elastic stress system and it was thought that no great difficulty would be encountered in correlating existing work on overstrain of thick cylinders subjected to internal pressure, with the shrink-fit problem.

A substantial part of the review is therefore concerned with this important aspect, but the examination is by no means exhaustive.

(d) Presentation.

The list of Contents outlines the general scheme of classification for this Part, but some further explanation is desirable.

The main sections deal with interference fits, thick cylinders and crankshafts, in this order. It is necessary to examine the simpler problem of the rotationally symmetrical assembly before proceeding to the crankshaft case, as the additional complexity of shape can only be satisfactorily resolved after conditions in the simpler case have been established.

The sub-headings of the interference fit section, are, with one exception, concerned with particular aspects of the stress conditions. All previous work has dealt with grip strength on an empirical basis, the measurements from which the stress conditions could be estimated, having been entirely omitted in many investigations. The attention given to any

particular paper is determined by the evidence of stress, and not of grip, contained therein. One sub-section reviews very briefly the very considerable fund of empirical knowledge of factors affecting the strength of grip in interference fits.

In the sections dealing with overstrained cylinders and with crankshafts, discussion is classified by individual papers and not by particular aspects of the subject matter.

A final section containing a very brief list of the more striking features of the review and the conclusions which may be drawn therefrom, is included at the end of this Part

2. INTERFERENCE FITS.

A. Fit Allowance - Definition and Unit.

The discrepancy in free size between the mating diameters of two cylinders before assembly, is known as the fit allowance. The process of assembly consists of deforming the parts by force or temperature, thereby inducing circumferential strains on the cylindrical surfaces of both elements of such magnitudes that the sum of the changes in diameters is equal to the initial discrepancy. The stresses consequent on the deformations are functions of the circumferential strains and therefore of the fractional changes in diameters. It is thus more convenient to deal with fractional fit allowances obtained by dividing the dimensional discrepancy by the diameter of either mating cylinder resulting in a non-dimensional fit allowance of the order of strain and equal to the sum of the circumferential strains of both elements when the fit is effected. A convenient unit for the fit allowance is 1×10^{-3} strain, hereafter referred to as 1 mil. Values of fit allowance in the papers reviewed below have been converted to mils, unless otherwise stated, in order to facilitate comparison.

B. Variation of Fit Allowance.

(a) Force Fits.

In a large number of practical cases, both elements of the assembly are rotationally-symmetrical. By making the assumptions that stress in the direction of the cylinder axis is zero, and that the limits of elasticity are not exceeded in either element, the interface normal pressure can be evaluated in terms of the fit allowance, using the equations of plane stress in thick cylinders, due to Lamé, which can be found in almost any standard text book on the Strength of Materials. The relationship of interface pressure to fit allowance is, on this basis, linear.

Early records of force-fitting by McGill (21) give the apparent coefficients of friction in 206 assemblies, obtained by using this two-dimensional thick cylinder theory and the axial load to make the fit. The records show that the coefficient varies widely. The fit allowances would, however, in most cases cause overstraining of the hollow element, rendering the elastic theory invalid, and resulting in incorrect pressure values.

Russell and Shannon (31) carried out experiments on force-fitted ring and plug assemblies. Permanent enlargement of the bore and outside diameters of the ring occurred for fit allowances in excess of 0.4 mils. The dimensions of the plug

were unaffected. When the elastic limit of the material was raised by cold-working, overstrain did not occur until a fit of 0.67 mils was exceeded. Both values, however, are substantially lower than would have been expected from the results of tensile tests of the material, using any of the proposed theories of elastic failure. The maximum axial loads required to make and separate the assemblies, compared with the fit allowance, indicated a departure from linearity at approximately the above values. Russell and Shannon's results are shown in Figs. 1 and 2.

The authors suggest, firstly, that the elastic limit is lower than that deduced from tensile test results, thus accounting for the permanent set of the ring elements, and secondly, that the friction force would hardly follow a straight line law up to the limit of proportionality, on account of the end effects, variations of friction and of contact area. The implication is that, if the latter variations were absent, the linear relationship would extend to a higher value of fit allowance than is shown in Fig. 1, in contradiction to the experimental evidence of overstrain. The explanation of the overstrain is also inadequate, since it implies that theories of failure, based on tensile tests are not applicable to thick cylinders. Cook and Robertson (4) showed that elastic breakdown in thick cylinders occurred at an internal pressure approximately mid-way

between pressures calculated on the St. Venant maximum strain criterion and the maximum shear stress criterion of Guest. Their results were shown by Haigh (13) to agree closely with the maximum strain energy criterion of failure.

In these circumstances, the permanent enlargements observed by Russell and Shannon must have been due to higher pressures than those calculated on the elastic thick cylinder basis, probably caused by deformations of the elements in the assembly process. Pressing-on and pressing-off graphs of the type shown in Fig. 3 suggest that such deformation takes place. These graphs may be taken as typical of force-fitting loads, as later work by Russell (32) (33) (34) shows little deviation from the general trend. The relationship of axial load to length of grip, is non-linear for both pressing-on and pressing-off. The pressing-off operation frequently gives a higher holding force after the plug has started to separate from the ring, due to lack of axial symmetry. Fig. 1 is plotted from the maximum loads - not necessarily the loads given by the complete assembly. The maximum holding force of the grip at a fit allowance corresponding to the Haigh criterion of failure must be regarded as coincidental, since the ring was considerably overstrained.

The deformation resulting from the pressing operation were noted by Horger and Nelson (16 (17) who observed that the

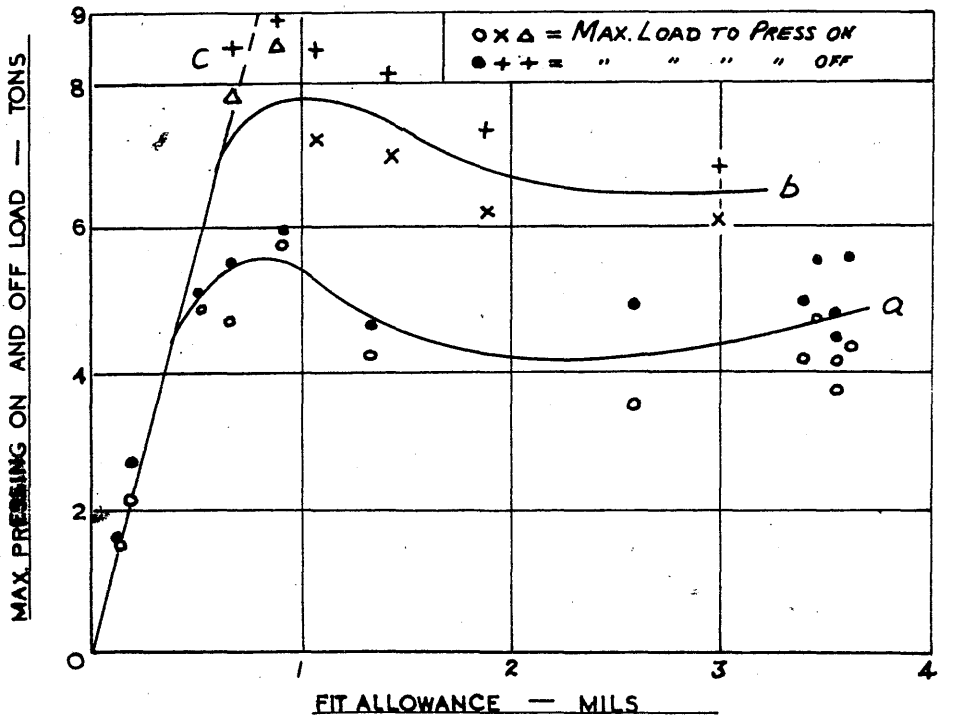

a — NORMAL RINGS
b,c — COLD-WORKED RINGS

GRIP STRENGTH V FIT ALLOWANCE — RUSSELL AND SHANNON

FIG. 1

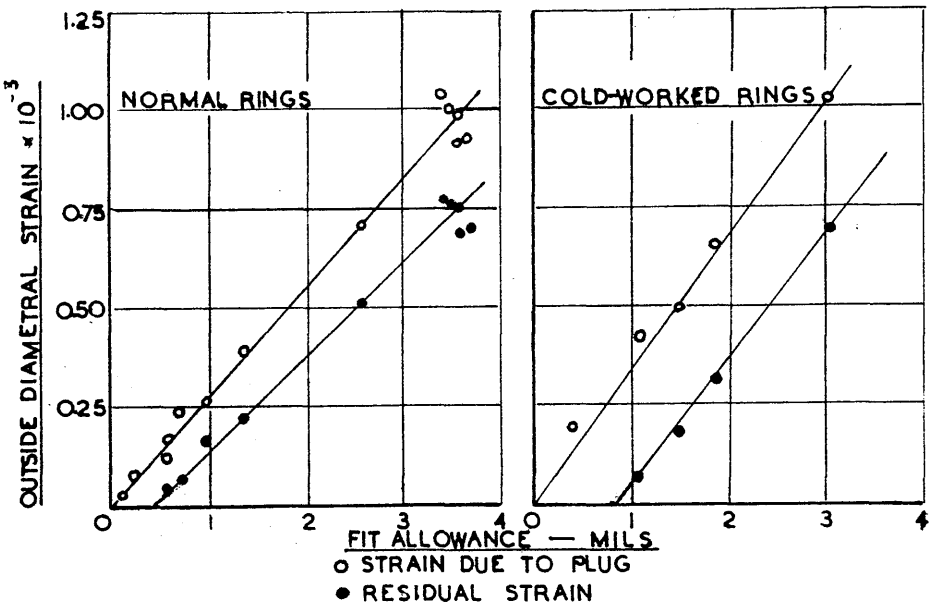

OUTSIDE DIAMETRAL STRAIN V FIT ALLOWANCE
(RUSSELL AND SHANNON)

FIG. 2

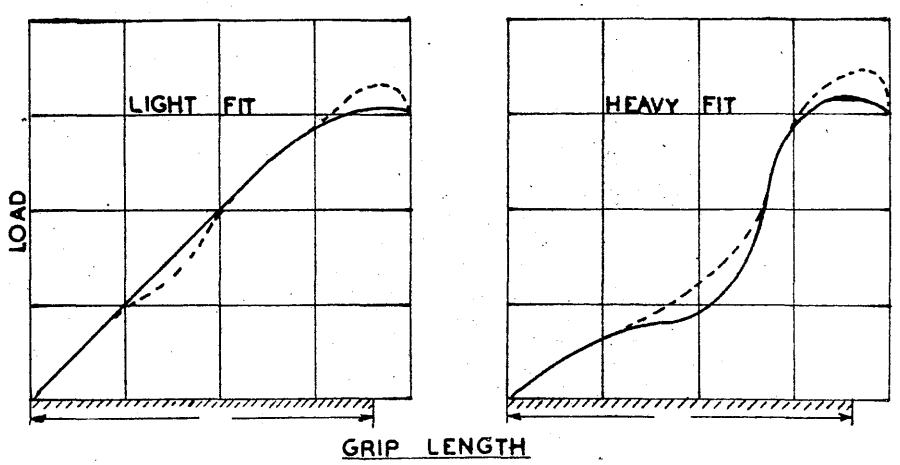

TYPICAL LOAD CURVES — RUSSELL

FIG. 3

bore of the hollow element remote from the entering plug diminished in diameter at first. It was stated that bell-mouthing at the entry and, leading to loss of pressure over the first part of the grip, occurred. No figures were given. The magnitude of this effect probably depends on the axial length of grip. Russell (33) gives the variation of residual dimensions of railway waggon wheel seats and bosses which registered low back pressure loads. The diagrams of straightness of boss and axle profiles clearly show the bell-mouthing at the entry end and in some cases clearance conditions at that end of the fit.

It is clear that the application of simple thick cylinder theory to force fits is an oversimplification, leading to incorrect pressure values, except when the fit allowance is sufficiently low to avoid overstraining the ring in the assembly operation. The value of this limiting fit will depend on other factors, such as the entry condition at the nose of the plug, which may have a fillet radius or an entry taper. It is probably on account of this variation of pressure from the values calculated by the thick cylinder theory that such wide variations in coefficients of friction are observed in force fits. Baugher (2) states that the coefficient of friction in shrink-fits is higher than in force fits. In the case of shrink-fits, overstraining of this type is not present, and it is possible that

higher pressures would be obtained with the same fit allowance.

(b) Temperature Fits.

The two classes of temperature fits, namely shrink - and expansion-fits, may for the purpose of this review, be grouped together. Different conditions exist mainly because the grip is realised at different temperature levels, and because the solid element cannot be assembled without a surface film of atmospheric moisture which affects the grip characteristic. The effect of variations of temperature on the elastic properties of materials has not hitherto been considered, and it is possible that the stress condition is not identical in the two types of fit.

The effect of varying the fit allowance in either shrink - or expansion-fits has not been investigated. It has been tacitly assumed by previous investigators that identical stress conditions would obtain in force and temperature fits. This is incorrect, as the following example shows.

In an investigation of the grip of force, shrink and expansion fits, Russell (32) stated that in a shrink-fitted assembly with a fit of 0.67 mils, no permanent deformation of the ring occurred. The material had not been work-hardened and was similar to, and probably the same as that used in his earlier force-fit experiments in which permanent set occurred at 0.4 mils. An expansion-fitted assembly with this fit

allowance also showed no permanent set. These two tests were part of a series which included force-fits with the same allowance. In the latter case, the dimensions after separation were not stated, but in a later series comparing the torsional grip of shrink - and force-fits, it is significant that the fit allowance was reduced to 0.33 mils.

Although temperature fits apparently maintain elastic conditions in the hollow element at a higher fit allowance than force-fits, it is not safe to assume that the full value of the fit allowance, based on any selected criterion of failure and elastic thick cylinder theory, can be realised without overstrain. Temperature strain occurs in the axial direction during assembly, and this cannot be relieved without slip of the mating surfaces during cooling, after the mating surfaces have established contact. If the slip is entirely prevented by friction, axial shearing tractions on the interface remain. The result is that the solid element is compressed and the hollow element extended axially, causing an effective increase in pressure since the corresponding radial and circumferential strains are prevented.

C. Grip Characteristics.

Fig. 3 is a typical pressing-on and pressing-off graph of load versus grip length for force-fits. Russell (32) states that the general characteristics were observed in numerous tests on force-fits. The grip strength at low fits is

roughly proportional to area for about three quarters of the grip length during pressing-on and pressing-off. The last quarter of the grip is effected at nearly constant load. The pressing-off is invariably accompanied by a rising load for decreasing grip which attains a maximum value in excess of the maximum pressing-on loads, thereafter falling to the starting value in the first quarter of the pressing-out, and decreasing linearly. With heavy fit allowances the same general trends are present but the linear relationship is modified. It seems likely that the major part of the grip is taken by the nose of the plug at first, and that the remaining part of the overstrained bore only begins to exert pressure and grip when the plug is more than half-way home.

The meagre data available on shrink - and expansion-fits seems to indicate that, in both types of assembly, the grip strength drops immediately the grip is broken. In the case of expansion-fits thepressing-out is similar in characteristic to the force-fit, but the shrink-fit shows less rise as the plug is removed.

Russell (34) carried out tests on breaking the grip by torque action. Force - and shrink-fitted assemblies with fit allowances of 0.33 mils were broken by torque, applied by a force at the end of a 60" lever. The forces in lbs. were as follows:

TABLE I.

	Initial Slip	2nd Slip
Force Fit	90	95
Shrink Fit	100	80

This seems to indicate that the drop in grip strength of the shrink-fit at first axial slip is also present in torsional slip, and that part of the increase in grip of force fits during pressing-off, may be due to changes in the surface asperities with change in direction of relative motion.

When the two assemblies were pressed-off the initial loads were identical and the graphs of load versus plug travel very similar. The shrink-fit showed a further slight drop in grip after the grip was broken axially.

It would seem that the method of assembly has some effect on the surfaces, and that even in cases where identical pressure and lubricant conditions appear to be present, the holding power of different types of assembly is subject to variation.

D. Factors Affecting the Grip.

The records of McGill (21) indicate that, even

allowing for errors in calculating interface pressure, the coefficient of friction varies widely, the values for steel shafts and hubs ranging from 0.077 to 0.33. Baugher (2) gives values from 123 press-fits with both ground and turned surfaces ranging from 0.03 to 0.25. The experiments of Russell (33) (34) in this field show that variations of the lubricant in a force-fit can cause difference of over 300% in the grip strength.

The influence of surface finish of the mating parts is not so well marked. The experiments of Sawin (35) indicate that the finer the finish the higher the grip strength. Baugher (2) disagrees with this view, stating that, in more than 100 press-fits in which the surfaces varied from ground to rough turned, practically no difference was observed. Baugher does, however, advocate ground finishes to obtain closer machining tolerances.

The effect of time on the grip strength was investigated by Russell (34). In tests of up to 32 months duration, the grip of force fits increased in the first 8 months and then became erratic. Shrink - and expansion- fits showed no definite tendency. The increase in grip strength of force-fits with time was noted by Baugher (2) and by Werth (41) who stated that the force required to press-off was 25% lower immediately after assembly than after 2 days time.

An explanation of the film and time variations put forward by Thomson, in the discussion of Russell's paper (34), is briefly as follows.

Solids possess free surface energy, electrochemical in nature, which acts at an appreciable distance from the surface. This attractive field causes the cohesion of clean dry solids and the formation of an adsorbed film in the presence of a lubricant. The adsorbed film reduced the free energy and thus the tendency to seizure, and the greater the degree of adsorption the lower is the friction between surfaces. Mineral oils have a low adsorption factor and the Russell experiments showed that Bayonne oil gave the highest friction value of a number of different films used, and was, in addition, the least affected by ageing. Fatty oils have higher adsorption factors and, in addition, tend to oxidise and become acidic. The acidity increases the oiliness and also attacks the surface of the metal, causing a decrease of grip strength with time. This was confirmed by results of the experiments which showed a tendency for the back pressure tonnage to decrease slightly after 8 months, where the assembly was made with fatty lubricant.

E. End Effect.

In one series of tests to investigate the effect of out-of-straightness of mating elements. Russell (32) used a

press-fitted assembly with grooves cut circumferentially in the bore of the ring element, thus reducing the area of contact. By boring out the intervening lands between the grooves, the grip area, and also thepressing-on and pressing-off loads, were progressively reduced. Russell concluded from this, that out-of-straightness of the surfaces would approximate to this bearing-band condition, and result in reduced grip strength. An analysis of the values, however, indicates that, though the reduction of area is accompanied by a reduction of grip, the smaller areas have a higher proportional grip strength than the area of the ungrooved ring. Russell's results are tabulated below, together with the % increase in grip strength calculated by the writer. The mean pressing-on and pressing-off loads were used.

TABLE II.

Test No.	Bearing Surface in^2.	Grip Strength Tons.	Fraction compared with Test 1.		% increase of grip compared with Test 1.
			Bearing Surface.	Grip Strength.	
1	5.900	9.95	1.000	1.000	0
2	4.484	8.79	0.760	0.883	16
3	3.068	7.29	0.521	0.733	41
4	2.336	6.80	0.396	0.684	73
5	1.522	5.01	0.258	0.504	95

An explanation for this increase of grip strength per unit area under bearing band condition, may be found by considering the deformation of the plug under a band of pressure. This problem was investigated by Barton (1), and later, using a slightly different mathematical approach, by Rankin (28). Assuming an infinitely long shaft with a finite band of pressure of uniform intensity over the breadth of the band, Rankin calculated the stress components and the shaft deformation adjacent to the pressure. The minimum diameter of the shaft occurs in the middle of the pressure band and the stresses and deformations "wash-out" as the shaft returns to its free diameter within a short distance from the pressure band. Assuming that the interface pressure in a shrink-fit is constant over the axial length of grip, the shaft deformations correspond to the case where a thin ring is shrunk over a relatively long shaft, as occurs in turbine rotor assemblies. Calculating the interface pressure of such an assembly by assuming that the decrease in diameter of the shaft follows from the Lamé plane stress equations involves some error. Rankin compared the decrease in diameter of the shaft, calculated from plane stress assumption, with the average decrease under the band of pressure on a long shaft, and relates the two values by a factor K, such that:

$$K = \frac{\text{radial deformation on plane stress assumption}}{\text{average radial deformation under pressure band}}$$

values of K were plotted by Rankin for varying band widths.

It would appear that, for widths in excess of about 0.3 times the shaft diameter, no appreciable error is introduced by the simplified calculation.

With the dimensions of bands given by Russell for Test No. 5, above, and assuming that there is no coupling between adjacent bands, the increase in radial pressures with the above correction amounts to about 25%, whereas the increase in grip is actually 95%. In this case, however, the ring bore is subjected to the same pressure band conditions and the average radial deformation of the bore must be smaller than that calculated by the plane stress theory. Pressure bands on infinite cylinders have been considered by MacGregor and Coffin (22). By making certain approximations with regard to the stress systems induced by deformation of the cylinder wall, the resulting solution is in closed form. Using MacGregor and Coffin's analysis, the radial deformation under a circumferential line pressure load equal to the bearing band load, compared with the corresponding deformation using the Lamé equations, has been evaluated. The deformation under the line pressure is less than $\frac{1}{50}$ of the Lamé deformation, and therefore for a given fit allowance the pressure is much higher. The comparison is, admittedly, highly approximate, since the ring used in Russell's tests was not infinite nor even long, and the calculated deformation should be modified to account for additional deformation

due to the other closely adjacent bearing bands. Nevertheless it appears that the higher proportional strength exhibited by bearing bands can easily be accounted for by an increase in pressure resulting from increased radial stiffness of the ring under bands of pressure.

With the dimensions of grip in marine crankshafts, it is unlikely that the pressure would be much in excess of that calculated from the plane stress assumption. Lloyd's Rules give an axial length of grip of 0.625 times thepin diameter and one end of the pin is nearly flush with the web surface. The correction on the above basis would be negligible.

It should be noted, however, that the radial deformation evaluated by Rankin are not compatible with the assumption on which they are based. The mating surfaces of the plug and ring must be deformed by the boundary tractions in such a way that the profiles and dimensions are identical. The tractions are equal and opposite at every point on the mating surfaces. These are the only two conditions imposed on the boundaries, and solutions on this basis have not been attempted. The accuracy of an assumed distribution of stress must be judged by the compatibility of deformations of the two parts on which the stress is acting. It is clear that the interface pressure in an interference assembly where the two parts are unequal in length must be highest at the ends of the grip and lowest in the middle.

The actual value of the maximum pressure is important in view of the pressure required to overstrain the ring bore, and also on account of the deleterious effect of radial pressure on the fatigue strength of the shaft.

F. Torque Distribution at Interface.

In the discussion on a paper by Baugher (2), an important contribution was made by Mansa. When an interference fit is used for transmitting torque, the circumferential friction tractions cannot be assumed to be uniformly distributed over the length of grip. The problem may be treated as one of torque distribution in a shaft with a changing cross-section. Fig. 4 shows the approximate distribution in the case considered. The flow of the equimomental lines, drawn at quarter torque intervals indicates that the first $\frac{1}{20}$ of the grip length transmits one quarter of the total torque. The ratio of torque transmitted to grip length will probably increase to an even higher value at edge. The dimensions, and particularly the transition fillet, modify the torque distribution to a great extent. In most shrink-fits there is no fillet, the assembly consisting of a shaft and collar, in which case slip would occur at the entry end for extremely low torque.

In his reply to this point, the author admits that slip of part of the grip is likely, and states that this does, in

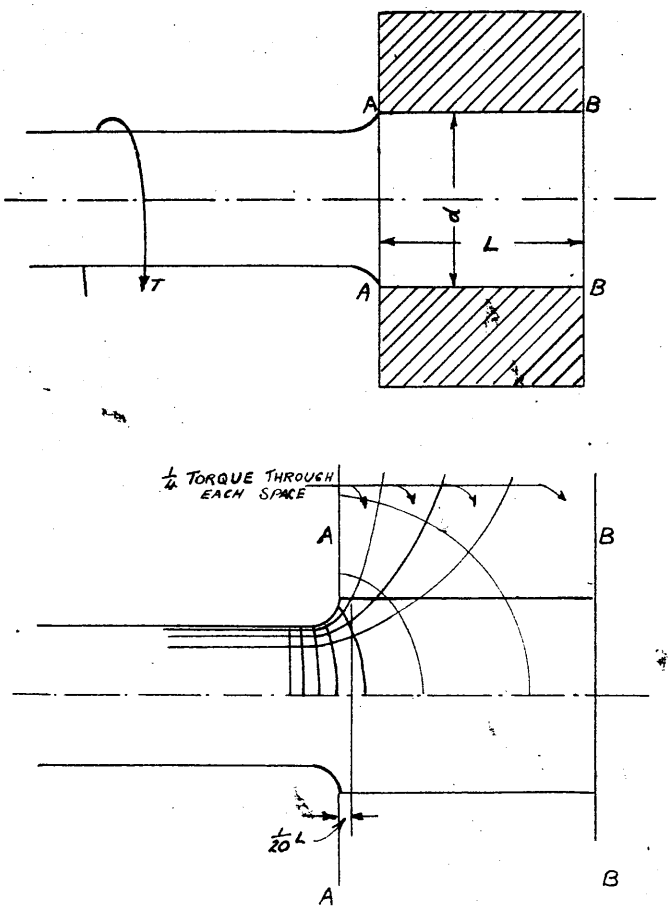

TORQUE DISTRIBUTION IN SHRINK-FIT (MANSA)

FIG. 4

fact, occur. He refers to unpublished work by Timoshenko and Jacobsen, which reports that the slip starts at the end AA, Fig. 4, and progresses with increase of torque until the entire grip is broken. The torque to initiate this slip does not increase with length of grip above about half the shaft diameter, but the maximum holding torque increases in proportion to the grip length.

This local failure of the grip by torque action is highly important where cyclic torques are imposed on the assembly, as is possible in the crankshaft fits. If relative movement occurs fretting corrosion and gradual loss of fit will result. The effect has been noted by the writer in some tests described in Part III of this thesis, in which a departure from torque-twist linearity was noted at torque values about one half of the ultimate grip strength. There are some features about the results, however, which suggest that local overstrain, and not relative movement, is the correct interpretation. Under the action of circumferential shearing forces, theprincipal stresses at the bore are displaced from the circumferential and radial directions and the maximum shear stress of the material is increased in magnitude, leading to overstrain and circumferential displacement of the bore layers.

G. Pulsating Loads on Fits.

An investigation carried out by Horger and Maulbetsch (15)

on the fatigue strength of shafting, showed that a press-fitted collar on a shaft seriously diminishes the fatigue strength. Fractures occurred just inside the end of the collar at which the bending moment in the shaft was greatest. In cases where a large number of reversals had taken place before fracture, the collar had become loose, and the fracture occurred in the middle of the grip.

This indicates that cyclic bending of the shaft progressively overstrains the fitted ring, with consequent progressive reduction of the interface pressure and destruction of the grip strength. It appears that the loss of fit depends on the number of reversals and corresponds to a creep of the overstrain through the ring material. This is of the utmost importance in the case of the built crankshaft where cyclic bending and torsion actions are imposed on the grip. The strength of assembly under superposed cyclic loading should not be inferred from the initial grip strength.

H. Axial Tractions in Temperature Fits.

In temperature fits the shrinkage of the ring or the expansion of the plug in the axial direction, as well as in the radial direction, is partially prevented. Even in the absence of temperature strain, axial strain due to radial

pressure would not be free to occur. The effect of this is to induce axial friction drag tending to extend the ring and compress the plug. Extension of the ring and contraction of the plug is accompanied by corresponding radial deformation tending to increase the fit allowance. The conditions are therefore complex.

Axial friction drag has been analysed by Goodier (11) but his assumption of an assembly long in relation to the diameter, renders the result of doubtful validity for the lengths of fit encountered in practice. Goodier shows that in a very thick cylinder the conditions remote from the ends of the cylinder are zero axial strain, instead of the zero axial stress implicit in the thick cylinder theory normally used. The effect of this is to increase the fit allowance by the factor $\frac{1}{1-\sigma}$ (or about 40% for mild steel). The identical result is derived by the writer in Part II, without the restriction of a very thick, or of a very thin, cylinder necessary in Goodier's analysis.

3. THICK CYLINDERS UNDER INTERNAL PRESSURE.

A. General.

The equations for the radial and circumferential stresses in an elastic thick cylinder, due to Lamé, are well known and universally used for shrink-fit calculations. The assumptions made in the derivation of these equations (e.g. Timoshenko (40)), are, in addition to the usual assumptions of elasticity, isotropy and homogeneity, that a condition of plane stress or of plane strain exists on planes normal to the cylinder axis, and that body forces are zero or constant. The stress distribution in the radial and circumferential directions is unaffected by axial stresses provided that these are uniformly distributed over the cross-section giving a condition of plane strain, e_z = constant.

The radial and circumferential stresses are greatest at the bore of the cylinder, and it is at this radius that elastic breakdown occurs under increasing bore pressure. The criterion of elastic failure of thick cylinders has not yet been definitely established and theoretical treatment of the stress conditions in overstrained cylinders varies according to the assumption made.

Cook and Robertson (5) carried out experiments on closed mild steel cylinders with a view to ascertaining the

correct failure criterion, and showed that breakdown of elastic conditions, as indicated by outside diameter measurements occurred at a pressure about mid-way between the pressure calculated on the Maximum Strain Theory of St. Venant and the Maximum Shear Stress Theory of Guest. Later, the experimental results were used by Haigh (13) to substantiate his Strain Energy criterion of failure.

Later work by Cook (6) (7), however, indicated that the "upper yield point" which can be observed in tension tests of carefully annealed mild steel specimens, had a counterpart in non-uniform stress systems. Cook's experiments on small steel cylinders with closed ends, demonstrated that the upper yield point was not constant, nor equal to the tensile test value, but varied as overstrain advanced through the wall of the cylinder.

The Shear Strain Energy criterion of failure, of Von Mises, has been used in theoretical analyses by Nadai (26), and by MacGregor, Coffin and Fisher (23). It is alleged that the failure of gun steel is more closely in accordance with this criterion, but its adoption leads to mathematical complexities in the analysis.

In a treatise by Macrae (24) dealing with the auto-frettaging process used in the manufacture of gun barrels, the shear stress criterion, as given by the lower yield point of a

tensile specimen, is selected. There is a substantial amount of experimental evidence in this treatise, that the behaviour of overstrained cylinders, within the limits of accuracy of measurement, can be calculated from the shear stress theory without appreciable error.

This theory of failure has also been used in a theoretical treatment by Sopwith (37) taking account of the compressibility of overstrained material, which is usually neglected when the plastic strain is large in comparison with the elastic strains. In the thick cylinder the inelastic material is bounded by elastic material which limits the amount of plastic strain to values of the same order as those occurring in the elastic region. On this account, theories which fail to account for the compressibility in the overstrained region must be considered to be approximate.

The analysis by Nadai (26) did not account for compressibility and in addition was based on zero axial strain, a condition not found in practice. Hill, Lee and Tupper (14) also use the zero axial assumption but take account of the incremental strain law for plastic strains. The solution is by graphical methods. All the other analyses referred to above, assume the plastic stress-strain law of Hencky, that the ratio of the principal shearing stresses is equal to the ratio of corresponding principal shearing strains.

The basic assumptions associated with inelastic stress and strain analysis of thick cylinders under internal pressure are enumerated in the next sub-section. The remaining sub-sections deal with the work of Cook, Macrae and Sopwith in greater detail.

B. Basic Assumptions in Overstrain Theory.

The variations in published theories of overstrained cylinders result from variations of the basic assumptions listed below.

(a) End Conditions.

In cases of closed cylinders under internal pressure, the end load of the pressure is communicated to the cylinder wall as an axial tensile load. Thus

$$\int_1^k p_z \; y \; dy = \frac{P}{2}$$

If the arrangement is such that the pressure is not accompanied by end load as is the case in shrink-fits and in certain autofrettaging arrangements, then

$$\int_1^k p_z \; y \; dy = 0$$

In addition to these equilibrium relationships, the assumption of plane strain

$$e_z = \text{constant}$$

is made. This is a necessary condition from physical consideration when the cylinder is long, but must be considered to be an

approximation for proportions of the order of length equal to diameter, as is usually the case in shrink-fits.

The assumption made by Nadai and by Hill, Lee and Tupper that

$$e_z = 0$$

is an artificial condition requiring an end load, initially unknown, computed from the resulting axial stress.

(b) Elastic Failure Criterion.

A universally applicable criterion of elastic failure of engineering materials has not been advanced. It is claimed that certain functions of the stress or strain conditions determine the incidence of overstrain in particular loading conditions and in particular materials. These functions must, as yet, be assumed to be approximations to more complex relationships.

For thick cylinders, two criteria havebeen selected, to correlate the observed behaviour of tensile test specimens and thick cylinders of the same material under internal pressure. These are

$$p_\theta - p_r = p_e$$

and

$$(p_\theta - p_r)^2 + (p_r - p_z)^2 + (p_z - p_\theta)^2 = 2p_e^2$$

The first is a criterion of maximum shear stress, and the second, of shear-strain energy, usually associated with Guest

and Von Mises respectively.

The shear stress criterion enables the radial depth of overstrain to be calculated from equilibrium considerations, independently of axial stress conditions, and therefore of end condition, and for this reason, as well as for the reason that, in mild steel cylinders, no great discrepancy occurs between calculated and measured external diametral extensions, it has been adopted by Cook, Macrae and Sopwith in their treatments of the subject.

Cook's analysis takes account of the possible difference of yield stress between initial elastic breakdown and subsequent plastic deformation.

Nadai and MacGregor, Coffin and Fisher, have analysed the problem, using the Von Mises criterion, which it is claimed, more closely represents the behaviour of gun steels. Hill, Lee and Tupper also use this criterion which they allege to be more satisfactory than the maximum shear criterion when the maximum energy dissipation during plastic deformation is considered.

(c) Plastic Stress-Strain Relationships.

The stress-strain relationship in the overstrained region usually adopted, is the Hencky hypothesis, which may be stated thus: the ratio of the principal shearing stresses is equal to the ratio of the corresponding principal shearing

strains, or

$$\frac{p_1 - p_2}{e_1 - e_2} = \frac{p_2 - p_3}{e_2 - e_3} = \frac{p_3 - p_1}{e_3 - e_1}$$

This is the relationship used by Cook, Nadai, Sopwith and MacGregor, Coffin and Fisher. Hill, Lee and Tupper use the more correct incremental strain law of Prandtl and Reuss, which may be reduced to the form

$$\frac{p_1 - p_2}{d(e_1 - e_2)} = \frac{p_2 - p_3}{d(e_2 - e_3)} = \frac{p_3 - p_1}{d(e_3 - e_1)}$$

If, as shown by Sopwith, the ratios of the principal shearing stresses are equal, then the latter reduces to the Hencky hypothesis.

(d) Compressibility.

Inelastic strain may be considered to consist of elastic strain which is recoverable on release of stress, and irrecoverable plastic strain which is accompanied by no volume change in the material.

When the plastic strains are large compared with the maximum elastic strains, the elastic component of total strain is usually neglected, and the material is therefore considered to deform plastically with no volume change.

In the case of the thick cylinder partially over-strained, the inelastic strains are limited to a magnitude

comparable with elastic strains, and the neglect of the elastic component of the strain is an approximation which may be important.

For overstrained material, the volume changes may be neglected, i.e.

$$e_r + e_\theta + e_z = 0$$

or included, in which case

$$e_r + e_\theta + e_z = \frac{1 - 2\sigma}{E} (p_r + p_\theta + p_z)$$

The volume changes were neglected in the earlier solutions by Nadai and Cook, but all later work has included this effect.

(e) Tensile Stress-Strain Curve.

The flat-topped stress-strain curve given by tensile tests of annealed steel specimens, as shown in Fig. 5, is usually assumed, in the development of overstrained cylinder theory. The material does not exhibit strain-hardening characteristics until considerable overstrain occurs, and the flow criterion in the overstrained region may be taken to be that corresponding to the criterion of failure adopted. A variation of this occurs in Cook's treatment and will be discussed later.

Macrae allowed for strain hardening by attaching

simple geometrical properties to the tensile diagram.

The analysis of MacGregor, Coffin and Fisher enables an arbitrary tensile test diagram to be employed. An assumption made that the relationship between "effective stress" and "effective strain" is the same for all kinds of deformations. These terms are defined as

$$\text{"Effective Stress"} = \frac{\sqrt{2}}{2}\left\{(p_r - p_\theta)^2 + (p_\theta - p_z)^2 + (p_z - p_r)^2\right\}$$

$$\text{"Effective Strain"} = \frac{\sqrt{2}}{3}\left\{(e_r - e_\theta)^2 + (e_\theta - e_z)^2 + (e_z - e_r)^2\right\}$$

(f) Configuration of Overstrained Region.

The assumption is made in all cases that a definite rotationally-symmetrical region ofoverstrain exists, in a partially overstrained cylinder, as shown in Fig. 6. The plastic front progresses radially under increasing pressure, but maintains a circular boundary at the junction with the elastic region.

This assumption is almost essential for a mathematical approach to the problem. It is well-known, however, that the progression of overstrain is a piece-meal process and is accompanied by unsymmetrical radial deformations which produce out-of-roundness at the external diameter. The process of yielding is discussed in some detail by Cook (7), and by Muir, in the discussion of Cook's paper.

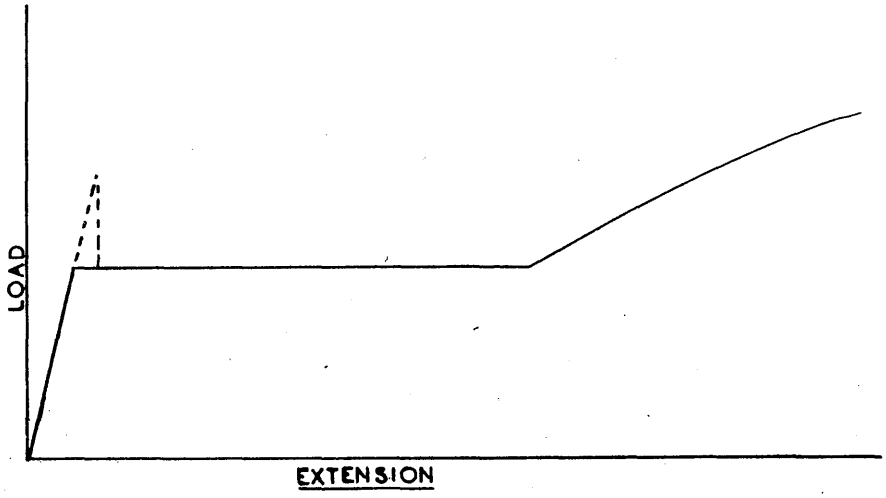

TENSILE TEST DIAGRAM FOR MILD STEEL

FIG. 5

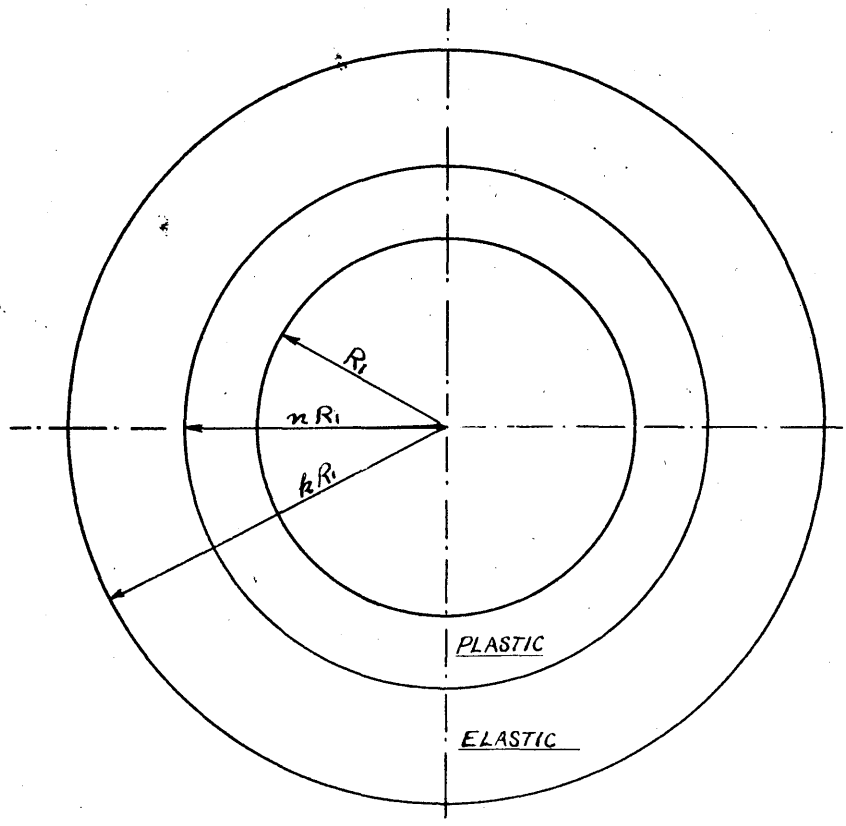

PLASTIC REGION OF OVERSTRAINED CYLINDER

FIG. 6

C. Theoretical and Experimental Work by Cook (7).

(a) Experimental Results.

The numerous assumptions inherent in most theoretical treatments of overstrained cylinders, make it essential to compare derived relationships with experimental results, obtained from measurements of cylinders under bore pressure. Such experiments are few in number, the most reliable data having been obtained by Cook from measurements of circumferential and axial strain at the outside diameter under increasing internal pressure. The effect of variations in the basic assumptions on the predicted values of these measureable quantities is relatively slight, and it is necessary to obtain accurate results, if reliable conclusions are to be drawn. The experimental results in this paper were obtained with extreme care, and the accuracy of the measurements cannot be questioned.

The experiments were carried out on small mild steel cylinders, with varying wall thicknesses. The bore-size varied from $\frac{3}{4}$" to $\frac{1}{4}$" and the diameter ratio from 1.167 to 4.000. A parallel length of $3\frac{1}{4}$" was faired into enlarged ends, screwed for pressure connections. All specimens and tensile test pieces were carefully machined and subsequently annealed for 20 mins. at 900°C., in vacuo, afterwards cooling by radiation. Tensile test results were obtained on a specially designed machine, described by Cook in an earlier paper (6) allowing the

upper yield point to be observed.

The results show that, without any reasonable doubt the pressure required to maintain plastic flow in a completely overstrained cylinder wall, corresponds to the Tresca maximum shear stress hypothesis for plastic flow, based on the lower yield shear stress in the tensile test. Relationships based on the Von Mises flow criterion, indicate that pressures in excess of those observed would be required to overstrain the cylinders completely. In the case of the cylinder with the 2:1 diameter ratio, the pressure computed from MacGregor, Coffin and Fisher's work is 10% in excess of the observed value. Cook himself states that 10-16% greater pressures are required using the formula derived by Nadai, on the basis of the Von Mises criterion. It must therefore be concluded that for mild steel cylinders, the Tresca flow hypothesis is more accurate. On this account, theories based on the Von Mises criterion, have not been reviewed in detail.

The pressure required to initiate overstrain is, however, much in excess of that calculated on the basis of a lower yield point in tension, and indeed, in excess of that corresponding to the upper yield point. The earlier work of Cook and Robertson (4) indicated that the maximum shear stress at the elastic failure point in cylinders was independent of wall thickness for a given bore diameter, but varied inversely with the

diameter. Cook suggests that there is a connection between the rate of change of maximum shear stress with radius, and the critical value observed. In the paper under discussion, however, the critical shear stress did not increase proportionately to the reduction in diameter, although the higher values were observed in the tubes with the smallest bores. The highest value was 15% in excess of the average tensile upper yield shear stress.

It is possible that the tensile test did not indicate the true maximum. An eccentricity of loading of 6×10^{-3} inches on the tensile specimen would be sufficient to elevate the local stress due to bending and direct action, to that observed in the thick tubes. At the same time, even this small eccentricity is probably unreasonably high for the type of loading system employed by Cook(7).

It might be supposed that initial failure could be based on a different flow criterion than the subsequent plastic deformation. The Von Mises criterion based on the upper yield tensile stress does, in fact, give slightly better agreement between the calculated and observed critical pressures, than the upper shear stress criterion. When the subsequent progression of overstrain is considered, however, it becomes clear that no matter which criterion is adopted an explanation of the experimental results cannot be obtained, unless some variation in the

initial failure criterion is assumed. The elastic failure criterion appears to be a function not of stress condition only, but of the state of progression of overstrain and possibly of the absolute size of the specimen.

The idea that the elastic failure criterion for each element of the material is arbitrarily fixed by its location, is, however, untenable. The difficulty may be avoided by assuming the local stress condition to be different from the average, as given by average loads and average deformations. The material fails locally under the local stress system and measurements merely indicate an integrated effect of a number of local failures. There are two points in experimental work which tend to support this view. The rotational symmetry of the tube is destroyed after overstrain begins, indicating that variations of stress do, in fact, exist. Secondly, considerable care was taken to ensure that the tensile and cylinder specimens were free from tool marks or residual stresses, both of which tend to set up local stresses in excess of the average, and consequent local failure before the average failure. Presumably the upper yield point would not be observed unless considerable care was exercised in those respects.

It was noted by Cook that the upper value of the yield point in the tensile specimen could not be attained after overstrain had commenced, when the specimen was unloaded, and sub-

sequently reloaded. The presence of overstrained material apparently inhibits higher stress values in material which had previously demonstrated an ability to withstand such stresses. There is difficulty in reconciling this fact with the behaviour of overstrained cylinders, in which the yield point in elastic material, is apparently greater than that in contiguous overstrained material. The elevation of the initial breakdown point is to be expected, but subsequent overstrain should occur with the lower value of yield shear stress at the inner boundary of the elastic ring.

While speculation regarding the process of overstrain is undesirable, the question of the value to be attached to the maximum elastic shear stress after overstrain has commenced, is one which cannot be avoided in the shrink-fit investigation. It is considered that overstrain will commence at the lower value of shear stress on account of the residual machining stress and the probability of local concentrations. This, however, does not preclude a higher shear stress being attained during the progress of overstrain. Nevertheless, a definite viewpoint must be taken on this important issue.

For the following reasons, the upper yield point in shear has been rejected in shrink-fit calculations.

(i) The experiments of Macrae, reviewed in the next section,

indicate that calculations based on the lower value of yield stress at the inner boundary of the elastic shell, are not seriously in error, when applied to gun steel forgings, and that the tensile test diagrams for such steels are comparable with mild steel diagrams.

(ii) Cook's results show that the value of the upper yield stress falls rapidly with the progression of overstrain, and also that increasing the specimen size tends to depress the values attained.

(iii) It is thought that the elevation of the yield point in the elastic region is due to the initial high value at the commencement of overstrain, and would not occur without this initial elevation. In this connection it is visualised that the release of strain energy at the breakdown of elastic conditions causes localised slip in the material in advance of the general plastic front. The material would then contain a transition zone in which the stress conditions would be highly complex and in which neither the constancy of shear stress nor the Lamé stress relationships could adequately represent the average conditions. The breadth of the transition zone apparently diminishes as the overstrain progresses, and so the calculated maximum elastic shear stress approaches the lower yield value.

(iv) In a shrink-fitted assembly, out-of-roundness during overstrain is to some extent prevented by the local unloading

action which would consequently occur, the plug being relatively rigid. This tends to induce a more ordered progression of overstrain.

(b) Theoretical Work.

The following exceptions to the notation listed at the beginning of the thesis are used in this section.

s = Variable maximum shear stress in the elastic zone.

s' = Constant maximum shear stress in the plastic zone.

Radial equilibrium of an element of overstrained material under constant shear stress s' leads to the equation

$$y \frac{dp_r}{dy} = p_\theta - p_r = 2s' \qquad \text{----------(1)}$$

Since s' is constant this equation can be integrated directly, the constant being given by boundary condition

$p_r = -P$ at $y = 1$

Hence

$$p_r = s' \log y^2 - P \qquad \text{----------(2)}$$

The radial pressure, $-p_r$, is assumed to be continuous at $y = n$, and in the elastic cylinder the Lamé equations give

$$p_r = \tfrac{1}{2} p_\theta)_k \left(1 - \frac{k^2}{y^2}\right) \qquad \text{----------(3)}$$

$$p_\theta = \tfrac{1}{2} p_\theta)_k \left(1 + \frac{k^2}{y^2}\right) \qquad \text{----------(4)}$$

From (2) and (3), eliminating $p_r)_n$

$$P = s' \log n^2 + \tfrac{1}{2} p_\theta)_k \left(\frac{k^2}{n^2} - 1\right) \qquad \text{----------(5)}$$

Also

$$p_\theta)_n - p_r)_n = 2s$$

Therefore from (3) and (4)

$$s = \tfrac{1}{2} p_\theta)_k \frac{k^2}{n^2} \qquad \text{----------(6)}$$

Equations (5) and (6) contain measurable quantities P and $p_\theta)_k$ and unknown quantities s , s' , n . Cook assumed that s' would be equal to the value given by the lower tensile yield point and hence n and s were calculated from the experimental results. s varied with n , between a value in excess of that given by the upper yield in tension, and a value closely corresponding to s' at $n = k$.

In his analysis of axial stress Cook made the following assumptions.

(i) Incompressibility of overstrained materal,

$$e_\theta + e_r + e_z = 0 \qquad \text{----------(7)}$$

(ii) The Hencky flow hypothesis,

$$\frac{p_r - p_\theta}{e_r - e_\theta} = \frac{p_\theta - p_z}{e_\theta - e_z} = \frac{p_z - p_r}{e_z - e_r} \qquad \text{----------(8)}$$

(iii) The axial strain, e_z , constant in a long tube

From (7)

$$\frac{du}{dr} + \frac{u}{r} + e_z = 0$$

Integrating

$$\left.\begin{aligned} e_r &= -\tfrac{1}{2} e_z - \frac{C}{r^2} \\ e_\theta &= -\tfrac{1}{2} e_z + \frac{C}{r^2} \end{aligned}\right\} \qquad \text{----------(9)}$$

where C is a constant of integration.

The value of C was found by assuming the circumferential strain continuous at $y = n$. This condition leads to a discontinuity in the axial stress, since the conditions $e_\theta + e_r + e_z = 0$ applies to one side of the interface and

$$e_\theta + e_r + e_z = \frac{1 - 2\sigma}{E} (p_\theta + p_r + p_z) \quad \text{to the other.}$$

From (8) and (9) the axial stress in the overstrained region was derived in the form

$$p_z = s' (\log y^2 + \beta y^2 + 1) - P \qquad \text{----------(10)}$$

where β is a function of the stresses at $y = k$, given by

$$\beta = \frac{3(p_z)_k - \sigma p_\theta)_k)}{(1-2\sigma) n^2 (p_\theta)_k + p_z)_k) + (1+\sigma) k^2 p_\theta)_k}$$

From (10) the axial stress in the overstrained region could be computed. The average value of p_z found by integrating (10) from 1 to n , was compared with that obtained from axial equilibrium considerations, the axial stress in the elastic region being uniform and equal to the measured value at the outside diameter. The agreement was rough. This is probably due to the assumption of incompressibility and the consequent discontinuity of axial stress. The average value based on equilibrium conditions must be considered to be the correct value, within the limits imposed by the experimental determination of axial stress in the elastic region.

In Part II of this thesis an analysis is given, based on the same assumptions as that of Cook, with the exception that the maximum shear stress is assumed to be that given by the lower yield point, in both regions. The assumption of incompressibility again leads a discontinuity in axial stress at $y = n$, and it is shown that if the axial stress be made continuous the value is given by the arithmetic mean of the hoop and radial stresses in both regions. In this case, the compatibility equation is not satisfied, the constant in equation (11) being infinite. The simplification effected by this, however, gives relationships which are not seriously in error in the case of closed cylinders, and are suitable for rapid computation.

In Fig. (7) Cook's experimental results for axial and radial extensions at the outside diameter for a cylinder with a 2:1 diameter ratio are shown, together with curves obtained from the theory developed in Part II, and curves computed from the equations given by Sopwith (37), allowing for compressibility in the plastic region. The latter two sets of curves were plotted from the shear stress corresponding to complete over-strain in the cylinder and not the value given by Cook from the average tensile tests.

It can be seen that theory based on the assumption of continuity of maximum shear stress at the boundary of the two regions is inadequate, even when compressibility effect is included. The latter has little influence on the outside radial extensions, but axial strains are seriously affected.

D. Theoretical and Experimental Work by Macrae (24).

This treatise by Major Macrae describes a large number of experiments carried out in connection with the design and manufacture of autofrettaged gun barrels. A theoretical treatment for the radial and circumferential stress conditions in an open-ended thick cylinder is developed from certain assumptions, which are open to criticism, but which nevertheless lead to relationships closely corresponding with experimental observations, and not seriously in error compared with later theoretical work.

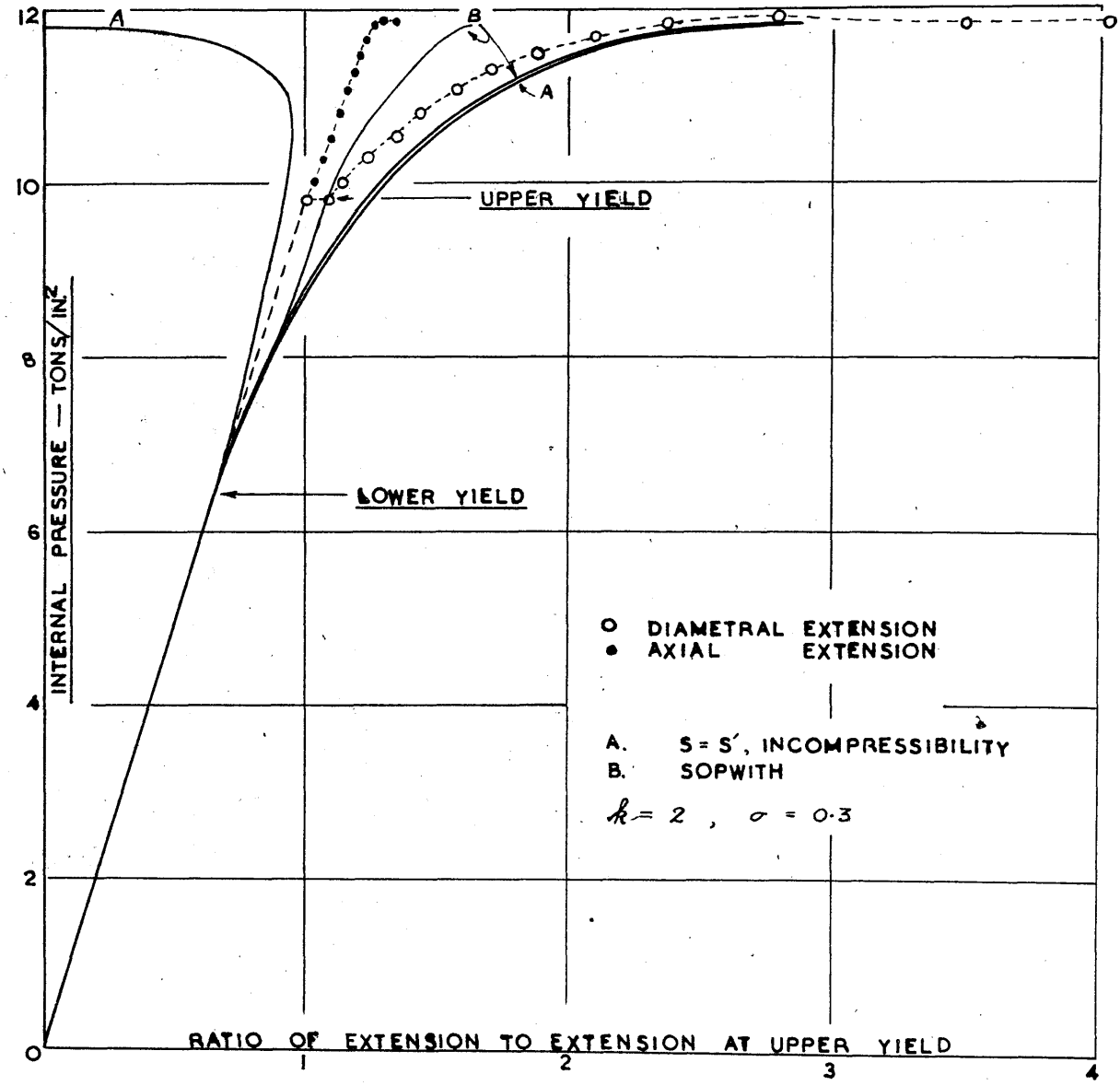

EXPERIMENTAL RESULTS BY COOK

FIG. 7

A very large number of tensile and compression tests on various kinds of steels, subjected to various heat and strain treatments are reported. The empirical data furnished by these tests is of fundamental importance, and merits a brief statement of the properties of overstrained steel.

(a) Tensile and Compression Tests of Various Steels.

Over 2000 such tests were carried out by Macrae to determine the properties of metals strained beyond the elastic limit in tension and compression. Various gun steels, medium carbon steels, mild steel (0.15% - 0.22% C), gun metal, and maganese bronze, were examined and showed the same tendencies, though differing slightly in detail.

The terminology adopted by Macrae for strains in excess of the maximum elastic values was "Overtension and Overcompression". The tensile load-extension diagram was divided into ranges as shown in Fig. 8. Low temperature heat treatment, denoted by L.T.T., was used to improve the elastic properties. This consisted of soaking for one hour at temperatures varying from 200°C to 400°C, the optimum value for each material being determined experimentally.

The mechanical properties of steel subjected to overtension, overcompression and L.T.T., singly or together, are briefly as follows:

(i) Young's Modulus is not affected by strain or thermal treatment.

(ii) Overtension reduces the compressive elastic limit to zero, and overcompression reduces the tensile limit to zero.

(iii) Overtension followed by L.T.T. at zero stress increases the tensile elastic limit to at least the overtension stress, but does not fully restore the compressive elastic limit.

(iv) Overtension followed by overcompression to the limits shown in Fig. 9, followed by L.T.T. increases both tensile and compressive elastic limits. The same result may be achieved with the diagram inverted, i.e. overcompression followed by overtension. Further increases in elastic limits can be obtained after a second cycle of operations.

(v) The treatment in (iv) increases the indentation hardness and slightly lowers the impact strength.

(vi) The treatment in (iii) has little effect on the fatigue strength. No results were obtained for treatment (iv).

(vii) Overtension, followed by L.T.T. under reduced load, has an effect similar to that under zero load. The trend is not clearly defined here. For mild steel, which had been overtensioned in the yield range, L.T.T. under reduced tensile load increased both elastic limits to values in excess of the originals.

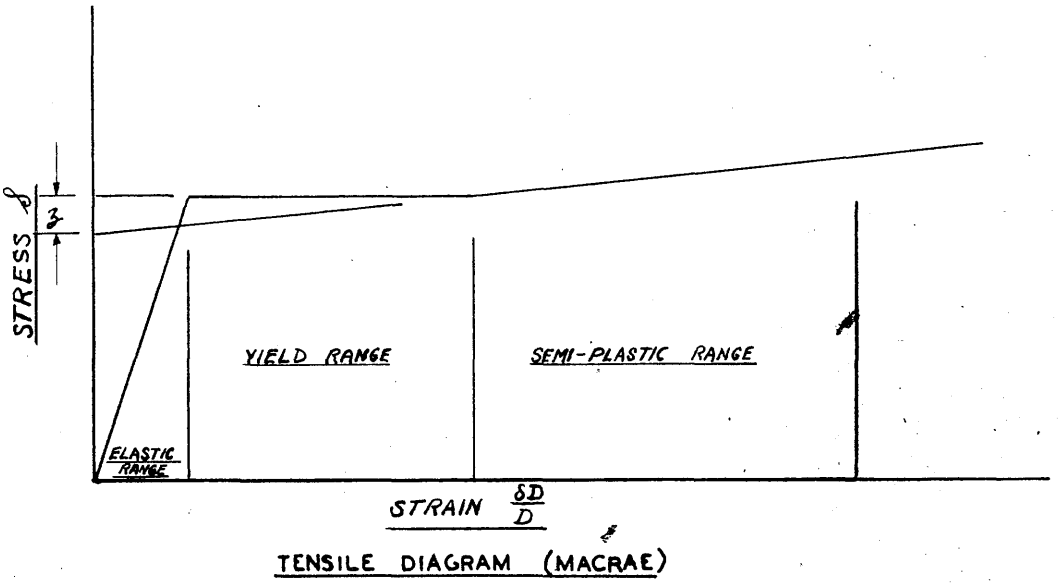

TENSILE DIAGRAM (MACRAE)

FIG. 8

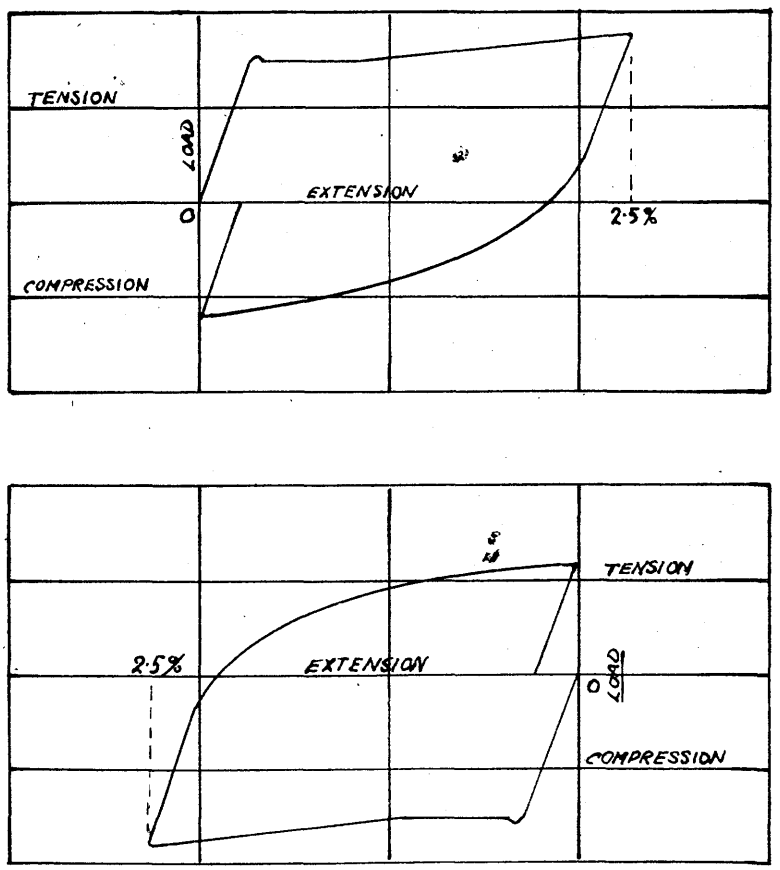

OVERTENSION AND OVERCOMPRESSION OF STEEL

FIG. 9

(b) Autofrettage Experiments.

A number of experiments were carried out on gun-steel test cylinders and on actual gun forgings. The results of eleven experiments on 3" cylinders, with diameter ratios between 2 and 4, are reported in some detail. The cylinders, about 18" in length, were machined from gun forgings and subjected to a predetermined maximum internal pressure under open-end conditions, measurements being taken of outside diameter and internal pressure up to the maximum value. Measurements of bore and external diameter were taken before and after application and release of pressure. The cylinders were stabilised by L.T.T. and the pressure re-applied. In some cases pressure in excess of the original value was applied. Axial lengths were measured, before, during and after applications of pressure.

From the series of experiments, Macrae obtained experimental evidence that his theory for overstrained cylinders was substantially correct. Among many deductions made, the following are noteworthy.

(i) The curve of external diametral expansion against pressure agreed with the theoretical expansion, calculated on the maximum shear stress criterion of failure

(ii) The external diametral expansion recovered elastically

on release of pressure.

(iv) Measurements of permanent set at the bore and external diameter were in the inverse ratio of the diameters.

These statements merit closer examination.

(i) The agreement between the calculated and measured external deflection is, on the whole, mediocre. It is doubtful whether measurements obtained by comparative methods could establish the criterion of failure with certainty. The curves show experimental scatter in the elastic range exceeding the limits of accuracy of measurement, stated by Macrae as $\pm$ 0.0001".

(ii) The elastic return of external diametral expansion on release of pressure is an important assumption in the theoretical treatment, yet only one curve is included showing experimental measurements obtained during the removal of autofrettage pressure. In this diagram the experimental points indicate a small, but significant departure from linearity, in excess of the probable experimental error. Other evidence on the elastic recovery of the outside diameter, to which attention is drawn in the treatise, shows the linear relationship on application of pressure to the stabilised cylinder, not the release of autofrettage pressure.

(iii) The relationship between residual deflections and diameters must be considered to be very approximate . Accuracy

of internal measurements is generally less than that of comparable external measurements. The method by which the measurements were obtained was not stated, but the external deflection measurements indicated that a 5% error in each residual deflection would be quite possible, giving a possible 10% error in ratio.

(c) Theoretical Treatment.

The stress and strain relationships for the overstrained cylinder were approached via the stress-strain diagram of a tensile test. The shear stress in the cylinder $\frac{p_\theta - p_r}{2}$ was identified with the shear stress in a tensile test specimen under a tensile stress S , termed the Equivalent Simple Stress, i.e. $p_\theta - p_r = S$

Corresponding to S and therefore to $(p_\theta - p_r)$ there is a tensile strain $\frac{\delta D}{D}$ in the test piece, i.e. the test-piece strains are identified with the diameter D of the cylinder at which the shear stress has the same value as has the tensile specimen with strain $\frac{\delta D}{D}$.

In the elastic cylinder $(p_\theta - p_r)$ varies inversely as the square of the diameter and therefore S and $\frac{\delta D}{D}$ vary in a like manner.

For the overstrained cylinder, Macrae stated that $\frac{\delta D}{D}$ again varied inversely as the square of the diameter. This

must be regarded as an assumption, since no attempt at proof was given. It is not easy to see the precise implications of the statement. In general terms it must be regarded as an obscure relationship between plastic stress and strain.

One further statement in the analysis is questionable. The change in length after application and removal of over-straining pressure was found to be negligible. From this, Macrae, assuming conservation of volume, concluded that the cross-section area remained constant, and therefore residual circumferential strains varied inversely as the squares of the diameters. Conservation of volume is not applicable between a cylinder, initially free from stress, and one containing a residual stress system.

Denoting the residual circumferential strain at diameter D as $\frac{\delta d}{d}$, and using the experimental observation which has already been criticised, that the outside diameter recovers elastically, it follows that the residual test-piece strains are everywhere equal to the residual circumferential cylinder strains, since the test-piece recovers elastically from a strain $\frac{\delta D}{D}$, inversely proportional to D, and at the outside, the radial stress being zero, the cylinder and test-piece strains are equal. This leads to the equations:

For Test Piece.

$$\text{Total Strain} = \text{Plastic Strain} + \text{Elastic Strain}$$

$$\frac{\delta D}{D} = \frac{\delta d}{d} + \frac{p_\theta - p_r}{E} \qquad \text{-----(11)}$$

For Cylinder.

$$\text{Total Strain} = \text{Plastic Strain} + \text{Elastic Strain}$$

$$e_\theta = \frac{\delta d}{d} + \frac{p_\theta - \sigma p_r}{E} \qquad \text{---(12)}$$

Equation (13) implies that all diameters recover elastically, and therefore neglects the overcompression of the bore layers on release of overtension. p_θ and p_r are elastic stresses corresponding to overstrain pressure P .

From (11) and (12)

$$e_\theta = \frac{\delta D}{D} + \frac{(1 - \sigma)}{E} p_r$$

where p_r is given by the Lamé equations, i.e.

$$p_r = - \frac{P}{k^2 - 1} \left(\frac{k^2}{y^2} - 1\right)$$

therefore

$$e_\theta = \frac{\delta D}{D} - \frac{(1 - \sigma)}{E} \frac{P}{k^2 - 1} \left(\frac{k^2}{y^2} - 1\right) \qquad \text{----------(13)}$$

At bore

$$e_\theta)_1 = \frac{\delta D}{D})_1 - (1-\sigma)\frac{P}{E}$$

i.e.

$$e_{\theta})1 = k^2 \frac{\delta D}{D})_k - (1 - \sigma) \frac{P}{E} \qquad \text{----------(14)}$$

At exterior

$$e_{\theta})k = \frac{\delta D}{D})_k$$

and

$$\frac{\delta D}{D})_k = \frac{P_\theta}{E})k \qquad \text{----------(15)}$$

since the Equivalent Simple Stress is equal to the hoop stress at the exterior.

The radial and hoop stresses for the plastic and elastic zone are derived by Macrae in the usual way from radial equilibrium considerations. They are given by equations equivalent to (2) (3) and (4) above.

The unique manner in which strain-hardening effects are accounted for, is noteworthy. As shown in Fig. (8) the idealised test-piece diagram is divided into three zones. In the semi-plastic zone a linear relationship of stress and strain is assumed, the slope and intercept of the line being constant for a particular kind of steel.

The Equivalent Simple Strain for a particular diameter is known, by assumption, and the right-hand side of equilibrium equation (1) may therefore be expressed in terms of the constant yield stress and the diameter variable (together with the diagram constants). The integration is possible, giving

$$p = s \left\{ \log n^2 + \beta \log n'^2 - \frac{n^2}{k^2} + 1 + \frac{\beta}{2s} (n'^2 - 1) \right\}$$

where $n' = \frac{\text{Radius of exterior of semi-plastic zone}}{\text{Internal Radius}}$

β = Strain-hardening constant shown in Fig. 8.

Axial stresses are entirely ignored. It is stated that changes in the length of the cylinder due to application of auto-frettage pressure may be neglected. This is, no doubt, fortuitous, since the cylinder must shorten by a measurable amount under elastic stresses. It then presumably lengthens during overstrain so that the nett change in length may be neglected. On return to zero pressure, the reverse occurs, and if the length is still unchanged it indicates that inelastic strains have been induced during removal of pressure. For example, an 18" long cylinder with k = 2, would shorten by 3×10^{-3} inches approximately at the elastic failure pressure.

In spite of the assumptions made in deriving the equations of stress and strain, the bore strain calculated by Macrae's method agrees very closely with the bore strain given by the more correct analysis of Sopwith. Fig. 10 shows the comparison for a 2:1 cylinder. Outside diametral strains are identical for the scales used in this graph.

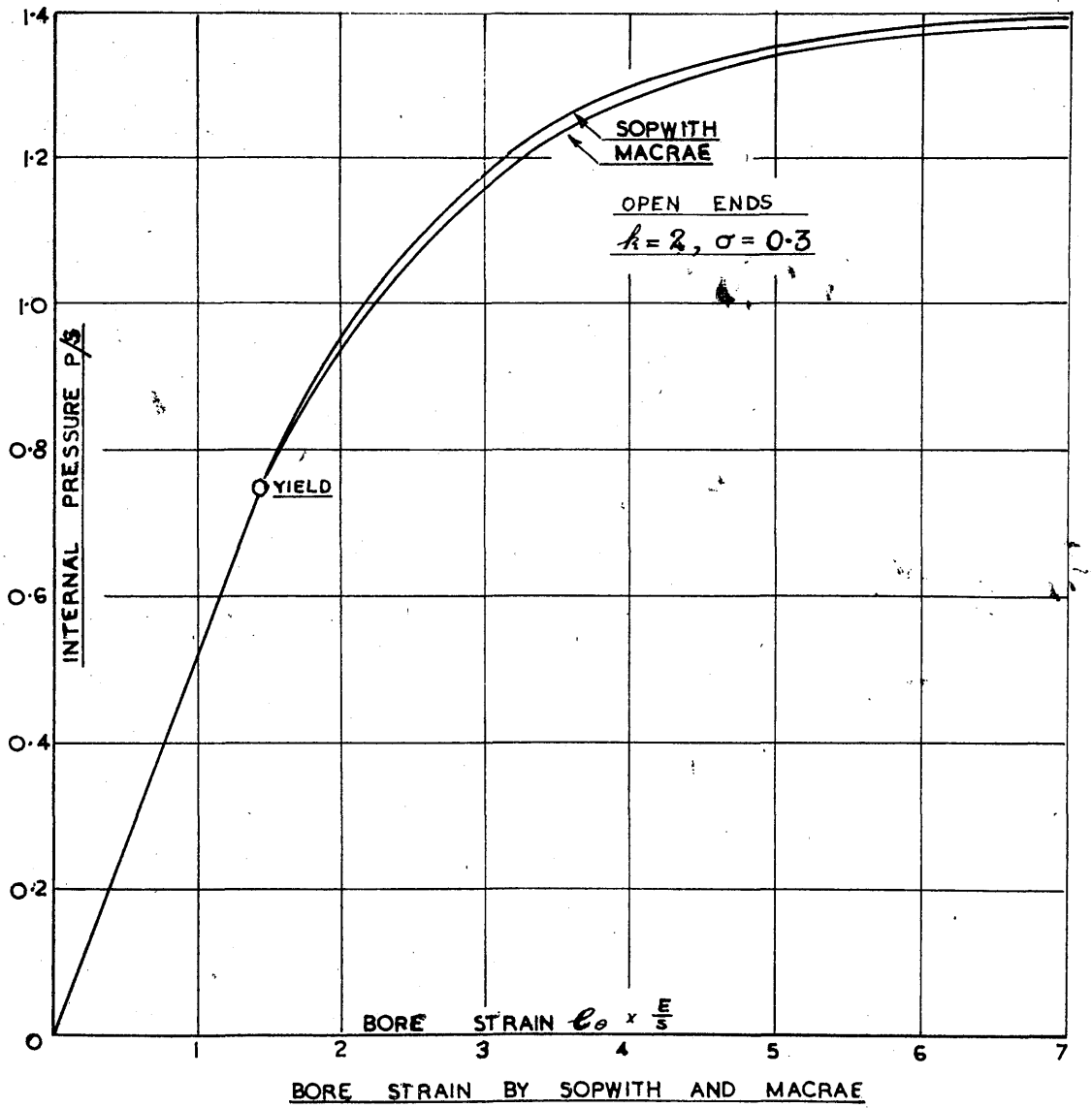

BORE STRAIN BY SOPWITH AND MACRAE

FIG. 10

E. Theoretical Work by Sopwith (37).

The mathematical difficulties encountered in taking account of compressibility of overstrained material were overcome by Sopwith with substitutions and one close approximation. Solutions of the stresses and strains in an overstrained cylinder, are given for either open or closed end conditions. The analysis is based on the following assumptions.

(i) The maximum shear stress $\frac{p_\theta - p_r}{2}$ in the plastic region is constant and equal to the yield shear stress of the tensile test. The same maximum shear stress is assumed at the inner boundary of the elastic region.

(ii) The plastic stress-strain relationship is given by the Hencky total strain hypothesis of plastic flow

$$\frac{p_r - p_\theta}{e_r - e_\theta} = \frac{p_\theta - p_z}{e_\theta - e_z} = \frac{p_z - p_r}{e_z - e_r}$$

(iii) The plastic material is compressible in accordance with

$$e_r + e_\theta + e_z = \frac{2(1 - \sigma)}{E} (p_\theta + p_r + p_z)$$

(iv) The axial strain is constant over any cross section i.e., the cylinder is assumed to be long.

(v) The axial stress and end load are in equilibrium, i.e.,

$$\int_1^k p_z \, y \, dy = 0 \quad \text{or} \quad \frac{P}{2}$$

(open or closed ends respectively)

These assumptions lead to the same equations for radial and circumferential stresses given in sub-section 3.C.(b) above, by making $s = s'$.

Plastic Region ($1 < y < n$)	Elastic Region ($n < y < k$)
$p_r = p_\theta = s(\log \frac{y^2}{n^2} \mp 1 + \frac{n^2}{k^2})$ *	$= sn^2(\frac{1}{k^2} \mp \frac{1}{y^2})$ *

* Upper sign with upper suffix.

In order to evaluate the axial stress p_z and the strains e_θ , e_r , e_z , assumptions (ii), (iii), (iv) and (v) above must be used.

The equations derived by Sopwith are:

Plastic Region ($1 < y < n$)	Elastic Region ($n < y < k$)
$p_z = s(\frac{n^2}{k^2} - 2W_2 - 2aW_3)$	$= s(\frac{n^2}{k^2} - 2(1 - 2\sigma)\, a)$
e_z = constant $= \frac{s}{E}(1 - 2\sigma)(\frac{n2}{k^2} - 2a)$	
$e_r = \frac{s}{E}(1 - 2\sigma)(\frac{n^2}{k^2} - W_6 + aW_1)$	$= \frac{s}{E}\{(1 - 2\sigma)(\frac{n^2}{k^2} + 2\sigma a) - (1+\sigma)\frac{n^2}{y^2}\}$
$e_\theta = \frac{s}{E}(1 - 2\sigma)(\frac{n^2}{k^2} + W_5 + aW_1)$	$= \frac{s}{E}\{(1 - 2\sigma)(\frac{n^2}{k^2} + 2\sigma a) + (1 + \sigma)\frac{n^2}{y^2}\}$

W_1 , W_2 , W_3 , W_5 , W_6 , are functions of $(\frac{y}{n})^2$ tabulated in Sopwith's paper for various value of $(\frac{y}{n})^2$ with $\sigma = \frac{2}{7}$ and 0.3; a is a constant depending on the end conditions and n . Values of a_o , a_c (open and closed ends respectively) are

tabulated for values of $(\frac{1}{n})^2$.

Sopwith compares his solution with the solution of Hill, Lee and Tupper (14) based on the incremental strain hypothesis. For k = n = 2 the axial stress agrees within 5%, showing that no great error is introduced by the Hencky flow hypothesis.

A comparison with the Von Mises criterion of failure is also given. It is shown that the analysis will satisfy the condition with closed ends, within 1% error, if a fictitious shear stress between 14.7% and 15.5% higher than the yield shear stress is adopted. For open ends the errors are much greater.

4. BUILT CRANKSHAFTS.

A. Available Information.

At the present time, built crankshafts are usually designed in accordance with the recommendation of Lloyd's Register of Shipping. The rules for scantling sizes and other recommendations are generally the result of practical experience. To the writer's knowledge, no papers are available containing theoretical or experimental evidence on the grip or stress condition of shrink-fits in marine crankshafts. This is hardly surprising, since the review of papers in Section 1 above, indicates that in simple shrink-fitted assemblies the interface pressure and stress condition have neither been definitely established, nor correlated to the fit allowance, and that there is disagreement about the influence of other factors affecting the grip.

Furthermore, no information is available from which the factors contributing to failure of a shrink-fit might be assessed. Apparently failures have not been investigated, or reports are not released for general publication.

In these circumstances, a survey of previous work yields little of value or relevancy to the present investigation. Two papers by Dr. Dorey, however, contain some recommendations for the design of built shafting; also the plane stress dis-

tribution in a perforated plate similar in shape to a crank web, has been determined by Coker and Levi (3), using photo-elastic methods. The relevant sections of these papers provide some guidance, and are reviewed in the following sub-sections.

B. Papers by Dorey (9) (10).

These papers are concerned with the general design of shafting, and consequently the sections dealing with shrink-fit stresses are quite brief. The following features were discussed by Dorey.

(a) Scantling Sizes.

Lloyds Rules for scantling sizes are given as

$h = 0.625d$ $t = 0.438d$ where h, t and d are as shown in Fig. 11. Dorey points out that increasing the h dimension is more effective than increasing t , in providing increased grip strength. The relationships between h and t for constant grip strength at constant fit allowance, and for constant grip strength at constant hoop stress, were demonstrated by curves. Fig. 12 reproduced from Dorey's later paper, shows these relationships.

Further comment on the Rules for scantling sizes is desirable, as Fig. 12 suggests that the proportions are derived from the intersection of the two curves. This is incorrect.

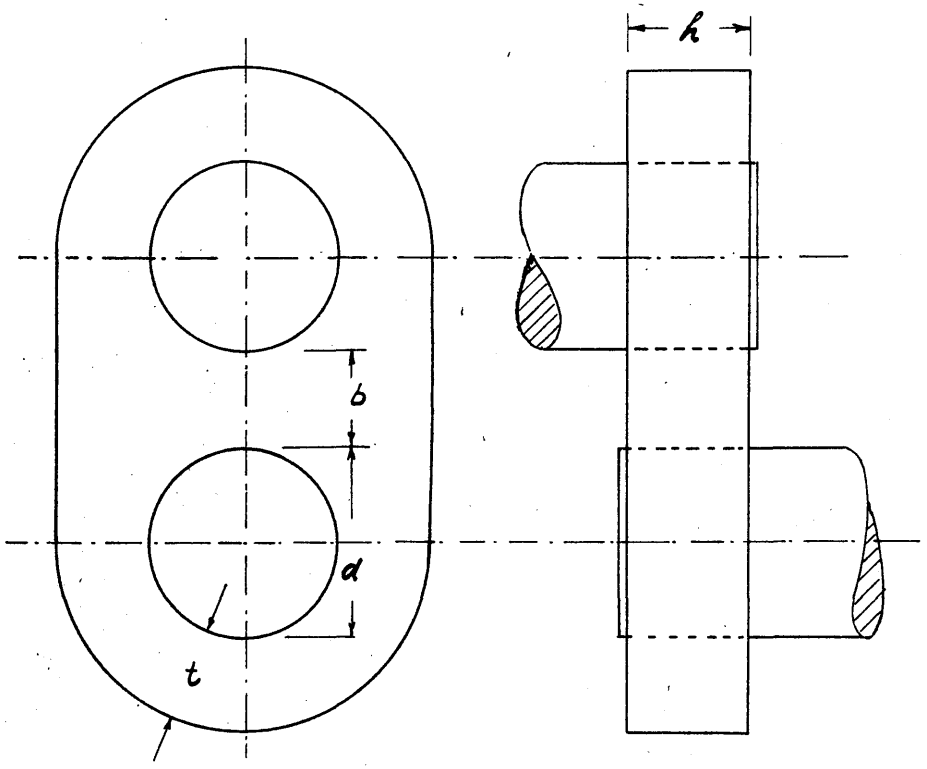

WEB SCANTLINGS

FIG. 11

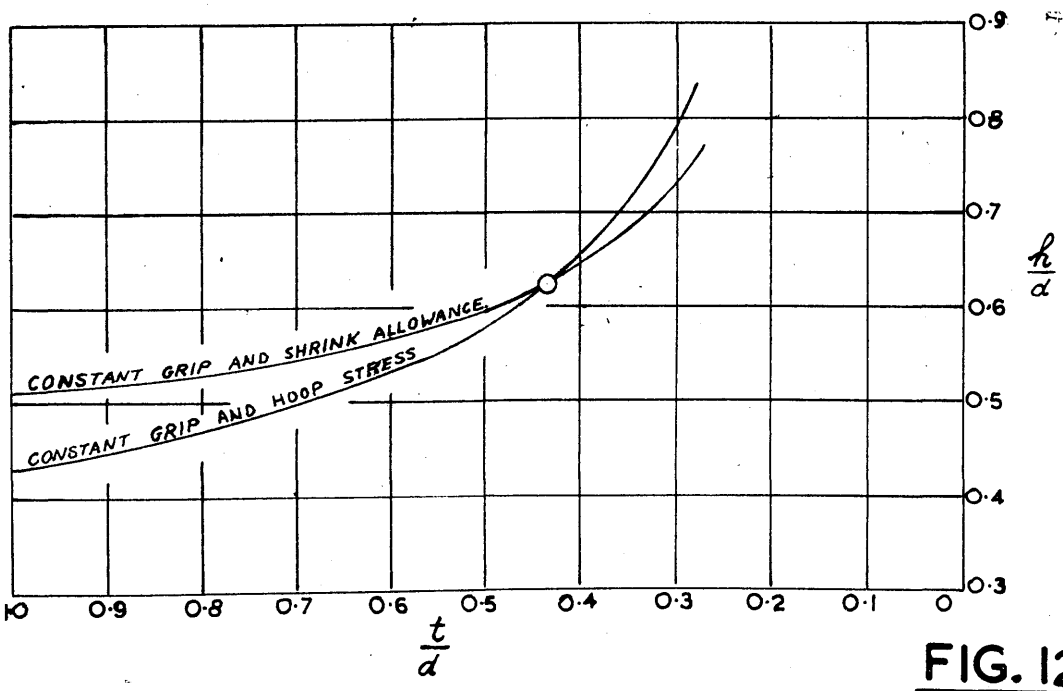

FIG. 12

Both curves represent relationships between h , d , and t derived from Elastic Thick Cylinder Theory applied to the circular ends of the web, relationships which contain a number of constants. By substitution of the recommended proportions, the constants are eliminated and hence the derived relationships are necessarily satisfied by the substituted values, and both curves necessarily intersect at these values. The derivation of the curves is, of course, given in Dorey's paper.

The basis for the recommended scantlings is, however, not mentioned. It would appear that the proportions are within limits, arbitrary. The form of both curves in Fig. 12 suggests that the ratio of h to t was selected from consideration of the asymptotic tendencies of the curves. The mean value of the points on each curve nearest to the origin of co-ordinates, corresponds very closely to the ratio $h/_t$ selected by Lloyd's. There does not appear to be any special significance in this, however, In the absence of other factors affecting proportions, it might be thought that the optimum ratio of h to t should correspond to minimum volume of material, from considerations of economy. The volume is very approximately proportional to ht^2 and since the hyperbolic shape of the curves indicates that ht is approximately constant, some economy would result from decreasing t and increasing h . The precise ratio for minimum volume could be evaluated.

Having selected the ratio $h/_t$, the values in terms of shaft diameter are still arbitrary. These values are fixed by the required area of grip, and are therefore empirical. Using a coefficient of friction of 0.2 , Dorey shows that the interface pressure must be at least equal to the torsional shear stress in the shaft. Lloyds proportions give on this basis, a factor of safety which varies with the fit allowance and the working stress of the shaft.

(b) Fit Allowance.

Using Thick Cylinder theory and the Haigh criterion of failure, the required tensile test-piece strength for varying fit allowances was tabulated. It was shown that for 28 - 32 ton mild steel the fit allowance should not exceed 1.25 mils. This takes no account of the stress concentration at the bridge-piece between the two pins.

(c) Stresses at Bridge-Piece.

The combined effect of pin and journal on the stress between the holes in the web was shown by a family of curves for varying thickness of bridge. The derivation of these was not given, but appears to be as shown in Fig. 13. The maximum pressure and hoop stress obtained by this method do not agree well with photo-elastic values, the discrepancy increasing as the width is reduced.

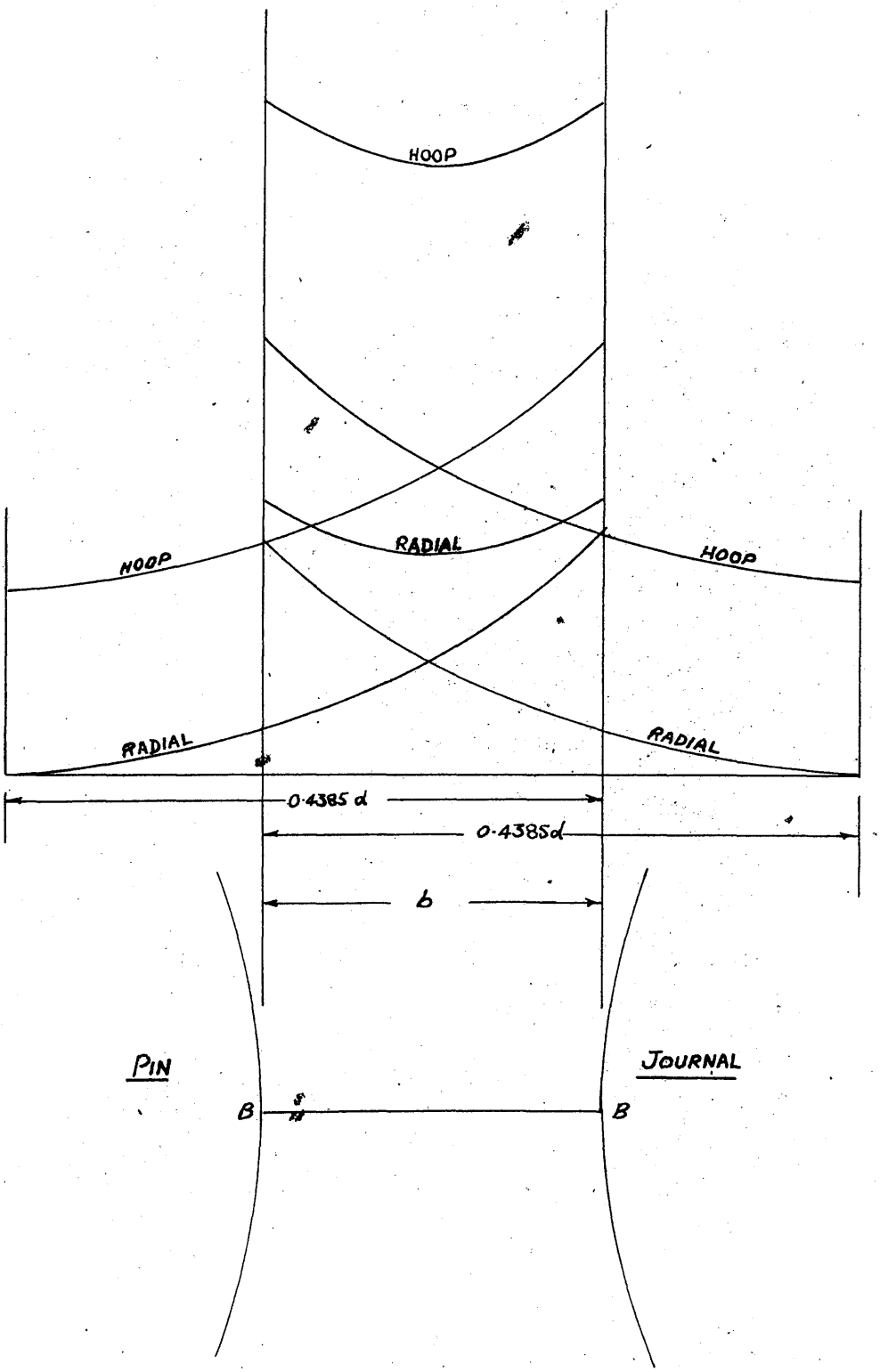

SUPERPOSITION OF STRESS AT BRIDGE PIECE

FIG. 13

It was recognised by Dorey that overstrain would occur at the fit allowances generally used, but no serious consequences were envisaged.

(d) Dowel Pins.

The practice of fitting dowels in the grip after shrinking, as a precautionary measure, was not discouraged so long as care was taken not to separate the grip surfaces by excessive dowel pressure. It was thought that drilling the dowel holes would not relieve the grip to any extent on account of the circumferential friction tending to prevent any general redistribution of stress. This may or may not be the case. The precise grip conditions in the presence of dowels is highly complex.

(e) Web Materials.

The use of good quality steel is recommended in order to avoid excessive overstrain.

C. Photo-Elastic Analysis.

The distribution of stress in a transparent photo-elastic model of a crank-web was investigated by Coker and Levi (3). Two closely-adjacent holes, symmetrically positioned on the long centre-line of a rectangular plate, were expanded radially, the resulting two-dimensional stress pattern being determined for three widths of the bridge between the holes.

The photoelastic pattern showed that the corners of the rectangle were practically free from stress, the isochromatics being circular and concentric with the holes, round the outer half of each hole. The shape can thus be compared with a crank web having semi-circular ends and straight sides, tangential to the end semi-circles, a shape very commonly used.

In each case the highest stresses occurred in the bridge between the holes, the magnitude of both radial and hoop stress increasing as the thickness of bridge was decreased. The distribution across the bridge was similar to that shown in Dorey's paper (9) , obtained from the superposition of two Lamé systems, but the magnitudes were different. Fig. 14 shows the variation of both principal stresses with bridge thickness. The values given by Dorey's method are also shown. Stresses are given as ratios, the basis of comparison being the average interface pressure shown in Coker's paper with b = 0.5d.

In comparing relative magnitudes of principal stresses obtained by photo-elastic methods, it should be borne in mind that the isochromatic or fringe pattern shows variations of principal stress difference. The magnitude of this quantity at any point is estimated from a known value at one point and from the fringe sensitivity of the material, determined experimentally. The sum of the principal stresses can be found by a number of methods, the one used in this paper being by measure-

ment of lateral strain in the thickness of the plate, given as 0.186 inches. Measurements of this order of magnitude require extreme care, and the possibility of substantial experimental errors in both the sum and the difference of principal stresses cannot be overlooked. Without considerable practical experience of the technique it is not possible to estimate the experimental errors, but the distribution of stress on the transverse centre-line of the plate, shown in this paper, fails to satisfy the essential equilibrium requirement.

The peripheral distribution of circumferential and radial stress adjacent to the bores is shown in Fig. 15. If the interface pressure is distributed as shown, the relative magnitudes on each side of the transverse centre line of the hole must be modified in order to maintain equilibrium of the pin. The increase in pressure towards the outside quarter points is probably due to the square corners of the plate, and would not be expected to occur in the oval web shape. The decrease at the inner quarter points is a feature of this type of stress system.

$f = \frac{\text{STRESS AT BRIDGE}}{\text{INTERFACE PRESSURE}}$

o RADIAL STRESS } COKER
□ HOOP STRESS }

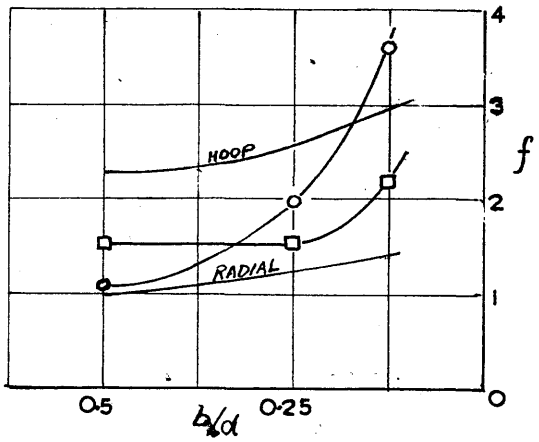

MAXIMUM STRESSES AT BRIDGE PIECE

FIG. 14

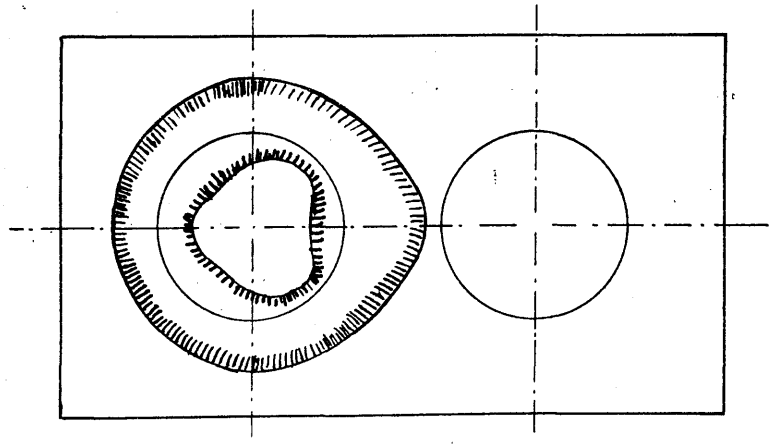

RADIAL AND HOOP STRESS ROUND PINS — COKER

FIG. 15

5. SUMMARY AND CONCLUSIONS.

A. Interference Fits.

(a) Fit Allowance.

(i) The experiments of Russell and Shannon on force-fits indicated that the maximum grip occurred at a value of fit allowance corresponding to elastic failure based on the Haigh criterion and simple thick cylinder theory. In view of the experimental evidence that the hollow element was considerably overstrained at this fit allowance, the association of the pressure conditions with elastic theory is misleading.

(ii) In none of the papers reviewed has any attempt been made to analyse the pressure and stress conditions in assemblies overstrained by excessive fit allowances.

(iii) There is ample evidence in Russell's later work that the stress conditions in temperature fits and force-fits with the same fit allowance are not identical.

(iv) No experimental evidence of the effect of varying the fit allowance in any type of shrink- or expansion-fitted assembly has been published.

(b) Grip Strength.

(i) Russell's investigations into the influence of film conditions on the grip of assemblies have demonstrated that the

friction grip is highly sensitive to variations in the adsorbed primary film, and that time has an important influence on the load required to separate assemblies. It is possible that other variables which were not investigated have an equally important influence.

(ii) The results of experiments in which interface pressures are deduced from stripping loads, should be regarded with caution on account of the variable nature of friction grip, even under closely controlled conditions.

(c) Static Loading of Assemblies.

(i) It is clear from Russell's work that damage occurs with the plug either entering or leaving the ring during force-fitting or stripping. It is possible that similar damage occurs in stripping a shrink-fit by axial displacement.

(ii) Local grip failure in shrink-fits at low torque is mentioned in Baugher's work. This is possibly due to local overstrain and not to relative movement of the surfaces.

(iii) If either of the effects (i) or (ii) above occur, measurements of permanent set in the hollow element will not correspond directly to the shrink-fit pressure, owing to the additional overstrain caused by separation of the assembly.

(d) Dynamic Loading of Assemblies.

The very meagre evidence of the behaviour of assemblies

under pulsating bending loads, suggest that a serious loss of fit occurs after a large number of reversals. The grip strength under static loading may be relatively unimportant in assemblies which are subjected to cyclic force actions.

(e) Axial Grip.

The prevention of free axial straining which necessarily occurs during the assembly of shrink- and expansion-fits has not previously been included in calculations of pressure. In a long assembly the fit is increased by about 40% if no axial slip occurs. This may be regarded as a maximum value, the actual value being dependent on the coefficient of friction, and on the length of the assembly.

(f) Temperature Effect.

No reference has been found in any paper reviewed, to the change of elastic constants with temperature in shrink- and expansion-fits.

B. Thick Cylinders.

(a) Experimental.

(i) Cook's experiments on carefully prepared mild steel tubes under pressure indicate that the upper yield point phenomenon exhibited by mild steel in tension can be observed in complex

stress systems. The values are not directly comparable.

(ii) Macrae's experiments with gun-steel cylinders, the material of which had tensile properties similar to mild steel, gave no indication that the yield stress in the cylinders was higher than the lower yield stress of the tensile test.

(iii) It is concluded that the elevation of yield point results from careful preparation and annealing of specimens for both tensile and cylinder experiments. It would not be expected to occur in shrink-fits, but the evidence is insufficient to make this conclusion reliable.

(b) Theoretical.

It is possible to derive theoretical relationships for the stresses and strains in an overstrained cylinder if certain assumptions are made. In the absence of experimental evidence theories based on fewest assumptions must be regarded as the most accurate.

C. Built Crankshafts.

(i) A photo-elastic analysis of the general pattern of stress in a perforated plate, similar in shape to a crank web, showed the presence of high stresses between the two holes. The accuracy of the analysis was not high, as the results indicated a lack of essential equilibrium on at least two

sections.

(ii) With the above exception there is no published theoretical or experimental evidence of the type of stress system in crankshafts resulting from the method of assembly.

(iii) Present design is based on established practice; the influence of various factors affecting the shrink-fitted assembly is still a matter of opinion and conjecture.

PART II

THEORETICAL WORK.

1. DISCUSSION OF THE PROBLEM.

In almost every practical application of shrink-fitting two elements, the mating surfaces of both elements at which the friction grip is developed are cylindrical. It may be that some advantage could be gained by modifying the shape of the grip surface by, for example, axial splining or circumferential helical grooving of the basic cylindrical shape, but attention will be confined, in this investigation, to the cylindrical grip.

In a plane perpendicular to the cylinder axis the profile of the mating surfaces is circular. The stress system in this plane is radically simplified if the other boundaries of the elements are concentric circles, and if the boundaries and stress system are assumed invariant in the direction of the cylinder axis. The case is referred to as rotationally symmetrical, and approximates to the conditions in a number of practical assemblies.

The stress system in the built crankshaft results from two adjacent assemblies. Complete rotational symmetry does not exist, but by St. Venant's principal the stress system at the outside semi-circular parts of the web remote from the bridge may be regarded as approximately rotationally-symmetrical, and due to the adjacent shrink only.

The rotationally symmetrical stress system is the simplest case of the shrink-fit problem. It is therefore convenient to examine this case in some detail, before proceeding to the more general web shape. All the features of the simple case will be present in the crankshaft assembly, together with the other more complex features, due to what may be termed the "shape-factor".

(a) Rotational Symmetry.

(i) Axial Variations.

Previous investigators have assumed that the stress system could be calculated without appreciable error by the Lamé equations. These well-known equations are applicable to conditions of either plane stress or plane strain, the former being assumed for shrink-fits. This is, at best, a fair approximation, as shrinkage in the axial direction induces axial shearing stresses at the interface, and therefore normal and shearing stresses on the cross-section. The boundary loading and deformation are interdependent, as the only necessary conditions are continuity of stress and deformation at the mating surfaces. It is therefore necessary to set up three-dimensional stress and strain relationships for both parts of the assembly and obtain a simultaneous solution, based only on the discrepancy in free size. This is not yet possible. One set of boundary conditions (either stress or deformation) must

be assumed, and the compatibility of the other set examined.

Three-Dimensional solutions for elastic stresses in solids of revolution are not easily derived, and in view of the indeterminate nature of the boundary conditions (axial shrinkage may not be entirely prevented) it does not appear to be worthwhile to develop this rigorous approach.

An overestimate of the effect of axial shrinkage may be obtained by assuming that the shrinkage is entirely prevented and that the stress system consequent on this deformation is a uniformly distributed axial tension and compression in the female and male elements respectively. This is equivalent to Goodier's (11) assumption of a long cylinder, in which the friction preventing axial shrinkage was confined to the ends, and therefore bending and shearing stresses in any section of the cylinder wall near the middle of the grip were of a low order. The derivation given below is not restricted to very thick or very thin cylinders necessary in Goodier's analysis.

A Lamé stress system for the cross-section of the grip is not incompatible with uniform tension or compression in the axial direction, since a condition of plane strain exists. The magnitude of stress is increased, however.

(ii) Overstrain.

The restriction of plane strain in the cylinder cross-

section allows the analysis of stress conditions to be extended to include the effects of fit allowances causing overstrain. From the section concerned with overstrained cylinders in Part I, it will be noted that the three-dimensional aspect cannot be ignored. The strains in the plane of the cross-section are functions of the axial stress system consequent on overstrain; and are therefore functions of the end load on the cylinder. For this reason the effect of axial shrinkage must be investigated before the effect of overstraining the cylinder, as the relationship of interface pressure to bore deformation in the plastic condition is a function of the axial stress condition. The shrink-fit corresponds neither to open nor to closed end conditions but to an end condition which, with the maximum axial effect discussed in (i) above, is equivalent to an end load of double the magnitude of the closed-cylinder end load.

(iii) Thermal Stressing.

The fitting process involves heating the female part of the assembly to a temperature in excess of that corresponding to a bore strain equal to the fit allowance. The excess of temperature is necessary for practical reasons and the amount is incalculable.

Changes of mean temperature must necessarily be accompanied by thermal gradients, and therefore by stress systems.

These are unimportant providing the magnitudes are such that elastic conditions are maintained, but the maximum rate of heating compatible with this is usually indeterminate. Furthermore the rate of cooling immediately after assembly cannot be controlled, as the rate of heat transfer from female to male element is determined by the conductivity for the material and the intersurface transfer coefficient only. The evidence presented in Part III of this thesis indicates that thermal stressing is an important feature of shrink-fitting.

During the transfer of heat after assembly the thermal stresses are accompanied by a build-up of boundary stress loading. Without making an investigation of this transient stress system it is impossible to assess the importance. Timoshenko (40) shows that with steady heat flow across the wall of a long cylinder, the axial and circumferential stress at the bore are equal in magnitude, and tensile for heat flow inwards. The stresses are therefore of like kind to those set up by prevention of shrinkage. For fits in which plastic deformation occurs, an excess of temperature, and therefore temperature gradient, is present when overstrain begins. The stress system in which the overstrain is propagated is complex

No account of thermal stressing has been taken in this theoretical investigation, as the effect clearly necessitates a further investigation of considerable magnitude.

(iv) Temperature Change of Elastic Properties.

The temperature changes in shrink-fitting are accompanied by changes in the values of elastic constants and limits of elasticity. The changes are like the constants themselves, empirical, and little data is available for reference. Indeed, it is doubtful whether comparative variations selected from published data, instead of from actual tests, would be more reliable than say, values of Young's Modulus. In experimental work it is usual to measure the elastic constants at room temperature by tensile tests of representative material but temperature variations require more elaborate test apparatus and are rarely measured.

The temperature at which thermal equilibrium is attained, is dependent on the excess of temperature necessary to give adequate clearance to the male element during the fitting. When the axial length of fit is large, for example in the case of a tail shaft liner, very large clearances are necessary for the assembly, and the amount of heat received by the shaft before the fit is taken up is considerable. The fit allowance is therefore only a guide to the temperature of the material when thermal equilibrium is attained. The effect of changing elastic constants will be examined later in this Part.

(b) Crank Web Shape.

(i) Boundary Condition.

In the absence of rotational symmetry, the stress system cannot be derived without making assumptions regarding the boundary loading. A condition of uniform radial pressure at the interface does not, in general, result in a circular deformation of the profile of the hollow part and hence the deformations of the two parts are not compatible. It will be assumed that the male part is a solid cylinder; there is no complication in the case where the crank pin and journal are bored for oil-ways or lightness, providing the hole in concentric with the grip surface.

Assuming that the conditions approximate to plane stress, a further assumption is necessary regarding the circumferential distribution of stress. An infinite number of self-equilibrating systems of radial pressure are possible, and a further infinity of systems can result from circumferential friction drag. Having selected a system satisfying the compatibility of deformations, the difficulty of formally integrating the elastic differential equations of plane stress remains.

As a solution of stress components is obtained for a particular stress field, the shape selected for examination should

be one which is commonly used in built crankshafts. The oval web shape in Fig. 11 is commonplace but the boundary is discontinuous in the first and higher derivatives and cannot therefore be represented in closed form by any plane co-ordinate system.

The Relaxation Methods developed by Professor Southwell are admirably suited to problems in which difficulty with boundary discontinuities is encountered and a solution by these methods is presented in Section 5 below.

(ii) Axes of Symmetry.

The web shape selected has two geometrical axis symmetry. The stress system will be symmetrical about the transverse axis only if the fit allowance on both pins is identical and if the deformations are entirely elastic. The restriction of identical allowances is not serious, this being the usual practise. If the allowances are not equal, a different system results from each combination, and no general solution is possible.

When conditions of overstrain are present, the symmetry can be preserved only if the overstrain occurs at the same instant of time in both fits. The time restriction is necessary with inelastic stress analysis, in which the sequence of events must be observed. It is doubtful whether symmetry in conditions of overstrain can be realised in practice.

In most cases after one pin is fitted the web is reheated for the other shrink-fit. When both fits made with one heat, there is necessarily a short time delay between entry of pin and journal. Overstrain will occur at the pin which was fitted earlier and will modify the stress system in the process of being set up by the second pin, so that a different configuration of plastic region will result.

(iii) Stresses at End of Web.

It was stated earlier that the plane stress distribution at the semi-circular end portions of the web might approximate to simple thick cylinder conditions over a limited range of rotation, being remote from the influence of the other pin. This is the case only if the hoop stress resultant force at the bridge is equal in magnitude to half of the bursting force due to pressure in both bores, or the hoop resultant force at each end section is half of the bursting force in one bore, as the Lamé distribution necessitates.

If the requisite force is not carried by the bridge, then equilibrium dictates that the end portions carry a tensile load in excess of the Lamé resultant and that, in addition, bending actions tending to reduce the curvature are set up, thereby increasing the hoop tensile stress at the bore.

In these circumstances, application of St. Venant's principle is unsound.

(iv) Ring Theory Applied to Web Shape.

The considerations discussed in sub-section (a) above, apply also to the web shape. It is not possible, however, to estimate the effect of axial friction, overstrain, and thermal stress, with reasonable accuracy. Qualitatively, these effects should show the same tendencies in both types of assembly. At present, only experimental work can provide a sound correlation.

2. AXIAL SHRINKAGE.

At the time that the surfaces come into contact in the shrinking process, the thermal strain in the ring, measured relative to the thermal strain datum of plug temperature, is equal to the fit allowance. The temperature of each part is assumed to be uniform throughout, and therefore no thermal stresses are present. During the return to thermal equilibrium it will be assumed that no slip occurs between the fitted surfaces and points initially in contact remain in contact. Therefore the superficial strain difference at every point in every direction is at all time equal to the initial strain difference, that is, equal to the fit allowance.

After thermal equilibrium is restored, the strains at the interface may be related by the following two independent equations.

$$\Delta = (e_\theta)_R - (e_\theta)_P = (e_z)_R - (e_z)_P \quad \text{----------(16)}$$

where suffices R , P refer to the ring and plug elements of the fit respectively.

If the assembly is long, plane cross sections remain plane except near the ends (this is a necessary physical condition) and a condition of plane strain may be assumed, with the principal axes of stress and strain in the directions of the co-ordinates.

The strains in (16) may be expressed in terms of the

principal stresses as follows:

$$E\Delta = (p_\theta - \sigma \overline{p_z + p_r})_R - (p_\theta - \sigma \overline{p_z + p_r})_P \quad \text{------(17)}$$

$$E\Delta = (p_z - \sigma \overline{p_r + p_\theta})_R - (p_z - \sigma \overline{p_r + p_\theta})_P \quad \text{------(18)}$$

the ring being of the same material as the plug, and the usual $+^{ve}$ tensile convention of stress and strain being observed.

Axial equilibrium of the assembly requires that

$$\int_1^k (p_z)_R \, y \, dy = - \int_0^1 (p_z)_P \, y \, dy$$

If p_z = constant over the cross section, then

$$(k^2 - 1)(p_z)_R = - (p_z)_P \quad \text{----------(19)}$$

The radial and hoop stresses at the interface may be expressed in terms of the interface pressure P according to the Lamé equations

$$(p_r)_R = (p_r)_P = (p_\theta)_P = - P \quad \text{----------(20)}$$

$$(p_\theta)_R = + \frac{k^2 + 1}{k^2 - 1} P \quad \text{----------(21)}$$

Substituting (19) (20) and (21) into (18) and solving for $(p_z)_R$

$$(p_z)_R = \frac{E\Delta}{k^2} + \frac{2\sigma P}{k^2 - 1} \quad \text{----------(22)}$$

Substituting (19) (20) (21) and (22) into (17)

$$E\Delta = (1 - \sigma) \frac{2k^2}{k^2 - 1} \cdot P \qquad \text{----------(23)}$$

The corresponding expression derived from the usual assumption of plane stress, is

$$E\Delta = \frac{2k^2}{k^2 - 1} \cdot P \qquad \text{----------(24)}$$

(23) and (24) show that the assumption of plane strain, with no axial slip, leads to a theoretical interface pressure $\frac{1}{1 - \sigma}$ times that obtained on the assumption of plane stress.

It may be shown that

	Ring	Plug
e_z	$+ \frac{\Delta}{k^2}$	$- (k^2 - 1) \frac{\Delta}{k^2}$
p_z	$+ \frac{2P}{k^2 - 1}$	$- 2P$

$$\text{end load} = 2\pi r_1^2 \cdot \int_1^k (p_z)_R \, y \, dy = 2\pi r_1^2 \cdot \int_0^1 (p_z)_P \, y \, dy = 2\pi r_1^2 \cdot P \qquad (25)$$

For a closed cylinder subjected to internal pressure P , the end load is equal to $\pi r_1^2 P$; the axial grip load is therefore twice the closed-cylinder end load. This is important when inelastic strains are induced, as the relationship of bore strain to internal pressure depends on the axial stress in the cylinder.

The identical increase in interface pressure was derived by Goodier (11), using the Duhamel equations for thermal stresses. The analysis required that the cylinder be either very thick or very thin, compared with the plug diameter; a condition of zero axial strain in the ring was found in the former case. This follows from

$$(e_z)_R = \frac{\Delta}{k^2} \longrightarrow 0 , \quad k \longrightarrow \infty$$

For a thin cylinder

$$(e_z)_R \longrightarrow \Delta , \quad k \longrightarrow 1$$

Goodier's analysis showed that the axial friction drag was maximum at the ends and diminished rapidly with axial distance into the grip. For distances in excess of the pin diameter the friction was of a low order. With the usual short assemblies, the condition of plane strain would not be attained. The above analysis shows the maximum possible effect; the actual effect can only be found experimentally.

---

3. OVERSTRAINED CYLINDERS.

As shown above, prevention of free shrinkage in the axial direction has the effect of inducing a higher value of interface pressure than the value calculated on the plane stress asumption, and also of inducing a tensile end load on the hollow element, the maximum value of which is double the end load corresponding to the interface pressure acting on a closed-ended cylinder.

When the cylinder remains entirely elastic the interface pressure may be related explicitly to the fit allowance by transposing (23) and (24) above, in the two extreme cases of free axial shrinkage and of maximum friction drag in a long cylinder. The actual value will depend on the length of the assembly and on the friction grip of the surfaces.

In order to extend the analysis to overstrained conditions in the hollow element the two cases of zero and maximum end load must be developed. In this case, however, it is not practical to develop an explicit expression for interface pressure in terms of the fit allowance. Both may, however, be expressed in terms of the parameter n, the radius of overstrain.

In Part I the analytical work of Sopwith was discussed. His solution is free from the assumption of incompressibility and

from the consequence of the assumption that all stresses and strains cannot be continuous at the plastic boundary. In view of the experimental evidence by Cook that flow takes place in mild steel cylinders according to the Shear Stress Criterion when the cylinder is completely overstrained, Sopwith's solution is probably the best available. It is worthwhile, however, to examine the possibility of using the more approximate analysis based on incompressibility for the shrink-fit problem, as computation is considerably simplified, especially when comparing assemblies with varying k values.

Two cases are examined below. In the first case the solution is based on continuity of e_θ , e_r at the plastic boundary. The axial stress is then discontinuous. In the second case the axial stress is made continuous and in consequence the compatibility condition of e_θ , e_r is not satisfied. The bore strains in both cases are compared with those given by Sopwith's solution.

(a) Continuity of Strains.

The following assumptions are made.

(i) Constant Shear Stress in the plastic region

$$p_\theta - p_r = 2s = \text{constant}, \quad 1 < y < n \qquad \text{---------(26)}$$

(ii) s , e_θ , e_r continuous at $y = n$ ----------(27)

(iii) Plastic Stress Strain relationship

$$\frac{e_\theta - e_z}{p_\theta - p_z} \equiv \frac{e_z - e_r}{p_z - p_r} = \frac{e_f - e_\theta}{p_r - p_\theta} = \gamma , \quad 1 < y < n \quad --(28)$$

(iv) Plastic material incompressible

$$e_\theta + e_r + e_z = 0 \qquad ----------(29)$$

(v) Plane cross sections remain plane

$$e_z = \text{constant} \qquad ----------(30)$$

Radial equilibrium requires that

$$y \frac{dp_r}{dy} = p_\theta - p_r$$
$$= 2s \text{ , from (26)} \qquad ----------(31)$$

Integrating

$$p_r = 2s \log y + C$$
$$= 2s(1 + \log y) + C \qquad ----------(32)$$

In the elastic region the Lamé equations are

$$p_\theta = A \overset{+}{-} \frac{B}{r^2} \quad * \qquad ----------(33)$$

* The upper sign with the upper suffix.

A , B , C are constants given by conditions at $y = n$ and $= k$.

From (33) at $y = n$,

$$p_\theta - p_r = 2s = -\frac{2B}{n^2}$$

$$B = -Sn^2$$

and at $y = k$,

$$p_r = 0 = A - S\frac{n^2}{k^2}$$

$$A = +S\frac{n^2}{k^2}$$

Therefore in the elastic region

$$p_\theta = S n^2\left(\frac{1}{k^2} \pm \frac{1}{y^2}\right) , \quad n < y < k \qquad \text{----------(34)}$$

From (32) and (34) at $y = n$

$$(p_r)_n = s \log n^2 + C = S n^2 \left(\frac{1}{k^2} - \frac{1}{n^2}\right)$$

$$\therefore C = S\left(\frac{n^2}{k^2} - 1 - \log n^2\right)$$

Equations (32) then become

$$p_\theta = S\left(\log \frac{y^2}{n^2} + \frac{n^2}{k^2} \mp 1\right) \quad 1 < y < n \qquad \text{------(35)}$$

At $y = 1$, $p_r = -P$

$$P = S\left(\log n^2 - \frac{n^2}{k^2} + 1\right) \qquad \text{----------(36)}$$

From (28) ,

$$e_\theta - e_r = \gamma (p_\theta - p_r)$$

$$= 2 S \gamma$$

Therefore from (29) ,

$$e_{\frac{\theta}{r}} = -\tfrac{1}{2} e_z \pm S\gamma \ , \qquad \text{----------(37)}$$

For compatibility of e_θ , e_r

$$\frac{d}{dy}(e_\theta . y) = e_r \qquad \text{----------(38)}$$

i.e. $y \frac{de_\theta}{dy} = e_r - e_\theta = -2 S\gamma$,

Also from (37)

$\frac{de_\theta}{dy} = S \frac{d\gamma}{dy}$, e_z being constant over the cross section.

$\therefore \ y\frac{d\gamma}{dy} = -2\gamma$

Integrating

$$\gamma = \frac{D}{y^2} \qquad \text{----------(39)}$$

D is a constant found from the value of γ at $y = n$

At $y = n$, since e_θ , e_r are continuous,

$$\gamma = \frac{e_\theta - e_r}{p_\theta - p_r} = \frac{1}{E} \frac{(p_\theta - \sigma \overline{p_r + p_z} - p_r + \sigma \overline{p_\theta + p_z})}{p_\theta - p_r}$$

$$= \frac{1 + \sigma}{E}$$

$$\therefore \ \frac{1 + \sigma}{E} = \frac{D}{n^2}$$

or

$$\gamma = \frac{1+\sigma}{E}\,\frac{n^2}{y^2} \qquad \text{----------(40)}$$

The axial stress may now be expressed in terms of the axial strain e_z and functions of y in both regions, and evaluated by integrating over the cross section and equating to the appropriate end load.

Elastic Region.

$$p_z = \text{constant} = 2\sigma s\,\frac{n^2}{k^2} + Ee_z \qquad \text{----------(41)}$$

Plastic Region.

$$p_z = p_r + \frac{e_z - e_r}{\gamma}\,, \quad \text{from (28)}$$

Substituting (35) (37) (40)

$$p_z = s\left(\log\frac{y^2}{n^2} + \frac{n^2}{k^2}\right) + \frac{3E}{2(1+\sigma)}\,\frac{y^2}{n^2}\,e_z \qquad \text{--------(42)}$$

The discontinuity in p_z at $y = n$ is obvious from these equations.

For axial equilibrium

$$\int_1^n p_z\,\gamma\,dy + \int_n^k p_z\,y\,dy = 0\,,\ \frac{P}{2}\,,\ P$$

the appropriate value of the R.H.S. of the equation being selected from the end conditions. The expressions for p_z given by (41) (42) above are substituted in the first and

second terms of the L.H.S. and the integration carried out, e_z being constant with respect to y.

The following values of e_z are found:

(i) Open ends, zero and load

$$e_z = \frac{s}{E}\frac{n^2}{k^2}\frac{(k^2-n^2)(1-2\sigma)+(1-k^2/n^2)-\log n^2}{\frac{3}{4(1+\sigma)}\left(\frac{n^4-1}{n^2}\right)+k^2-n^2} \qquad \text{----(43)}$$

(ii) Closed ends, and load $= \frac{P}{2}$

$$e_z = \frac{s}{E}\frac{n^2}{k^2}\frac{(k^2-n^2)(1-2\sigma)}{\frac{3}{4(1+\sigma)}\left(\frac{n^4-1}{n^2}\right)+k^2-n^2} \qquad \text{----------(44)}$$

(iii) End load $= P$

$$e_z = \frac{s}{E}\frac{n^2}{k^2}\frac{(k^2-n^2)(1-2\sigma)-(1-k^2/n^2)+\log n^2}{\frac{3}{4(1+\sigma)}\left(\frac{n^4-1}{n^2}\right)+k^2-n^2} \qquad \text{---(45)}$$

The axial stress is then given by (40) and (41) and the strains in the plastic region by (37), using the appropriate value of e_z.

The strains of interest are the circumferential strains at the outside and bore, given by

$$(e_\theta)_k = 2\frac{s}{E}\frac{n^2}{k^2}(1-\sigma^2)-\sigma.e_z$$

$$(e_\theta)_1 = \frac{s}{E}n^2(1+\sigma)-\tfrac{1}{2}e_z \qquad \text{----------(46)}$$

(b) Continuity of Axial Stress.

With the same assumptions as in (a) above, the analysis is identical up to the point where particular values must be inserted in equation (39) to find the constant of integration D. Continuity of e_θ, e_r is replaced by continuity of p_z.

The constant is carried through to the point where equations analogous to (41) (42) are found for both regions and the values equated at $y = n$.

For the plastic region

$$p_z = p_r + \frac{e_z - e_r}{\gamma}$$

substituting (35) (37) and (39), at $y = n$

$$p_z = s\frac{n^2}{k^2} + \frac{1}{D}\cdot\frac{3}{2}\cdot e_z n^2$$

equating to $p_z = 2\sigma s\frac{n^2}{k^2} + E e_z$

$$D = \frac{3}{2}\,\frac{n^2 e_z}{E e_z - s(1-2\sigma)n^2/k^2}$$

and $$p_z = s\left(\log\frac{y^2}{n^2} - (1-2\sigma)\frac{y^2}{k^2} + \frac{n^2}{k^2}\right) + \frac{y^2}{n^2} E e_z \quad ---(47)$$

This replaces equation (42) above, (41) is, of course, unchanged. The expression for e_z, in this case is

$$e_z = \frac{s}{E}\left\{(1 - 2\sigma)\frac{n^2}{k^2} + m\,\frac{\log n^2 - n^2/k^2 + 1}{k^2 - \frac{n^4 + 1}{2n^2}}\right\} \text{-----(48)}$$

where m has the values -1 , 0 , $+1$ in the three end conditions corresponding to open, closed and double end load, respectively.

Equations (43) (44) (45) may be put in a similar form

$$e_z = \frac{s}{E}\left\{\frac{(1 - 2\sigma)\, n^2/k^2\,(k^2 - n^2) + m\,(\log n^2 - n^2/k^2 + 1)}{\frac{3}{4(1+\sigma)}\left(\frac{n^4 - 1}{n^2}\right) + k^2 - n^2}\right\} \text{(49)}$$

The result in the case of the closed ended cylinder, $m = 0$, is of interest. Equation (48) becomes

$$e_z = \frac{s}{E}(1 - 2\sigma)\frac{n^2}{k^2}$$

and therefore,

$$p_z = s\left(\log \frac{y^2}{n^2} + \frac{n^2}{k^2}\right) = \frac{p_\theta + p_r}{2} \qquad 1 < y < n$$

and $$p_z = s\frac{n^2}{k^2} = \frac{p_\theta + p_r}{2} \qquad n < y < k$$

This simple relationship of p_z to p_θ and p_r , suggested by Cook, is in good agreement with Sopwith's solution for closed ends.

In this case when $m = 0$ the constant D becomes infinite, i.e. the compatibility equation is not satisfied due

to the incompressibility assumption. The strains may be evaluated using equation (46) and the value of e_z given by (48). This is effectively a compromise between the discontinuities inherent in the assumptions. The result may be compared with Sopwith's solution for bore strain shown in Fig. 16. The curves given by equations in (a) and (b) above are practically identical, but the agreement with Sopwith's solution is poor. It may be concluded that neglect of compressibility in the plastic region leads to serious discrepancies in the bore strain, and therefore it is not possible to develop relationships capable of more rapid numerical computation without introducing appreciable errors. Fig. 16 suggests that compressibility might be neglected if the Sopwith curve corresponding to double end load were required. Equation (34) with $m = 0$, i.e. closed cylinder end load, could be used without serious error. This enables the computation to be rapidly carried out.

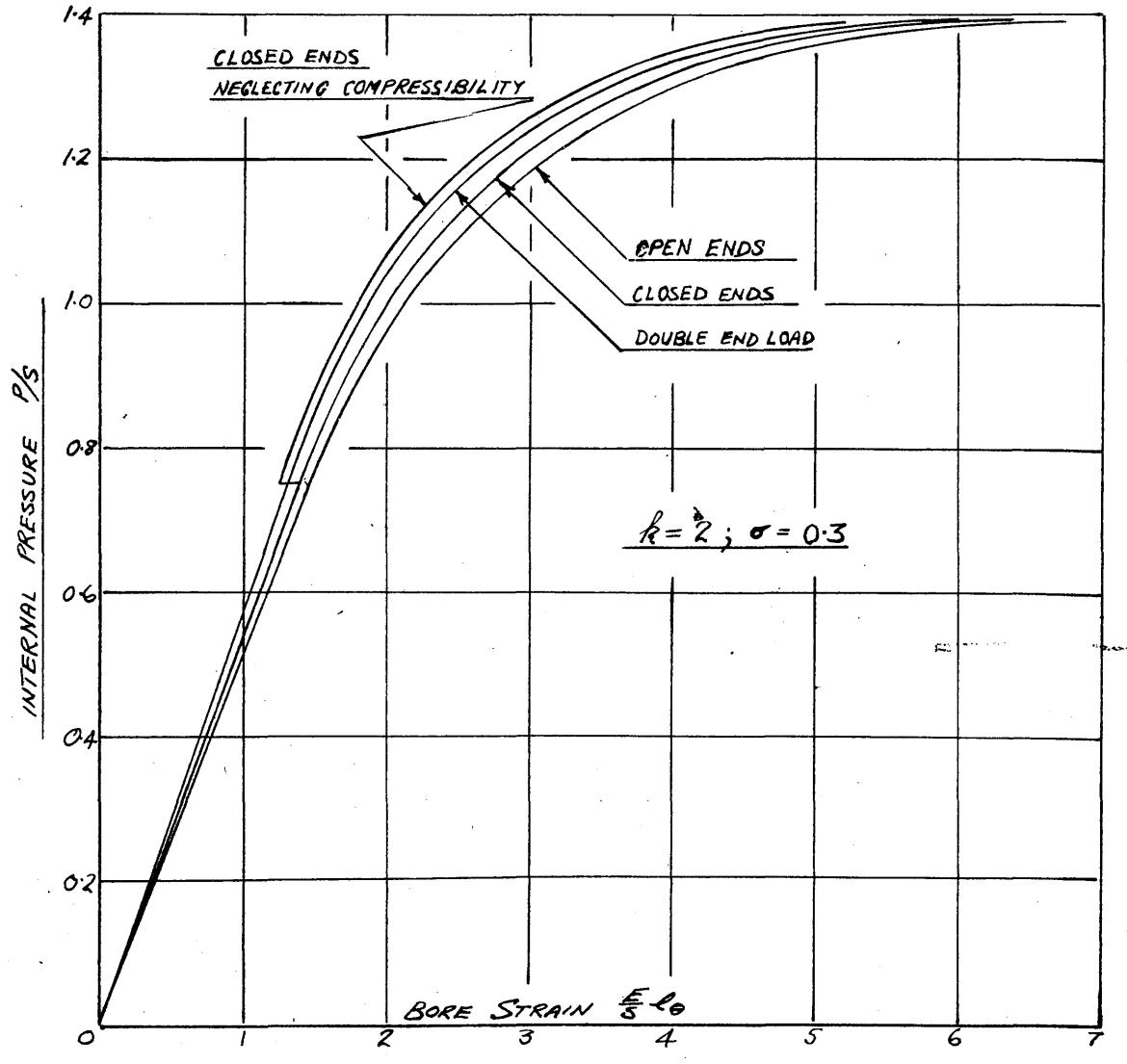

EFFECT OF END LOAD AND COMPRESSIBILITY

FIG. 16

4. TEMPERATURE CHANGE OF ELASTICITY.

For inelastic straining of the hollow element it is inconvenient to express the strains as functions of the bore pressure, but the radial depth of plastic flow may be used as a parameter in developing algebraic relationships for these quantities. Explicit relationships of interface pressure and strain for both elements of the fit may be shown graphically. In this way the pressure and fit allowance, which is the arithmetic sum of the bore circumferential strains of both elements, are easily related by a diagram of the type shown in Fig. 17. The bore strains for both parts are plotted against interface pressure to right and left of the vertical pressure axis and the fit allowance corresponding to any pressure value is the length of the horizontal line AB to the strain scale used for abscissa.

The pressure-strain relationship for the solid part may be taken as linear, as the maximum shear stress is always considerably less than that in the hollow part, and experimental evidence indicates that the solid part remains elastic at the pressures developed in shrink-fits.

The relationships developed in Section 3 above show that the strains are functions of the ratio of elastic constants $\frac{E}{s}$ for a given depth of plasticity, and that the pressure is a

function of s. The variations of these quantities when the ring is heated to fitting temperature necessitate different diagrams for different values of elastic constants, but this can be avoided by a non-dimensional plot of $\frac{P}{s}$ against $\frac{E}{s} e_\theta$ as shown in Fig. 18. The length of AB is now $\frac{E}{s}\Delta$, to the strain scale.

The maximum value of the quantity $\frac{E}{s}\Delta$ is the criterion which determines the furthest point from the origin on the strain curve for the hollow element, and hence the maximum depth of plasticity in the ring and the amount of permanent set produced. The value at the elevated temperature at which thermal equilibrium is attained in the shrinking process, is in excess of the value found by using the room temperature constants, and so a higher value of $\frac{P}{s}$ (though not necessarily of P), and greater permanent set, are produced by the increase in value of $\frac{E}{s}$ with rise in temperature, than would be indicated by the final value of P, or of grip strength if this were used to measure P. Conversely, the values of permanent set, measured after the assembly was separated, would indicate an incorrectly high value of pressure if the room temperature value of s were used in the calculation.

Little data is available on the variations of elastic constants with temperature. The results obtained by Lea and Crowther (19) for mild steel, (the chemical analysis was not

quoted) are plotted in Fig. 19 which may be used in conjunction with Fig. 18 to estimate the final pressure and strain conditions in the fit.

An approximation is necessary in arriving at the temperature at which thermal equilibrium is attained. As discussed in Section 1. above, an excess of temperature is given to the hollow part, the amount of the excess being variable, depending on the type of assembly. If this excess be neglected the temperature t above room temperature of the hollow part before assembly is given by

$$t = \frac{\Delta}{c}$$

where c = coefficient of linear expansion of the material.

During build-up of pressure the loss of heat by convection and radiation may be assumed negligible, compared with the transfer of heat to the cold plug, and the thermal equilibrium temperature t_e is given by

$$t_e = \frac{k^2 - 1}{k^2} t = \frac{k^2 - 1}{k^2} \frac{\Delta}{c}$$

the axial length of plug and ring being assumed equal. The values of t_e may be used in conjunction with Lea and Crowther's results to obtain Fig. 20 which shows the ratio $\frac{E'}{s'} \div \frac{E}{s}$ against Δ for varying k values, the dashes denoting the values at the elevated temperature. The assumed value of c is 11 millionths

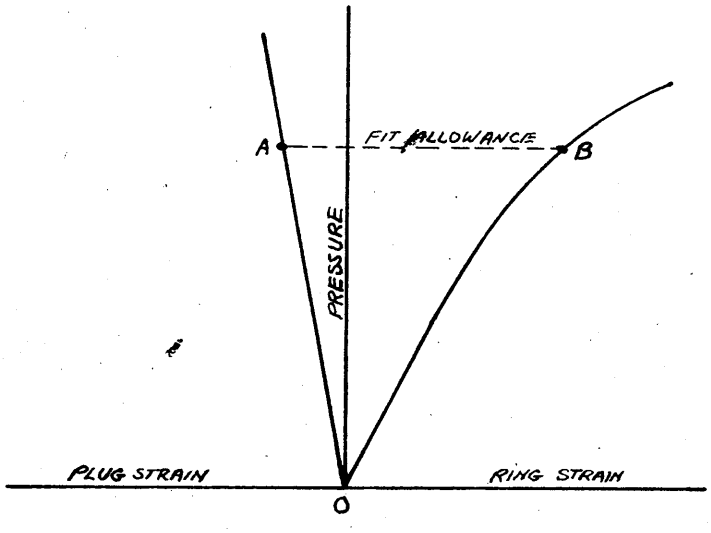
A
FIT ALLOWANCE
B
PRESSURE
PLUG STRAIN
RING STRAIN
O

FIG. 17

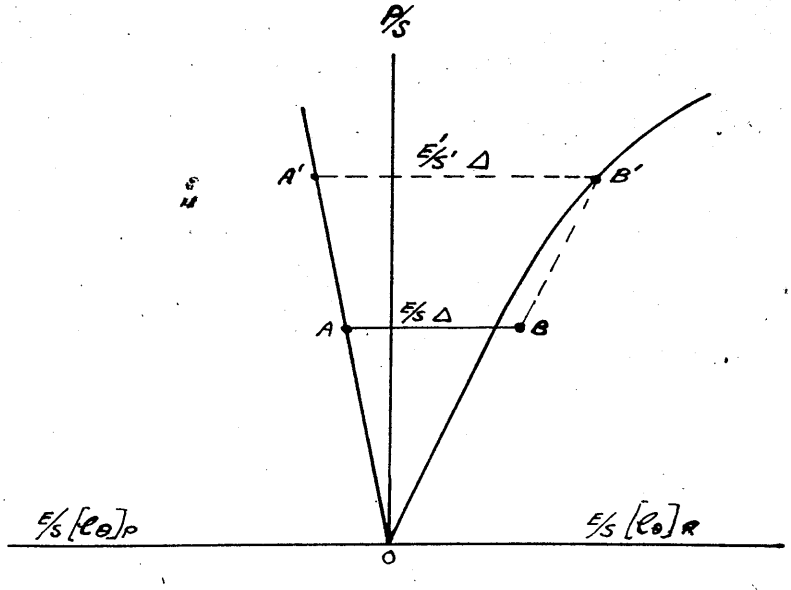
P/S
A'
E'/S' Δ
B'
A
E/S Δ
B
E/S [ℓθ]P
E/S [ℓθ]R
O

FIG. 18

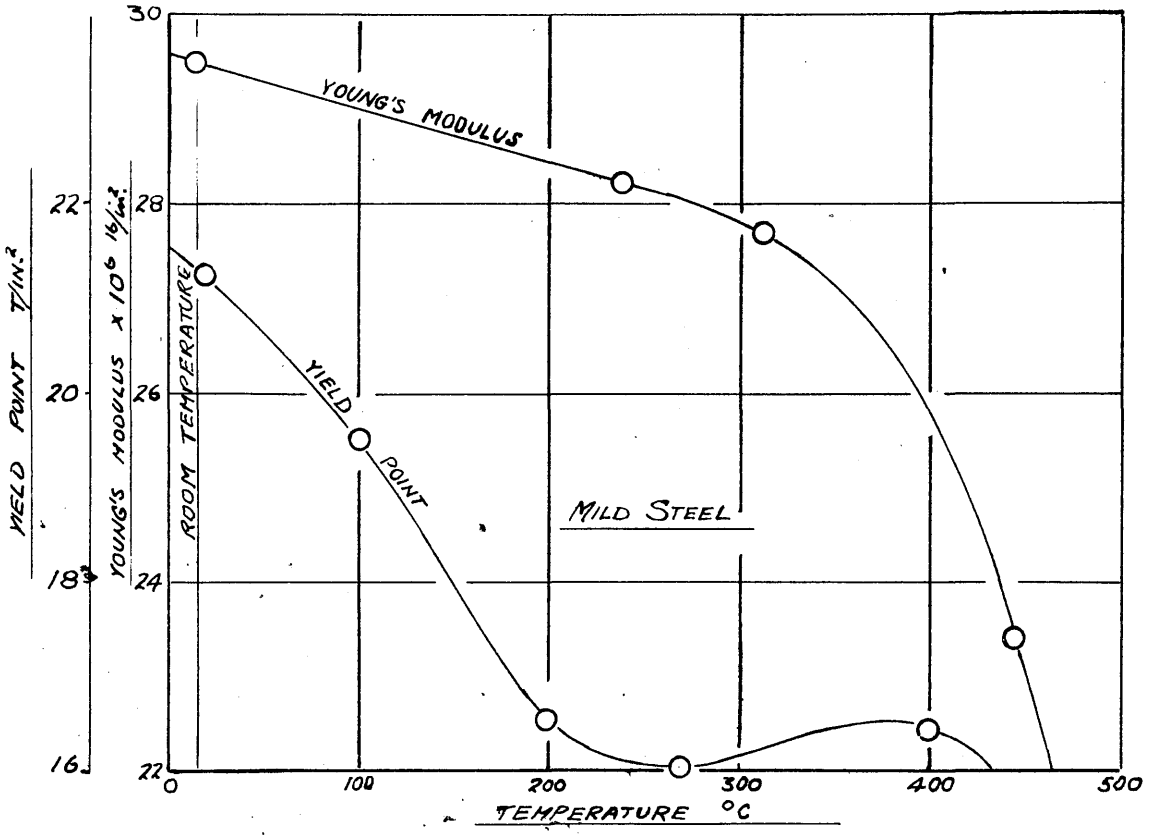

VARIATION OF ELASTIC CONSTANTS WITH TEMPERATURE
(LEA AND CROWTHER)

FIG. 19

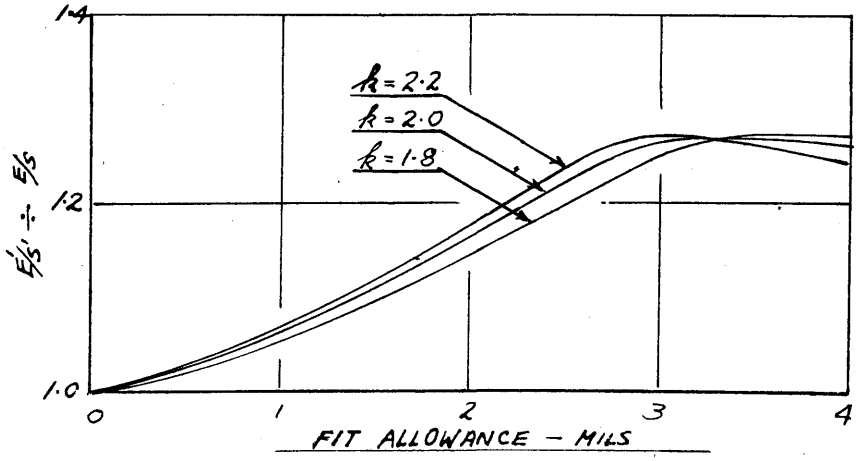

FIG. 20

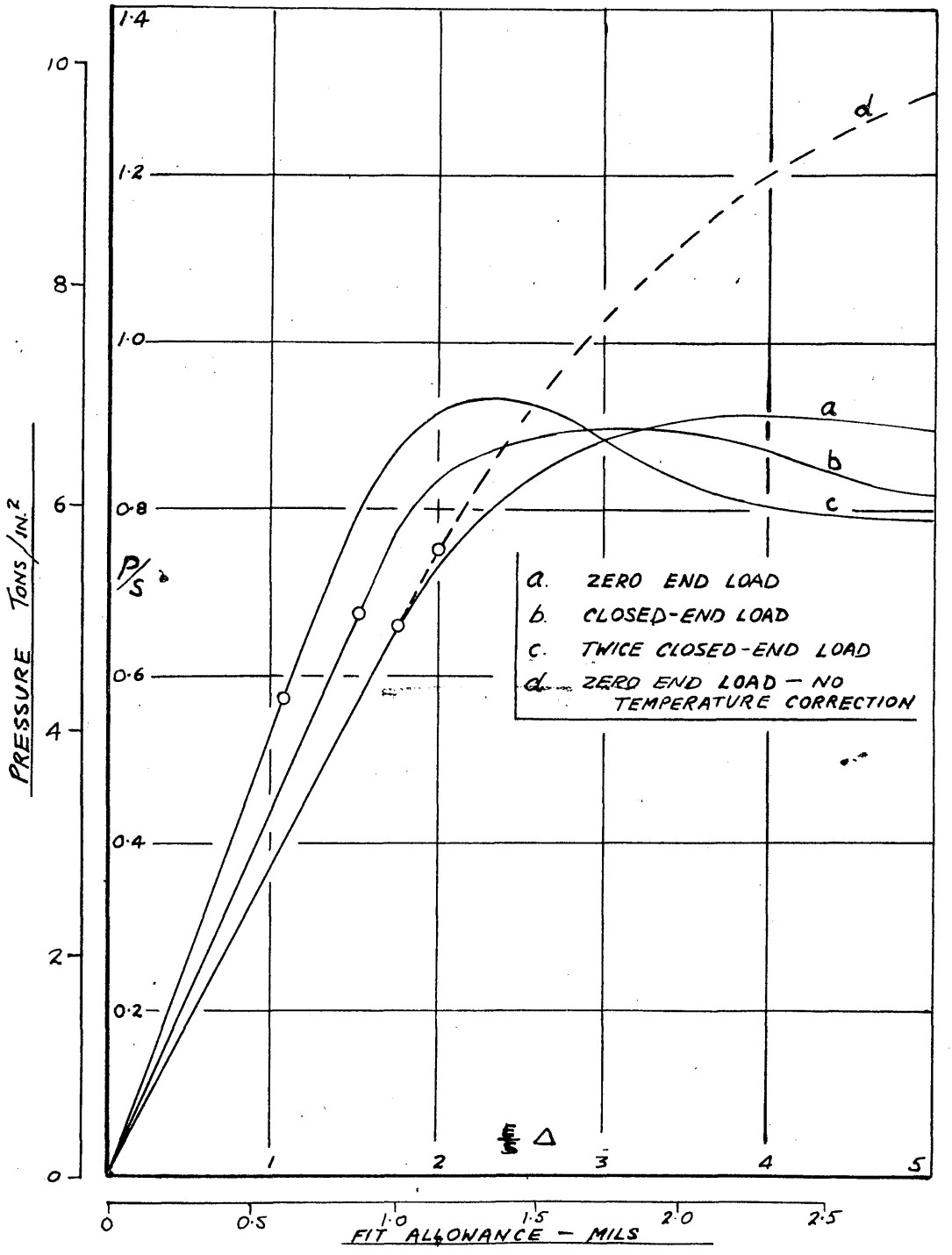

PRESSURE V FIT ALLOWANCE WITH END LOAD AND TEMPERATURE CORRECTIONS

FIG. 21

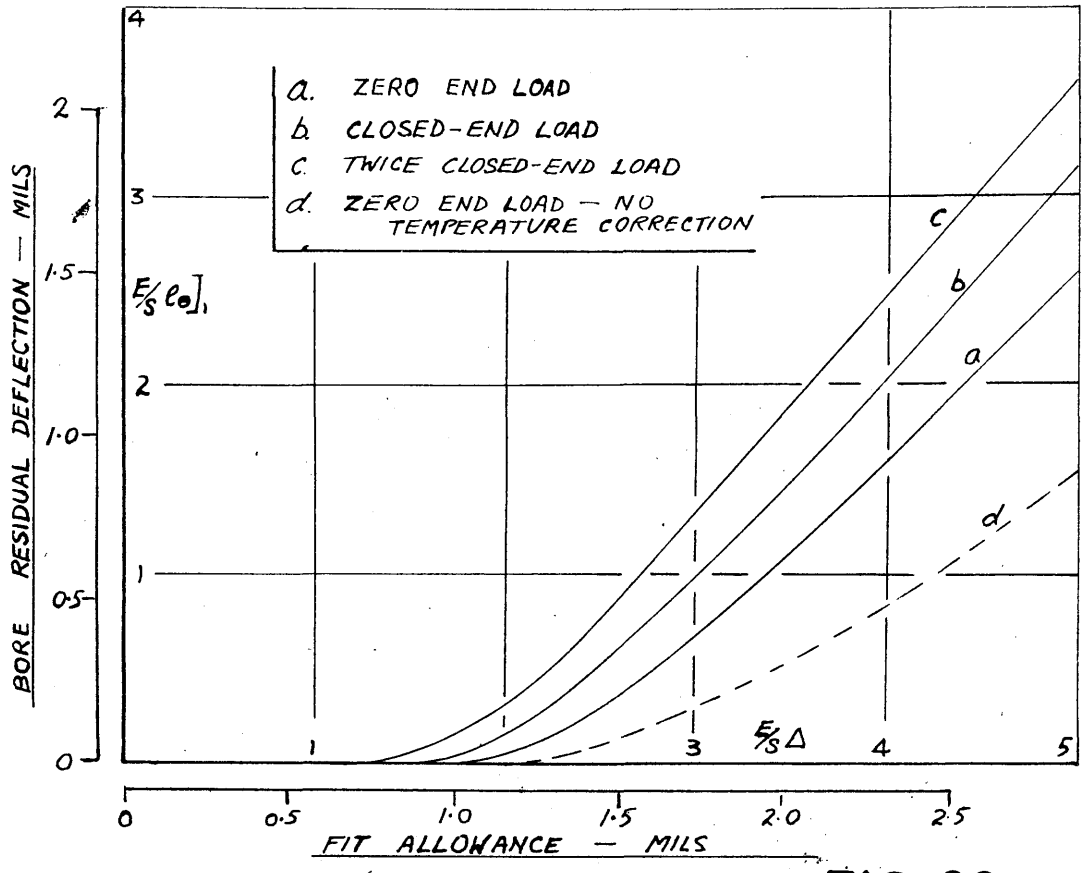
a. ZERO END LOAD
b. CLOSED-END LOAD
c. TWICE CLOSED-END LOAD
d. ZERO END LOAD — NO TEMPERATURE CORRECTION
BORE RESIDUAL DEFLECTION — MILS
E/S ℓθ]1
E/S Δ
FIT ALLOWANCE — MILS

FIG. 22

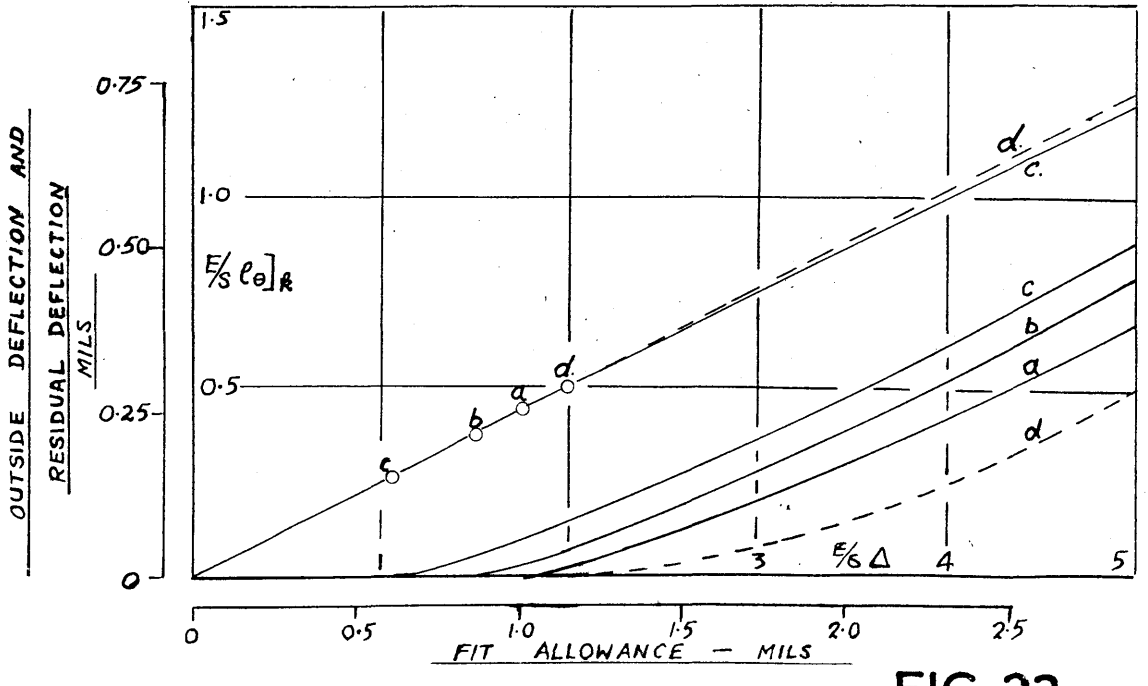
OUTSIDE DEFLECTION AND RESIDUAL DEFLECTION — MILS
E/S ℓθ]R
E/S Δ
FIT ALLOWANCE — MILS

FIG. 23

per ^{o}C , and room temperature, $15^{o}C$.

Using Fig. 20 the relationship of interface pressure fit allowance may be determined graphically. It is necessary to assume that elastic strains occur on reduction of overstrain pressure for the amount of reduction resulting from change of elastic constants. This has experimental support, as Macrae (24) showed that the outside diameter recovered elastically on release of autofrettage pressure, though the linear relationship was not maintained as the pressure approached zero.

Fig. 21 shows the relationship of interface pressure to fit allowance for full and zero axial grip, and for zero axial grip with no temperature effect in a ring and plug assembly, the ring diameter ratio being 2:1 and Poisson's Ratio 0.3. Non-dimensional scales, and scales for common values of Young's Modulus and Yield Shear Stress of 13000 T/in^2 and $7\frac{1}{2}$ T/in^2 are given.

The bore residual deflection, and the outside diametral deflections with the plug fitted and plug removed are shown in Figs. 22 and 23 respectively. Fig. 23 shows very clearly that the deflections with the plug fitted provide practically no indication of the state of pressure or overstrain in the cylinder. Curves a and b lie in the narrow zone between the two curves c and d shown.

In deriving the curves of residual deflection it was assumed that the cylinder recovered elastically for the complete removal of fit pressure. This is an approximation. Fig. 9 shows the effect of reversing the direction of shear stress in the overtensioned layers of the cylinders, which will behave inelastically as the pressure approaches zero. The loss of compressive elasticity will not be so serious as Macrae's tests showed, as mild steel exhibits a self-annealing tendency with time, and the cylinder may be expected to behave nearly elastically if the fit is not separated for a considerable time after assembly.

5. PLANE STRESS SYSTEM IN CRANK WEB SHAPE.

(a) Assumptions.

The stress system in a crank web due to the assembly of the crank and journal pins is, as in the simple ring-and-plug case, three-dimensional, due to the prevention of free axial shrinkage, and to lack of axial symmetry. For the relatively short length of grip common in built crankshafts, the effect of axial grip is likely to be confined to the vicinity of the gripping surfaces, and, as the web slab alone is almost invariably of constant shape in the direction of the shaft axis, the variation of stress in that direction is due only to the extensions of the pins beyond the slab faces. The effect of this is to cause a local increase in the interface pressure at the entry side of the pin, but the pressure may be assumed constant over the major part of the grip. With these qualifications, plane stress conditions in the web slab may be assumed.

The system can now be obtained for any given set of boundary conditions, on the assumption that only elastic actions occur. The boundary conditions are zero stress at the outside, but at the bores the stress and deformation are inter-dependent, and some assumption regarding the boundary loading must be made. Coker's photo-elastic analysis of a similar problem showed that

the bore radial pressure was non-uniform in the circumferential direction, but his results were inaccurate. In view of the other assumption necessary for a theoretical approach, a condition of uniform pressure of equal intensity in both bores of the web plate is a reasonable approximation to the boundary conditions in a problem of this type.

The differential equations of equilibrium and compatibility can now be formally integrated if the boundary profile can be expressed as a function of the selected co-ordinates. In the case of the crank web shape shown in Fig. 11 , the boundary shape is discontinuous, and the well-known Relaxation methods developed by Southwell (38) (39) are more convenient.

One further assumption must be made. The web plate is multiply-connected, and it is impossible to ensure that the displacements will be single-valued when using the Relaxation technique. Timoshenko (40) discusses multiply-connected bodies, and shows that the distribution of stress depends, in general, on Poisson's Ratio. The restriction vanishes if, as in this case, the forces on each boundary are in equilibrium. It is, however, necessary to make an assumption regarding the stress at one section connecting two boundaries, and simple thick cylinder conditions are assumed for the section BC shown in Fig. 26 . This is in good agreement with experimental results presented in Part III.

These assumptions are summarised below:

(i) Elastic stresses only are induced by the fitting of crank and journal pins.

(ii) The system is one of plane stress with no body forces, the stress planes being perpendicular to the axis of crank and journal pins.

(iii) Uniform and equal radial pressures are induced by the assembly process.

(iv) Simple thick cylinder stresses occur at radial sections on the long centre-line at the end of the web (Section BC , Fig. 26).

(b) Finite Difference Approximation.

The derivation of the differential equations of elasticity are found in any standard text-book on the Theory of Elasticity. In the case of plane stress or plane deformation with zero or constant body forces, the equilibrium and compatibility equations satisfy:

$$\left(\frac{\partial^2}{\partial x^2} + \frac{\partial^2}{\partial y^2}\right)(p_x + p_y) = 0$$

Introducing the Airy Stress Function ϕ , defined by

$$p_x = \frac{\partial^2 \phi}{\partial y^2} \; ; \; p_y = \frac{\partial^2 \phi}{\partial x^2} \; ; \; p_{xy} = \frac{\partial^2 \phi}{\partial x \partial y} \qquad \text{----------(50)}$$

then

$$\left(\frac{\partial^2}{\partial x^2} + \frac{\partial^2}{\partial y^2}\right)\left(\frac{\partial^2 \phi}{\partial x^2} + \frac{\partial^2 \phi}{\partial y^2}\right) = 0$$

or

$$\nabla^4 \phi = 0 \qquad \text{----------(51)}$$

where

$$\nabla^2 = \left(\frac{\partial^2}{\partial x^2} + \frac{\partial^2}{\partial y^2}\right)$$

In polar co-ordinates

$$\nabla^2 = \left(\frac{\partial^2}{\partial r^2} + \frac{1}{r} \cdot \frac{\partial}{\partial r} + \frac{1}{r^2} \cdot \frac{\partial^2}{\partial \theta^2}\right)$$

For the case of circular symmetry, derivatives with respect to θ vanish, and the general solution of (51) is

$$\phi = A \log r + Br^2 \log r + Cr^2 + D \qquad \text{----------(52)}$$

A , B , C , D , being constants of integration. The stress components are

$$p_r = \frac{1}{r} \cdot \frac{\partial \phi}{\partial r} = \frac{A}{r^2} + B(1 + 2 \log r) + 2C$$

$$p_\theta = \frac{\partial^2 \phi}{\partial r^2} = \frac{A}{r^2} + B(3 + 2 \log r) + 2C \qquad \text{---------(53)}$$

$$p_{r\theta} = 0$$

In the case of a complete ring it can be shown that displacements are single valued only if $B = 0$, in which case the above expressions for p_r , p_θ reduce to the Lamé equations.

In the web shape the function ϕ is required to satisfy equation (51) at all points within the boundary and to satisfy the stresses (50) at the boundaries. The Biharmonic Equation may be considered to be solved if specific values of ϕ are found for a number of points in the stress field, the number being sufficiently large to enable the values at all other points to be inferred from the known values by interpolation. The specific values of ϕ satisfy the equation in the immediate vicinity of their co-ordinates and for infinitesimal variations of the co-ordinates only, but with diminished accuracy the equation is satisfied by values at control points spaced apart at finite increments. The accuracy of the approximation depends on the size of the increment, increasing with the distance between the points.

The finite-difference approximation to the differential equation (51) fixes the relationship between adjacent values of the stress function at every point inside the boundary. In the case where values of the function are defined at the node points of a square-mesh net covering the stress field as shown in Fig. 24, the Biharmonic relationship of adjacent values

is

$$20\,\phi_0 - 8\,\Sigma\phi_{1..4} + 2\,\Sigma\phi_{5..8} + \Sigma\phi_{9..12} = 0 \quad (54)$$

the points 0 to 12 forming a symmetrical pattern grouped round the 0 point, as shown in Fig. 27. The stresses given by (50) above in terms of these values, are

$$(p_x)_0 = \frac{\phi_2 + \phi_4 - 2\,\phi_0}{a^2}$$

$$(p_y)_0 = \frac{\phi_1 + \phi_3 - 2\,\phi_0}{a^2} \qquad \text{----------(55)}$$

$$(p_{xy})_0 = \frac{\phi_5 - \phi_6 - \phi_7 - \phi_8}{4a^2}$$

Equations in the form (54) above are set up for every node point within the boundary, the values being known at the boundary from the given conditions of stress. If there are m points at which the values of ϕ are unknown, then m equations can be set up, and the stress analysis reduces to a solution of m simultaneous equations.

In equation (55), terms of the order of a^6 and higher are neglected. The expressions for stresses neglect terms in a^4 and higher powers of a. The degree of approximation depends on the higher differentials of ϕ, of which these powers of a are factors, and no precise estimation can be made. In general, if the stress values are changing rapidly, the solution is less reliable than if a fairly uniform

stress system predominates.

(c) Boundary Values.

Considering a small element of the plate at the boundary, acted on by surface stresses of component intensities X and Y , the equilibrium equations, with directions as shown in Fig. 25 are,

$$\left.\begin{aligned} X\,ds + p_x dy - p_{xy}\,dx &= 0 \\ Y\,ds - p_y dx + P_{xy}\,dy &= 0 \end{aligned}\right\} \qquad \text{----------(56)}$$

Substituting for p_x , p_y , p_{xy} from equations (50)

$$X\,ds + \frac{\partial^2 \phi}{\partial y^2}\,dy + \frac{\partial^2 \phi}{\partial x \partial y}\,dx = 0$$

$$\text{or} \quad X\,ds = -\,d\left(\frac{\partial \phi}{\partial y}\right)$$

$$\text{or} \quad \int_I^{II} X\,ds = -\left[\frac{\partial \phi}{\partial y}\right]_I^{II} \qquad \text{----------(57)}$$

Similarly,

$$\int_I^{II} Y\,ds = \left[\frac{\partial \phi}{\partial x}\right]_I^{II} \qquad \text{----------(58)}$$

Now considering the clockwise moments about point II, the plate thickness being 1 unit,

$$dM = X\,ds\,(y - y_{II}) - Y\,ds\,(x - x_{II})$$

$$= -d\left(\frac{\partial \phi}{\partial y}\right)(y - y_{II}) - d\left(\frac{\partial \phi}{\partial x}\right)(x - x_{II})$$

Integrating by parts

$$\left[(M)\right]_I^{II} = \left[\left(\frac{\partial \phi}{\partial y}\right)(y_{II} - y)\right]_I^{II} + \int_I^{II}\left(\frac{\partial \phi}{\partial y}\right) dy$$

$$+ \left[\left(\frac{\partial \phi}{\partial x}\right)(x_{II} - x)\right]_I^{II} + \int_I^{II}\left(\frac{\partial \phi}{\partial x}\right) dx$$

and since

$$\int_I^{II}\left(\frac{\partial \phi}{\partial x}\right) dx + \int_I^{II}\left(\frac{\partial \phi}{\partial y}\right) dy = \int_I^{II} d\phi = \left[\phi\right]_I^{II}$$

$$\left[(\phi)\right]_I^{II} = \left(\frac{\partial \phi}{\partial y}\right)_I (y_{II} - y_I) + \left(\frac{\partial \phi}{\partial x}\right)_I (x_{II} - x_I) + \left[(M)\right]_I^{II} \qquad --(59)$$

Knowing the boundary stresses, values of ϕ and its gradients can be calculated for all points on one boundary. The values are arbitrary at one point, corresponding to the lower limit of integration, since the stresses are given by second differentials of the function. On an unloaded boundary the integrals (57)(58) are zero, and if the arbitrary value of gradient be also zero then the R.H.S. of equation (59) is zero and ϕ is constant on the boundary. This constant value may also be made equal to zero.

Since the crank web shape and boundary loading are symmetrical about two perpendicular axes, one quarter only need be considered. Proceeding counterclockwise from A to B in Fig. 26, the function and its normal gradient are zero up to the point B , the outside being unstressed. The shear stress from B to C is zero, but the normal stress causes a change in ϕ and $\frac{\partial \phi}{\partial x}$ from B across the section BC . These changes, and hence the starting value at the loaded boundary are unknown and cannot be derived, unless an assumption is made regarding the hoop stress at BC.

For a ring shape subjected to bore pressure only, the contours of stress function must be circles concentric with the outside and bore, and the stress function must maintain a constant value on the inner boundary. The hoop stress distribution is given by the Lamé equation. In the web shape, if the hoop stress at BC be given by this equation, the stress function is also constant on the inner boundary, and the computation of boundary values considerably simplified. Partly because of this simplification, and partly because experimental evidence indicated that the stresses were not very different from the Lamé stresses, this assumption was made, and the values in the inner boundary CD calculated from equations (57), (58), (59).

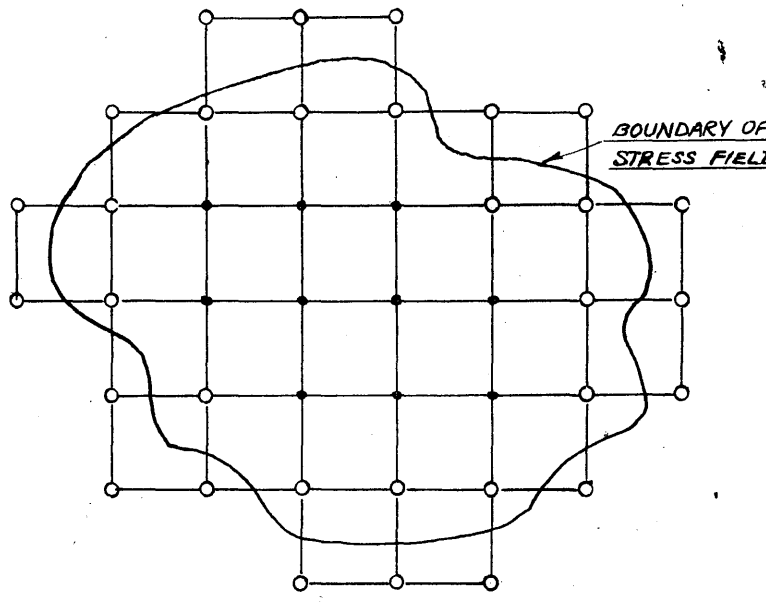

○ FUNCTION DEFINED BY BOUNDARY TRACTIONS

• FUNCTION COMPUTED BY RELAXATION

FIG. 24

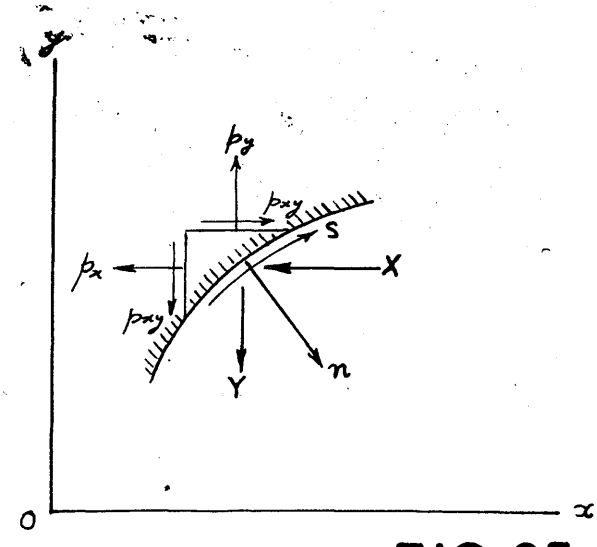

FIG. 25

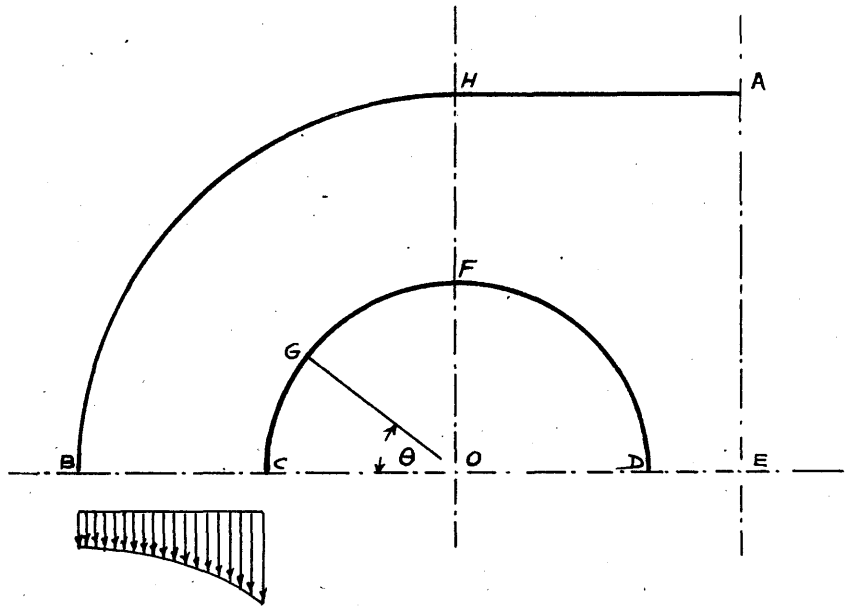

FIG. 26

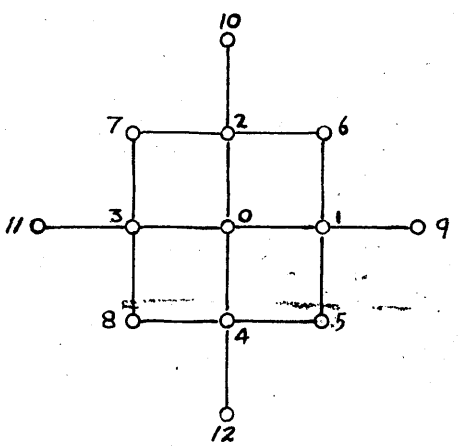

FIG. 27

The stress function for a thick cylinder from (52) above, is

$$\phi = A \log r + Cr^2 + D$$

substituting boundary values given by $p_r = 0$ at $r = r_k$ and $p_r = P$ at $r = r_1$; and assigning the arbitrary value $\phi = 0$ at $r = r_k$,

$$\phi = \frac{Pk^2 r_1^2}{3}\left\{\log \frac{k}{y} - \tfrac{1}{2}\left(1 - \frac{y^2}{k^2}\right)\right\}$$

and $$\frac{d\phi}{dr} = \frac{Pk^2 r_1^2}{3r_1}\left\{-\frac{1}{y} + \frac{y}{k^2}\right\}$$

$$= \frac{Pkr_1}{3}\left\{-\frac{k}{y} + \frac{y}{k}\right\}$$

These formulae enable the values of ϕ and $\frac{\partial \phi}{\partial x}$ to be computed for the point C at which $y = 1$, but the mesh size and web proportions must be considered before numerical values can be assigned.

The shape selected for investigation was the common straight-side web with the thickness of eye-piece and bridge-piece equal to half the pin diameter. This corresponds to one of the cases investigated by Coker. The minimum mesh size to which the analysis was carried was $a = \frac{r_1}{10}$ and the stresses were required to a numerical accuracy of $\frac{P}{100}$. The numerical values of $\frac{\partial \phi}{\partial x}$ and ϕ at C can now be computed by substituting $P = 100$ units of stress, $r_1 = 10a$, and $k = 2$, giving

$$\phi_c = 4242a^2$$

$$\left(\frac{\partial\phi}{\partial x}\right)_c = 1000a \quad ; \quad \left(\frac{\partial\phi}{\partial y}\right)_c = 0$$

At any other point G on the inner boundary, where CG subtends angle θ at the pin centre $\left(\frac{\partial\phi}{\partial n}\right)_G = \left(\frac{\partial\phi}{\partial x}\right)_G \cos\theta - \left(\frac{\partial\phi}{\partial y}\right)_G \sin\theta$

$$\left(\frac{\partial\phi}{\partial n}\right)_G = \left[1000a - 100 \times 10a\ (1 - \cos\theta)\right]\cos\theta - \left[0 - 100 \times 10a \sin\theta\right]\sin\theta$$

$$= 1000a$$

$$= \left(\frac{\partial\phi}{\partial n}\right)_c$$

similarly $\left(\frac{\partial\phi}{\partial s}\right)_G = 0$, and therefore

the values of ϕ and $\frac{\partial\phi}{\partial n}$ are constant on the loaded boundary.

Along DE and EA boundary values are not assigned to ϕ, as these values are subject to relaxation, points on either side of the centre line having identical values due to symmetry.

(d) Computation.

Guided by the values of ϕ and its gradient at the boundaries, trial values may be assigned to every node point. These values will not, in general, satisfy equation (54) exactly, and the R.H.S. will be equal to some quantity R different from zero, termed the residual. By systematically altering the

local values of ϕ, the residuals can be reduced to insignificant values, the final values of ϕ satisfying the Biharmonic Equation within the finite difference approximation determined by the mesh size, and within the numerical approximation of the computation. Both approximations may be improved to any desired extent at the cost of labour in computation.

Altering the trial value of the function at any node point alters the residual at that point and at adjacent points, the changes being determined by the influence of the value of the function at the point on surrounding residuals. An influence pattern may be constructed for a change of 1 unit in the node-point value of ϕ at the centre of the pattern. The pattern, which is, of course, identical for all node points is shown in Fig. 28.

The value and gradient of the function being fixed at the boundaries the values at two rows of nodal points adjacent to the boundaries may be fixed, but owing to the finite mesh size these values are approximate only, and must be changed at intervals as the computation proceeds, guidance being obtained from the inner node points.

The convergency of the process is much slower than in the case of Poisson's Equation and the Laplace Equation, where solutions can be obtained quite rapidly by the Relaxation

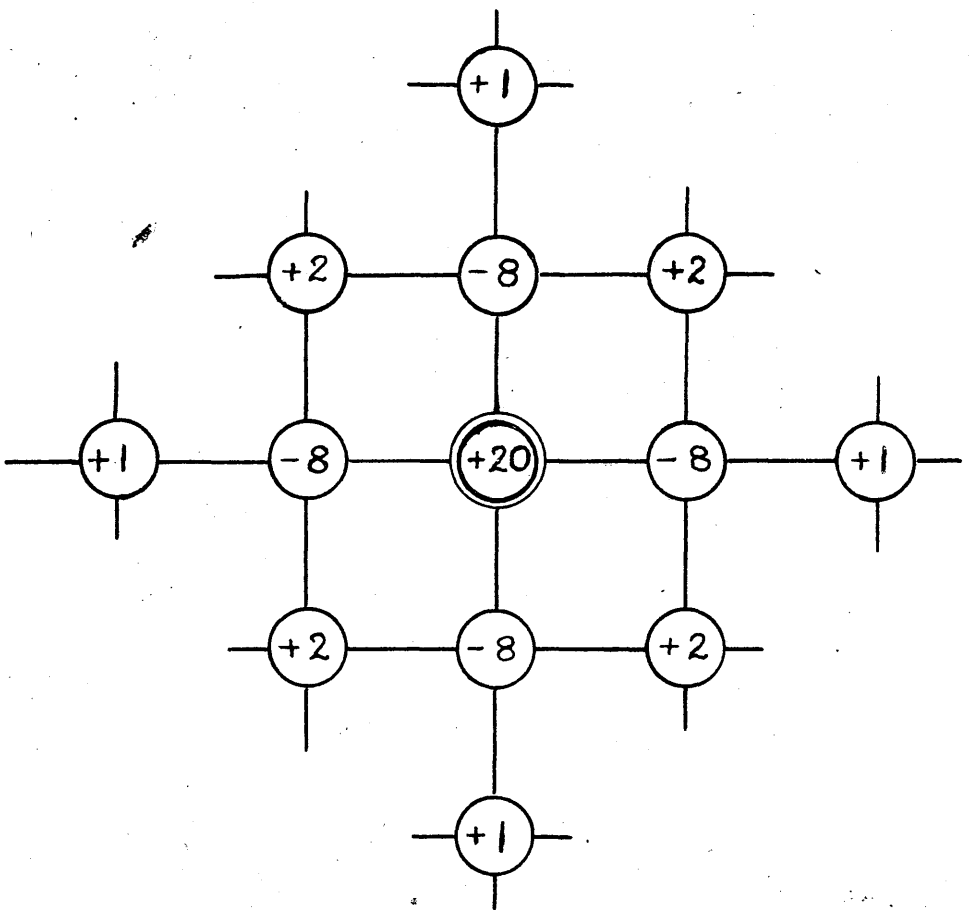

CHANGE OF RESIDUALS FOR $\delta\phi_0 = +1$

FIG. 28

technique. The labour entailed in arriving at a solution for the crank throw of the web in Fig. 26 precluded further solutions being obtained showing the effect of varying the thickness of bridge-piece.

(e) Results.

The final values of stress function at the node points and the unliquidated residuals, are shown in Fig. 29. The stress function values are such that a change of 1 unit at any node point would increase the value of some residual. Contours of stress function are shown in Fig. 30.

Using equations (55) the stress components were calculated for every node point. These values (to the scale of 100 units of bore pressure) are shown in Fig. 31. The values to right and left of the node point above the horizontal lines are p_x , p_y , respectively. The shear stress p_{xy} is shown below the horizontal line. It will be noted that at the section F H (Fig. 26) the shear stress values are very small and the stress conditions all round the circular end portions of the web are very nearly given by thick cylinder equations. This is brought out more clearly in the contours of maximum principal stress - the hoop stress, in the case of the end portions.

The principal stresses and inclination of principal planes were calculated from the normal and shear stresses in the

usual way. Contours of major principal stress are shown in Fig. 32, and contours of maximum shearing stress in Fig. 33. The trajectories of principal stress are shown in Fig. 34 which is approximate only, the lines having been sketched by eye from the directions of principal stresses at the node points. It is possible to employ the relaxation technique to plot the course of any trajectory accurately, but the value of such a plot does not warrant the additional computation.

The stress distribution at various sections of the web and round the peripheries are shown in Fig. 35. Coker's results, where applicable, are also shown in this diagram.

The radial stiffness of the web with both pins fitted may be calculated from the average hoop stress round the bore, and compared with the stiffness of a simple ring under the same bore pressure. In this way the stresses induced by a given fit allowance may be compared with the stresses in a simple ring assembly. The average bore diametral strain in the web is

$$\frac{1}{E}\left\{(p_\theta)_{av.} - \sigma p_r\right\}$$

and the ratio

$$\frac{\text{web diametral strain}}{\text{ring diametral strain}} = \frac{\frac{1}{a^2}\left(\frac{\partial^2 \phi}{\partial n^2}\right)_{av.} + 100\,\sigma}{167 + 100\,\sigma}$$

$$= \frac{197 + 30}{167 + 30}$$

for $\sigma = 0.3$

The plug diametral strain is the same in both cases and equal to $-P(1-\sigma)$ or -70. For the same hoop stress in the circular ends of the web as in a simple ring the ratio of the required fit allowances is therefore $\frac{197 + 30 + 70}{167 + 30 + 70} = 1.11$, the lower radial stiffness of the web requiring the higher fit allowance.

There is a stress concentration in the web at the bridge-piece. The maximum stress in the web occurs at the interface at the points D (Fig. 26). At this point the shear stress concentration factor is $\frac{254 + 100}{167 + 100} = 1.325$ so that if elastic conditions prevail in both the web and the corresponding simple ring and plug assembly, the maximum fit allowance in the web is limited to $\frac{1}{1.325 \times .9} = 0.84$ of the maximum fit allowance in the simple assembly and for this fit allowance the interface pressure is 0.755 times the maximum possible interface pressure for elastic conditions in the simple assembly.

ϕ_0 | R_0

VALUES OF STRESS FUNCTION

AND RESIDUALS

FIG. 29

CONTOURS OF STRESS FUNCTION

FIG. 30

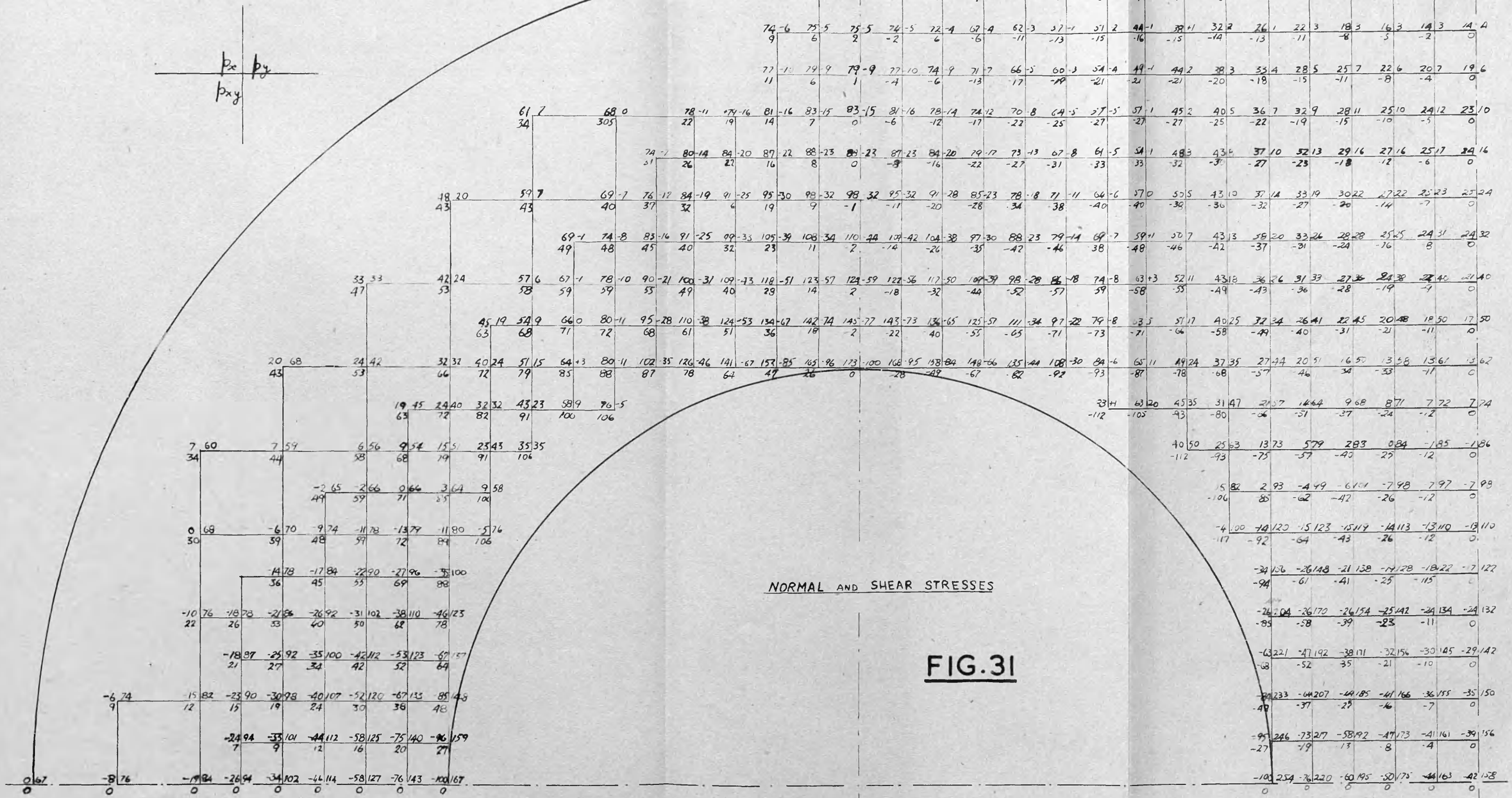

NORMAL AND SHEAR STRESSES

FIG. 31

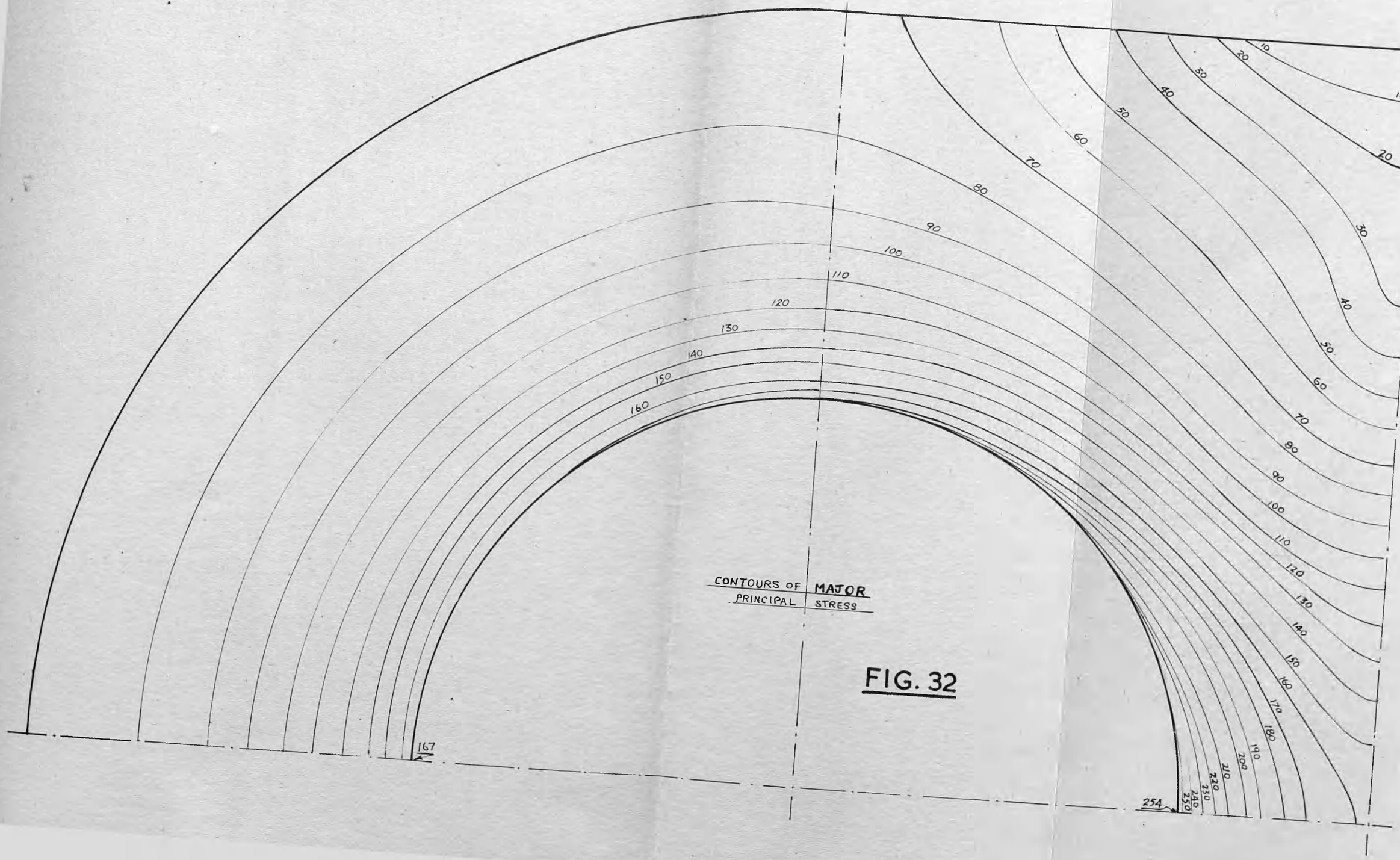
10
20
30
40
50
60
70
80
90
100
110
120
130
140
150
160
167
254
CONTOURS OF MAJOR
PRINCIPAL STRESS

FIG. 32

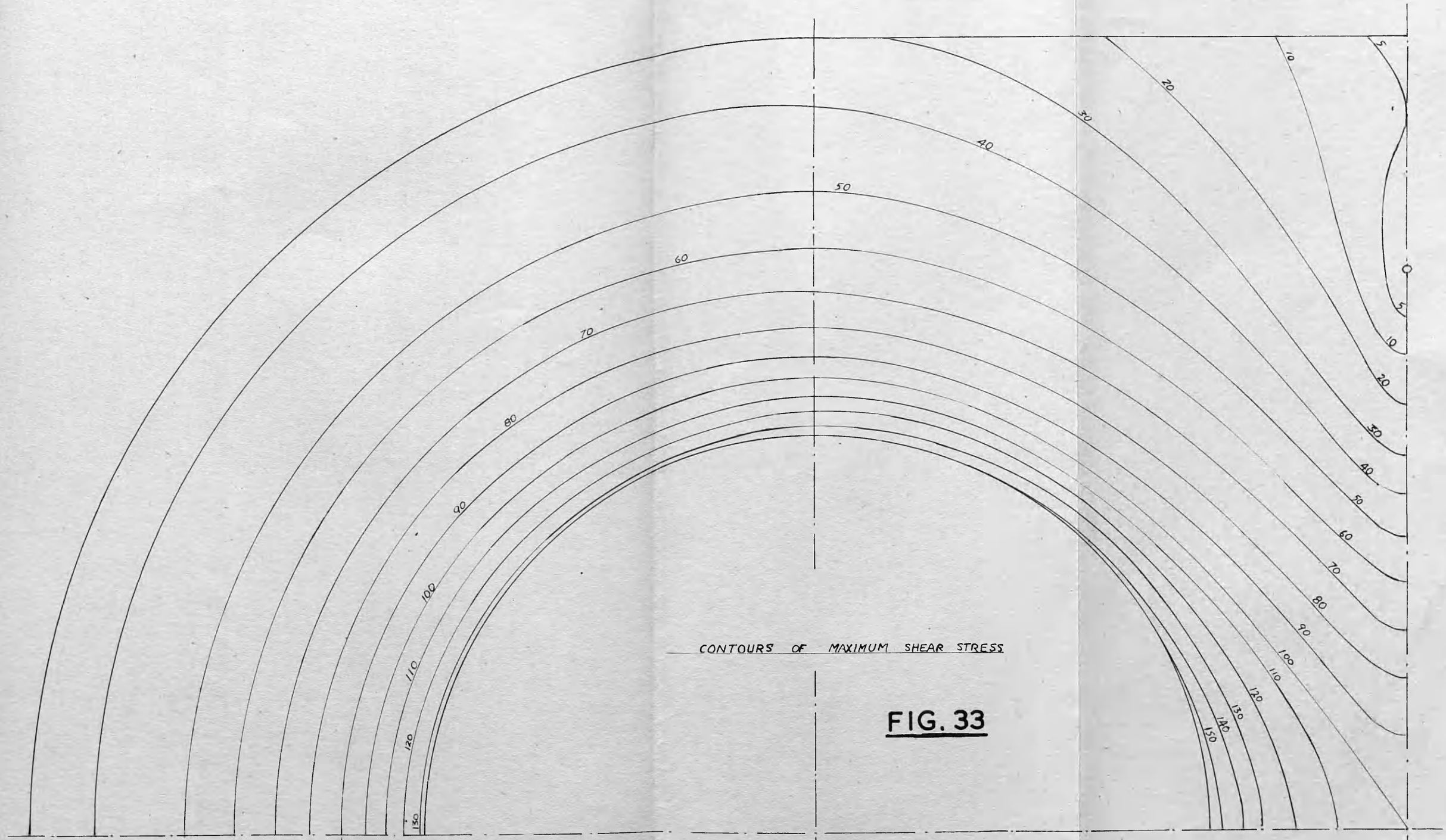

CONTOURS OF MAXIMUM SHEAR STRESS

FIG. 33

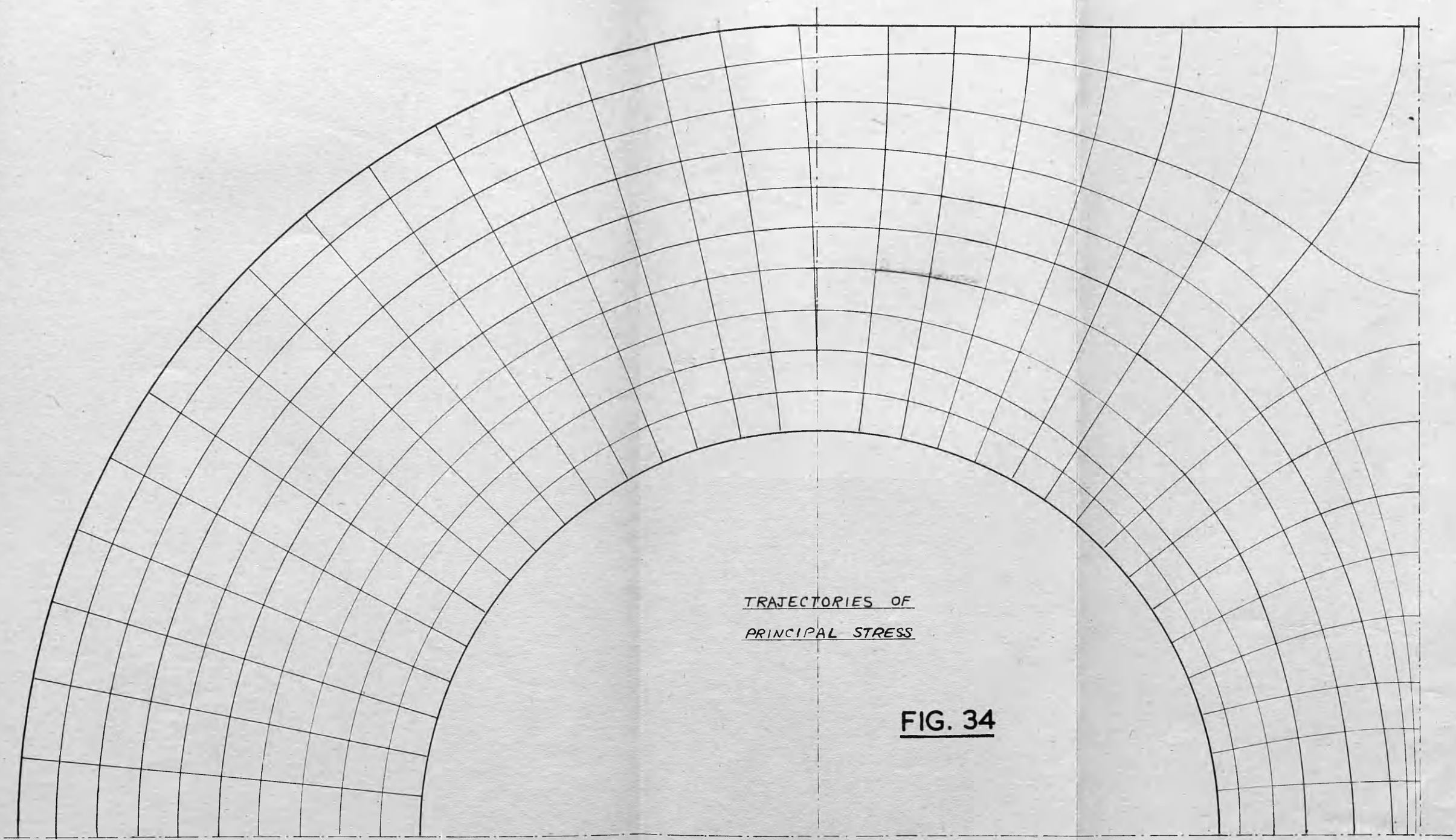

TRAJECTORIES OF
PRINCIPAL STRESS

FIG. 34

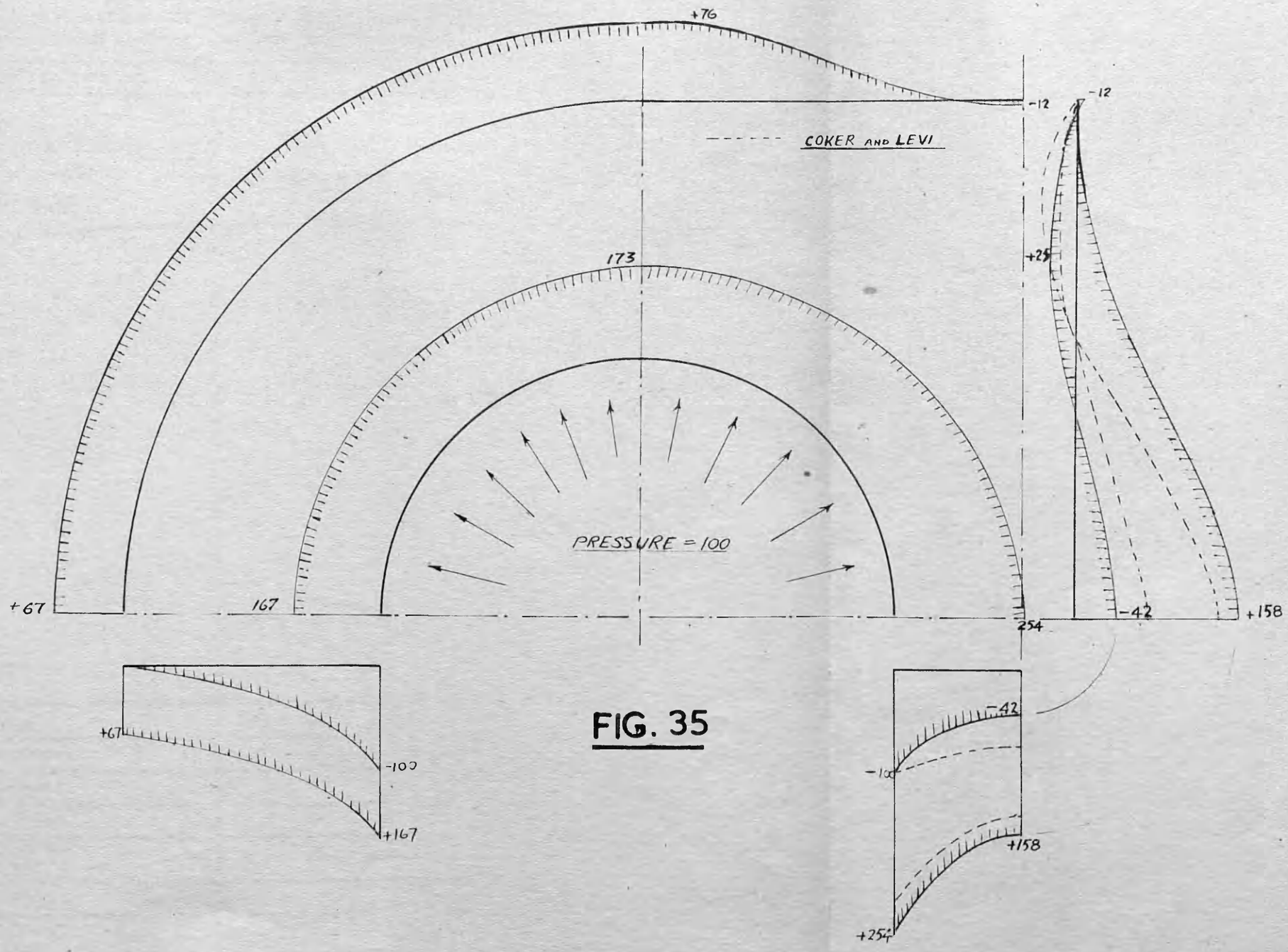
+76
-12
COKER AND LEVI
-12
+25
173
PRESSURE = 100
+67
167
254
-42
+158
+67
-100
+167
-42
-100
+158
+254

FIG. 35

6. SUMMARY AND CONCLUSIONS.

(a) General.

(i) The stress system of a shrink-fit is essentially three-dimensional. Two-dimensional analysis is at best a good approximation, the degree of approximation depending on the proportions of the assembly.

(ii) The type of problem presented is one in which the boundary values of stress and deformation are interdependent, the only condition imposed being the initial discrepancy in size of the unstressed components.

(iii) In the absence of rotational symmetry, development of stress relationships in overstrained assemblies presents formidable difficulties.

(iv) A number of secondary effects such as prevention of free axial shrinkage, change of elasticity with temperature, and thermal stressing during heating and after assembly, have not hitherto been thoroughly investigated.

(b) Axial Shrinkage.

(i) The restriction of a very thick or very thin cylinder, in the analysis of the effect is unnecessary. For the time being the cylinder must be assumed to be long compared with the diameter, in which case the pressure in the middle region,

calculated on the assumption of plane stress, is increased by the factor $\frac{1}{1-\sigma}$ if the axial shrinkage is entirely prevented.

(ii) The tensile end load on the cylinder is twice the end load on a closed-ended cylinder with the same internal pressure.

(iii) When the cylinder is not long the average pressure will lie between the plane stress value and that given by the factor in (i) above.

(iv) Shearing tractions p_{zr} at the interface will warp the end planes of the ring and plug and the stresses there will not, in general, represent the average pressure and hoop stress in the assembly.

(c) Overstrained Cylinders.

(i) Published work analysing the stress conditions in overstrained cylinders can be applied to estimate the stress system in an overstrained shrink-fit.

(ii) Neglect of compressibility of plastic material introduces a discontinuity in either stress or strain at boundary between the plastic and elastic regions. Two solutions with different types of discontinuity, are given. The results for bore strain are almost identical, but are in error compared with the more exact analysis of Sopwith, which takes account of compressibility.

(iii) One of the given solutions, for the case of the closed-ended cylinder, leads to the result that the axial stress is the arithmetic mean of circumferential and radial stress in both regions. This enables rapid, but approximate computation of strains to be carried out.

(d) Temperature Change of Elasticity.

(i) The amount of permanent set in the hollow element depends on the ratio $\frac{E}{s}$ which may be appreciably higher when the fit pressure is developed, than the room temperature value.

(ii) The consequences of this change in the values of elastic constants are:

1. The bore permanent set and the interface pressure do not necessarily correspond at room temperature.
2. The maximum possible value of interface pressure does not correspond to the fit allowance for complete overstrain of the ring element, but to a reduced fit allowance, and partial overstrain.
3. The interface pressure is less than that calculated without the correction for temperature.
4. The pressure can be increased slightly before further overstrain begins.

(iii) Outside diametral deflections before and after assembly provide no indication of the temperature and axial grip effects.

(e) Plane Stress System in Crank Web Shape.

(i) On the assumption of plane stress, elastic conditions, and symmetrical uniform pressure in both bores, the stress system for the shape and proportions of a crank web commonly occurring in marine engineering practice, was evaluated by the Relaxation technique. The principal stress and trajectories at a number of reference points in the plane view of the web are given. The stresses at any other point may be inferred by interpolation.

(ii) From the above solution, the average radial deformation of the holes in the web is greater by 15% than the deformation of the simple cylinder of the same dimensions as the eye-piece, and subjected to the same bore pressure. Allowing for plug deformation, the allowance required for a web is 11% greater for the same thick cylinder stress in the eye-piece. Conversely, for the same fit allowance, the thick cylinder stress in the eye-piece of a web is 90% of that in the corresponding simple ring.

(iii) The overlapping of adjacent stress fields at the bridge-piece induces high stresses, the maximum value of principal shearing stress being 32½% greater than the thick cylinder principal shearing stress at the bore of the eye-piece.

(iv) For the same maximum principal shearing stresses in a web as in an equivalent simple ring, the fit allowance in the

web would require to be 84% of the fit allowance in the ring, and under these conditions the interface pressure in the web would be 75% of that in the ring. With the 28 - 32 ton mild steel normally used in marine crank webs, the limiting fit allowance is about 1 mil.

NOTE. The above figures refer only to crank webs with the shape and proportions given in the analysis.

PART III

EXPERIMENTAL WORK.

1. EXPERIMENTS ON RING AND PLUG ASSEMBLIES.

A. Introductory.

As stated in the Introduction, the work on crankshaft assemblies is only part of an extensive investigation of shrink-fits. A large number of tests on ring-and-plug assemblies have been carried out for this line of research, but it would be outwith the scope of this thesis to discuss the rotationally-symmetrical case of the shrink-fit in great detail. It is, however, necessary to include some such tests to establish the experimental basis for the analytical work in Part II, much of which cannot yet be extended to the more complex web shape.

Two series of tests on rings and plugs are presented below. In the first series the fit allowance is varied, and the interface pressure due to the fitting process deduced from measurements of the ring element; the plugs were removed by boring in order that the effects due to the fitting process alone might be examined. In the second series, the axial friction drag resulting from the prevention of free axial shrinkage is demonstrated. It was considered that this important effect should be established by direct measurement.

B. Variation of Fit Allowance.

(a) Apparatus and Procedure.

(i) Specimens.

A series of 16 mild steel rings and plugs having a nominal bore size and axial length of 3", were prepared. The rings were annealed and finish-bored with a fine-feed wet scrape, giving a bore surface finish of about 16 micro-inches on the Taylor-Hobson Talysurf machine. Measurements of bore and outside diameter were made, and the mating plugs finished to size by the same method, the range of fit allowances being from 1 to $2\frac{1}{2}$ mils.

(ii) Measurements.

The measurements of cylindrical surfaces were taken as the mean of six readings from three axial positions and orthogonal diameters. Outside measurements were made by a Sigma vertical comparator set to slip gauges: inside measurements were obtained by a Mercer dial gauge bore comparator set to a ring standard. The estimated accuracy of an individual measurement was 1/10,000 ", the sensitivity being about 1/100,000" for outside measurements and about 1/50,000" for bore measurements. Measurements were made before assembly, after assembly and after removal of pins.

(iii) Shrinking Process.

After cleaning and degreasing, the rings were heated to shrinking temperature by soaking for 3 - 4 hours in a Birlec electric furnace. The temperature of each ring was raised to about 50°F in excess of the calculated fitting temperature in order to preclude pre-seizure during assembly. The plug was dipped in sperm oil and quickly inserted in the hot ring. The assembly was then allowed to cool in air.

(iv) Removal of Pins.

After measuring the outside diameter, the plugs were removed on an ordinary centre lathe by drilling and progressively boring out until the remaining shell could be easily collapsed and removed. The rings were again measured.

(v) Tensile Tests.

Representative values of Young's Modulus and the Yield Point were determined from the mean of four tensile test pieces machined from different parts of the bar stock.

(b) Results, Discussion and Analysis.

(i) Results.

The results are shown in Table 3 and Fig. 36 below:

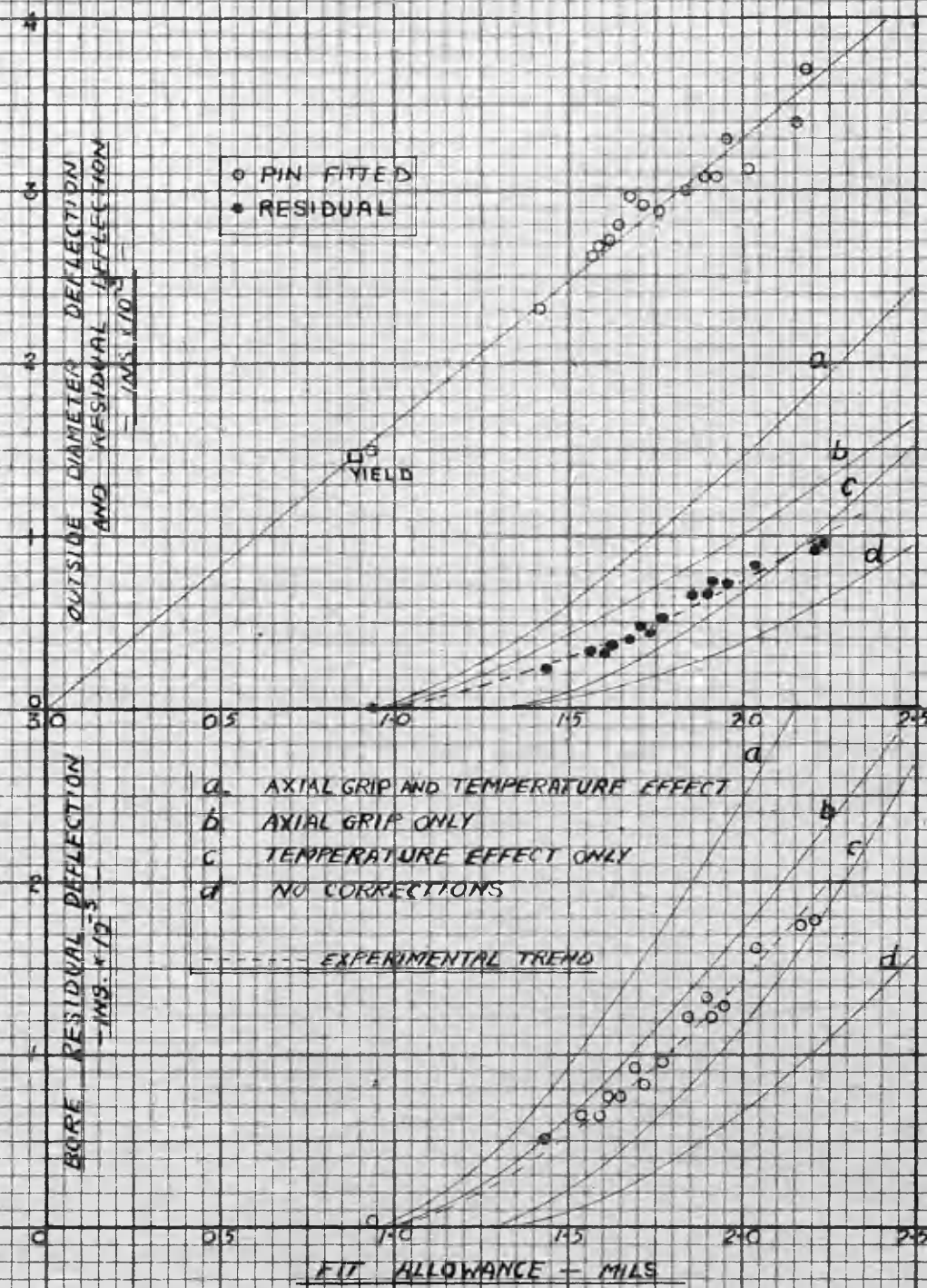
PIN FITTED
RESIDUAL
YIELD
OUTSIDE DIAMETER DEFLECTION AND RESIDUAL DEFLECTION = INS. x 10⁻³
BORE RESIDUAL DEFLECTION = INS. x 10⁻³
a
b
c
d
0
0.5
1.0
1.5
2.0
2.5
a. AXIAL GRIP AND TEMPERATURE EFFECT
b. AXIAL GRIP ONLY
c. TEMPERATURE EFFECT ONLY
d. NO CORRECTIONS
EXPERIMENTAL TREND
FIT ALLOWANCE - MILS

FIG. 36

TABLE 3

Bore Diameter	3.10 inches
External Diameter	3.96 inches
Diameter Ratio, k	1.925
Young's Modulus	13.400 T/in^2
Yield Point	16.7 T/in^2

The fit allowances used in this series were confined to the region just beyond the elastic limit of the ring with a view to ascertaining the conditions at the interface in the early stages of plastic flow. Graphs of outside diametral deflection with the pins fitted, and outside and bore residual deflections to a base of fit allowance, are shown. Theoretical curves obtained graphically from plots of Sopwith's solution for a thick cylinder according to the method discussed in Part II Section 4 , are shown in Fig. 36 .

(ii) Deflection - Pins Fitted.

As shown in Fig. 23 , the outside diametral deflections provide no indication either of the yield point, or of the effects of temperature and axial friction drag. The experimental results in Fig. 36 are in good agreement with the theoretical curve. The yield point shown is that corresponding to full axial grip (double end load in Part II Section 2), without temperature

correction.

It should be noted that the slope of the theoretical curve of outside deflection is not affected by the elastic constants of the material, since both ordinates and abscissae contain the factor $\frac{E}{s}$. In the elastic range the slope is independent of, and in the post-elastic range only slightly dependent on the axial friction drag. This may readily be shown as follows:

For elastic conditions

$$E(e_\theta)_k = p_\theta)k - \sigma p_z)k$$

and

$$p_z)k = \frac{2P}{k^2 - 1} \qquad \text{for maximum axial grip.}$$

$$= \frac{2}{k^2 - 1} \left(\frac{k^2 - 1}{2k^2} \cdot E\Delta \cdot \frac{1}{1 - \sigma} \right)$$

$$= \frac{E\Delta}{k^2} \cdot \frac{1}{1 - \sigma}$$

also

$$p_\theta)k = \frac{E\Delta}{k^2} \frac{1}{1 - \sigma}$$

Hence

$$e_\theta)k = \frac{\Delta}{k^2}$$

The identical result is obtained for no axial grip, p_z being zero and the factor $\frac{1}{1 - \sigma}$ becoming unity. The slope

of the outside diametral strain curve is therefore $\frac{1}{k^2}$ in the elastic range.

The maximum discrepancy between any experimental value and the theoretical line is about 0.0003" or about 0.005% strain. Bearing in mind that the plotted values on both axes are differences of fine measurements made by comparative methods, the agreement is good.

(iii) Residual Deflections.

The theoretical curves of bore and outside diameter residual deflections correspond to conditions of full and zero axial grip, with and without the correction for change of elastic constants with temperature according to Lea and Crowther's results for mild steel. Both sets of residuals lie between the curve of full axial grip with no temperature correction and zero axial grip with temperature correction.

Any combination of these two effects could give a curve which would coincide with the experimental results. The experimental trend suggests, however, that the temperature correction is not significant. In general, temperature correction tends to increase the slope of the curve, while axial friction drag displaces the curve to the left. The slope of the experimental trend is rather less than that of the axial drag curve without temperature correction, while the residual

deflections start at a fit allowance corresponding closely to the full axial grip. It would appear that the critical fit allowance for overstrain could be calculated without appreciable error, from the full theoretical pressure given by conditions of no axial slip, and that as the fit allowance is increased the axial drag tends to diminish. It is remarkable that in a short cylinder the conditions appear to correspond so closely to the analysis based on a cylinder of infinite length with axial load distributed as a uniform tensile stress in the cylinder wall.

The apparent insignificance of temperature correction may be accounted for as follows:

1. The results of Lea and Crowther, which were used to calculate the correction, may be an overestimate for the 28 - 32 ton steel used in this series of tests.

2. In the analysis in Part II Section 4, the heat loss by radiation was assumed to be negligible compared with the interchange of heat between the two elements in the fitting process. It is quite possible that the interface transfer coefficient is small and that temperature equilibrium is not attained for an appreciable time after fitting; the equilibrium temperature may therefore be quite low.

In order to separate the effects of temperature and axial friction drag it would be necessary to either

1. Measure the temperatures during the fitting and apply a correction based on values of elastic constants obtained by high temperature tests on the actual material of the ring, or
2. Arrange a combination of shrink - and expansion-fitting in which the mean temperature was close to the ambient.

The latter might introduce other complications with regard to the axial grip, as the surface film condition would be effected by unavoidable atmosphere condensation on the cold plug.

(iv) Interface Pressure.

The pressure may be calculated from the outside diametral change on removal of plug, and also from the residual fit, defined as the difference of the initial fit and the residual strain of the ring bore in mils, if elastic recovery on release of the shrink-fit pressure be assumed.

The pressure for full axial grip is $\frac{1}{1-\sigma}$ times the pressure calculated on the basis of plane stress conditions. The residual deflections in Fig. 36 show that the full axial grip is not developed, and the calculated pressure would therefore be higher than the correct value if the factor $\frac{1}{1-\sigma}$ were

used: for the same reason the plane stress value would be incorrect, but low. It is necessary to assume some factor for the end load due to friction drag between the value unity and the value $\frac{1}{1-\sigma}$. This factor may be written as $\frac{1}{1-m\sigma}$ where m has the value zero in the plane stress case, and unity in the case of full axial grip. A value of m between 0 and 1 would correspond to partial restraint on axial shrinkage.

The interface pressure is then given by

$$P = \frac{1}{1-m\sigma} \cdot \frac{k^2-1}{2k^2} \cdot E\,\Delta_r \qquad \text{----------(60)}$$

$$= \frac{1}{1-m\sigma} \cdot \frac{k^2-1}{2} \cdot E\,e_\theta)_k \qquad \text{----------(61)}$$

where Δ_r = residual fit as defined above.

From (60) and (61) the value of interface pressure P was calculated and plotted against fit allowance in Fig. 37. The value of m was taken as $\frac{3}{4}$, by inspection of the experimental trend of residual deflections in Fig. 36. The latter show that the axial grip is diminishing as the fit allowance is increased and better agreement with the calculated curves of interface pressure could no doubt be obtained by varying the value of m.

The points adjacent to the higher fit allowances lie outside the calculated curves and indicate a high value of interface pressure. These points may be brought within the

two curves by using a value of m less than $\frac{1}{2}$.

The value chosen for the empirical factor does not in general correspond to the fraction of end load taken by the ring. The selection of the value is somewhat arbitrary and pressures calculated by this method are suspect. It must be admitted that, by suitable choice of m, any pressure curve within wide limits could be constructed.

Pressures calculated on the basis of residual fit and of outside diametral changes, are in fair agreement.

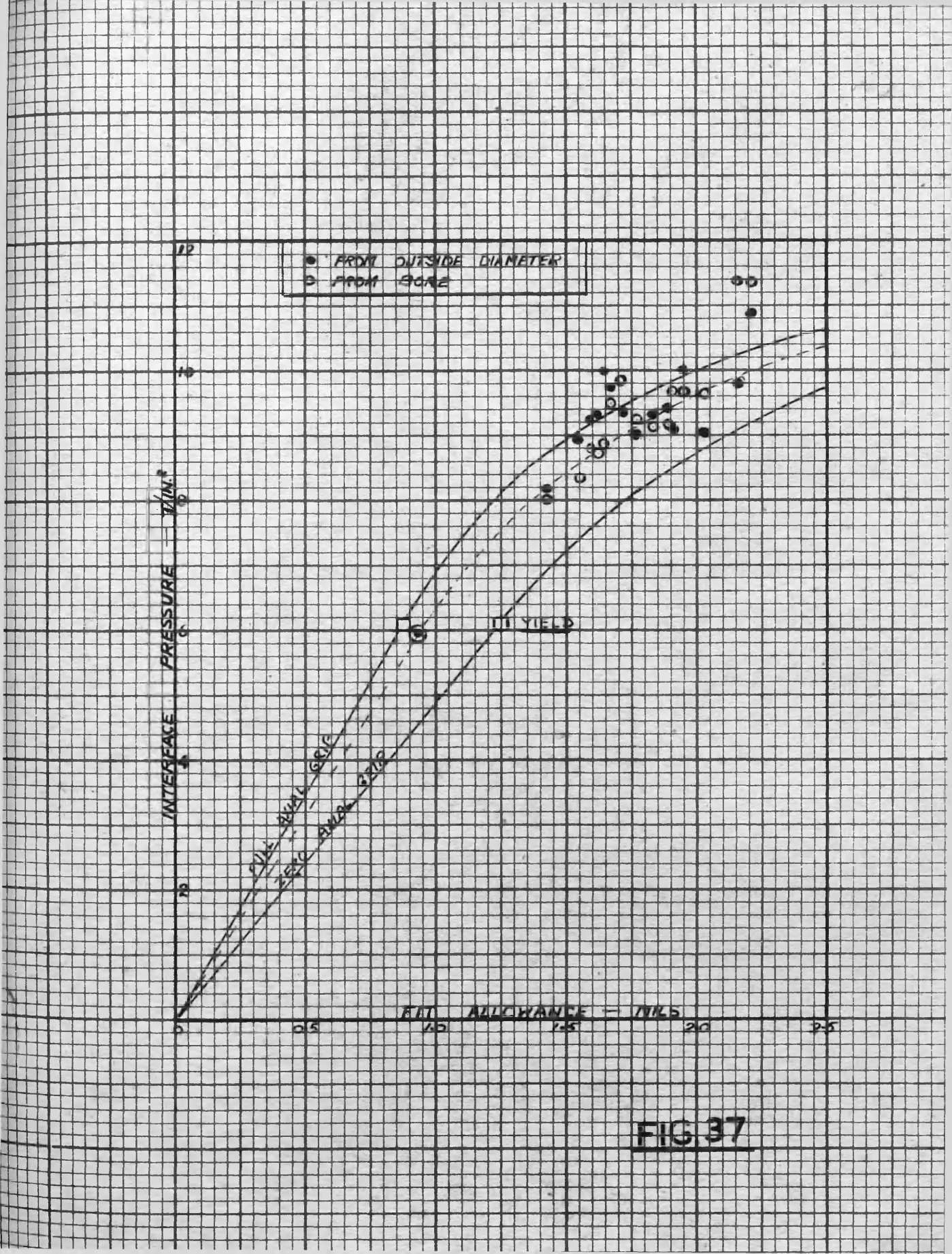
FROM OUTSIDE DIAMETER
FROM BORE
INTERFACE PRESSURE — TONS/IN.²
12
8
4
0
0·5
1·0
1·5
2·0
2·5
FIT ALLOWANCE — INCHS
YIELD
CYL. RADIAL GRIP
ZERO AXIAL GRIP

FIG 37

C. Demonstration of Axial Friction Drag.

(a) Apparatus and Procedure.

Two rings were machined with a number of wide grooves on the ends and outside circumference, the narrow lands between the grooves being accurately surfaced to form fine measurement references. A diametral cross-section of the machined rings is shown in Fig. 38 . Plugs were machined to sizes corresponding to fit allowances of 1.35 and 2.73 mils, and shrink-fitted according to the procedure outlined in sub-section B. above. Axial and outside diametral measurements were taken on two orthogonal diameters at each of the prepared surfaces before and after shrink-fitting, thus allowing the deformation of the ring profile due to the fitting to be measured.

(b) Results and Discussion.

The average changes of axial length at varying radii are plotted in Fig. 39 with the best smooth curve corresponding to the plotted points. Each point is the average of eight measurements, two on each of four radii at right angles.

The trend of the profiles of the end surfaces is quite definite in both cases.

The restraint on free axial shrinkage results in the bore layers of the ring being appreciably extended, but the extension "washes out" with increase of radius; at the outside

diameter the axial length of the ring is hardly greater than a ring under plane stress. The deformations corresponding to plane stress conditions for the different fit allowances are shown by the horizontal lines.

The amount of friction drag is not proportional to the fit allowance, possibly because of variations in the friction coefficients.

The deformations of the ends in Fig. 39 are not necessarily elastic deformations, since the fit allowance in both cases was sufficiently large to cause overstrain. The plugs were not removed in this experiment and no estimate can be made of the permanent deformations of the rings in the axial direction.

The extensions of the bores of both rings may be compared with the extensions calculated on the basis of plane strain and elastic conditions, for conditions of full and zero axial grip. With full axial grip

$$\delta_z)_1 = + \epsilon_z)_1 \times 3 = + \frac{\Delta}{k^2} \times 3 \text{ ins.}$$

and with zero grip

$$\delta_z)_1 = - \sigma e_\theta)_k \times 3 = - \sigma \frac{\Delta}{k^2} \times 3 \text{ ins.}$$

The theoretical and measured extensions for $\sigma = 0.3$ are shown in Table 4 below.

TABLE 4

Fit Allowance - Mils	Extensions - inches		Measured Extensions - inches	% Grip
	Full Grip	Zero Grip		
1.35	0.0011	- .00033	- . 00017	11
2.73	0.00204	- .00061	- .00039	38

The last column shows the amount of grip in each case, measured as the fraction of bore extension compared with the maximum possible extension from zero to full grip.

The values of measured extensions are considerably lower than the evidence in the previous sub-section would suggest. The above values based on elastic conditions, are not however, strictly accurate, and the degree of approximation cannot be assessed. Also it is impossible to allow for the effect of non-uniform axial stressing.

This experiment merely verifies that partial prevention of axial shrinkage as shown by the warpage of end plane of the hollow element, does, in fact, occur.

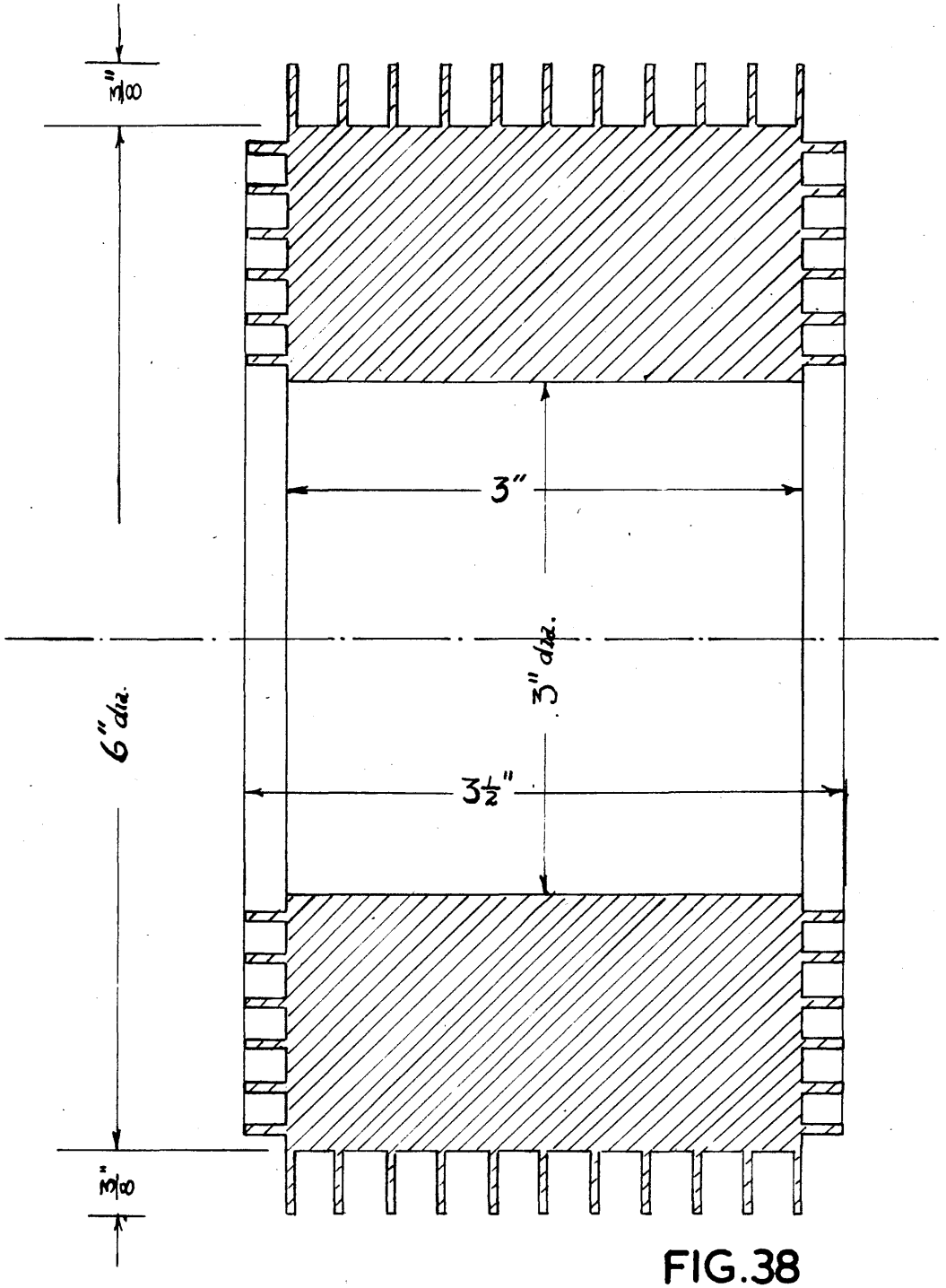

FIG.38

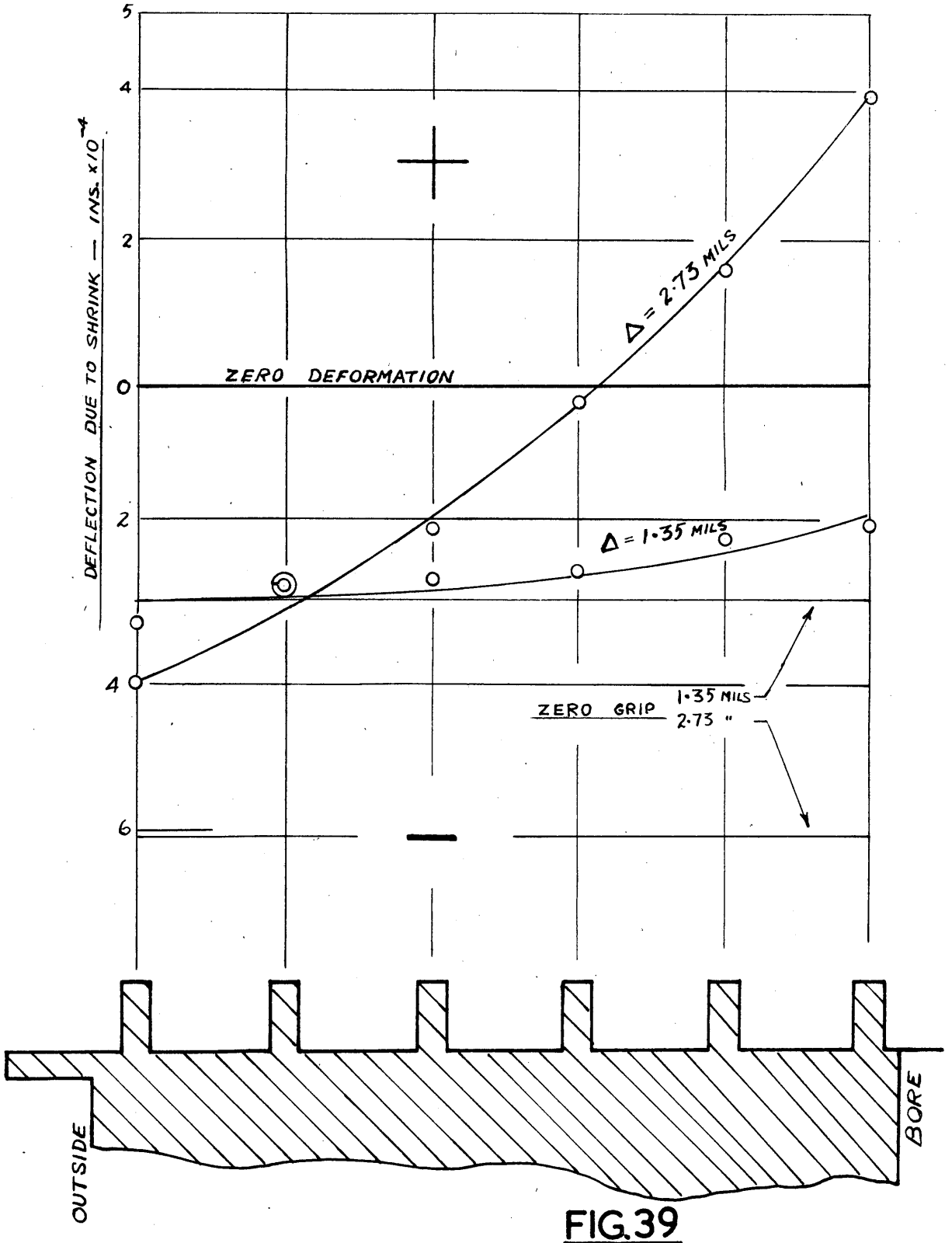
5
4
2
0
2
4
6
DEFLECTION DUE TO SHRINK — INS. x10⁻⁴
ZERO DEFORMATION
Δ = 2.73 MILS
Δ = 1.35 MILS
ZERO GRIP
1.35 MILS
2.73 "
OUTSIDE
BORE

FIG. 39

2. MODEL CRANK WEB TESTS.

(a) Introductory.

The tests carried out in connection with the investigation of built crankshafts consisted of simultaneous investigations of the stress system and strength of grip of full size crankshafts and of sections of model shafts. The latter series of tests were designed to establish the holding power of shrink-fitted crank pins and journals under various types of external force actions.

The predominant external force action in a crankshaft is that of static torque. Two series of tests were carried out to determine the influence of variation of surface finish and of variation of surface film condition on the grip strength of shrink-fits in model webs. The models were approximately geometrically similar to the full-scale crank webs investigated in Section 3 . Details are given in the following sub-section.

In carrying out the experimental work it was noted that the deflection of the assembly under torque was non-linear. A preliminary investigation of this was carried out with a rather crude indicator constructed at short notice. The results show that failure under torque action is a gradual process, corresponding to a progressive screwing of the pin within the grip length until a point is reached at which the twist penetrates

the entire grip and failure by torsional slip occurs. The indications are that relative movement of the mating surfaces does not occur, but the material of the web becomes plastic at the entry side of the grip, allowing the torque to be more evenly distributed over the grip length. The apparatus was not designed to investigate the mode of grip failure, and the results are somewhat less acurate than is desirable in view of the importance of the effect.

(b) Apparatus and Procedure.

(i) Model Webs.

Four webs, approximately $\frac{1}{7}$ scale models of the scrap crankshaft webs used in the full scale tests, were machined from 28 - 32 ton m.s. plate. The principal dimensions are shown in Fig. 40 . The nominal bore diameter of the series was 3" , but the bores were left $\frac{1"}{16}$ undersize, and after the first series of tests subsequently annealed and rebored to $3\frac{1"}{16}$ for a second similar series. In both series of tests the bores were finished to four different representative machine finishes, namely dry-scrape, wet-scrape, ground and honed, and the surfaces of the two bores of a particular web were, as far as possible, identical. In the first series the fitting was carried out with both mating surfaces dry, but not specially cleaned, corresponding to the normal shop practice of assembling

crankshafts and denoted by "shop-dry". In the second series the fitting was carried out using sperm oil as a fitting lubricant, the procedure being as in Section 1. B. (a) (iii) above.

The pins were machined with a wet-scrape finish from 28 - 32 ton m.s. upset forgings flanged for attachment of levers, through which equal and opposite torques were applied to the grips. The apparatus for applying pure torque is described below.

(ii) Torquing Apparatus.

The arrangement of the apparatus is shown in Fig. 41. Plate 1 shows a web on test in a 25 ton horizontal Avery hydraulic testing machine. Pure couples are applied to the pins by means of equal and opposite forces on the ends of the transverse levers. The forces are transmitted through tie links to the ends of two rigid cross beams of box construction, which are connected by central ties to the grips of the horizontal testing machine. A dial gauge is arranged to measure the relative movement between the levers under load.

The torque applied to the shrink-fit is given by the tensile load of the testing machine and the dimensions of the apparatus. Errors, apart from those inherent in the testing machine, can only arise from dimensional inaccuracies and friction at the various linkages. The former may be disregarded

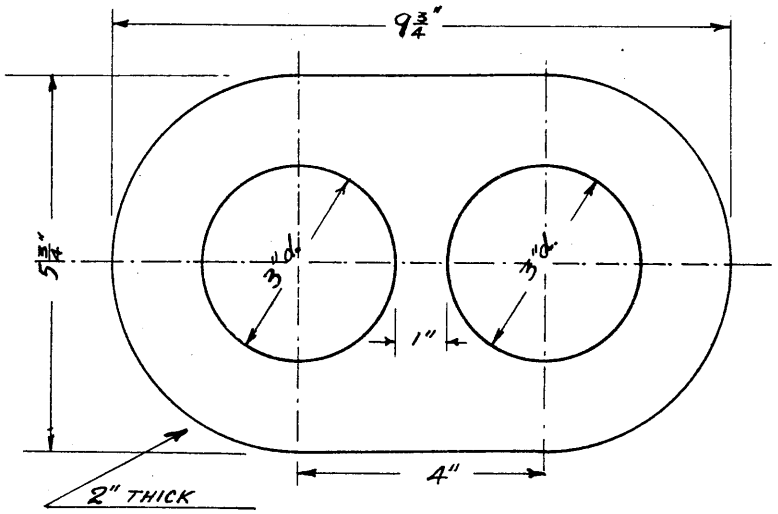

FIG. 40

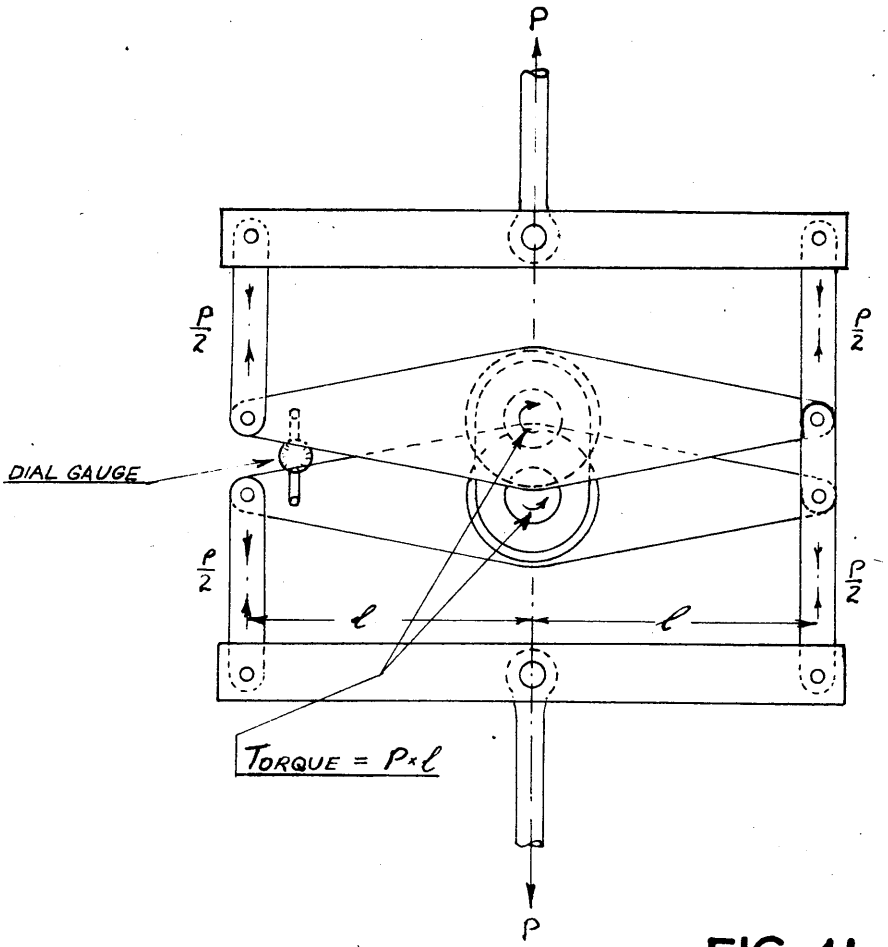

FIG. 41

PLATE 1

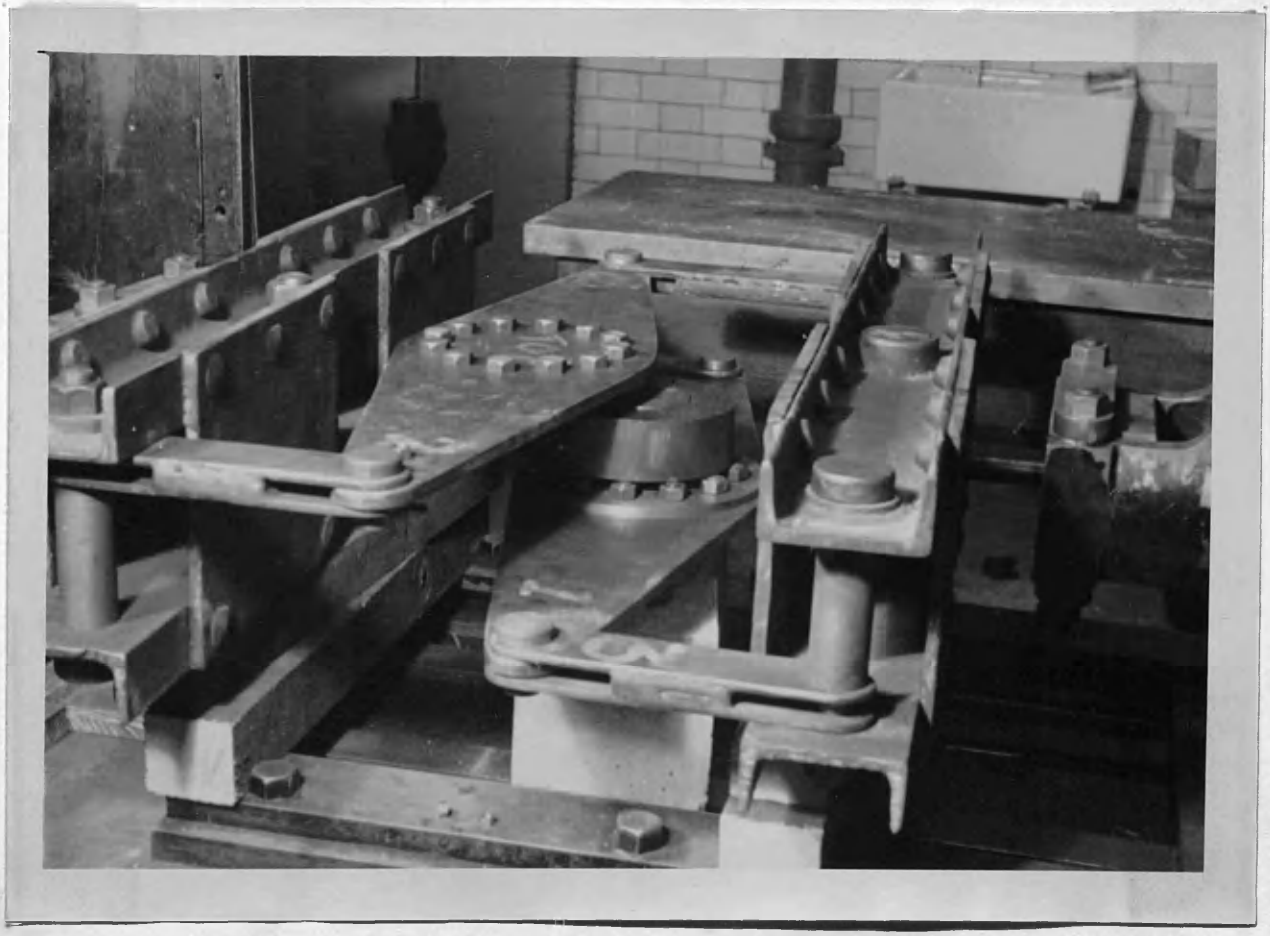

. TORQUING APPARATUS FOR MODEL WEB TESTS.

as not appreciable and the latter was estimated from the force required to produce transverse movement of the beams and levers under a longitudinal load equal to that required to cause failure. This correction was also negligible.

(iii) Procedure.

Measurements of dimensions and surface finish were made before assembly and after removal of pins. The holding power of this assembly was measured by

1. Static torque to cause slip at one grip.

2. Axial loads to cause slip of each grip.

Using the torquing gear described above, a web was subjected to increasing static torque in the tensile testing machine. Measurements of deflection of the two levers were made at increments of load up to the point at which failure of one of the shrink-fits occurred. The breakdown was indicated by a bumping noise, sudden increase of deflection, and a drop of the testing machine beam. The load was again increased and the second load to cause slip measured; the third load was measured in the same way.

After the torquing test the apparatus was dismantled, and the flanges machined off the pins in order to allow the push-out operation to be carried out. A bolster ring giving about $\frac{1"}{32}$ clearance on the pin size was used to support the

web and the pin which had failed by torque pushed into the bolster on a standard vertical 30 ton Avery testing machine. The first second and third slip loads were measured. The other pin was tested in the same way, and then removed completely and the grip strength of the former pin again measured.

This pin was removed and the surfaces of both pins and web examined; measurements of the fitted surfaces were checked.

(iv) Measurements.

The equipment used for the ring-and-plug tests in Section 1 above, was employed.

(c) Results, Discussion and Analysis.

The results for the shop-dry series are shown in Table 5 , and for the lubricated series in Table 6 .

(i) Grip Characteristics.

There is a tendency for the holding power of the grip to diminish with repeated application of the stripping load, but this tendency is not consistent in the shop-dry series, though quite definite in the lubricated series. The third axial and torsion loads may be regarded as a more definite indication of the variation of grip strength than the initial loads, as there is a tendency for time seizure to occur, especially in the presence of lubricant, making the initial grip strength somewhat

TABLE 5 - SHOP-DRY SERIES.

Web Number	1		2		3		4	
Bore Surface Finish	Dry Scrape		Wet Scrape		Ground		Honed	
Bore Identification	A	B	A	B	A	B	A	B
Bore Roughness (u ins.)	90	50	14	19	5	4½	5	6
Pin Roughness (u ins.)	35	35	16	12	19	9	6½	9½
Bore Diameter (ins.)	2.9367	2.9363	2.9370	2.9368	2.9430	2.9407	2.9430	2.9406
Pin Diameter (ins.)	2.9398	2.9396	2.9400	2,9400	2.9459	2.9434	2.9456	2.9433
Fit Allowance (ins.)	0.0031	0.0033	0.0030	0.0031	0.0029	0.0027	0.0026	0.0027
Fit Allowance (mils)	1.06	1.13	1.02	1.07	0.985	0.918	0.883	0.918
Torques (in.lbs.) Initial	97500	-	76500	-	-	85500	9700	-
Torques (in.lbs.) Repeated	75000	-	66000	-	-	85500	87000	-
Push-out Load (tons) Initial	27.9	31.9	24.05	29.4	22.8	24.85	26.6	24.5
Push-out Load (tons) Repeated	24.1	23.5	19.3	26.4	29.9	26.6	28.4	28.4

TABLE 6 - LUBRICATED.

Web Number		1		2		3		4	
Bore Surface Finish		Dry Scrape		Wet Scrape		Ground		Honed	
Bore Identification		A	B	A	B	A	B	A	B
Bore Roughness (u ins.)		52	66	14	12	$8\frac{1}{2}$	11	9	8
Pin Roughness (u ins.)		$5\frac{1}{2}$	4	$6\frac{1}{2}$	$3\frac{1}{2}$	13	13	19	17
Bore Diameter (ins.)		3.0030	3.0029	2.9998	2.9998	3.0399	3.0401	3.0402	3.0402
Pin Diameter (ins.)		3.0055	3.0054	3.0021	3.0021	3.0426	3.0426	3.0422	3.0425
Fit Allowance (ins.)		0.0025	0.0025	0.0023	0.0023	0.0027	0.0025	0.0020	0.0023
Fit Allowance (mils)		0.836	0.822	0.770	0.770	0.889	0.823	0.658	0.748
Torques (in.lbs.)	Initial	-	63000	54000	-	-	61500	57000	-
	Repeated	-	37500	33000	-	-	39000	31500	-
Push-out Load (tons)	Initial	30.4	22.0	12.9	18.4	17.9	13.3	9.4	13.0
	Repeated	9.0	9.0	6.1	6.4	9.3	4.6	5.8	7.0

variable. This discrepancy between initial stripping load and follow-up stripping load is a feature of interference fits noted by Russell and by Werth, in the case of force-fits, and is common knowledge in fitting shops. The time-effect was investigated by Russell (34) using various kinds of lubricant, but the time scale was much greater than familiarity with this kind of experimental work would suggest as appropriate. The seizure becomes appreciable in terms of minutes and hours, rather than weeks and months. This has become evident as a result of a large number of stripping tests on various types of assemblies.

It might be suggested that the decrease in holding power after the initial stripping load is due to release of axial grip and consequent decrease of interface pressure. There are two reasons why this explanation must be rejected.

1. The difference of initial and follow-up loads are generally much greater than the differences of interface pressure with zero and full axial grip.

2. The push-out loads in the case of the pins which had already been stripped by torque show the same tendency towards a high initial load, but the values of initial axial stripping loads are generally lower than in the case of the unbroken grip, because the time for seizure to develop was less in the former case, and perhaps

because the fitting temperature would induce a greater degree of seizure which would not be subsequently re-attained.

Nevertheless it is possible, indeed probable, that a release of interface pressure does occur at the initial cracking of the grip, but the effect is masked by the large decrease in the friction with disturbance of the contact conditions.

(ii) Coefficients of Friction.

It was intended that the fit allowance in both series of tests should remain constant, but machining tolerances made it impossible to guarantee precise dimensions. It is therefore necessary to reduce the values of grip strength to a common basis to facilitate a true comparison. The most convenient way of comparing the torques and push-out loads is via the coefficients of friction. These are shown in Table 7 .

The fit allowances in all cases were sufficiently low to allow the interface pressure to be deduced from elastic theory. In the case of the initial loads and torques an axial grip factor of $\frac{1}{2}$ is allowed. Subsequent loads and torques are assumed to be dependent on plane-stress conditions. A shape factor of 0.9 derived in Part II, Section 5 , is used in conjunction with ring theory, so that the interface pressure is given by

$$P = 0.9 \frac{1}{1 - m\sigma} \frac{k^2 - 1}{2k^2} E\Delta$$

where

$m = \frac{1}{2}$ or 0

and

$$\mu = \frac{2T}{\pi D^2 LP}$$

$$= \frac{F}{\pi DLP}$$

T = Torque to strip the grip.

F = Axial force to strip the grip.

D,L = Diameter and length of contact surface.

TABLE 7.

				Dry Scrape	Wet Scrape	Ground	Honed
Torques	Shop-dry	Initial		.280	.229	.284	.336
		Repeated		.254	.232	.334	.353
	Lubricated	Initial		.228	.207	.219	.252
		Repeated		.159	.150	.152	.165
Push-out load	Shop-dry	Initial	1	.304	.289	.232	.268
			2	.311	.279	.320	.356
		Repeated	1	.262	.306	.359*	.365*
			2	.269	.224	.342*	.380*
	Lubricated	Initial	1	.362	.246	.201	.173
			2	.314	.197	.190	.167
		Repeated	1	.126	.100	.132*	.110
			2	.129	.110	.086	.103

* Surfaces seized during push-out test.

Lines 1 and 2 of the push-out coefficients refer to the two pins, line 2 being the pin which had previously slipped under torque action. The repeated load coefficient was taken from the 3rd load or torque figure, as the holding power remained nearly constant thereafter.

The conclusions which may be drawn from Table 5 are, in the main, negative, and are listed below.

1. Comparing lines 1 and 2 push-out coefficients for all four conditions, it will be noted that the variation of the friction coefficient under apparently identical conditions is considerable. Measurements of surface finish before assembly and after separation revealed little change, therefore the torque could not have affected the surface finish to any appreciable extent. It would be expected that the initial coefficient would be higher in line 1 , since the surfaces had not been previously disturbed, but this is not always the case in the shop-dry series, though definitely so in the lubricated series. The variations are generally not so great in the latter series, and, for repeated stripping loads, the coefficients with one exception are fairly constant. In this series seizure occurred in Pin 1 of the ground web, with tearing of the surfaces and a high push-out load. In the shop-dry series, seizure occurred in both pins of the ground and honed webs.

2. The trend of variation of friction with surface finish

is not definite. The values in Table 7 are presented graphically in Fig. 42 , with the values from repeated loads and torques in the lubricated case heavily lined. A trend, if any, should be shown more definitely by the latter. The push-out loads have a lower coefficient than the torques, but the variation with surface finish is slight. With the honed surface there is a tendency for the friction to increase, although the micro-finish was approximately the same as for the ground surfaces. This may be attributed to a slight improvement in the geometry of the bore, as honing tends to suppress the machining inaccuracies such as out-of-roundness, lack of parallalism and tool-mark waviness. These effects are not contained in the Talysurf indication. The improvement with honing is shown by all lines in Table 7 , except those corresponding to initial push-out loads in the lubricated series.

3. The discrepancies between the coefficients of friction under torque and axial load are not consistent. The axial friction would be expected to be slightly higher than the circumferential friction for two reasons.

(i) The application of push-out load causes a slight increase in plug diameter, and hence in fit allowance and interface pressure.

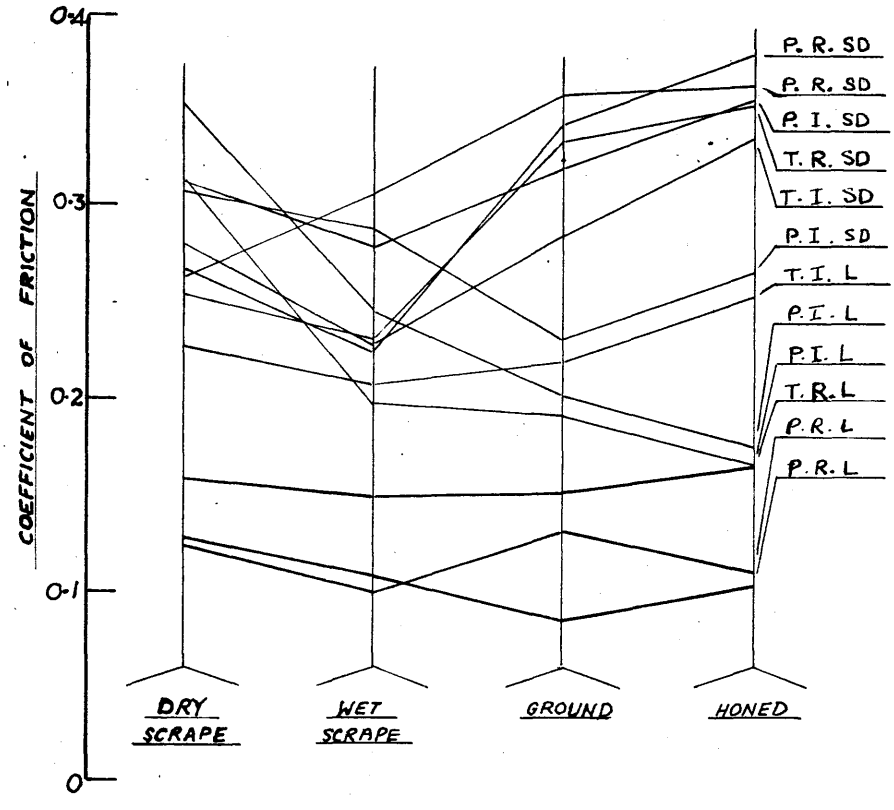

CODE:

P., T. — PUSH-OUT, TORQUE
R., I. — REPEATED, INITIAL
SD., L — SHOP-DRY, LUBRICATED

FIG. 42

(ii) The types of surface irregularities produced by machining processes suggest that slip should occur more readily in the circumferential direction. No explanation can be advanced for the reversal of this tendency in the lubricated repeated-load case, and the experimental results should therefore be confirmed before speculating on the cause.

4. The deterioration of grip in the presence of lubricant is evident both for initial and for repeated application of the stripping load. The lubricated friction value is dependent on the type of surface film and on time; it should not be assumed that the low coefficients with sperm oil are the minimum values which may be encountered in a crankshaft in service conditions. The repeated load values may be related to the values in a grip under pulsating force and torque actions, where the presence of engine oil due to breathing of the grip under pulsating bending is a define possibility. Dorey (10) observed that oil could be seen issuing from a shrink grip after running trials.

5. The subject of friction is fraught with uncertainty, and demands a major investigation of the nature of intimate cohesion of metallic surfaces. The micro-finish of surfaces of 100 μ-in. or less is clearly of secondary

importance. The macro-finish or waviness may not so readily be dismissed; the amount of waviness in any of the specimens examined was small. This test cannot be regarded as providing a useful indication of friction values for the design of built shafting.

(iii) Residual Measurements.

Measurements of dimensions and surface finish after separating the elements, were, within the limits of accuracy, the same as before assembly. In some cases the fit allowance might have produced a small amount of permanent set, but the amount was immeasurably small, and no serious inaccuracy in the calculation of interface pressure results from the use of the elastic formulae above.

(iv) Surfaces After Separation.

1. Shop-dry.

Except where seizure had occurred, the surfaces were clean and bright, with fine axial scratches of very minute depth, irregularly pitched round the circumference at about 5 to 10 per inch.

2. Lubricated.

The fine scratches were again apparent bu the surfaces were distinctly and uniformly oily. The oil could be readily

wiped off by hand leaving a bright surface.

(d) Mode of Torque Failure.

The torquing apparatus was fitted with a dial gauge at the position shown in Fig. 41 as a precautionary measure, in case the point of grip failure was not evident from other indications. Dial-gauge readings under increasing torque indicated that the deflection was non-linear. A typical torque-deflection diagram is shown in Fig. 44 .

It was decided to investigate the non-linearity by attempting to check the rotation of the entry side of each pin relative to the web surface, on the honed web of the shop-dry series. The apparatus did not permit any standard instruments to be employed, so simple gauges consisting of two arms, were constructed of sheet brass. One arm of the gauge was connected to the cylindrical surface of the pin, and the other to the flat surface of the web, both attachments being as close as possible to the entry of the grip. A sketch of the arrangement is shown in Fig. 43 .

The relative deflection of the ends of the arms was measured by the rotation of a standard 8 B.A. screw in a Tufnol bush, the cheese-head carrying a short pointer in the notch, reading on a circular paper scale divided into 36 divisions. Electrical connections to the screw and arm were as

shown, allowing the movement to be detected with very little force on the arms. The attachment of the arms to the surfaces presented great difficulty, owing to space restriction. Bonding was the only practicable method. This was carried out by cleaning and degreasing the surfaces of the gauges and points of attachment, using solvents, and applying a thin coat of Bostik sealing compound to one gauge arm only, setting in position, and clamping for 24 hours. The other arm was then attached in the same way. A similar gauge was then attached at the entry side of the other pin.

During the torquing test, readings were taken of the dial gauge and both pin gauges. The torque was applied in small increments up to approximately half the estimated slip torque and reduced to zero. This was repeated but the original maximum torque was slightly exceeded. On the third application loading was continued until failure of one grip occurred.

The deflections of the dial gauge and both pin gauges are shown in Figs. 45 , 46 , 47 . The graphs are approximately linear up to about 30,000 in.lbs. torque; thereafter the deflection increases at a greater rate. Failure occurred at Pin A under a torque of 97,500 in. lbs. Reducing the torque to zero leaves a residual deflection at all gauges; the recovery of the deflections with reduction of torque, and the deflections under re-applied torque, were linear and parallel

to the initial torque-deflection characteristics. The effect can be reproduced at a higher point on all curves, the process being strikingly similar to the behaviour of an overstrained tensile specimen.

The deflections of the pin gauges are contained within the deflection of the dial gauge, the pin gauges registering a portion of the latter deflection. The possibility of inelastic action at other parts of the apparatus may be disregarded, and the departure from the linear characteristic at the dial gauge should be accounted for by the combined pin gauge deflections. Fig. 48 shows the comparison of the pin gauge readings with the dial gauge reading.

It will be noted that the non-linearity is only partially accounted for by the measured deflections at the pins. This fact is of the utmost importance in deciding the type of failure occurring at the shrink-fits. Two possible explanations are as follows:

1. Partial slip of the mating surfaces could occur, allowing an increasing length of the fitted part of the pin to twist within the shrink grip, progressively decreasing the elastic stiffness of the assembly.

2. The transmission of torque across the fitted surfaces is equivalent to the application of circumferential friction drag, i.e. shearing stress, to the boundaries of a stress system

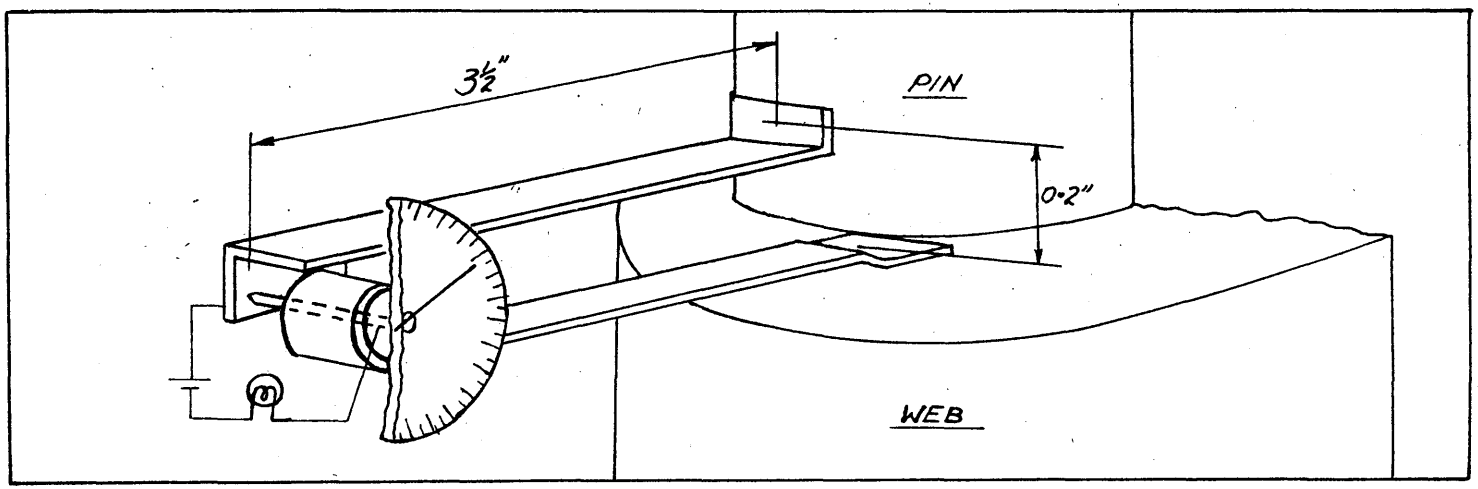

FIG. 43

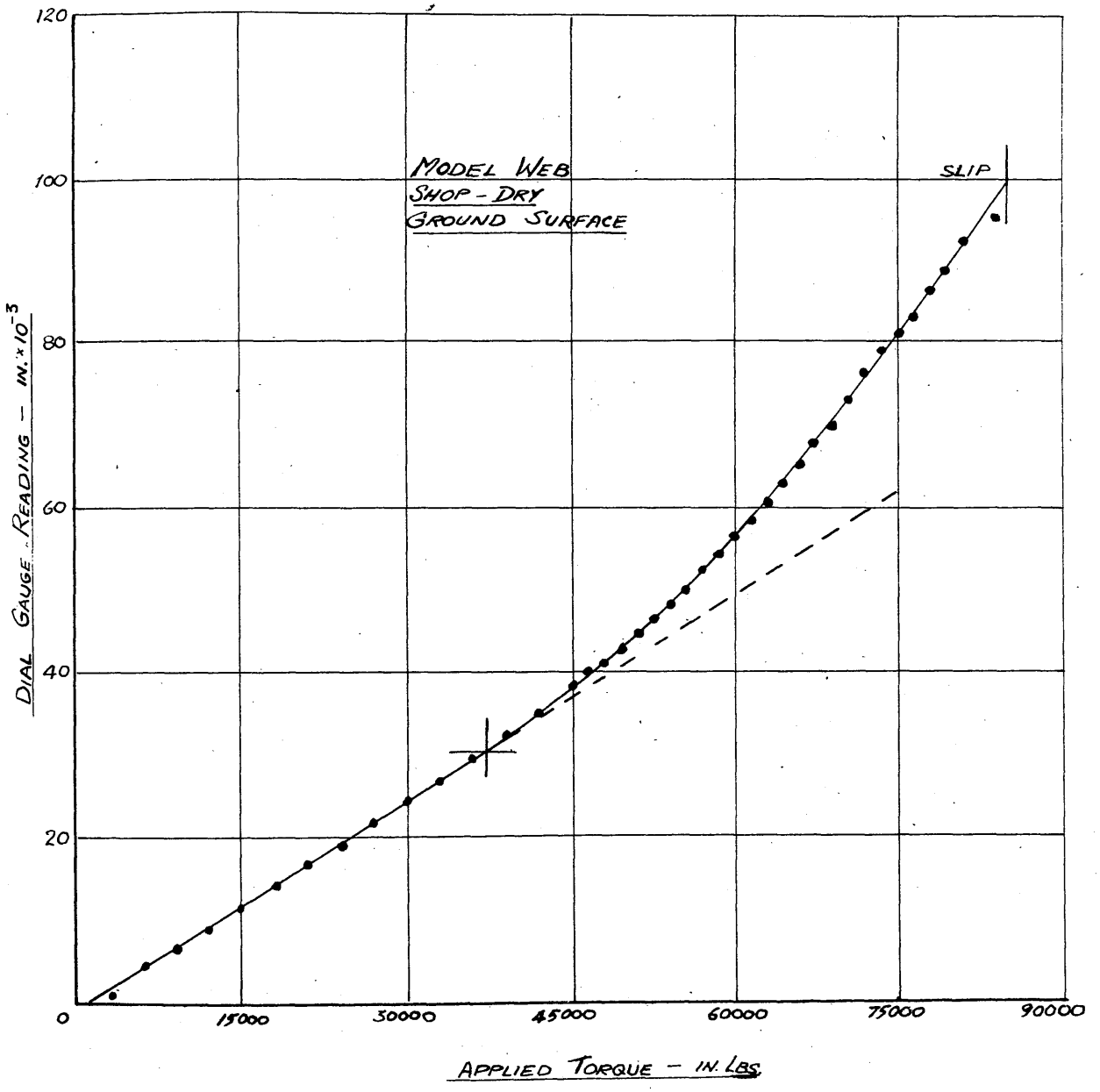
MODEL WEB
SHOP - DRY
GROUND SURFACE
SLIP
DIAL GAUGE READING - IN. * 10⁻³
APPLIED TORQUE - IN. LBS.
0
15000
30000
45000
60000
75000
90000
20
40
60
80
100
120

FIG. 44

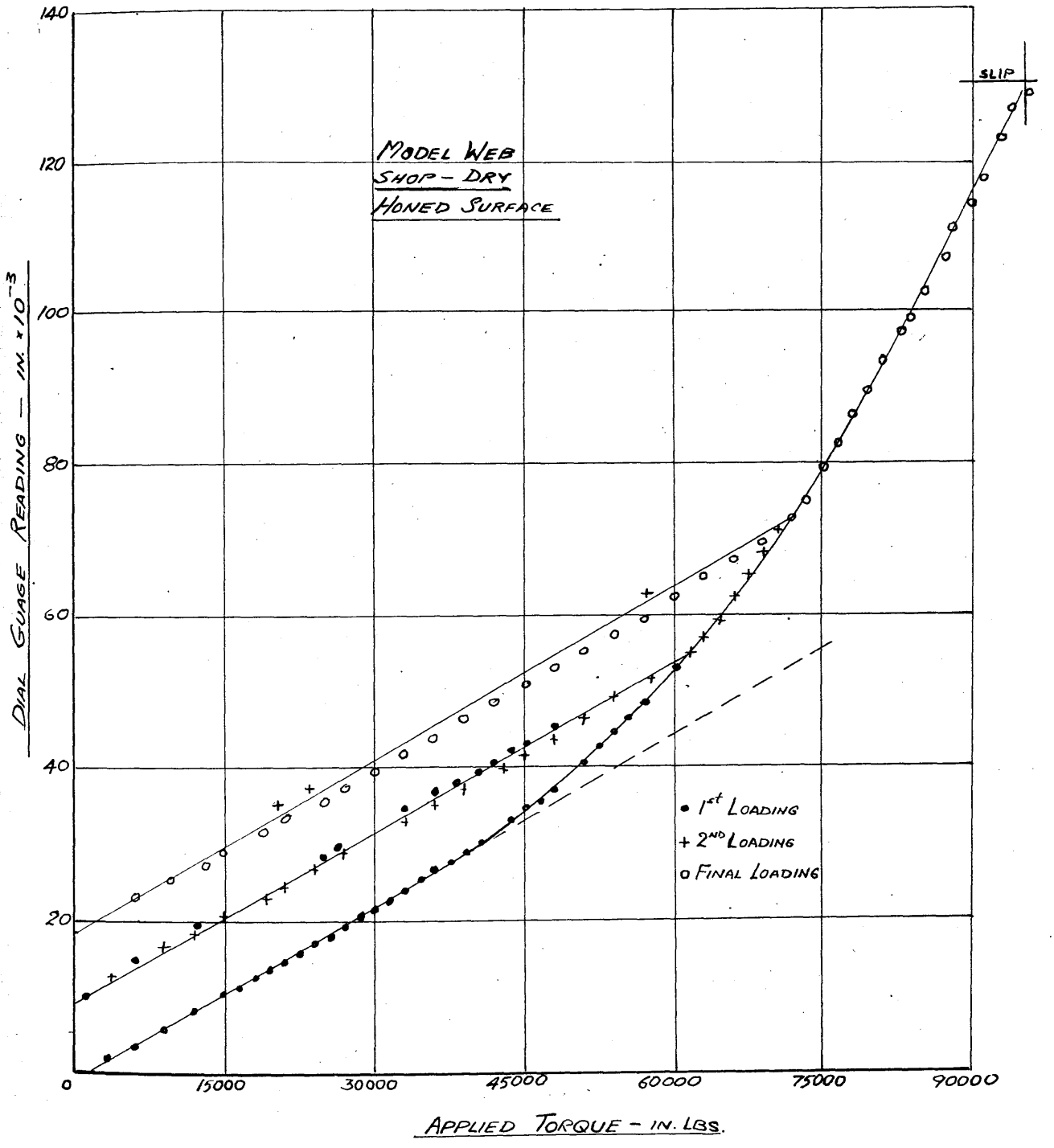
MODEL WEB
SHOP - DRY
HONED SURFACE
SLIP
• 1st LOADING
+ 2ND LOADING
o FINAL LOADING
DIAL GUAGE READING — IN. x 10⁻³
APPLIED TORQUE - IN. LBS.
0
15000
30000
45000
60000
75000
90000
20
40
60
80
100
120
140

FIG. 45

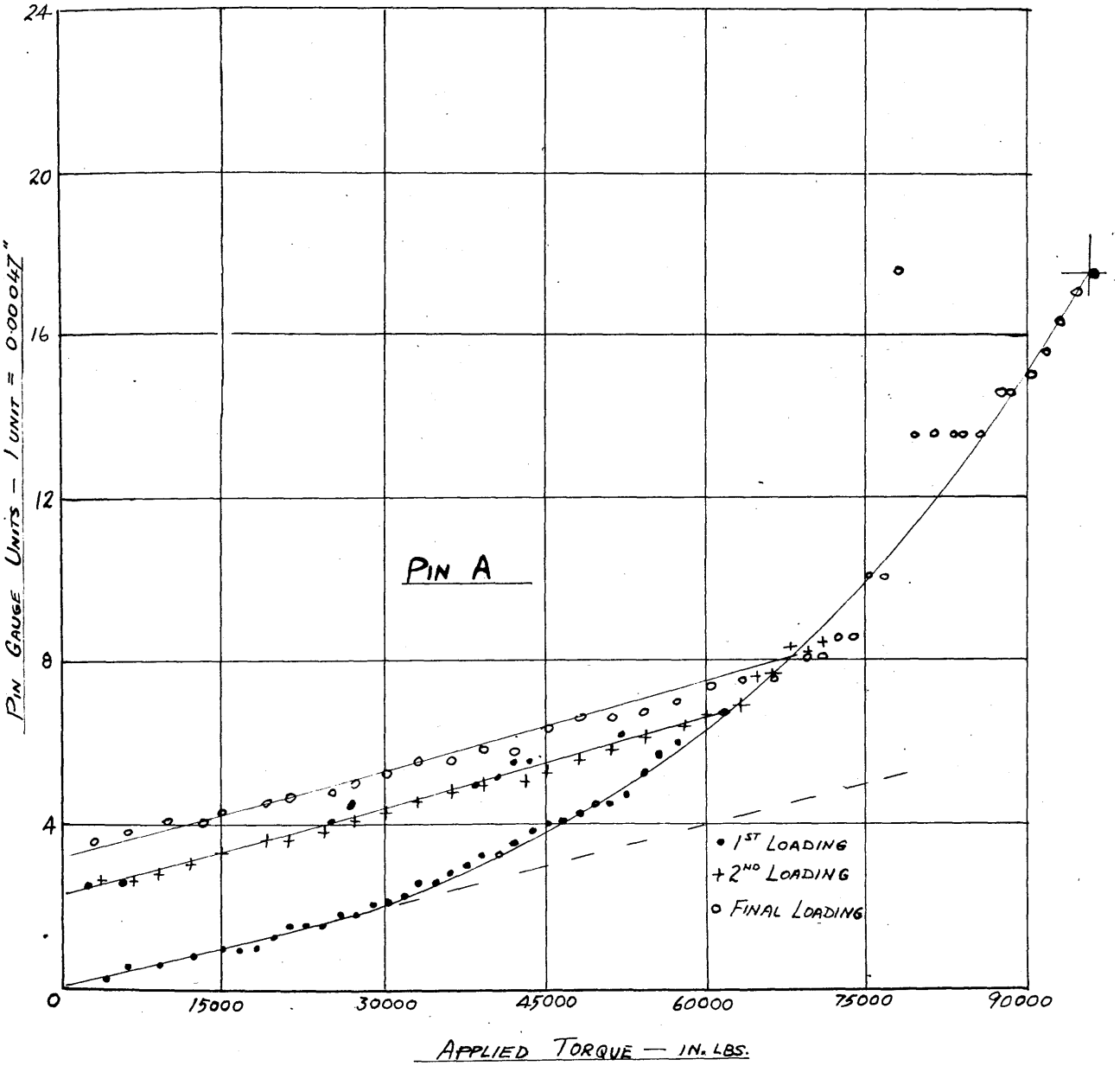
24
20
16
12
8
4
0
PIN GAUGE UNITS — 1 UNIT = 0.00047"
PIN A
15000
30000
45000
60000
75000
90000
APPLIED TORQUE — IN. LBS.
• 1ST LOADING
+ 2ND LOADING
o FINAL LOADING

FIG. 46

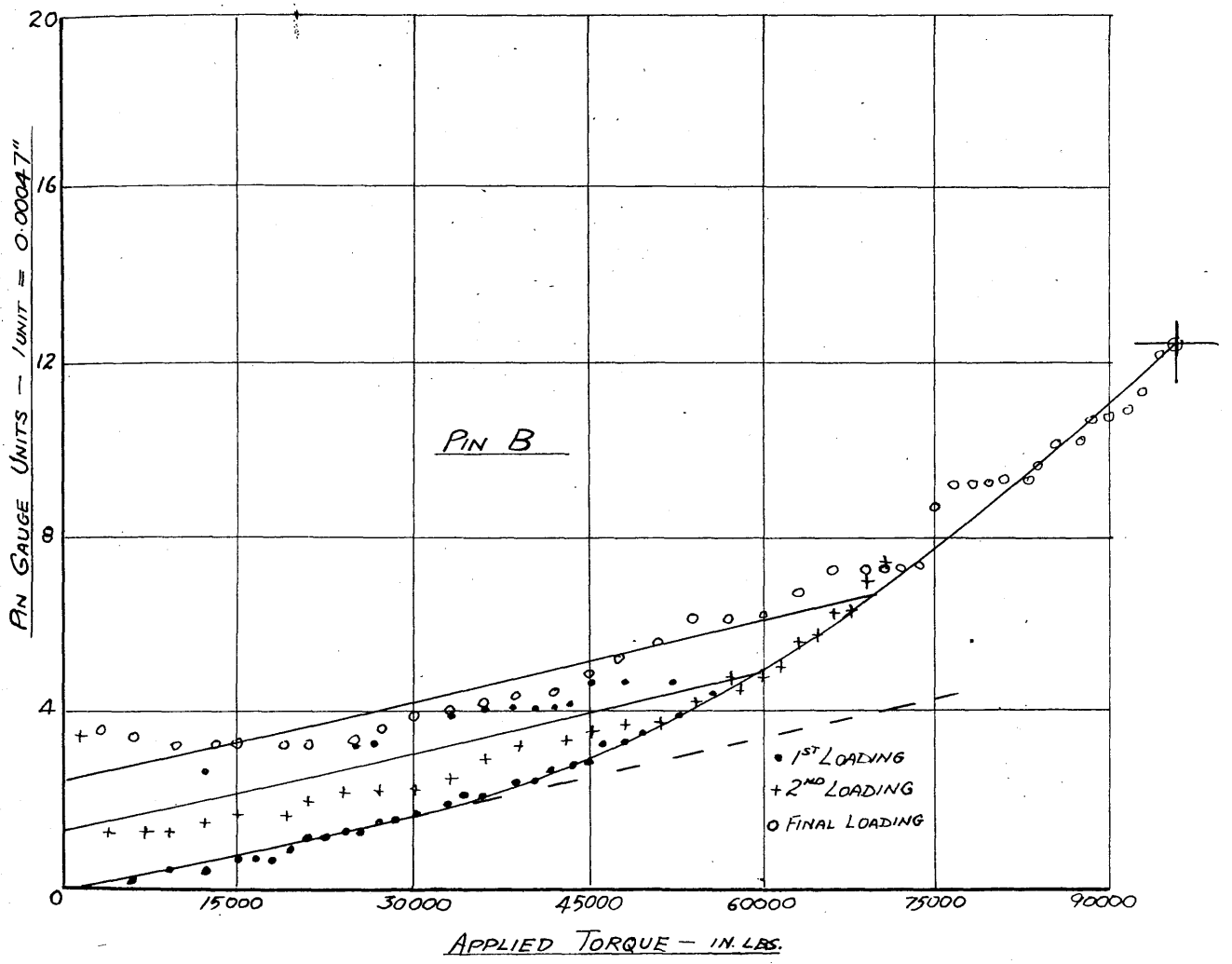
20
16
12
8
4
0
PIN GAUGE UNITS – 1 UNIT = 0·00047"
PIN B
1ST LOADING
2ND LOADING
FINAL LOADING
15000
30000
45000
60000
75000
90000
APPLIED TORQUE – IN. LBS.

FIG. 47

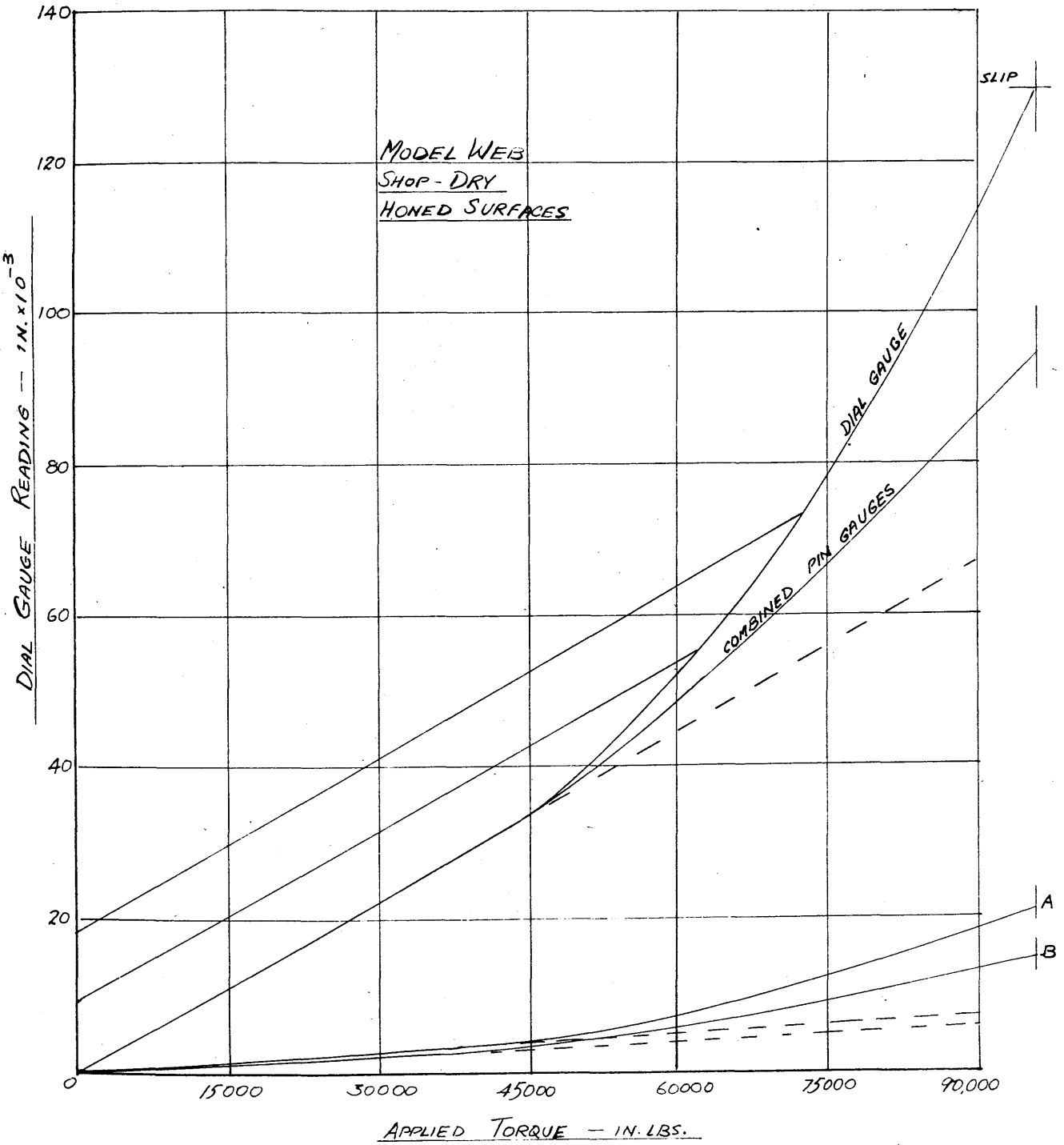
MODEL WEB
SHOP - DRY
HONED SURFACES
DIAL GAUGE READING — IN. x 10⁻³
140
120
100
80
60
40
20
0
15000
30000
45000
60000
75000
90,000
APPLIED TORQUE — IN. LBS.
SLIP
DIAL GAUGE
COMBINED PIN GAUGES
A
B

FIG.48

in which actual or incipient overstrain is present, thus inducing plastic flow.

The mode of failure under torque action was discussed in the paper by Baugher (2), reviewed in Part I , and the former explanation was advanced, presumably on the basis of similar experimental evidence. There are several reasons, however, why the latter explanation is more likely.

1. It is difficult to visualise the surface conditions within the grip in the event of partial slip. If relative movement has occurred at one point and not another, there must be a transition zone of discontinuity and therefore a zone of discontinuity of strain, and consequently of stress, on either or both of the elements, which is unlikely.

2. The relative movement at the entry side of the pins would be recorded on the pin gauges and the readings of both pin gauges should therefore account for the departure from the elastic straining of the apparatus recorded on the dial gauge. Fig. 48 shows the experimental discrepancy.

3. If the web is near the point of overstrain under the shrink stress system, as is extremely likely, the additional superposed stress system due to the torquing would be expected to produce plastic flow.

4. Inelastic strains occurring in the web, outwith the

radius of attachment of the pin gauge would not be recorded thereby, i.e. the plasticity penetrates the bore layers of the web to a greater radial depth than the gauge attachment, about 0.1" from the bore. The effect of such plastic strain is, of course, recorded on the dial gauge.

5. The experimental scatter in the pin gauge readings increases with the applied torque. This is consistent with an increasing amount of surface plasticity under the bonding of the gauge attachments. The higher degree of scatter with pin gauge B is probably due to less secure bonding at the initial attachment of the gauge.

If the pin and web assembly were regarded as of integral construction the sharp re-entrant corner between the pin and the web would be known as a "stress raiser". With a true 90° notch, the mathematical discontinuity of shape transition requires that, for practically all loading conditions, the stresses be infinitely large. In an integral assembly, overstrain would occur at quite low values of torque, allowing a more even transmission of torque from pin to web. If both elements of a shrink-fit behave elastically, there is no reason to believe that the friction stresses at the interface are different from the circumferential shearing stresses at the equivalent section of the integral component, and therefore either

slip or overstrain must occur with this design of assembly. On this account, shrunk assemblies should be designed with the transition fillet considered to be essential in the integral arrangement. Even in the absence of direct evidence of poor stress conditions at the entry of a shrink-fit, traditional design practice for stressed components has avoided the sharp transition of shape which results from the common practice shrinking directly on to a shaft without altering the diameter at the grip.

3. EXPERIMENTS ON FULL-SCALE CRANK WEBS.

A. Introductory.

On account of the physical dimensions of built crankshafts in marine engineering practice, it is impractical for economic reasons to carry out numerous investigations of the shrink-fit stress system in full-scale specimens, such investigations being necessarily destructive. Nevertheless it is essential that the results of experiments on ring-and-plug specimens and on model crank webs should be correlated to the full-scale component.

Three tests on webs cut from a scrap 21" diameter built crankshaft are described in this Section. The shaft had been in service for a number of years in M.V. "CLAM" and had been reconditioned in 1942 by the Sun Shipbuilding & Dry Dock Co., Chester, PA. new pins and journals being fitted at several cranks. The complete shaft, comprising two 3-throw sections, is shown in Fig. 49. The aft section had all pins and journals renewed and the two aft webs annealed. In the reconditioning, the original dowels at 45° points on bridge-piece, were ommitted and the cavities filled with weld metal. The vessel was scrapped about 1946; the aft portion of the shaft had therefore been in effective service for approximately four years.

Sufficient information about the work carried out was

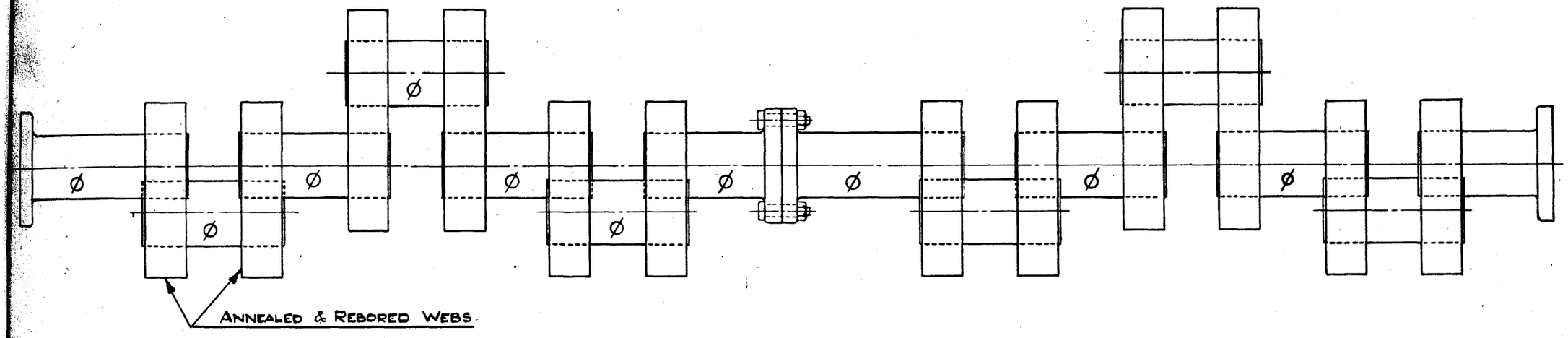

COMPLETE SHAFT

RENEWED PORTIONS INDICATED THUS: Ø

SCALE:- 1/40TH FULL SIZE

FIG. 49

obtained from the reconditioning firm, to justify making an investigation of the residual stress system and strength of grip, in the used shaft. A further investigation of the stress system was carried out after parts of the shaft had been annealed and rebored, the results of which correspond to the condition in a new shaft prior to service. A comparison of the results of these tests indicates the effect of operating conditions.

The stress analysis was carried out using wire resistance strain gauges, and a practical technique and suitable apparatus were developed as the test progressed. This method of strain measurement is still comparatively novel, and considerable time was spent investigating the scope, limitations and accuracy of gauges and associated apparatus. Improvements to the accuracy and reliability of the method, and economies in cost and in time of preparation and execution of tests, were made. A separate section is concerned entirely with a report of the development work carried out. In this section no details of the technique of electrical strain measurement are given.

B. Stress System in Used Crank Web - Pins Cut Out.

(a) Apparatus and Procedure.

(i) Specimens.

The aft section of the scrap crankshaft, comprising 6 webs, 4 journal pins and 3 crank pins, was cut up for test specimens. Three of the webs, Nos. 7 , 11 and 12 as shown in Fig. 50 , were each cut into three parts by slitting vertically on a band saw, resulting in nine slabs each about $3\frac{1}{4}$" thick of the plan form, shown in Fig. 51 . The aft section of the aft web (No. 12A) was selected for this test.

(ii) Removal of Pins.

The crank pin was removed by trepanning a circular groove about $\frac{1}{2}$" from the interface, allowing the centre piece to be removed. The shell was progressively bored out until it could be collapsed and removed by hand tools. The journal pin was then removed in the same way. Plate 2 shows the arrangements for carrying out this work.

(iii) Strain Measurements.

Strain measurements were made on the forward face of the web slab by a pattern of electrical strain gauges located round the crank pin as shown in Fig. 52 . Eight gauges were arranged round the journal on this face as shown in Fig. 52 and

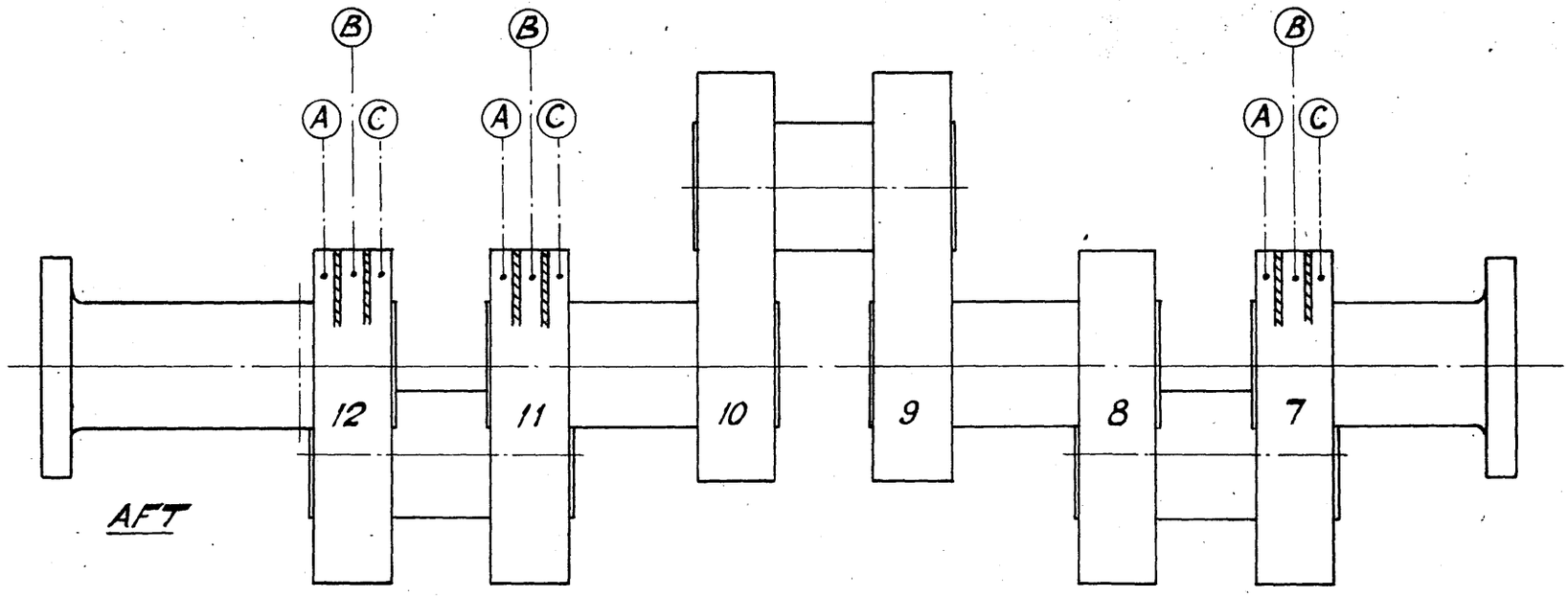

FIG. 50

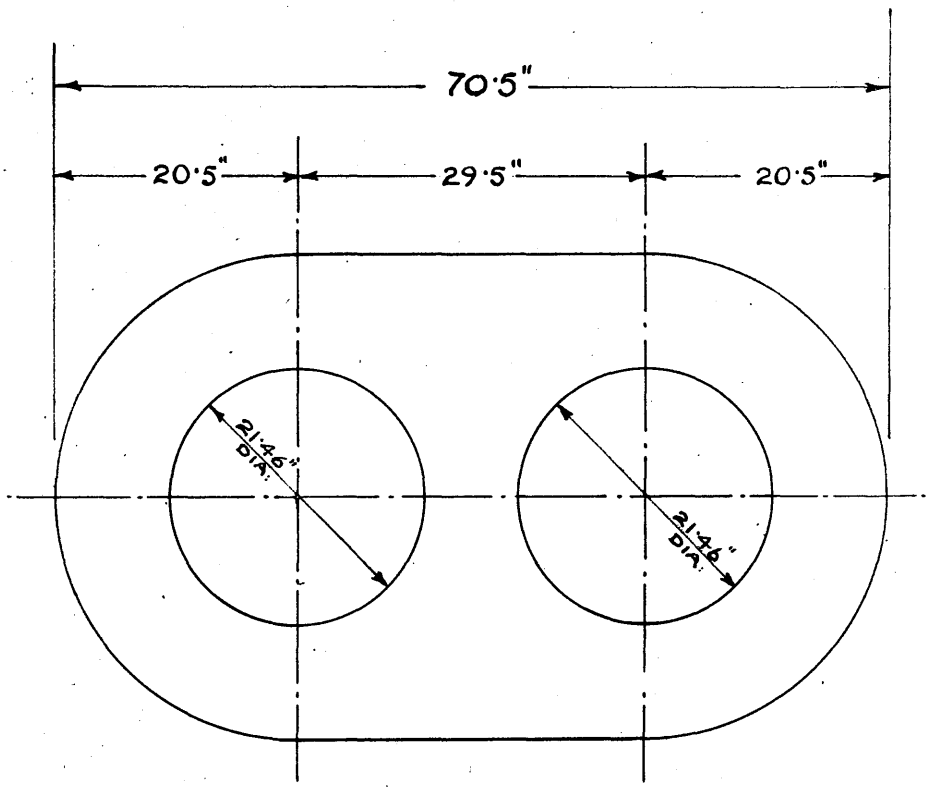

FIG:51

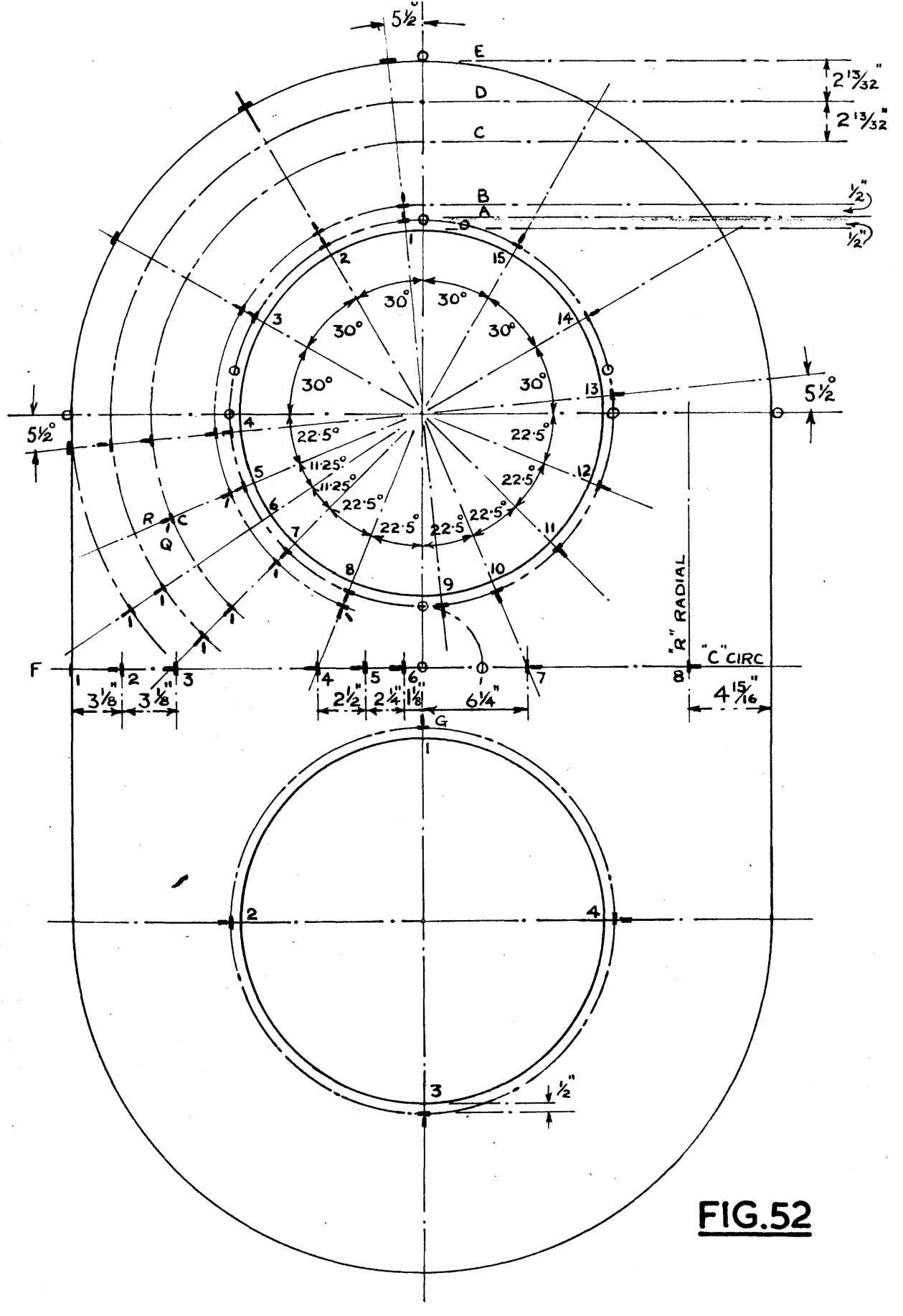
5½°
E
D
C
B
A
2 13/32"
2 13/32"
½"
½"
30°
22·5°
11·25°
5½°
5½°
R
C
Q
F
"R" RADIAL
"C" CIRC
3⅛"
3⅛"
2½"
2¼"
1⅛"
6¼"
4 15/16"
G
½"

FIG.52

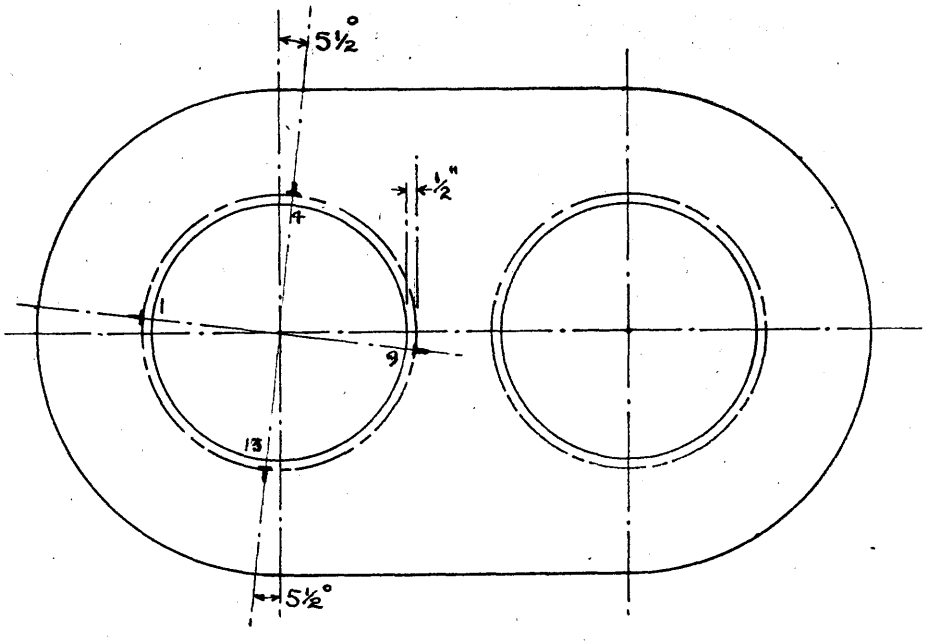

FIG:53

PLATE 2

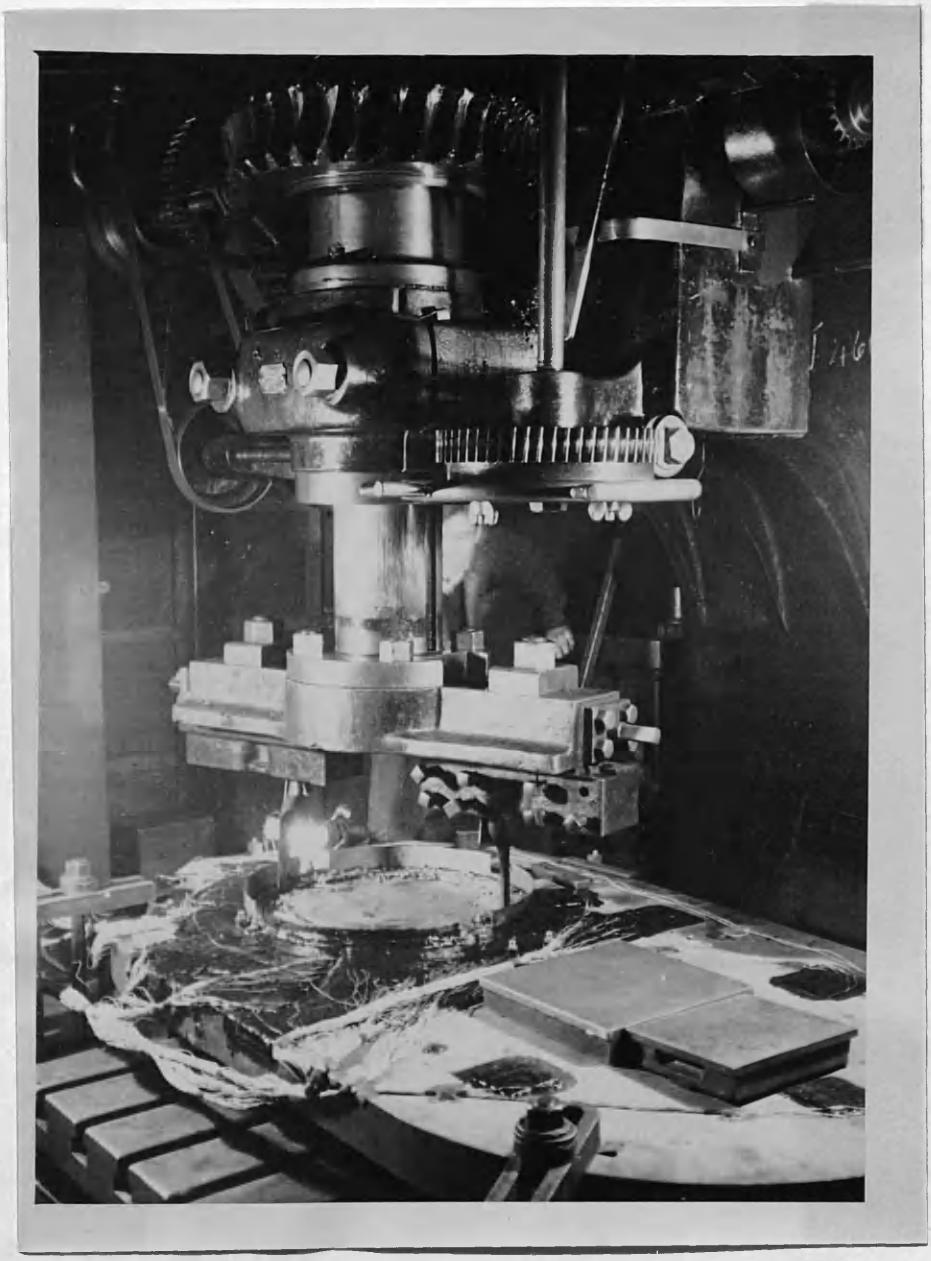

TREPANNING PINS FROM USED CRANK WEB.

a similar number round the crank pin as shown in Fig. 53 on the reverse, or aft face.

(iv) Length Measurements.

Mechanical measurements of selected dimensions were made by length bars and slip gauges, as a check on the electrical measurements. The measurements were made between the surfaces of $\frac{1}{2}$" ball bearings brazed to the ends of turned pedestals, which were screwed into holes bored and tapped in the face and edges of the web. The locations of those measurement points is shown by the small circles in ~~Fig. 51~~ TABLE II .

Plate 3 shows the forward face of the slab prepared with strain gauges and measurement points, before the gauges were wired and covered.

Readings of electrical gauges and measurements between gauge points were made before trepanning, after removal of crank pin, and after removal of journal pin.

(v) Bore Measurements.

After removal of crank and journal pins, the diameters of the bores were measured on four axes at two axial positions.

(vi) Tensile Tests.

Tensile specimens were cut from the web at points shown in Fig. 54 , on completion of the experiment.

PLATE 3

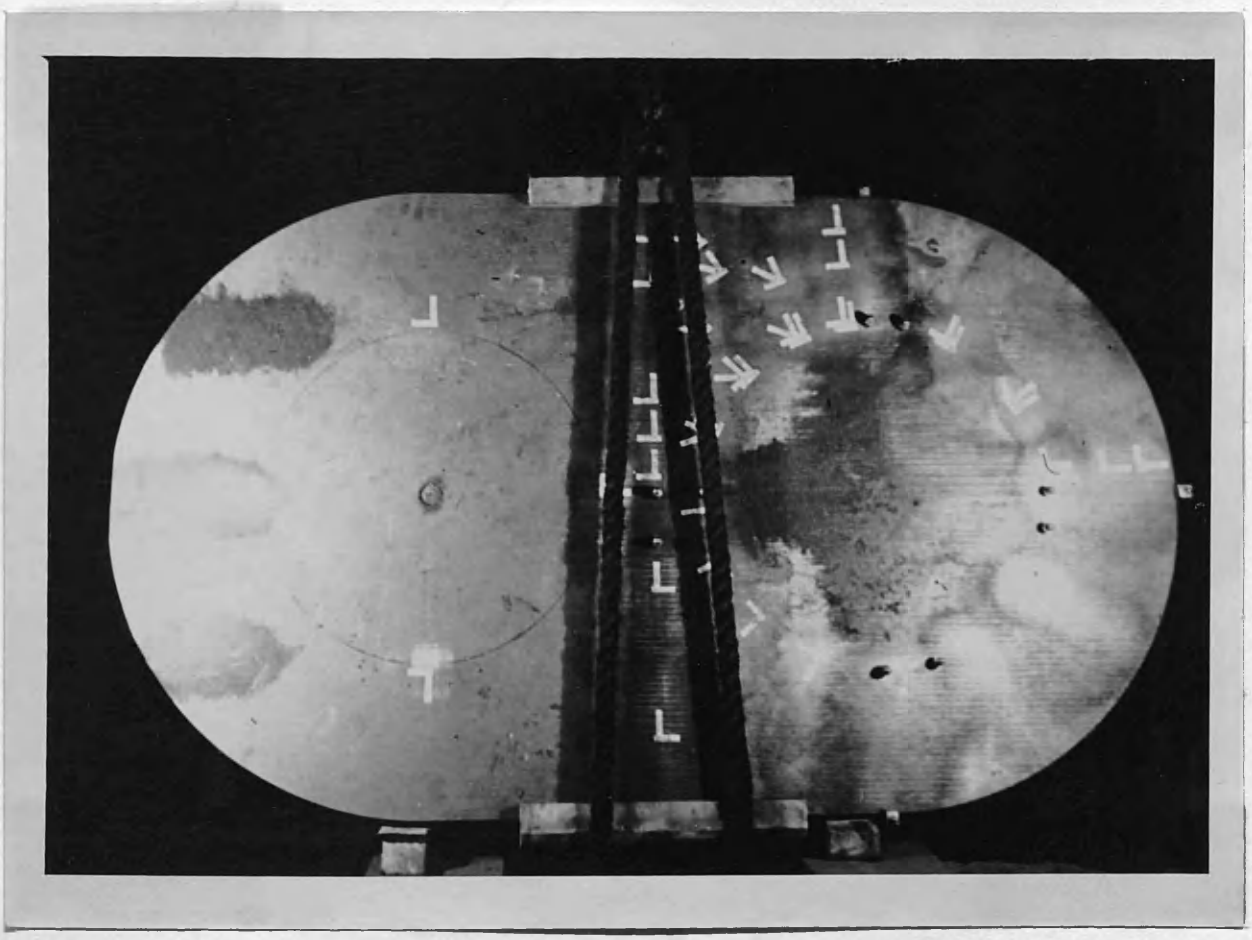

ELECTRICAL STRAIN GAUGE PATTERN

BEFORE WIRING (USED WEBS).

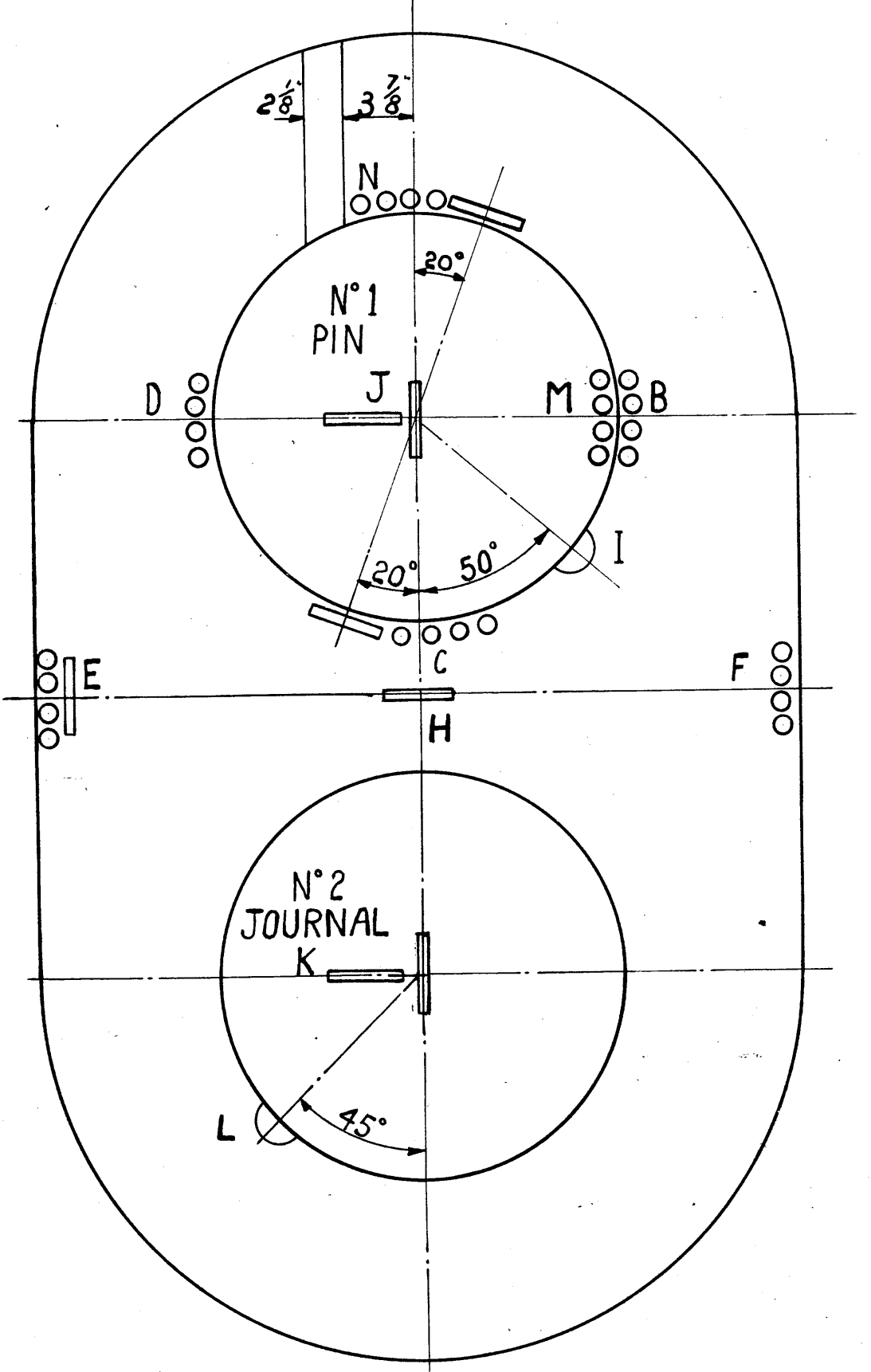

FIG:54

(vii) Surface Finish Measurement.

After separation the surfaces of pins and bores were examined by the Talysurf and Tomlinson surface finish recorders.

(b) Results, Discussion and Analysis.

(i) Mechanical Properties of Material.

It was not expected that the results of the tensile tests shown in Table 8 below, would indicate any definite trend in yield stress values or percentage elongation. Under stress systems such as exist in web shapes of this type, the plastic strains are comparable in magnitude with the elastic strains. The common characteristics of strain hardening, increase of yield stress and decrease of percentage elongation, are exhibited only if the plastic strains are allowed to develop fully to a magnitude considerably greater than the strain at the yield point. If the magnitude of the plastic strain is restricted to the same order as that of the elastic strains, such characteristics will not be manifested. The variations shown in Table 8 below, are not considered to be significant.

(ii) Stress System.

The summary graphs presented in Fig. 55 give the principal stresses derived from the strain readings, according to the two dimensional elastic formulae:

$$p_{1,2} = \frac{E}{1 - \sigma^2} (e_{1,2} + \sigma e_{2,1})$$

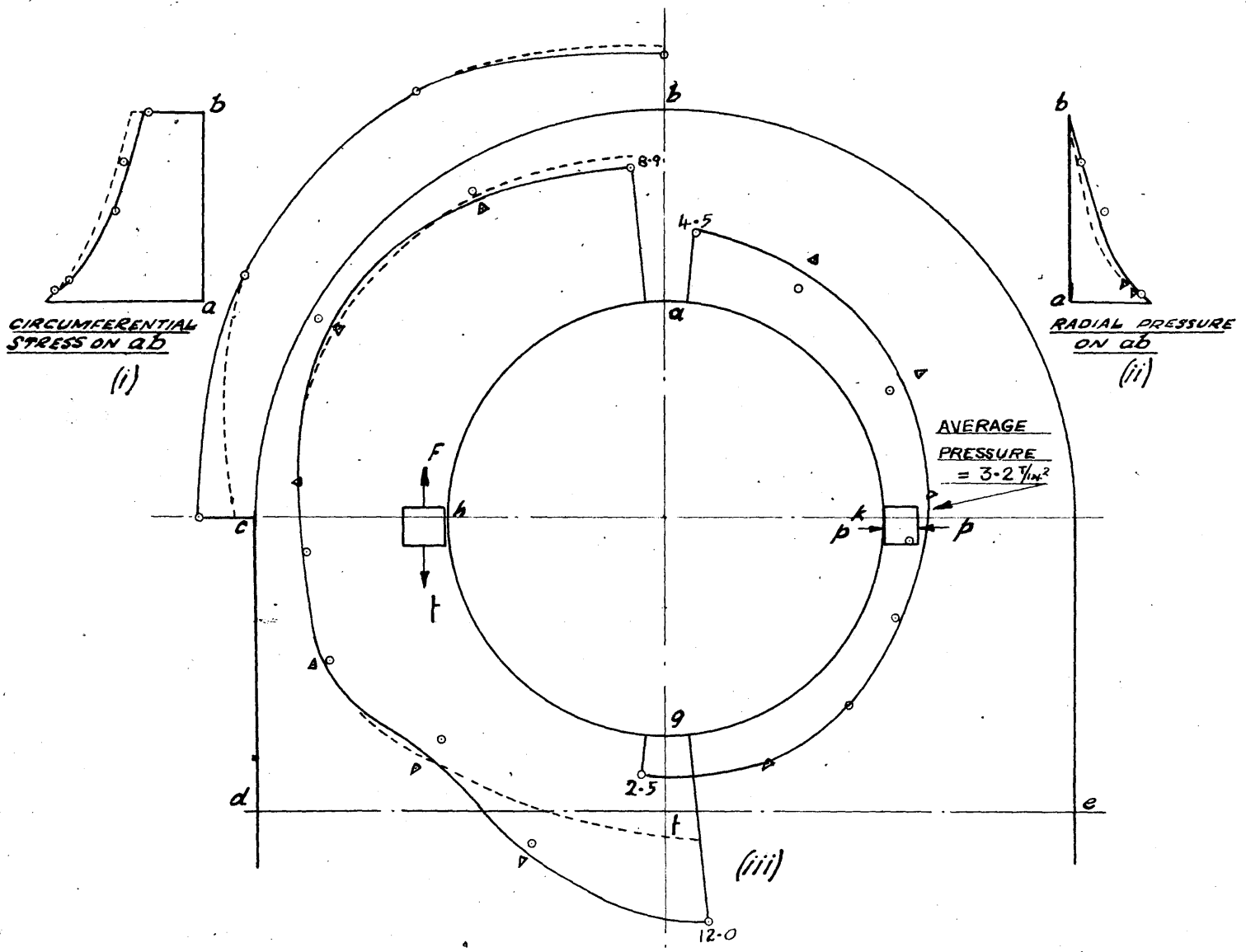

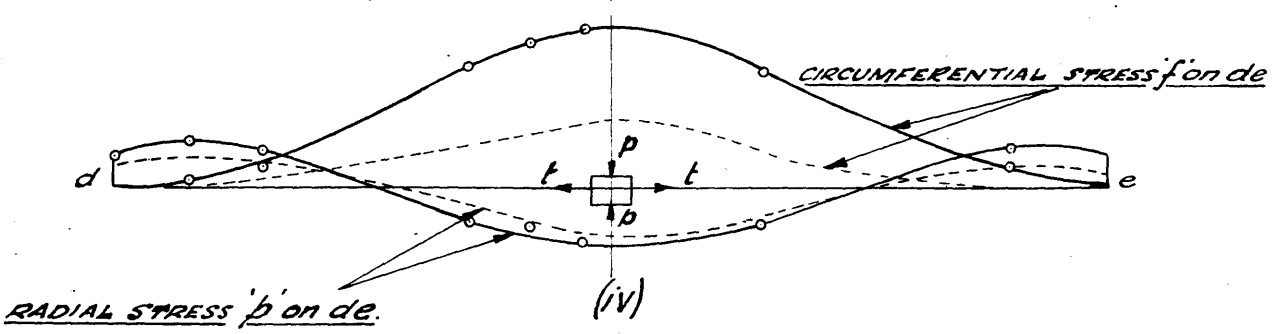

NOTE: DOTTED CURVES = PIN ONLY REMOVED
FULL CURVES = PIN & JOURNAL REMOVED
Δ POINTS FROM R. HAND HALF OF WEBS
o " " L. HAND " " "

SCALE: 1" = 10T/0" ⅝ X FULL SIZE

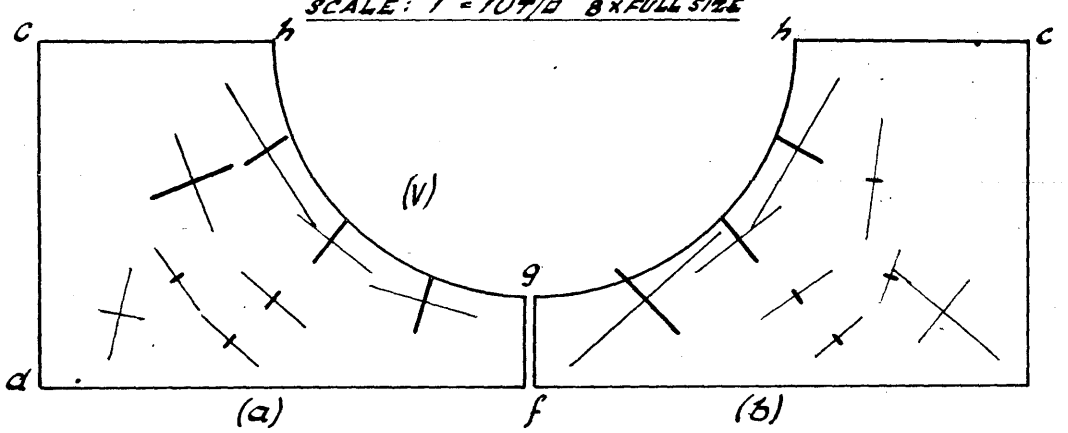

(v) DIRECTION & MAGNITUDE OF PRINCIPAL STRESSES IN PORTION "cdfgh"

(a) PIN ONLY OUT
(b) PIN & JOURNAL OUT

FIG. 55

TABLE 8

Yield Point T/in^2	Maximum Stress T/in^2	% Elong.	% Red. Area	Young's Modulus T/in^2	Remarks.
14.67	30.41	14	16.3	13,840	Average of two 'N' specimens.
14.78	31.19	24	29.9	13,400	Average of two 'B' & two 'D' specimens.
14.75	30.93	21	25.4	13,600	Average of two 'B' two 'D' & two 'N' specimens.
14.84	31.09	30	41.85	13,540	Average of two 'E' specimens.
15.50	30.76	17	21.6	11,500	Average of two 'C' specimens.
14.90	30.95	23	30.25	13,250	Average of all 12 specimens

It should be noted that all stress values quoted in the following are in fact "change of stress" values only, since the strain gauges do not differentiate between recoverable and residual stresses. Consequently if residual stresses are present the values quoted will not represent actual conditions.

Both tensile circumferential and compressive radial stresses vary round the bore in a manner symmetrical about the longitudinal axis of the web. The maximum value of the former appears to be situated on the axis between the bores while the latter exhibits its greater value about 30° from the axis at the bore remote from the bridge-piece.

The tensile circumferential stress on the outer periphery of the web shape appears - for all practical purposes - to be

uniform.

The radial distribution of stress across the eye-piece at section "ab" exhibits typical thick cylinder variation with maximum values of the circumferential and radial stresses at the bore.

The stress distribution along the bridge-piece at section "de" shows tensile stress values perpendicular to the longitudinal axis accompanied by compressive stress values parallel to the axis, in the middle portion. The latter changes from compression to tension, passing through a zero value at approximately the quarter points.

Directions and magnitudes of the principal stresses on one quadrant of the web between the bores are given in Fig. 55. It can be seen that the deviation in direction from the radial and tangential orientation is negligible, except in the vicinity of the bridge. The available readings, however, are considered to be too few to make this conclusion definite.

For purposes of comparison, Table 9 gives maximum stress values recorded by the gauges.

(iii) Effect of Successive Removal of Crank and Journal Pins.

The order of dismantling was crank pin followed by journal pin. In general it can be seen from Fig. 55 that the removal of the second element affected stress conditions

TABLE 9

Type of Stress	Position	Stress Tons/in^2	Fraction of Circumferential at bore
Circumferential	On axis at bore on bridge.	12.00 tensile	1
Radial	On bore remote from bridge 30° from axis.	5.22 Compressive	0.435
Circumferential at outside radius	On outer periphery 30° from axis.	4.81 tensile	0.40
Perpendicular to axis	On the axis at centre of web.	8.35 tensile	0.68
Parallel to axis	- do -	2.78 compressive	0.23

TABLE 10

	STRESS - T/in^2.			
Operation	Radial at bore 30° from axis remote from bridge.	Circumferential at bore on bridge.	Radial at centre of web on axis.	Perpendicular to axis at centre of web.
Crank pin only removed.	4.82	6.51	1.97	3.66
Both pins removed.	5.23	12.00	2.78	8.35
% change.	8	45	29	56

appreciably only in the material between the bores, as indicated, for example, by the stress distribution across the bridge. It should be noted that at this section the stress values shown are principal stresses only in the case of both pins removed (curve shown by full line). This is due to the fact that removing the crank pin creates a stress system unsymmetrical about the lateral centre-line of the web; consequently the orientation of the principal stresses at section "de" is not in the direction of the strain gauges.

The percentage relief of stress at selected points due to removing the second pin, and based on the final stress, is given in Table 10.

The percentages may be taken to represent the effect of fitting the second pin, provided that, on fitting the elements, elastic stresses only are induced. The relief of stress is probably elastic, which is not the case on fitting the pins with a fit allowance of 1.5 mils. If plastic flow takes place during the fitting process, the percentage stress increments quoted may not be truly representative.

(iv) Comparison of Stress System with Photoelastic and Superposition Results.

In Fig. 56 the results are compared with

1. Values given by photoelastic analysis (based on Coker's work) and

2. theoretical values obtained by the superposition of two thick cylinders. The latter process, slightly different from the superposition by Dorey's method shown in Fig. 13 , is illustrated in Fig. 57 .

The basis of comparison is the circumferential stress at the bore on the axis between the bores. The experimental, photoelastic, and theoretical circumferential stresses are assumed equal at this point. All other values were obtained by proportioning to this basic value.

Referring to Fig. 56 and noting that the experimental results are indicated by points, the photoelastic values by chain dotted lines, and the theoretical quantities are given by full lines, the proportional curves test the correspondence of the experimental results relative to each other and to the derived values. It is seen that, on the whole, good agreement is obtained with both the theoretical and photoelastic results, but that the experimental hoop stress round the eye-hole at the bore is consistently high. This is discussed in the next section.

(v) Interface Pressure.

The theoretical interface pressure in a web shape with overstrain fit allowances may be derived by the following approximate method. Due to the decrease in radial stiffness of the web compared with a simple ring of the same diameter ratio,

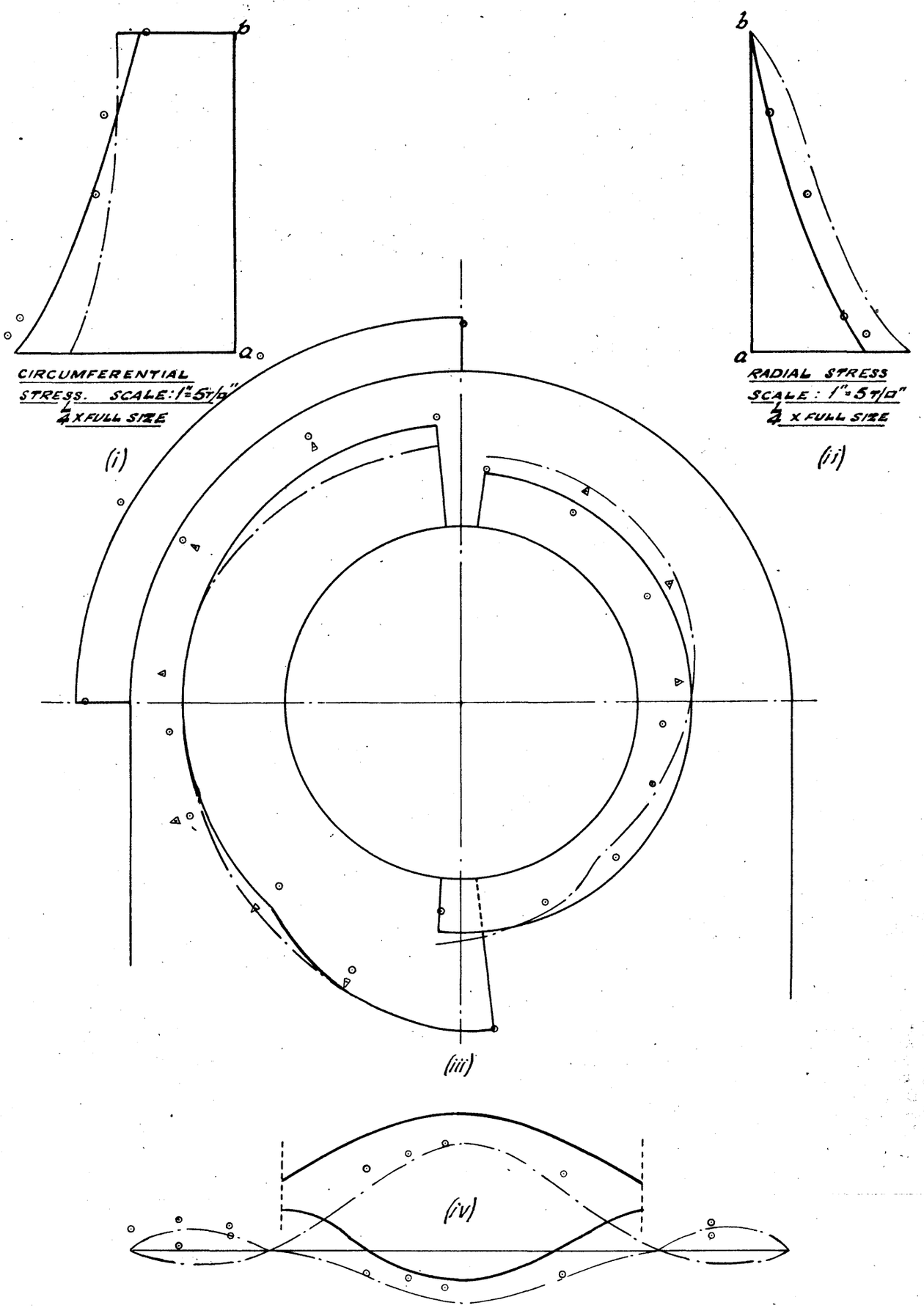

NOTE:- FULL CURVES FROM SUPERPOSITION OF TWO THICK CYLINDERS
CHAIN-DOTTED CURVES FROM PHOTOELASTIC ANALYSIS BY 'COKER'
△ Exp. Points from R. Hand half of web - pin & journal out
⊙ " " " L. Hand " " " - " - " "

SCALE:- ⅛ X FULL SIZE 1"=10T/□" EXCEPT AS NOTED

FIG. 56

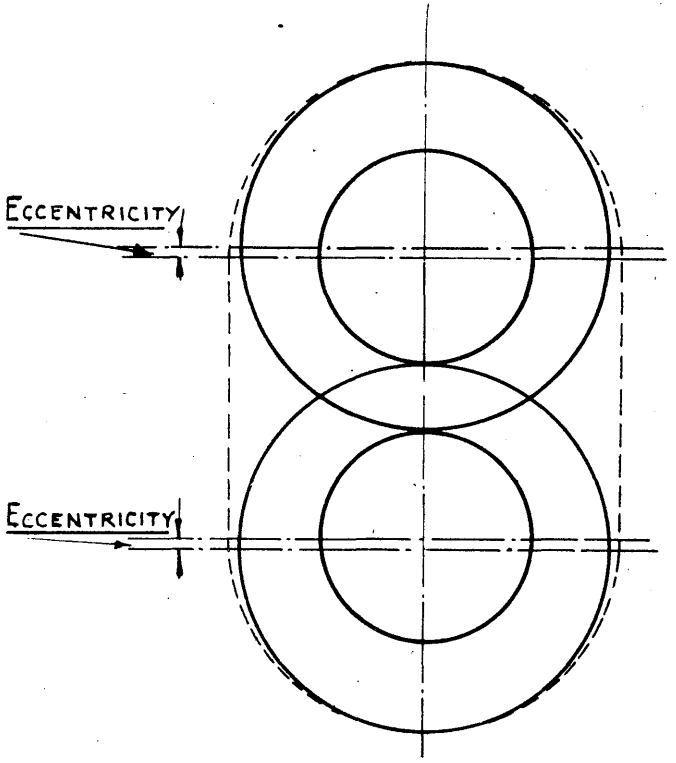

SUPERPOSITION OF TWO ECCENTRIC THICK CYLINDERS

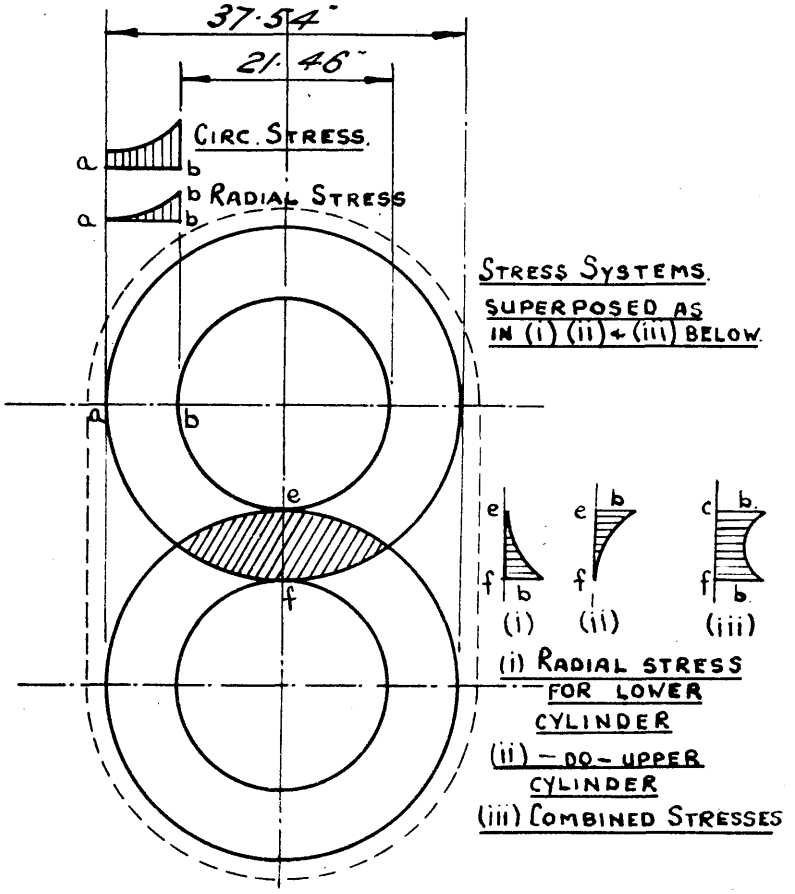

EQUIVALENT SUPERPOSITION OF TWO CONCENTRIC THICK CYLINDERS

(DIFFERENCE NEGLIGIBLE IN THIS CASE.)

FIG. 57

the web allowance is equivalent to a simple ring fit allowance of 0.9 x 1.5 = 1.35 mils, (see Part II, Section 5.). This fit allowance, with an axial grip factor of $\frac{1}{2}$ and no temperature correction would result in permanent set of the bores of 0.06 mils (obtained by graphical methods). The residual fit allowance of 1.35 - 0.06 = 1.29 mils would induce a pressure (or a release of pressure) under elastic conditions of

$$P = \frac{1}{1 - m\sigma} \frac{k^2 - 1}{2k^2} E\Delta r = 6.1 \text{ T/in}^2$$

assuming that m = 0 , owing to the short axial length of the slab.

The average radial pressure given by the experimental results in 3.2 t/in^2, or 52% of the calculated value. The explanation may be that the stress concentration in the bridge of the web shape causes a greater amount of permanent set than the ring theory suggests. The inferred value of residual fit of 1.29 mils is therefore in error. A more likely explanation is that service loading of the web had resulted in additional overstrain and loss of fit. The residual fit could not be checked from the bore measurements, as original sizes were not available, but a taper is shown by the bore measurements, suggesting bell-mouthing at this face of the web due to pulsating bending loads in service.

(vi) Comparison of Mechanical with Electrical Measurement.

The measurements by length bars were reduced to average strains at the location of the measurement points. These values are compared with the average of electrical strains in the vicinity in Table 11 . The agreement is satisfactory.

(vii) Bore Measurements.

After completion of the test, bores of both pin and journal holes were measured. The results are shown in Fig. 58 . It can be seen that the crank pin hole is oval with its long axis approximately perpendicular to the web axis and the journal stud hole oval with its long axis approximately parallel to the web axis. Measurements at inside and outside surfaces indicate, in general, an axial taper of about .002" , suggesting bell-mouthing of the web.

(viii) Surface Finish Records.

Figs 59 and 60 show typical surface records obtained by the Talysurf surface recorder. Plate 4 shows a 10x magnification photograph of the surface of the crank pin. Surface records of the equivalent mating surfaces of the web bores, by the Tomlinson macro surface recorder are shown in Fig. 61 . The surface roughness of the bores is clearly of a different order from that in the model webs reported in Section 2 above.

TABLE II

COMPARISON OF ELECTRICALLY & MECHANICALLY MEASURED STRAINS

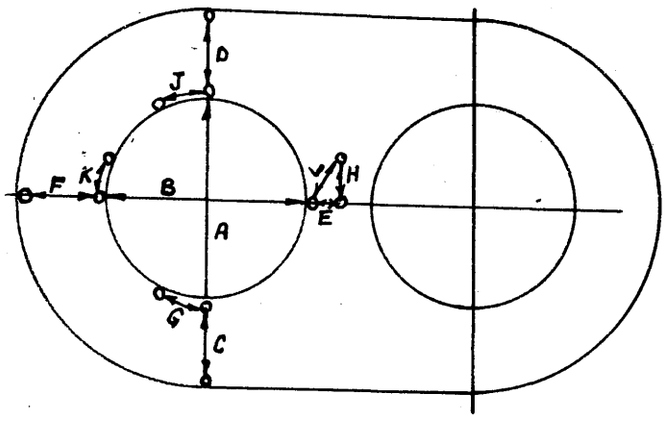

MEASUREMENT	MECHANICAL STRAIN $\times 10^{-6}$	ELECTRICAL STRAIN $\times 10^{-6}$	REMARKS (FOR GAUGE LOCATIONS SEE FIG 3)
DIAMETRAL A	843	634	CALCULATED FROM LAMÉ USING EXP. VALVES OF RADIAL & HOOP STRESS. (Hoop Stress = 9·62 T/in² Radial Stress 3·25 T/in²
DIAMETRAL B	783		
C	291	331	ARITH. AVERAGE OF VERTICAL GUAGES A4 & B4
D	356	300	2/3 OF READING OF VERTICAL GUAGE A9
E	529	456	MAX. RADIAL STRAIN AT BORE GAUGE A9
F	392	360	ARITH. AVERAGE OF RADIAL GAUGES A1, B1, C1, & D1.
G	830	724	CIRCUMF. GAUGE A4 (B4 = 825)
H	403	686	CIRCUMF. GUAGE F6
J	978	836	ARITH. AVERAGE OF CIRCUMF. GAUGES A12, 13, & 14.
K	967	782	ARITH AVERAGE OF CIRCUMF. GAUGES A1, A2, A15 & B1.

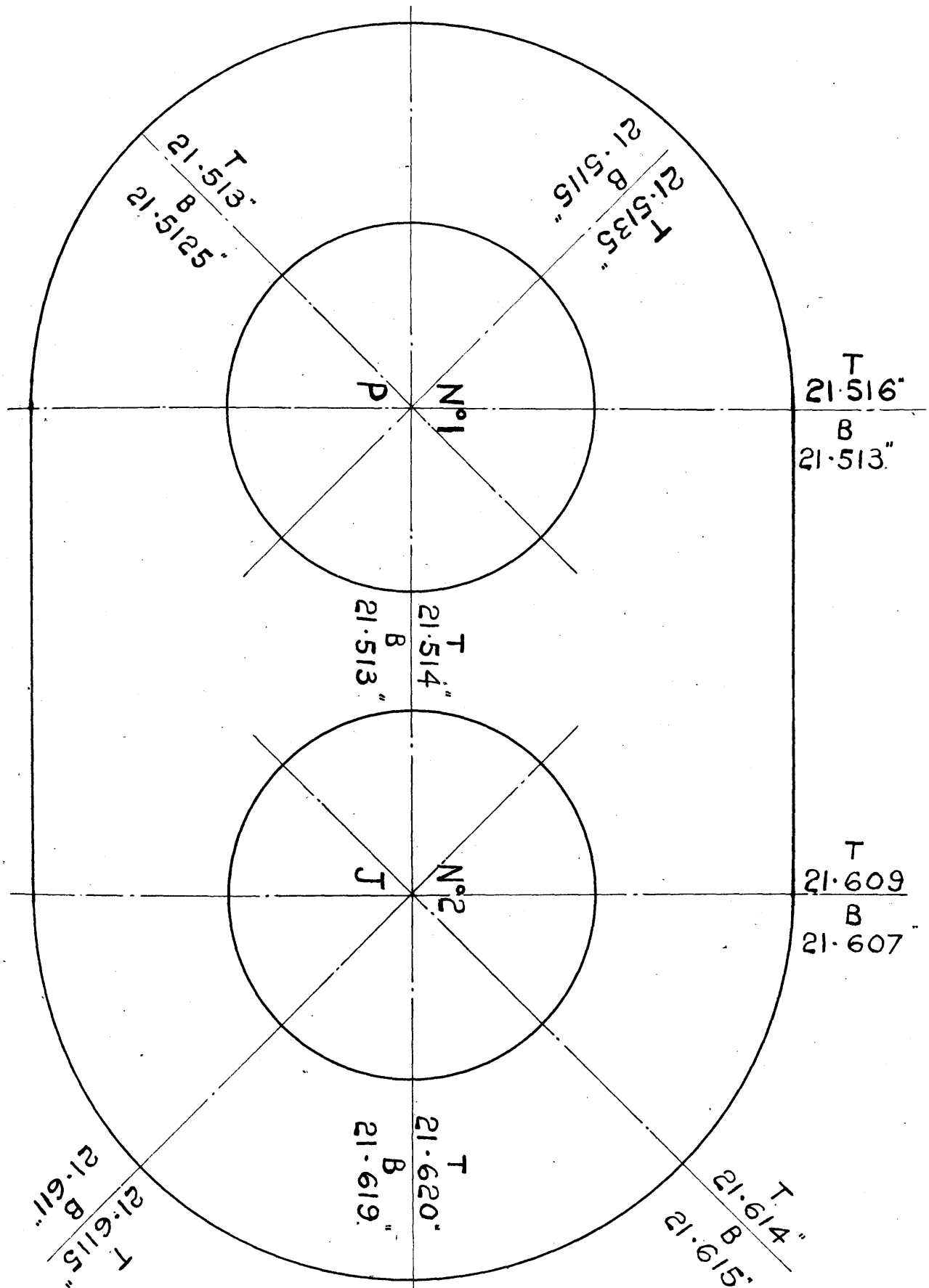
T
21·513"
B
21·5125"
T
21·5135"
B
21·5115"
P
N°1
T
21·516"
B
21·513"
B
21·513"
T
21·514"
J
N°2
T
21·609
B
21·607"
B
21·619"
T
21·620"
T
21·6115"
B
21·611"
T
21·614"
B
21·615"

FIG: 58

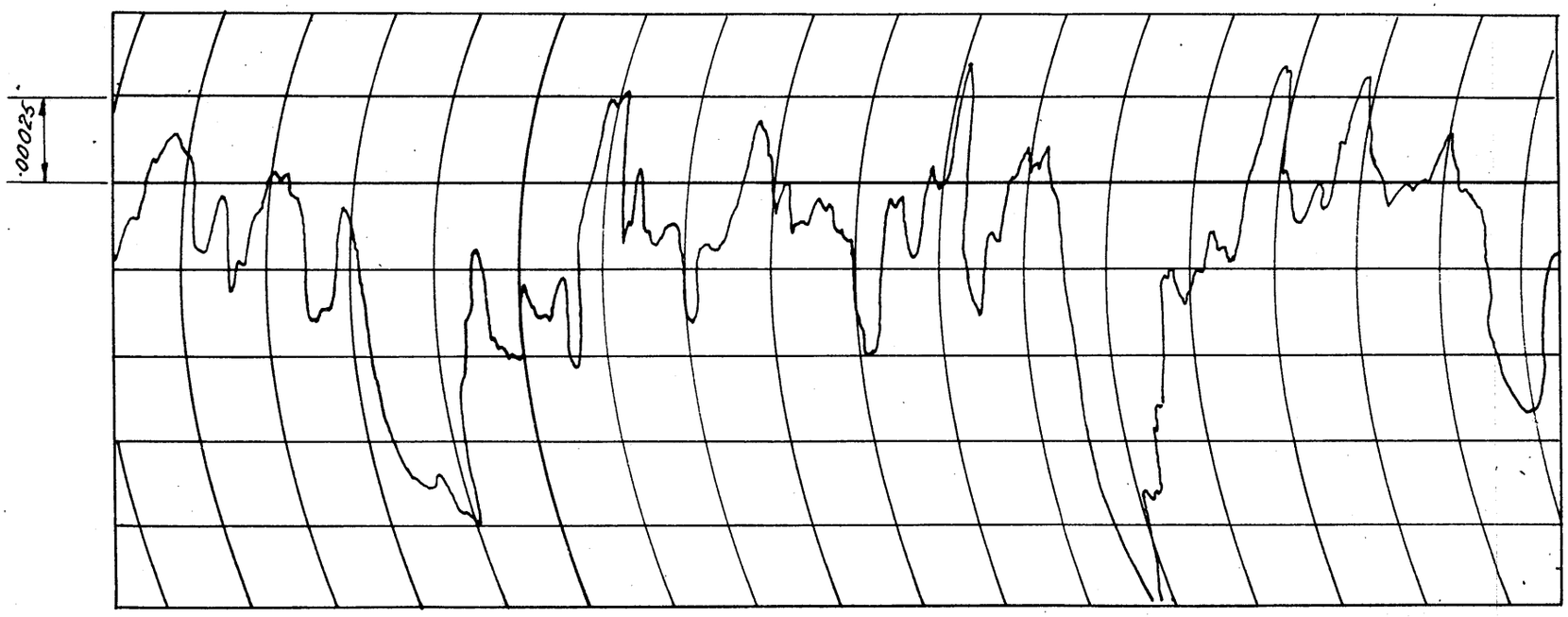

(a)

"TALYSURF" RECORD OF SURFACE FINISH.

MAG. { VERT. × 2,000.
HOR. × 200.

(b)

PHOTOGRAPH OF SURFACE.

MAG. × 10.

FIG. 59 CRANK PIN SURFACE.

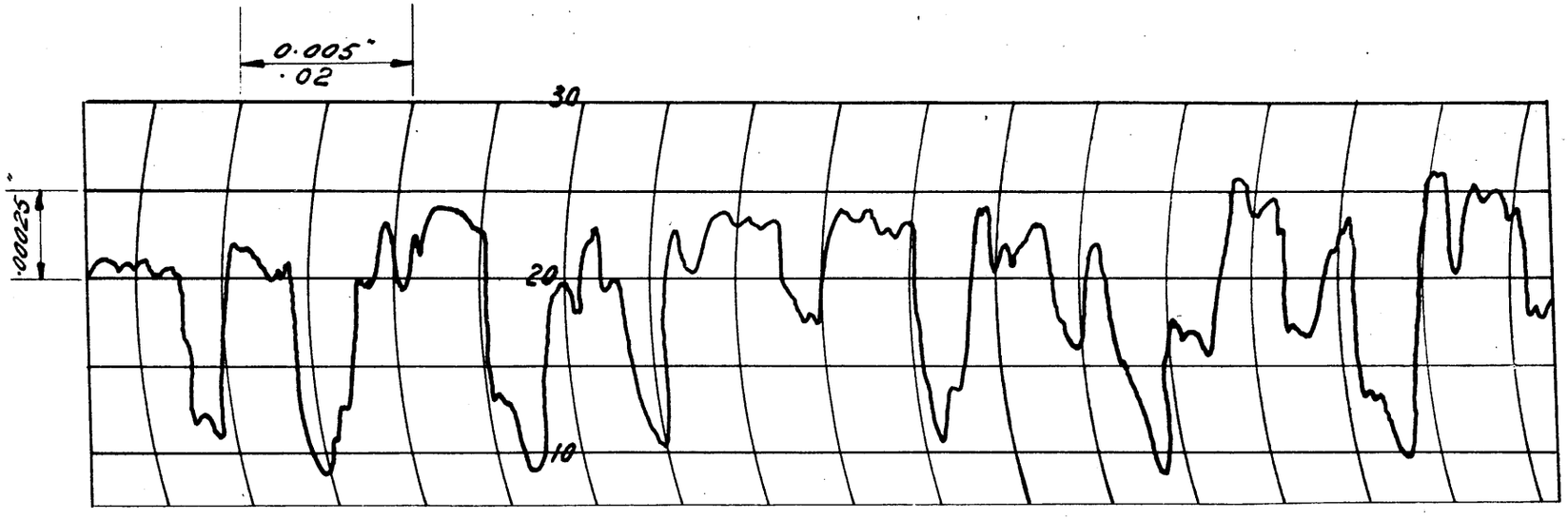

(a)

"TALYSURF" TRACE OF SURFACE

MAG. { VERT. ×2,000
HOR. ×200.

(b)

PHOTOGRAPH OF SURFACE
(MAG. × 10)

FIG. 60 JOURNAL SURFACE

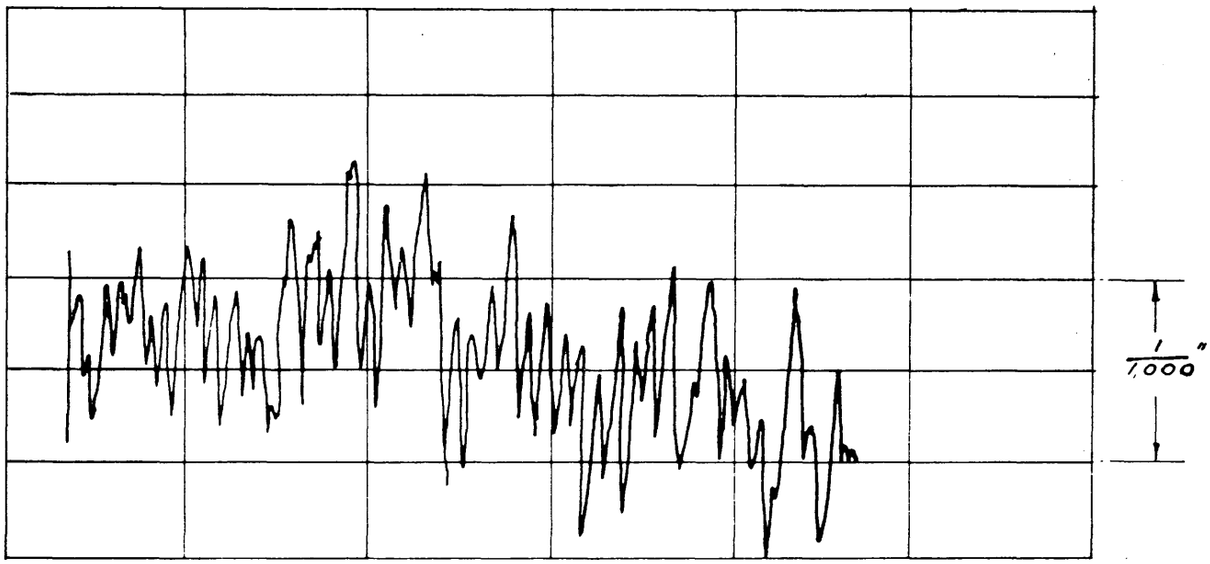

FIG 61 (a) SURFACE OF WEB "CRANK PIN" BORE

MAG:- VERT. × 1,000
HOR. × 6·9

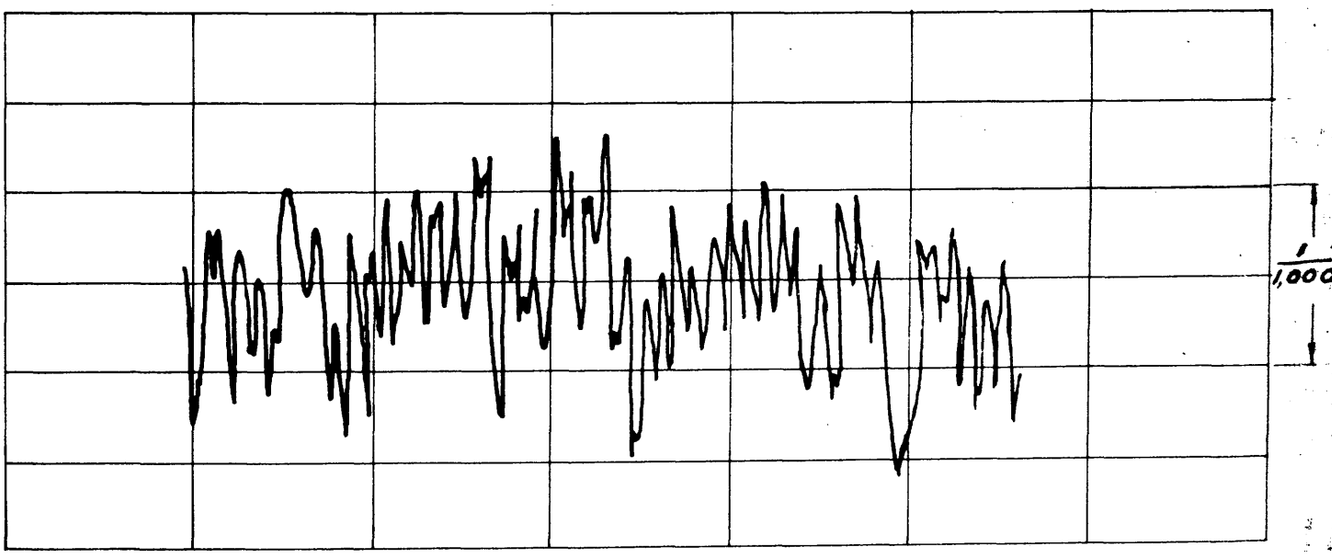

FIG. 61 (b) SURFACE OF WEB. "JOURNAL STUD" BORE.

MAG:- VERT. × 1,000
HOR. × 6·9

PLATE 4

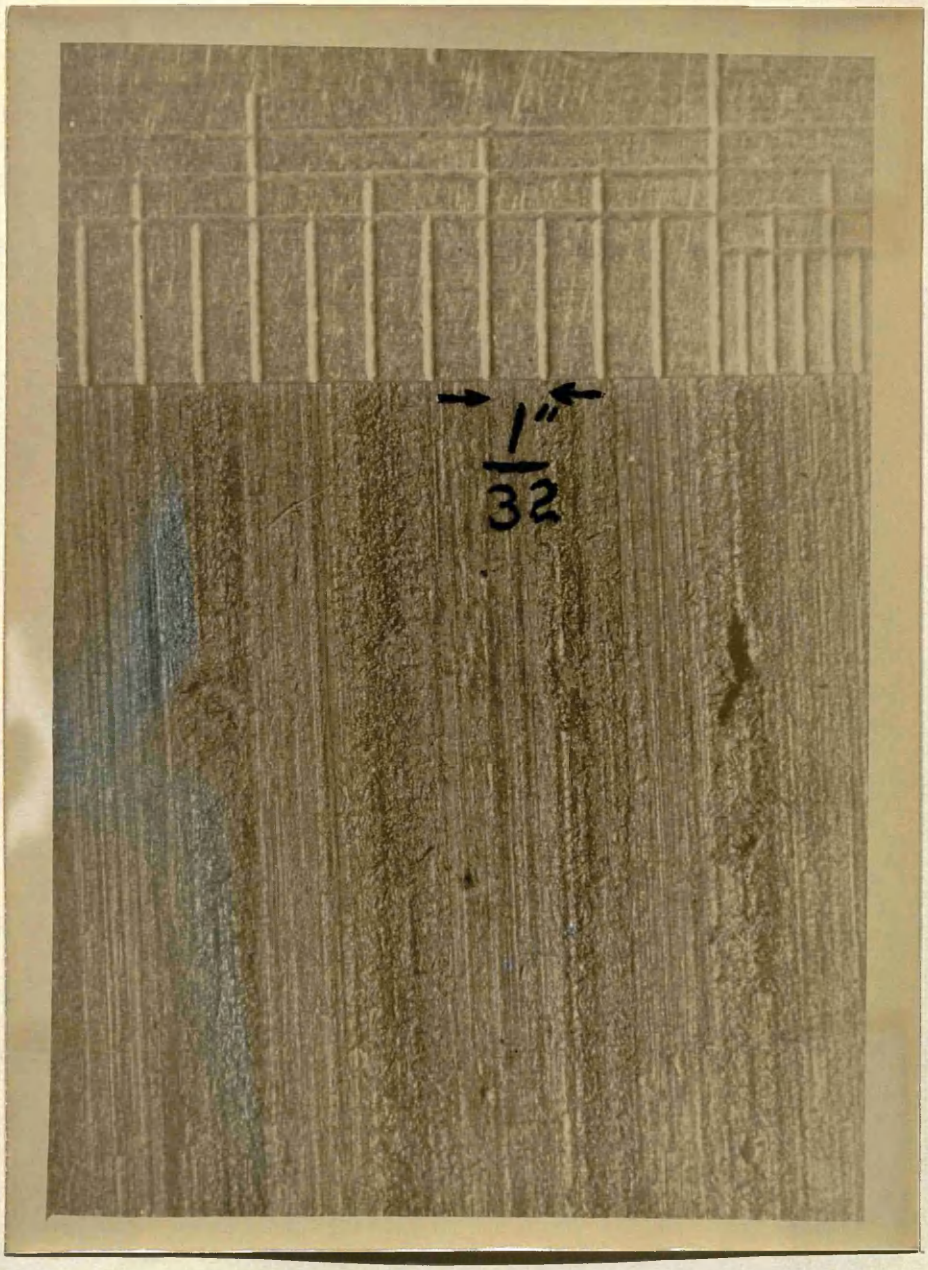

CRANK PIN SURFACE FINISH.

C. Stress System of Used Crank Web - Pins Pushed Out.

(a) Apparatus and Procedure.

(i) Specimens.

The three sections of web No. 7 were used for this experiment. The middle slab was prepared with electrical strain gauges round the crank and journal bores at 30° points as shown in Fig. 62 , but the outside slabs had no further treatment, beyond skimming of the surfaces after parting from the web.

(ii) Removal of Pins.

The crank and journal pins were removed by axial force in a 2000 ton vertical hydraulic press. The load was measured by a pressure gauge of the Bourdon type, calibrated by a compression test-piece in the platens. The test-piece elastic strain, measured by a Huggenburger tensometer, was calibrated up to 100 tons load in an Avery testing machine, and the test-piece used as a weigh-bar for the hydraulic press calibration. The two objectionable features of this method are that the calibration is indirect and that considerable extrapolation of the initially linear response of the pressure gauge was necessary. The method was tolerated only for the lack of a practical alternative, and errors estimated at $\pm$ 25 tons are possible at the maximum loads. Every care was taken to

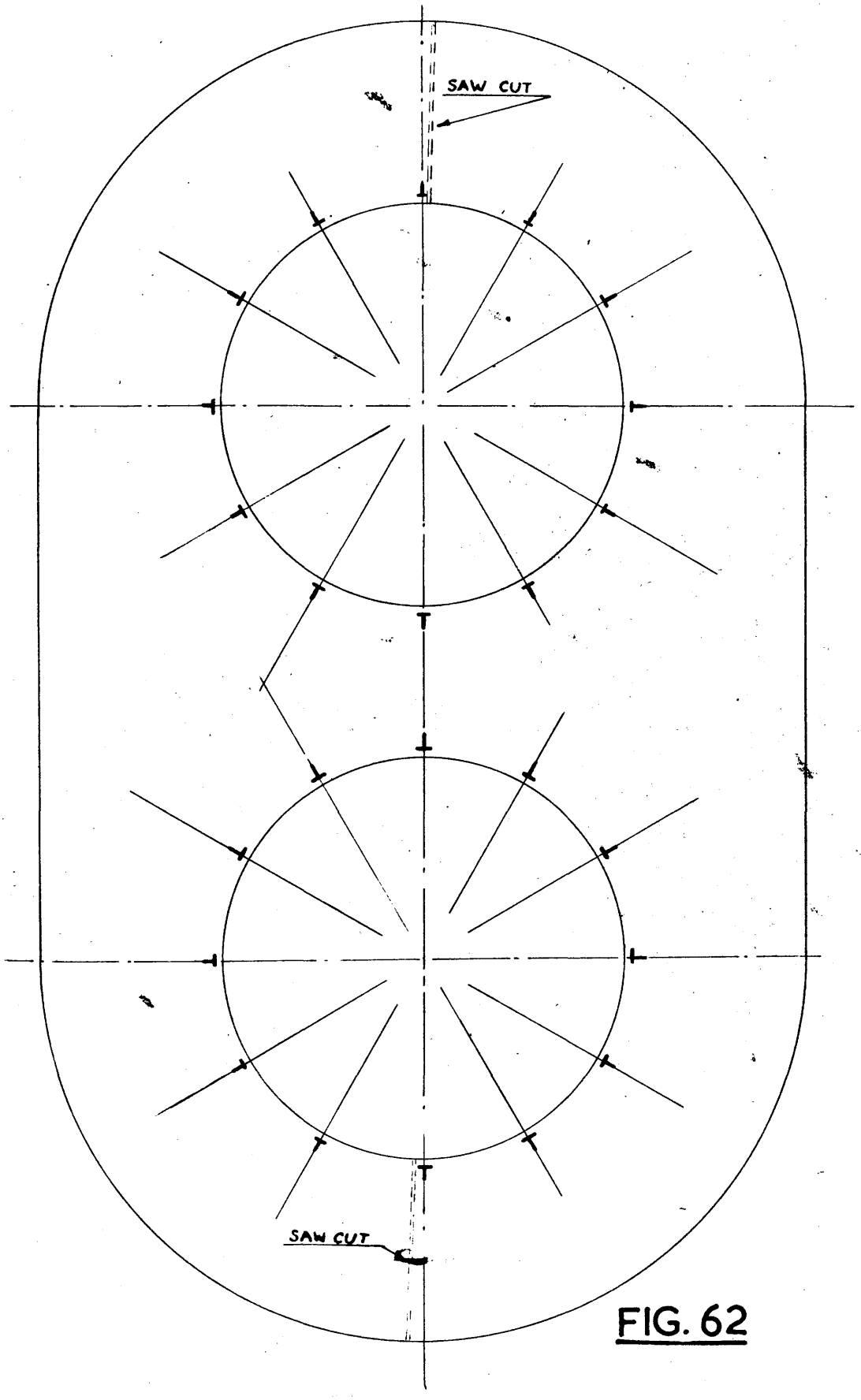

FIG. 62

allow for hysteresis effects by calibrating under increasing loads only. (The graph of push-out load, though falling with the area of grip, was obtained from successive slip loads towards which the pressure was rising). The calibration curve was in good agreement with the load calculated from the pressure and ram area, with an increasing discrepancy due to U-packing friction as the pressure increased.

Readings of pressure and ram traval.were taken as the pin was pushed out of the web. Five of the pins were successfully removed, but in one case the journal of 7 C. fouled the bolster ring; the results of this test are ommitted.

(iii) Strain Measurements.

Readings of the electrical strain gauges were taken before commencing the test on No. 7 B. slab, after removal of the crank pin and after the removal of the journal pin.

(iv) Bore Measurements.

After removal of pins the six bores were gauged with a stick micrometer set to a length standard, measurements being taken on four diameters and at two axial positions as before. In this case the pin sections were not destroyed by the removal, and the residual fit allowance was obtained from the difference of pin and bore diameters. The same number of measurements were made as for the bores; in this case a caliper micrometer set

to length standards was used.

(b) Results, Discussion and Analysis.

(i) Interface Pressure and Coefficient of Friction.

The graphs of push-out load against pin travel are shown in Fig.63 . In each case a high initial load was registered, followed by loads which diminished gradually and approximately linearly with pin travel. The graphs show the smooth curve extrapolated by dotted lined to indicate the initial seizure effect.

The intersection of the dotted lines with the ordinate at zero travel gives a load corresponding to the repeated coefficient of friction discussed in Section 2 above. The initial load corresponds to the partial seizure coefficient; the ratio of this to the repeated load coefficient is not constant.

The residual fit allowance was obtained from the pin and bore measurements, and hence the interface pressure calculated on the assumption of elastic release of stress. The pressure is given by

$$P = 0.9 \frac{1}{1 - m\sigma} \frac{k^2 - 1}{2 k^2} E\Delta_r$$

The average residual fits and calculated interface pressure are shown in Table 12 below.

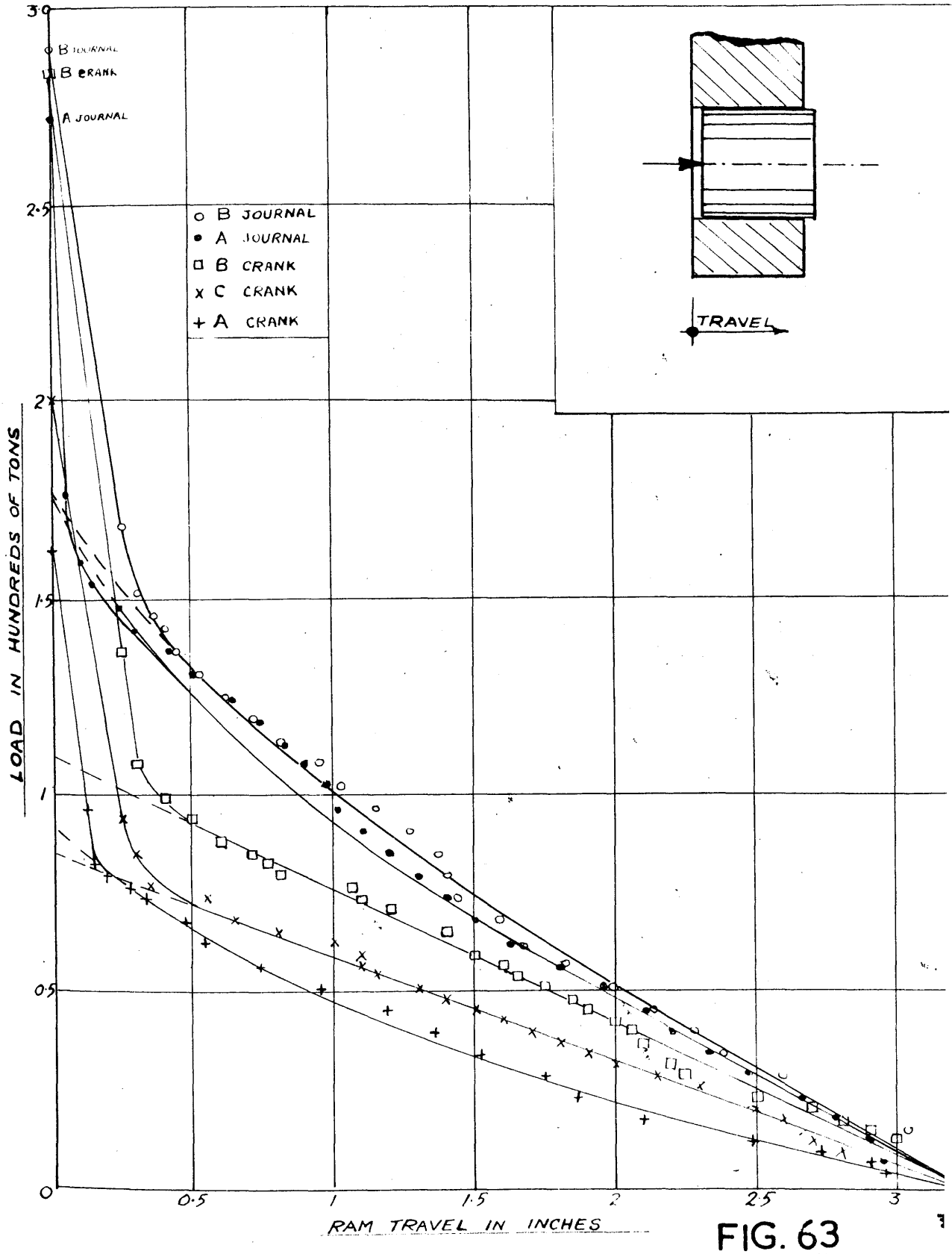
B JOURNAL
B CRANK
A JOURNAL
B JOURNAL
A JOURNAL
B CRANK
C CRANK
A CRANK
TRAVEL
LOAD IN HUNDREDS OF TONS
RAM TRAVEL IN INCHES
0
0.5
1
1.5
2
2.5
3
3.0

FIG. 63

TABLE 12

Slab		Residual Fit - mils.	Interface Pressure T/in^2.
7A	Crank	0.54	2.34
	Journal	1.00	4.34
7B	Crank	0.72	3.12
	Journal	1.04	4.50
7C	Crank	0.56	2.42
	Journal	0.86	3.72

From the above values of interface pressure the coefficients of friction corresponding to the initial and repeated loads are shown in Table 13 below.

TABLE 13

Slab		Loads - Tons		Coeff. of Friction.	
		Initial	Repeated	Initial	Repeated
7A	Crank	162	91	0.317	0.178
	Journal	272	109	0.285	0.115
7B	Crank	284	175	0.416	0.257
	Journal	290	176	0.294	0.179
7C	Crank	233	85	0.440	0.160
	Journal	-	-	-	-
			AVERAGE	0.350	0.178
			MINIMUM	0.285	0.115

The scatter observed in the model web experiments is again evident. It may be suggested that some variation is due to non-central axial loading, causing partial jamming of the pin in the bore. This is unlikely; the crank pin of 7B has a coefficient for repeated slip of 0.257 which is greatly in excess of the mean value. The push-out graph for this pin, however, was more consistently linear over the major portion than any of the other pins, showing that the pin was removed cleanly. The variations must be regarded as random.

Fig. 63 shows that the drop in friction does not occur suddenly when the grip is cracked; it appears that the minimum value is attained in the first $\frac{1}{4}$" of slip, suggesting that a distribution of surface film occurs due to the relative movement between the surfaces. In that event, the higher value of friction is more appropriate to the service conditions, where relative movement should not occur. However, it would be unsafe to assume, for design purposes, a higher value than the repeated value, since some slight working or breathing of the grip may occur, and the actual friction value is possibly lower than the initial stiction value. Also, the torsional friction value may not be so comparable with the axial value with surfaces of this order of roughness, as in the model web experiments. Clearly more information about interface friction under pulsating load conditions is required.

(ii) Stress System Round Pins.

The relief of stress measured by the electrical resistance gauges is shown in Fig. 64 . In the case of the journal pin the average pressure of 4.4 T/in^2 (measured about $\frac{1}{2}$" from the bore) compares well with the pressure of 4.5 T/in^2 calculated from the residual fit. The agreement is not so satisfactory in the case of the crank pin, the figures being 2.1 T/in^2 and 3.1 T/in^2 respectively.

The hoop stress at the bore corresponding to the interface pressure is given by

$$p_{\theta})1 = \frac{k^2+1}{k^2-1} P$$

The values for interface pressures of 3.1 and 4.5 T/in^2 are 5.4 and 7.9 T/in^2 respectively. The values shown in Fig. 64 are about 9.2 T/in^2 round the eye-holes in both cases. The crank pin hoop stress increases in the area of the bridge-piece, while the journal stress decreases.

There are two possible explanations of the high hoop stress; either the recovery of strain on release of the interface pressure is inelastic, or an axial traction exists at bore.

Considering the first of these, the effect of inelastic action on release of stress is to increase the strain measure-

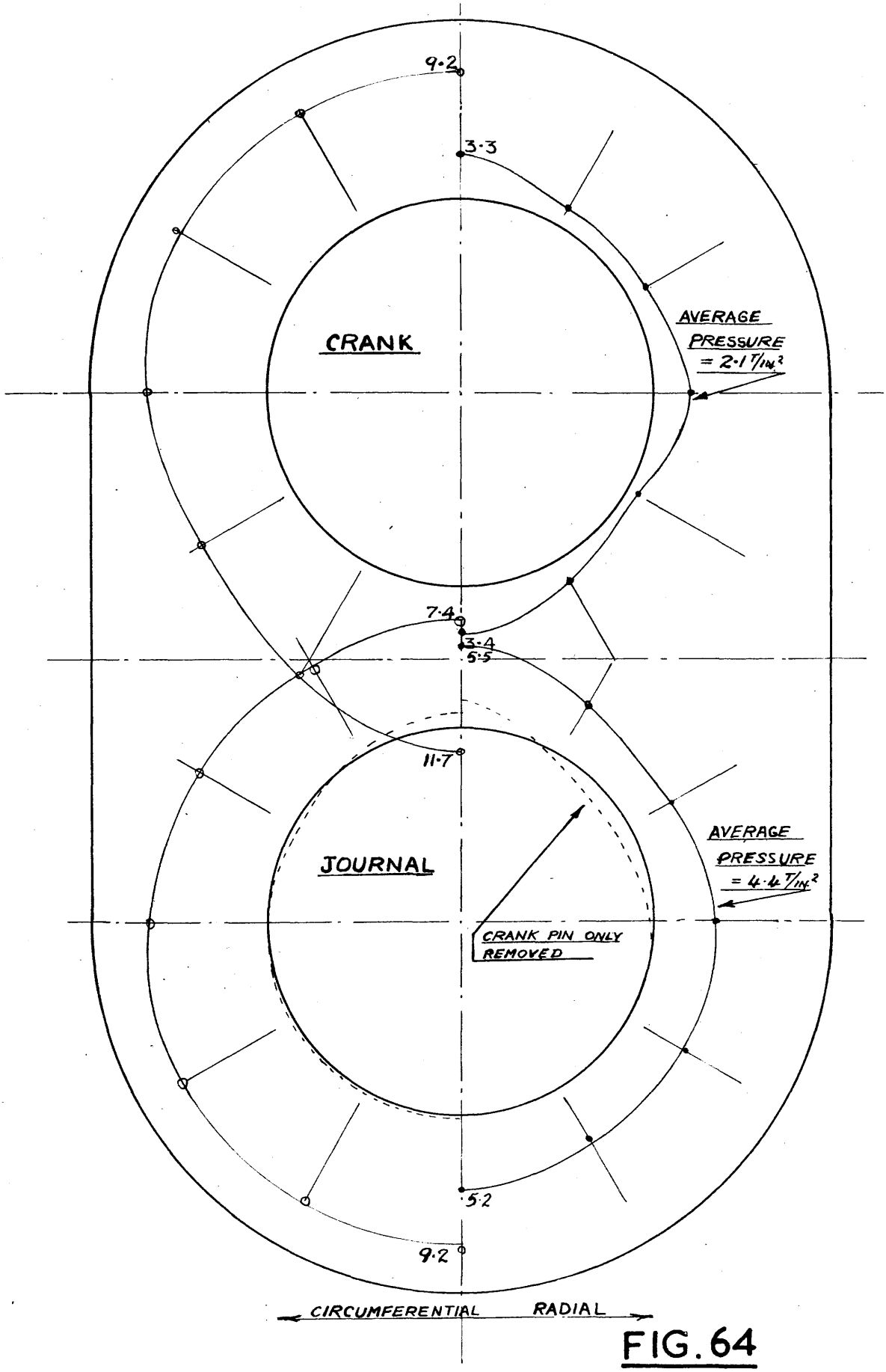
9·2
3·3
CRANK
AVERAGE PRESSURE = 2·1 T/IN²
7·4
3·4
5·5
11·7
JOURNAL
AVERAGE PRESSURE = 4·4 T/IN²
CRANK PIN ONLY REMOVED
5·2
9·2
CIRCUMFERENTIAL
RADIAL

FIG. 64

ment in both circumferential and radial directions. Both stresses would therefore appear to be too high. Within the elastic range the ratio of hoop to radial strain in a thick ring is given by

$$\frac{e_\theta)1}{e_r)1} = - \frac{(1 - \sigma) + (1 + \sigma) k^2}{(1 - \sigma) - (1 + \sigma) k^2} = - 1.35$$

It may reasonably be assumed that the ratio for a small degree of overstrain will not be substantially different from this value. The crank pin relief of pressure is low, while the hoop stress for this pin is as high as for the journal pin. This explanation of inelastic release of strain must therefore be rejected.

Axial friction drag is, however, a likely explanation. Although the axial factor was rejected in the calculation of interface pressure on account of the relatively short length of grip, there is every liklihood that localised stress actions occur adjacent to the interface, which have no significant effect on the average pressure, but which are recorded by strain gauges near the bore.

The effect on strain gauges adjacent to the interface of prevention of axial shrinkage can be qualitatively estimated by considering the method of analysis adopted by Goodier (11).

The three-dimensional stress system in the pin and

web after temperature equilibrium is attained, assuming that no slip between the surfaces occurs, may be reproduced with the algebraic signs of stresses reversed, by taking the complete assembly in an unstressed condition and uniformly heating the web to the fitting temperature. Alternatively the stress system will be reproduced with the correct stress sign by the temperature stress system in an initially unstressed integral body, in which the part corresponding to pin is heated to the fitting temperature while the web part remains cold.

The temperature stress system can be analysed in the orthodox way (see, for example, Timoshenko 1934) and consists of three distinct effects:

(1) A uniform hydrostatic pressure of magnitude $\frac{Ect}{1-2\sigma}$

(2) Surface tractions of magnitude $\frac{Ect}{1-2\sigma}$

(3) Body forces of magnitude $\frac{Ec}{1-2\sigma}\cdot\frac{\partial t}{\partial x}$, $\frac{Ec}{1-2\sigma}\cdot\frac{\partial t}{\partial y}$ etc.

In the case $t = \frac{\Delta}{c}$ therefore ct in the above expressions may be replaced by Δ, the fit allowance. The temperature being uniform over both pin and web, with a sharp discontinuity at the interface, the body forces containing terms $\frac{\partial T}{\partial x}$ etc. vanish, but the discontinuity in temperature is replaced by a surface stress equal to $\frac{E\Delta}{1-2\sigma}$ acting radially outwards on a surface within the integral body corresponding to the cylindrical interface in the composite assembly. This force,

together with the hydrostatic pressure, induces a stress system corresponding to the plane stress system in the pin and web assembly discussed in Part II.

The surface tractions of magnitude $\frac{E}{1-2\sigma}$ on the pin in the axial direction, together with the hydrostatic pressure, induce stresses corresponding to the effect of axial friction drag. This stress system, together with the probable distributions of stress and stress trajectories is illustrated in Fig. 65 .

The problem of the stress system due to distributions of pressure or tractions on the surfaces of a thick plate, was analysed by Sneddon (36) using Hankel transforms, but the results given by semi-infinite integrals are extremely tedious to compute.. No values are therefore shown in Fig. 65 , but it can be seen that the effect of this friction drag is to induce a radial tensile stress at the interface, the magnitude of the stress diminishing towards the middle of the grip. The average interface pressure in the assembly will therefore be greater than that recorded by gauges on the end faces. Also the bore circumferential stress on the end faces is probably tensile, for the following reason.

The usual equilibrium equation for an infinitesimal cylindrical element

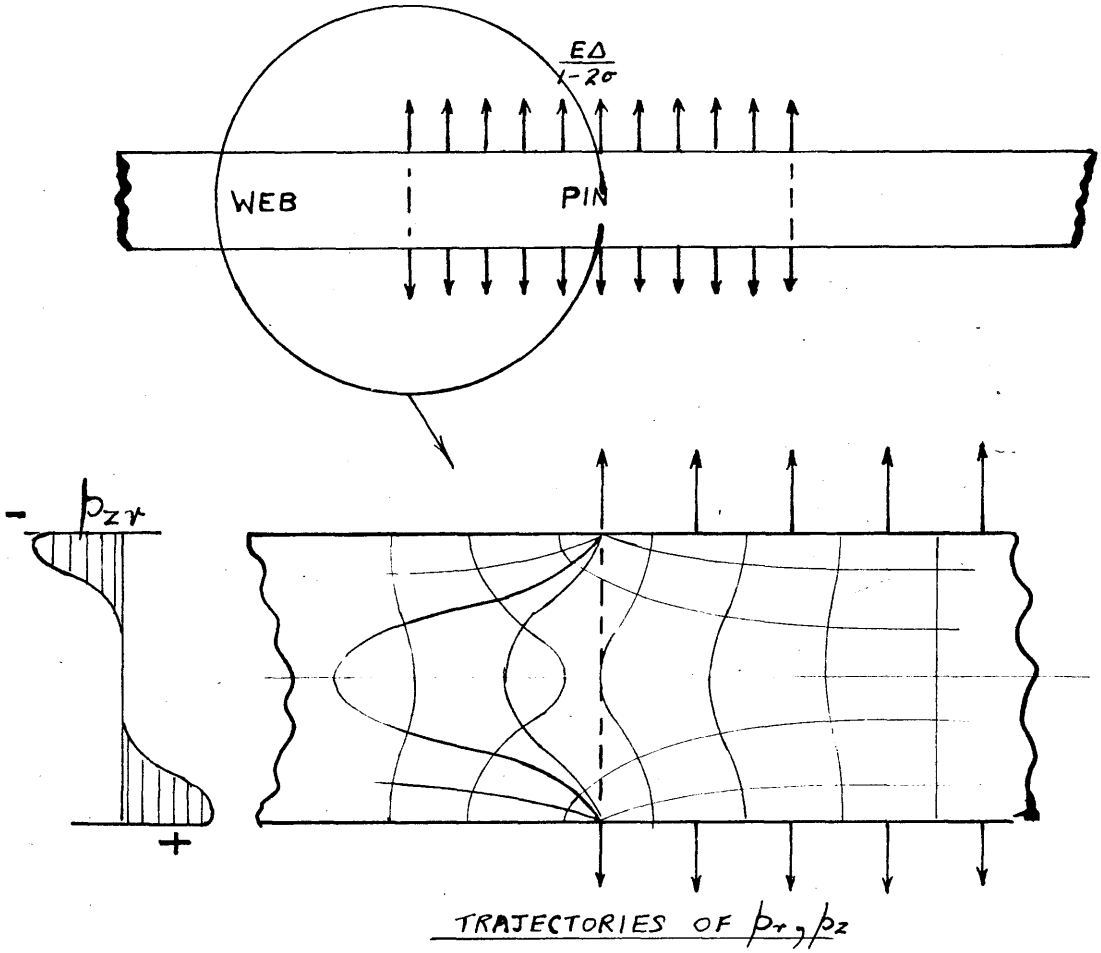

TRAJECTORIES OF p_r, p_z

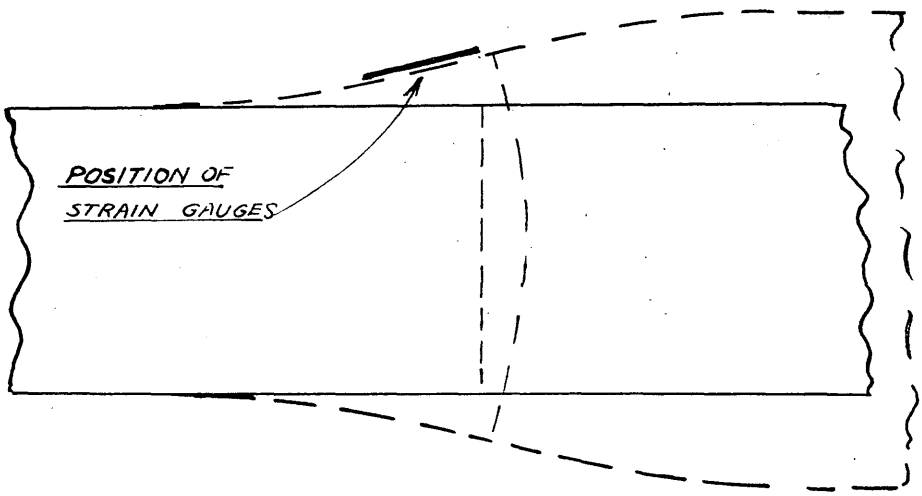

PROBABLE DEFORMATION OF RADIAL SECTION

FIG. 65

$$p_\theta = p_r + r\frac{\partial p_r}{\partial r}$$

becomes, in the presence of shearing stress p_{zr}

$$p_\theta = p_r + r\frac{\partial p_r}{\partial r} + r\frac{\partial p_{zr}}{\partial z}$$

The third term $r\frac{\partial p_{zr}}{\partial z}$ is very large and positive in sign near the ends of the grip*, the probable axial distribution of friction drag being shown in Fig. 65 . (The friction drag is actually p_{rz} with the sign convention adopted, and is positive on the upper half with the z axis upwards. Fig. 65 shows the complementary shear stress). The effect of axial drag on stresses near the bore on the end face is therefore to induce radial and circumferential tensile stress. Thus relief of stress due to removal of pins, measured on the end faces, indicates a high tensile hoop stress and a low radial pressure, compared with the average values.

This does not imply that elementary conditions of equilibrium of a half ring do not prevail. The tensile hoop stress due to the term $r\frac{\partial p_{zr}}{\partial z}$ in the above equation becomes compressive as the gradient of friction drag reverses in sign

---

* The shearing stress on a small element at the edge of the bore must be zero since no complementary shear exists on the end face, i.e., the friction drag increased rapidly with distance into the grip, very slight slip (or plastic flow in the case of an integral body) being inevitable at the re-entrant corner.

a short distance from the edge of the grip. The average hoop stress and the average pressure must, of course, always maintain equilibrium of the half ring.

Love's solution (20) for a circular area of uniform tension on a semi-infinite plate, used by Goodier in his analysis of the friction drag, indicated that the hoop stress on the surface at the edge of the tension area was tensile and in magnitude twice the radial tensile stress. This may reasonably be taken as a guide to the relative magnitudes of the corrections to be applied to the measured stresses in the case of the crank pin of 7B .

The average pressure of 2.1 T/in^2 should be increased by an amount δ and the hoop stress of 8.2 T/in^2 decreased by the amount of 2δ ; with this correction the stresses should be related by the thick cylinder formula

$$P_\theta = + \frac{k^2 + 1}{k^2 - 1} P = 1.75 P$$

i.e., $(9.2 - 2\delta) = 1.75 (2.1 + \delta)$

giving $\delta = 1.5$ T/in^2

and correcting the average interface pressure to 3.6 T/in^2.

The identical correction in the case of the journal pin gives pesssure as 4.8 T/in^2.

The ratio of these values of pressure compares well with

the ratio of measured residual fits, the pressure ratio of the journal to the crank being $\frac{4.8}{3.6} = 1.33$, and the residual fit ratio $\frac{1.04}{0.72} = 1.45$.

In the previous test in which the pins were trepanned out, the average pressure round the crank pin was 3.2 T/in^2, and the average hoop stress round the eye hole 9.0 T/in^2. Applying the above correction the average pressure becomes 4.1 T/in^2. In this case, however, the residual fit allowance could not be obtained as a check.

It was at first thought that the axial grip which undoubtedly occurs during assembly, would be lost through working of the pin under pulsating bending action. If the friction drag is lost, relative movement between the surfaces must occur, and no experimental evidence is available to support this. If, however, it can be established that the axial friction drag is maintained under service loading, the implication that no axial slip or movement occurs, leads to the conclusion of profound practical significance that the initial, or higher friction coefficient is likely to be attained, and that no serious opening of the grip surfaces occurs.

A disconcerting feature is that the axial grip correction is very much lower in the case of the journal fit, although both members are alleged to have had the same initial fit

allowance. This suggests either that the same amount of friction drag was not present during assembly due to vagaries of surface film conditions, or that the axial effect in this case had been "worked off" under pulsating torque action. The pulsating bending action on the journal is evidently not so severe as on the crank pin, but the torque loading is certainly greater. This is discussed under the next heading dealing with the residual measurements.

The former explanation is considered the more likely. Table 13 shows that the coefficients of friction for the crank pin in slab 7B. are very high indeed, and the presence of so large an axial grip correction may reasonably be attributed to the friction value.

(iii) Residual Measurements.

Fig. 66 shows the profiles of pins and bores obtained by direct measurement after separation. The parallelism of the pins was not noticeably affected, but both bores showed a serious degree of bell-mouthing. Measurements of the middle section could not be obtained as this section was used for another test described under (d) below, but the profiles sketched in Fig. 66 cannot be seriously in error.

The striking feature is that the loss of fit and degree of bell-mouthing is greater in the case of the crank pin,

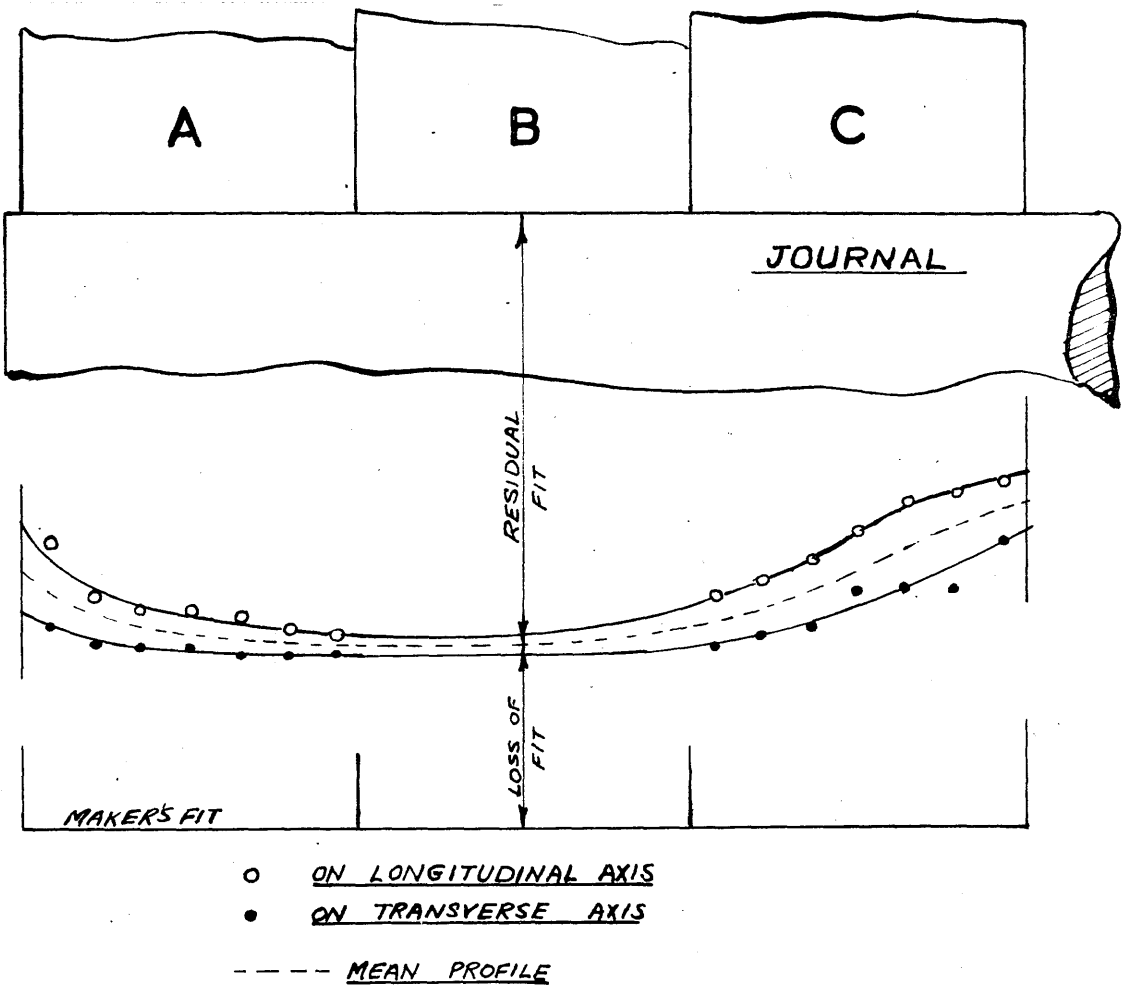
A
B
C
JOURNAL
RESIDUAL FIT
LOSS OF FIT
MAKER'S FIT
ON LONGITUDINAL AXIS
ON TRANSVERSE AXIS
MEAN PROFILE

FIG. 66

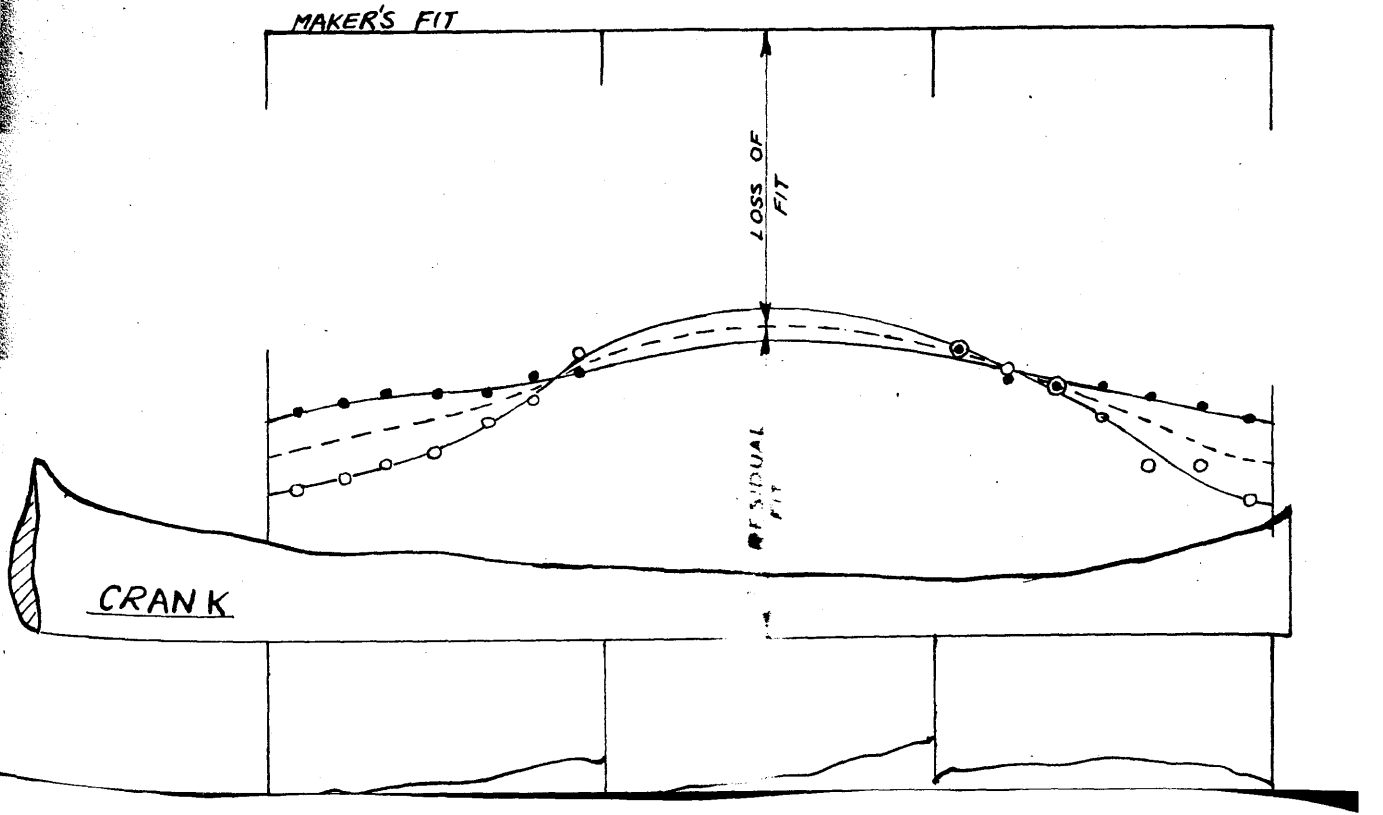
MAKER'S FIT
LOSS OF FIT
CRANK

indicating that conditions of pulsating bending are more severe.

The greatest effect in both cases is in the longitudinal direction of the web, corresponding to piston loading at top and bottom dead-centres, though the discrepancy between the profiles for the two axes is not large. It might be expected that the crank pin hole would be drawn in the transverse direction, as the tendency is for the journal torque to be transmitted to the next throw by bending and shear of the crank pin. With sufficient bearing constraint, the shaft would function as a structural member without necessarily transmitting any torque at the crank pin grip. Also, experience shows that troubles with crank pin shrink grips are very rare compared with journal grips, indicating that the crank pin torque is of a low order.

It should be noted that diametral measurements do not differentiate between a "drawing" of the hole at any particular part of the circumference, corresponding to a creep under steadily applied bending moment, and a true bell-mouthing corresponding to a complete reversal of direction of loading.

The bell-mouthing effects at the entry and at the blind end of the grip, are not appreciably different. The effects of the pin projection and the distribution of torque are

apparently not significant. In the case of journal pin there is a slight increase in the amount of bell-mouthing at the entry end, which may be due to the torque loading, but this is uncertain. It would be unwise to draw any conclusion therefrom.

D. Residual Stress System of Used Crank Web.

(a) Apparatus and Procedure.

After completion of the push-out test on slab No. 7B. the eye-holes of the web were cut from the outside to the bore along the longitudinal axis by a vertical band saw, in order to relieve the locked-up stress system due to overstrain. Strain readings of the electrical gauges were taken before commencement, after the crank eye cut, and after the journal eye cut.

(b) Results, Discussion and Analysis.

The relief of stress due to cutting is shown in Fig. 67 . Cutting of one eye portion has little effect on the other bore in the region of the bridge-piece. The values shown are not necessarily the maximum stresses, as only the section adjacent to the saw cut can be completely stress-relieved, though the residual stresses after cutting are likely to be of a low order everywhere except at the bridge-piece.

Round the eye hole the hoop residual stresses must be self-equilibrating, since no external forces are present. Cutting the section has the effect of applying equal and opposite bending moments to the sections on each side of the saw cut. The halves of the eye-hole therefore spring back by an amount equal to the deflection and rotation of an equivalent thick

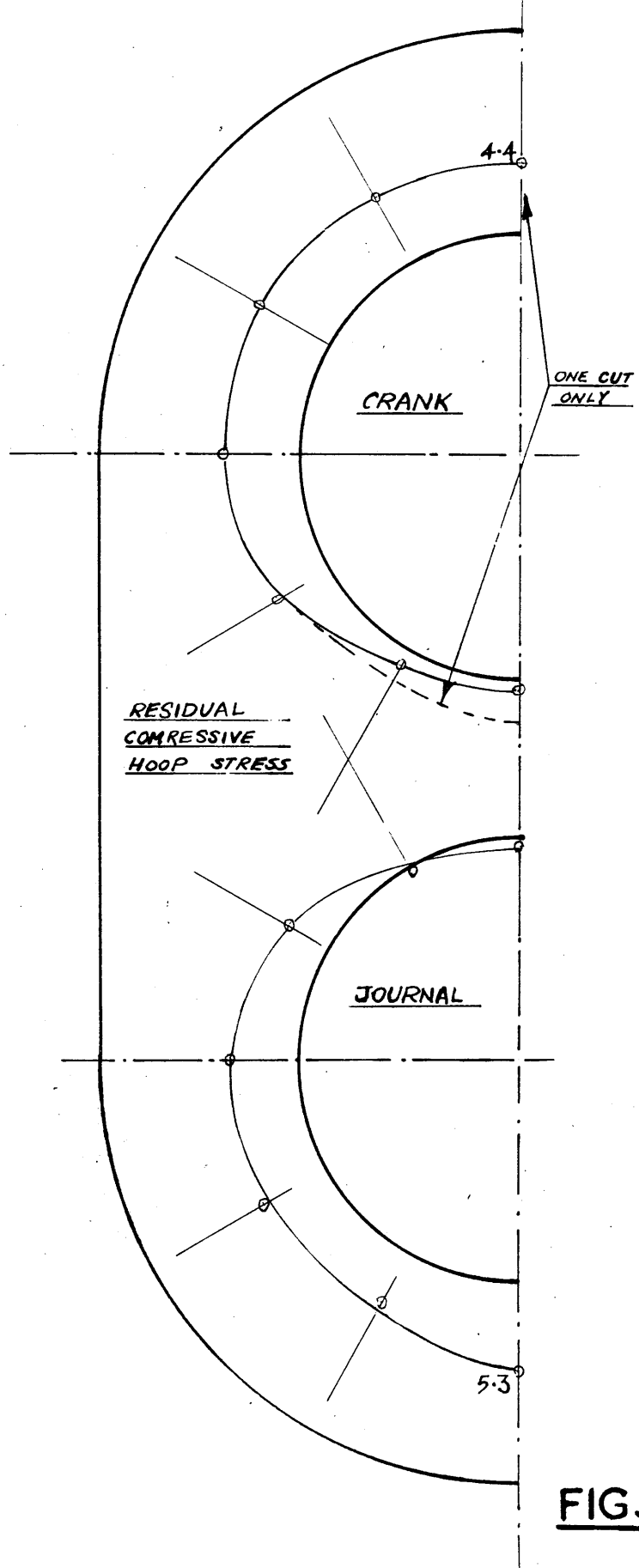
4·4
CRANK
ONE CUT ONLY
RESIDUAL COMRESSIVE HOOP STRESS
JOURNAL
5·3

FIG. 67

curved beam acted on by a moment equivalent to the residual stress distribution in a radial plane, the direction being such as to produce tensile stress (to cancel the residual compressive stress) at the inside of the beam.

Owing to the greater loss of fit at the crank pin discussed in Section C. above, it would be expected that the residual stresses at the bore would be higher at the crank pin. The results do not show this. The bore residual compressive stresses at the crank and journal are 4.5 T/in^2 and 5.3 T/in^2 respectively, indicating a greater radial depth of overstrain at the journal, in contradiction to the loss of fit given by the bore measurements.

The loss of fit is dependent on the figures of 1.5 mils obtained from the reconditioning firm in the U.S.A., and it would appear that some error in the initial fit allowance may have occurred.

The circumferential hoop stress at the bore, with the pin fitted is given by relief of stress on pushing out the pin and the residual stress by cutting the web (assuming that the stress is totally relieved). The bore circumferential stress in the assembly, before the removal of pins, was therefore

Crank $6.2^* - 4.5 = +1.7$ T/in^2

Journal $8.4^* - 5.3 = 3.1$ T/in^2

* Corrected for axial drag.

The circumferential hoop stress in the equivalent thick cylinder at maximum bore pressure, when plastic flow has penetrated to the outside, (n = k) is + 5.25 T/in^2, but the corresponding permanent set of the bore is about 2 mils, whereas the measured set, based on an initial fit of 1.5 mils is

Crank 0.46 mils.

Journal 0.78 mils.

The measured relief of stress on cutting the web is therefore considerably greater than the permanent set of the bore would indicate. Neither deficiencies in the theory of overstrained cylinders, nor experimental errors can account for the large discrepancy.

The most probable explanation is that residual compressive hoop stresses were present before assembly of the shaft. It will be recalled that this web is part of the aft section of the shaft which was entirely re-built, the original webs having been annealed and rebored. No details are available about the procedure adopted to stress-relieve the old webs, and in the circumstances it must be assumed that the original residual stress system was not entirely eliminated.

E. Stress System of New Crank Webs - Pins Cut Out.

(a) Apparatus and Procedure.

(i) Specimens.

Two of the slabs obtained by splitting the webs of the used crankshaft into three parts, as described in sub-section 3 (b) above, were dismantled and the pin sections discarded. The holes in the web slabs were rough-bored to slightly larger diameters in order to remove the bell-mouth effect, and annealed at 1100°F for five hours. The holes were then finish-bored with the surface-finish normally used in crankshaft work by Messrs David Rowan and Co. Ltd., Glasgow.

The bores were carefully gauged and new pin sections manufactured to a definite fit allowance.for each specimen. Denoting the two slabs as A and B the fit allowances were

Specimen A 1.00 mils.

Specimen B 2.00 mils

These fit allowances were selected to induce stress systems in the webs corresponding to fully elastic, and considerably over-strained, conditions; also the values chosen approximate to the limits of the range of fit allowances in common use.

(ii) Shrink-fitting Process..

The web slabs were heated by a pressure burner in each bore, the flame directions being changed at intervals in

PLATE 5

FLAME-HEATING CRANK WEBS FOR SHRINK-FITTING.

PLATE 6

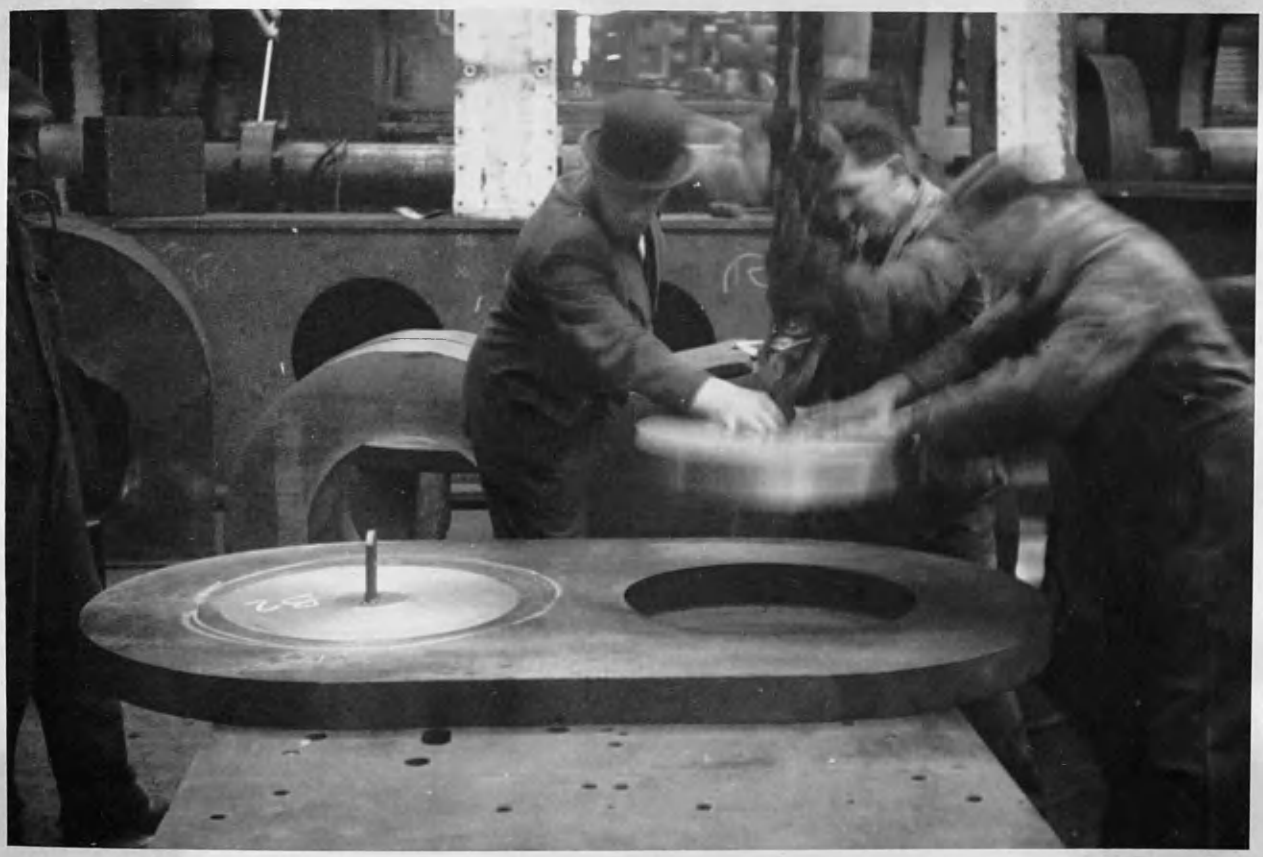

ASSEMBLY OF PIN SECTIONS.

order to heat the slabs as uniformly as possible. A sheet-metal cover was placed over the slab to minimise heat losses and distribute the burner gases. The heating arrangements are shown in Plate 5 . The bore sizes were checked at intervals with a stick gauge, the length of which was equal to the pin size plus $1\frac{1}{2}$ thousandths per inch of pin diameter, which is the normal excess fit allowed for work of this type.

When the gauge indicated that assembly could be carried out, the slab was transferred to a table and the bores quickly cleaned with a wet rag to remove soot. The pins, which had been previously wiped clean, were successively dropped into the holes and the assembly allowed to cool in air. Plate 6 shows the second pin about to be entered.

An assembly of both pins without reheating the web is referred to as a 'simultaneous' assembly, though a time delay (of the order of 20 - 30 seconds) necessarily occurs. On cooling, overstrain, if any, will take place at the pin which was first assembled, and the stress system in the web will not necessarily be symmetrical about the transverse centre line.

(iii) Strain Measurements.

After the shrinking operation electrical strain gauges, in the symmetrical pattern shown in Fig. 68 and Plate 7 , were attached to both slabs. Denoting the pins by Nos. 1 and 2 ,

FIG. 68.

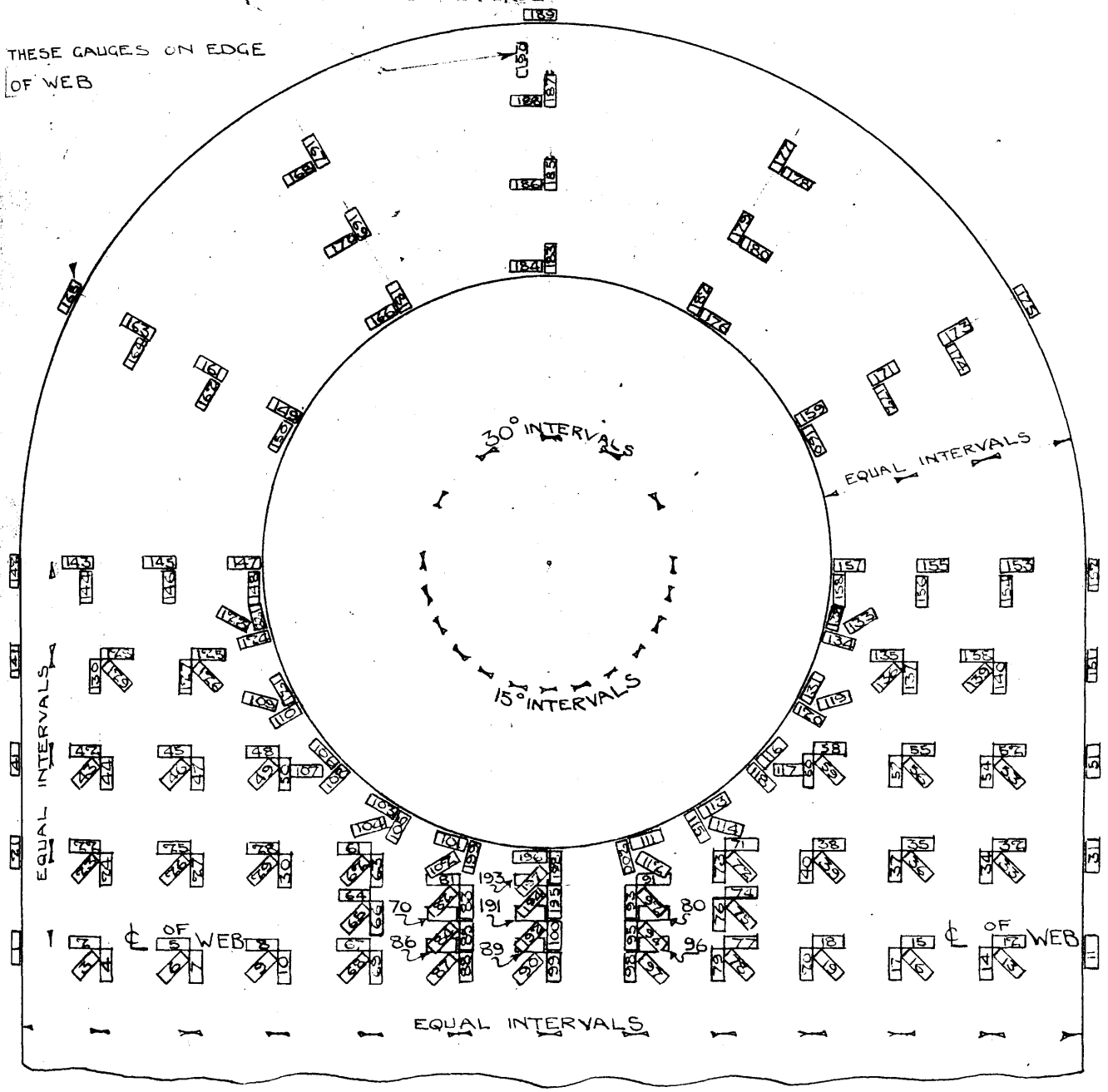

COMPENSATING GAUGE MOUNTED ON STEEL PLATE, POSITIONS UNMARKED, PROVIDED ADJACENT TO EACH GROUP OF 10 ACTIVE GAUGES Nºs 1-10; 11-20; ETC.,

POSITION OF STRAIN GAUGES
ON
EXPERIMENTAL CRANK WEBS
SCALE:- ½" = ONE FOOT

PLATE 7

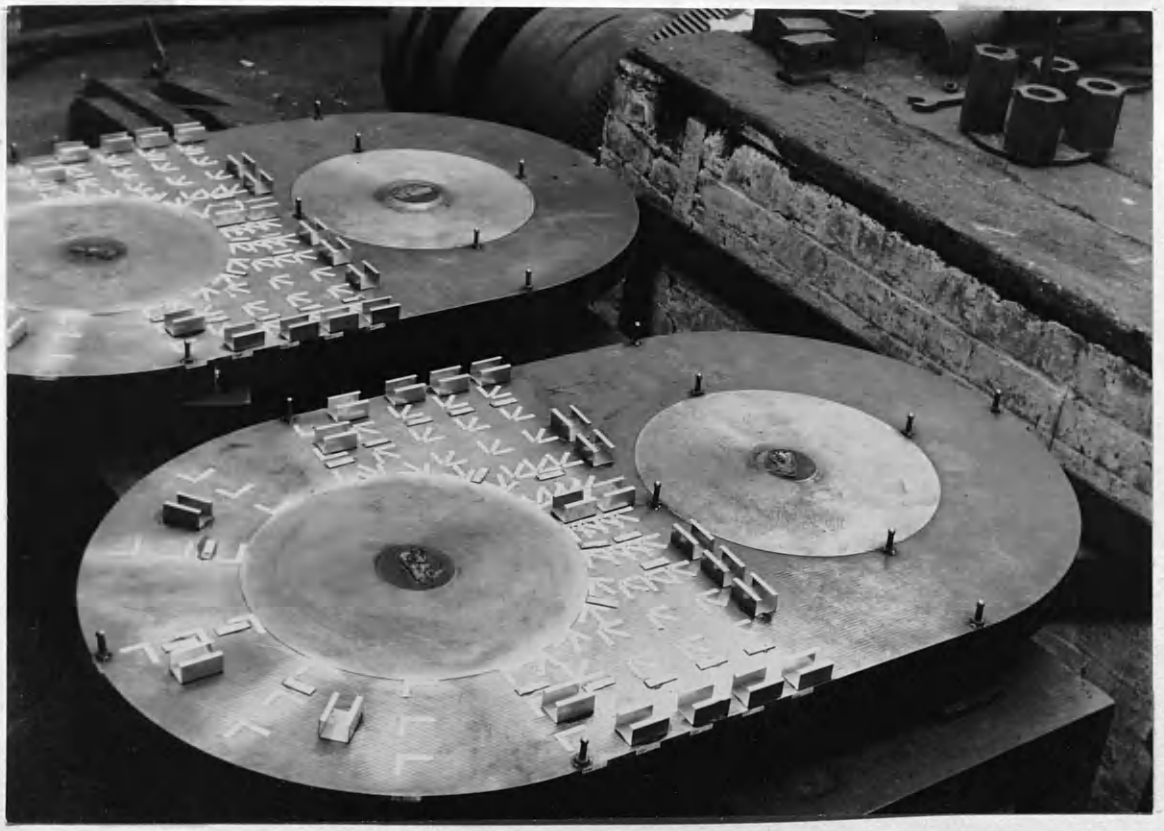

ELECTRICAL STRAIN GAUGE PATTERN

BEFORE WIRING (NEW WEBS).

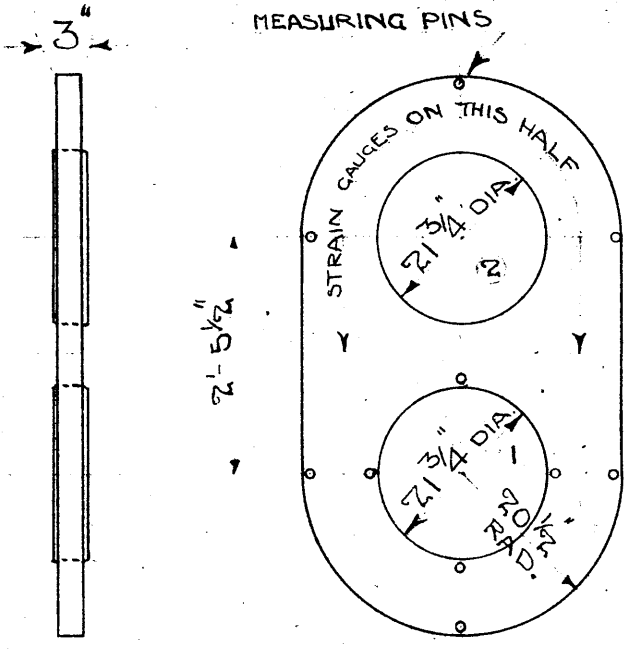

FIG.69.

PRECISION STEEL BALL
0·5000" DIA.

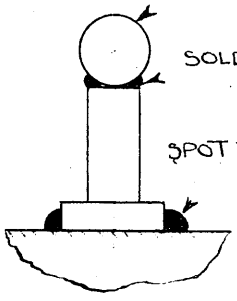

— DETAIL OF MEASURING PINS

EXPERIMENTAL WEB SHAPE

SCALE:- ½" = ONE FOOT

pin No. 2 was fitted first in both cases; the pattern of Fig. 68 was adjacent to this pin.

Readings were taken before and after removal of pins and after cutting web to relieve residual stress system.

(iv) Length Measurements.

Ten measurement pins were tack-welded to the surface of each web as shown in Fig. 69 . The majority were adjacent to No. 1 pin. Lengths between adjacent pins were measured at the various stages of the test by standard length bars wrung to slip gauges. The touch sensitivity and accuracy of measurement was not less than $\frac{2}{10,000}$ inch, and the accuracy of standards used was of a higher order.

(v) Bore Measurements.

The bores were gauged at the various stages of the tests with a stick micrometer set to length standards. Readings were taken at three axial positions on four diameters, giving a mean of twelve readings. The accuracy of measurement was not quite as high as for the length measurements but exceeded $\frac{4}{10,000}$ inch.

(vi) Surface Finish Measurements.

The bore surface finish was measured before assembly by the Tomlinson Macro Recorder, using a $\frac{1"}{16}$ diameter stylus. The tool marks were visible to the eye.

(vii) Removal of Pins.

The pins were successively dismantled by drilling three radial rows of 1" holes from the outside to the centre of each pin, allowing the sectors to be removed. The thin walls between the drilled holes were cut by hand tools. Plate 8 shows one slab set up for drilling on the table of an Archdale Radial drilling machine. The location of the holes and drilling sequence is shown in Fig. 70 .

After removal of pins the webs were cut by radial lines of holes at the eye-piece as shown, to relieve the residual stresses.

(b) Results, Discussion and Analysis.

(i) Stress Systems due to Removal of Pins.

The stress systems round the pins and outside edges, and at various sections are shown in Fig. 71 and 72 .

In the test an improved apparatus was used for the electrical strain measurements and the absence of the usual experimental scatter indicates the reliability of strain measurements. In a few cases only the experimental results are in error, due to faulty gauges.

1. Web A.

The stress system is almost, but not quite, symmetrical

FIG. 7Q

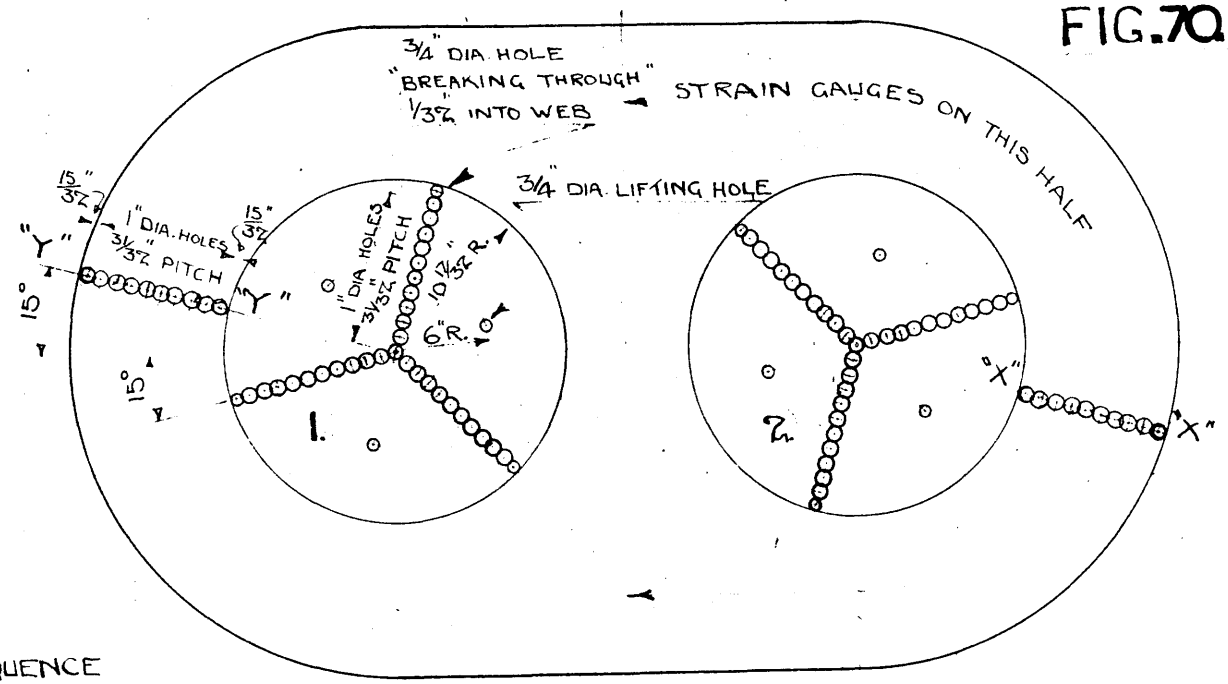

SEQUENCE

1.- Nº 1 DISC DRILLED OUT
2.- Nº 2 DISC DRILLED OUT
3.- WEB CUT ON "XX"
4.- WEB CUT ON "YY"

DETAIL OF DRILLING PROCEDURE

SCALE :- 1" - ONE FOOT

PLATE 8

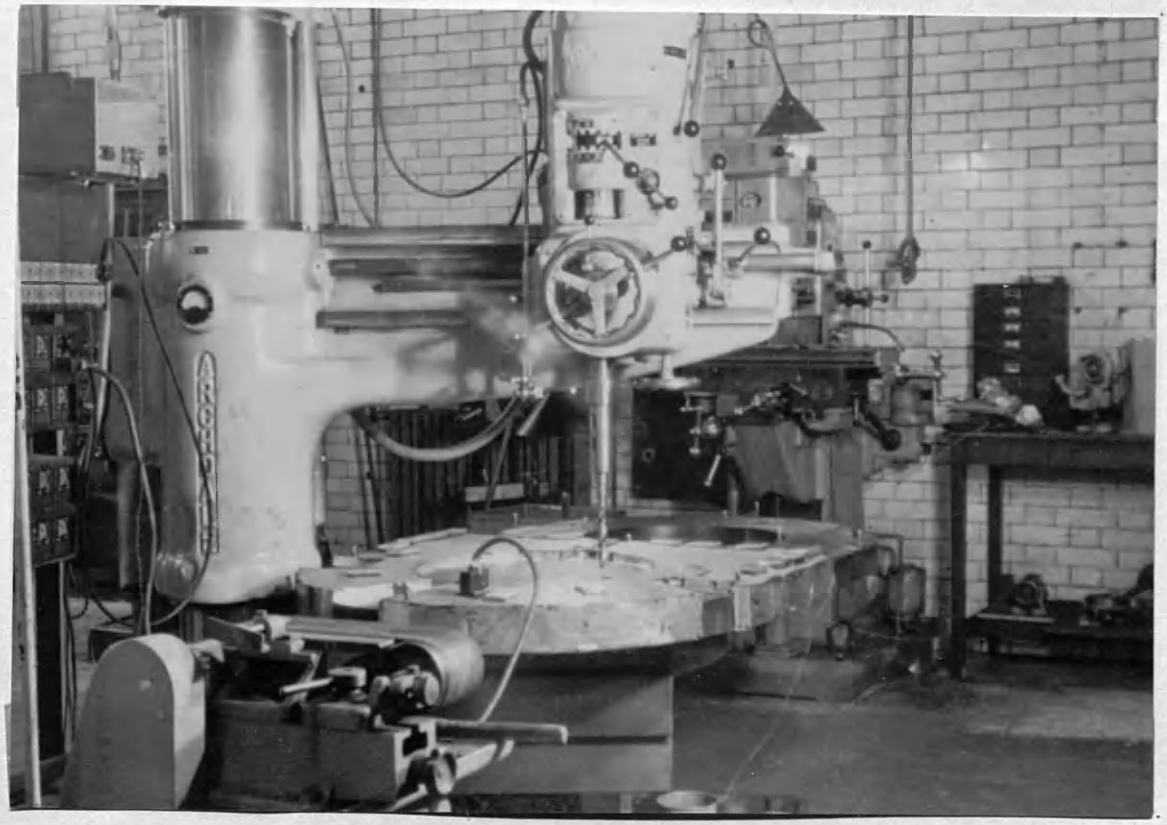

REMOVAL OF PINS IN DRILLING MACHINE.

STRESS DUE TO REMOVAL OF CRANK AND JOURNAL PINS

• RADIAL PRESSURE
o HOOP TENSION

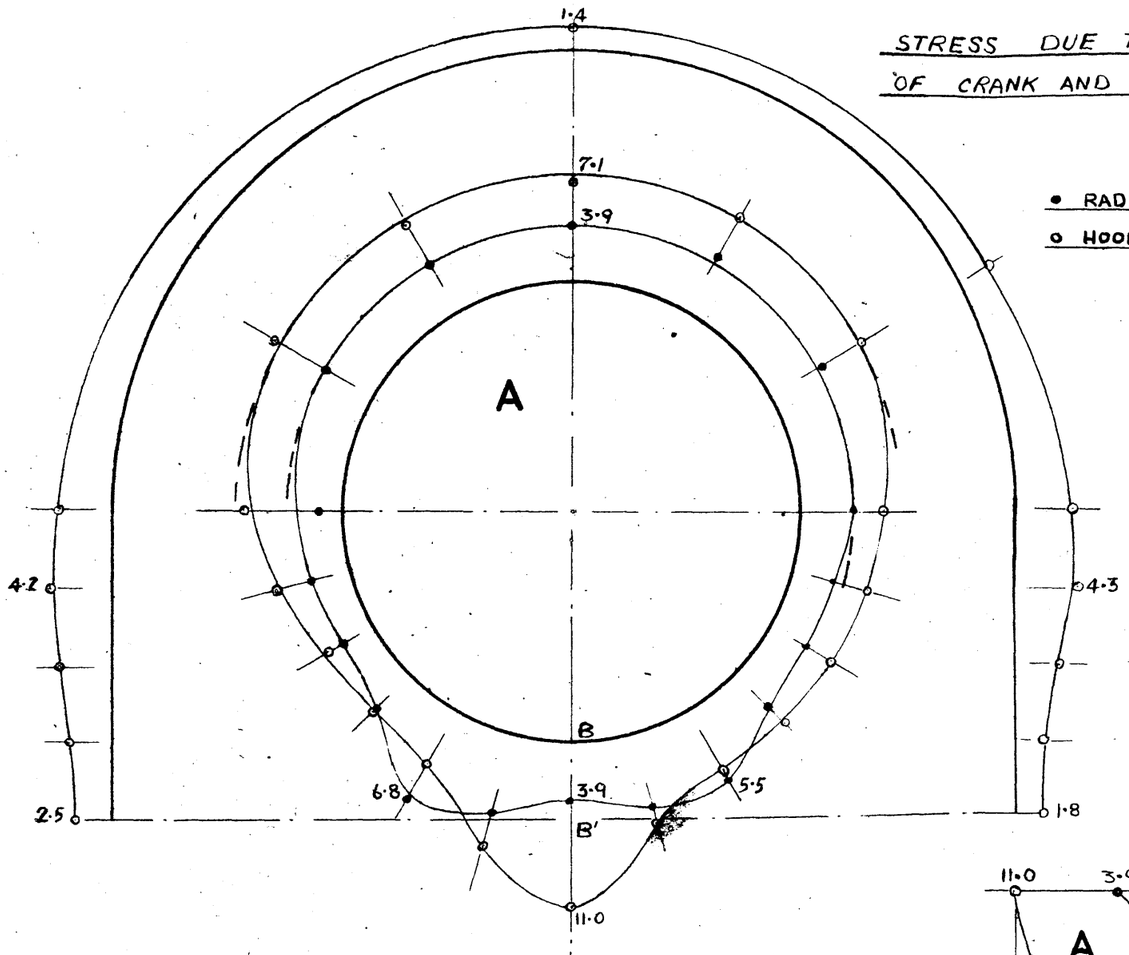

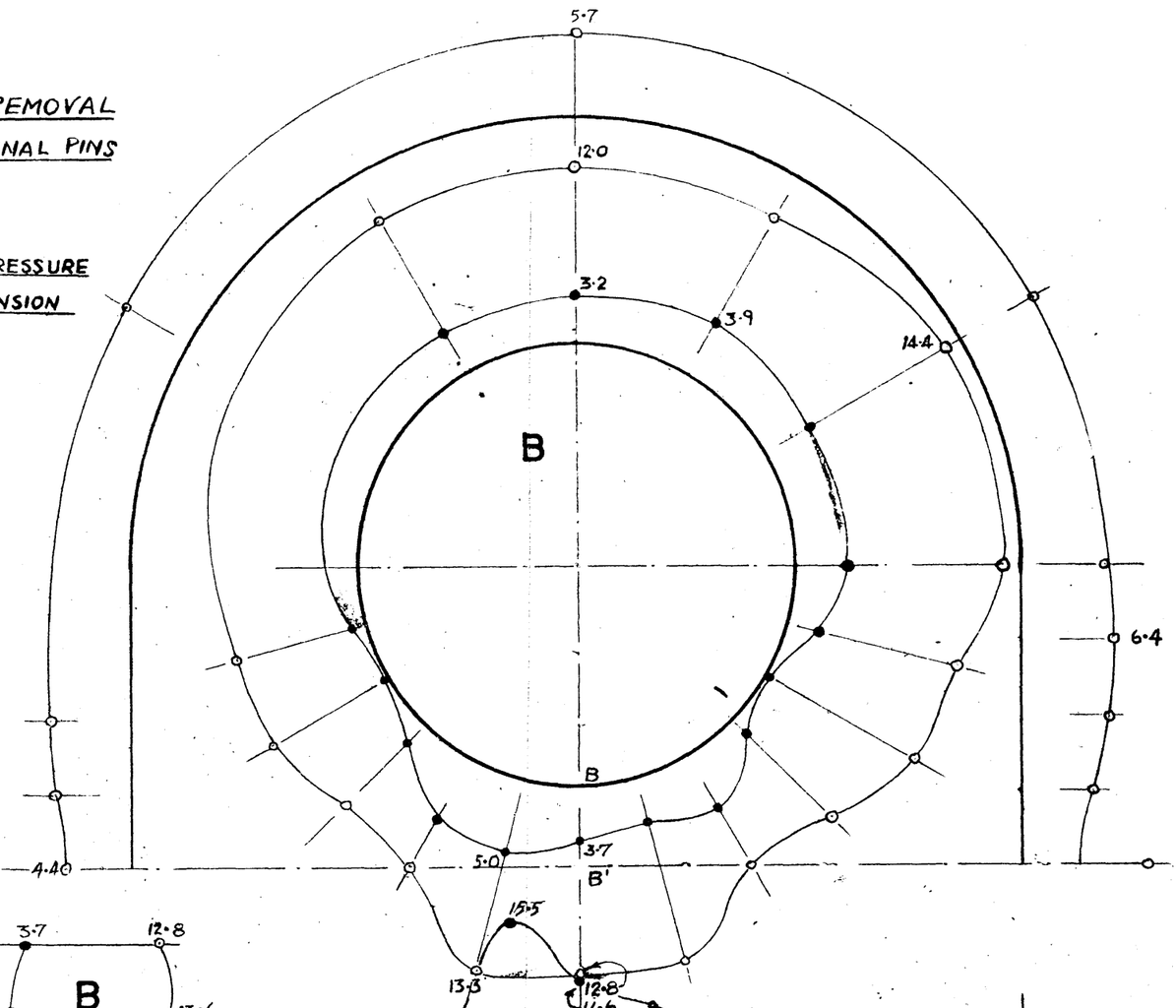

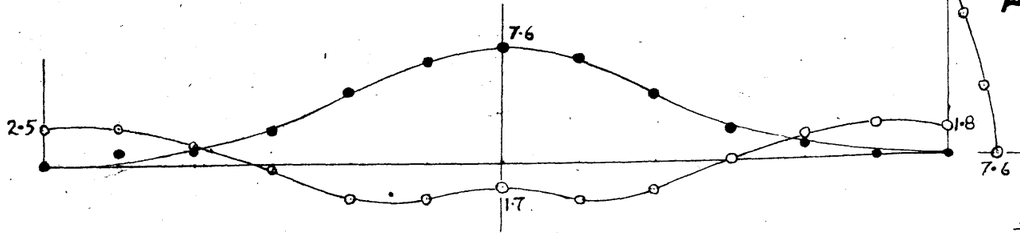

• TRANSVERSE DIRECTION
o LONGITUDINAL DIRECTION

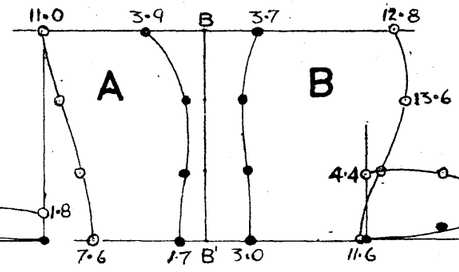

STRESS AT BRIDGE BB'

STRESS SCALE 1" = 10 T/IN.²

FIG.71

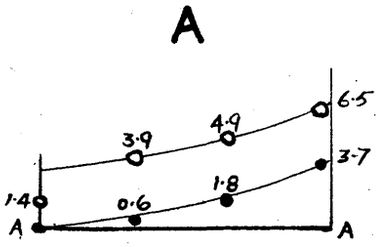

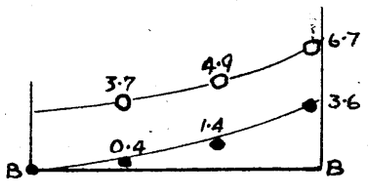

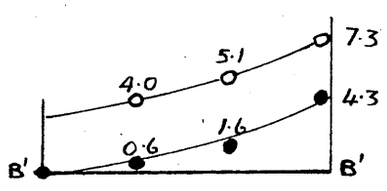

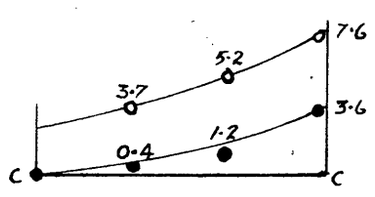

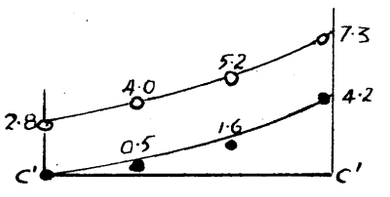

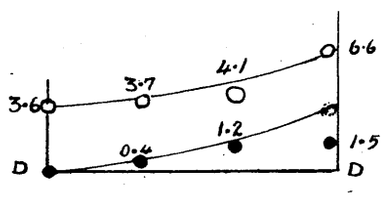

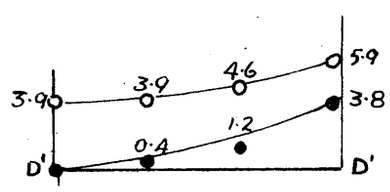

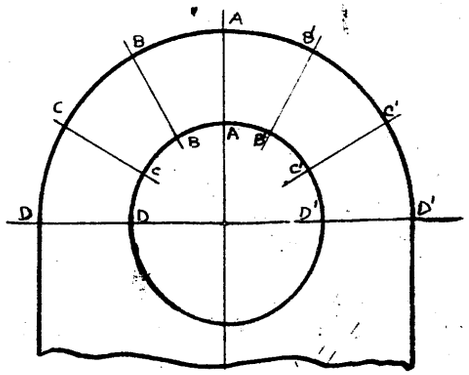

• RADIAL PRESSURE

○ HOOP TENSION

STRESS SCALE: 1" = 10 T/in.²

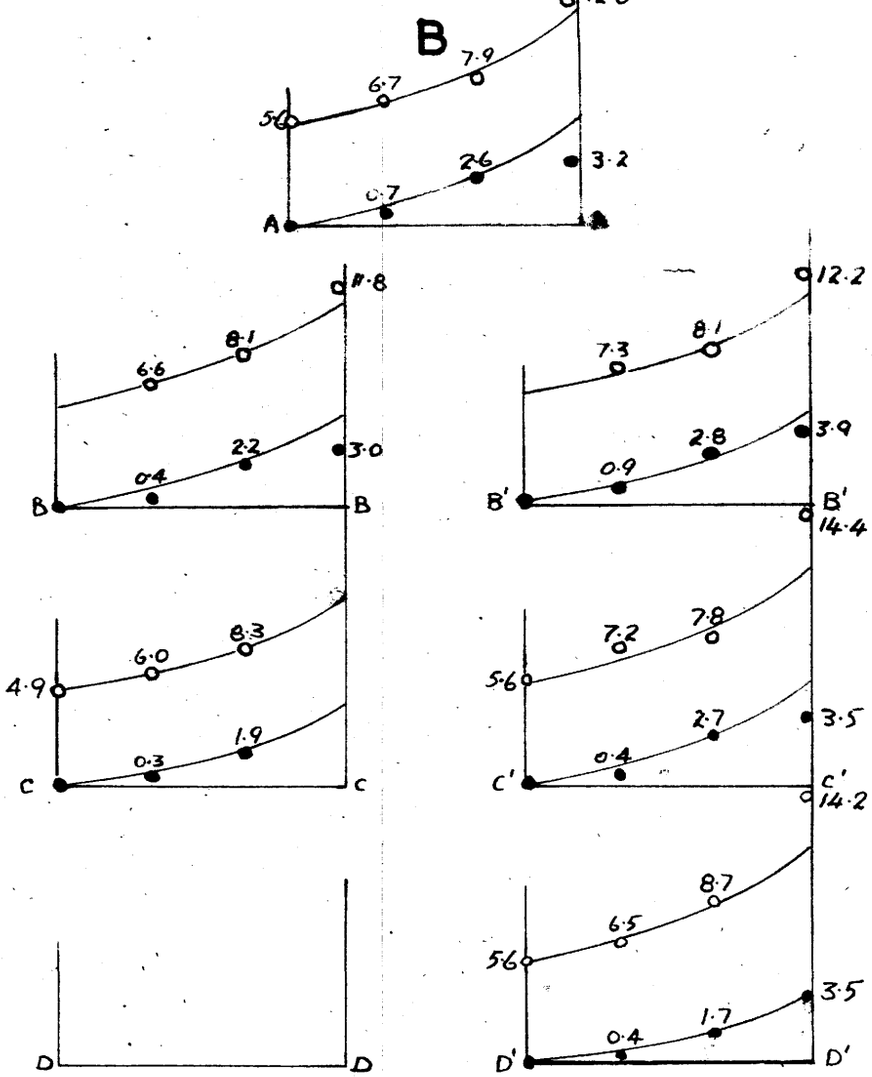

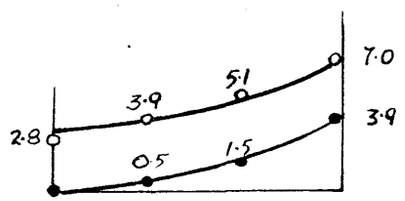

AVERAGE OF AA, BB, B'B', CC, C'C'

LAMÉ CURVES FOR

4·0 T/IN.² BORE PRESSURE

TABLE OF LAMÉ STRESS VALUES

RADIAL	3·2	3·9	4·9	6·9	4·0 T/in.² BORE PRESSURE
HOOP	0	0·6	1·8	3·9	
RADIAL	0	1·0	2·6	5·7	6·0 T/in.² BORE PRESSURE
HOOP	4·7	5·7	7·3	10·4	

OUTSIDE → BORE

STRESS ON RADIAL SECTIONS

CRANK AND JOURNAL PINS REMOVED

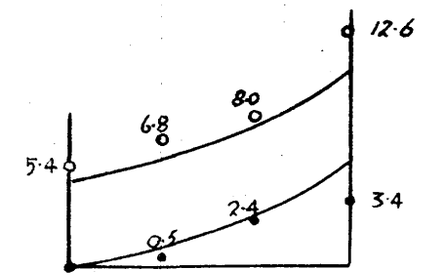

AVERAGE OF AA, BB, B'B', CC, C'C'

LAMÉ CURVES FOR

6·0 T/in.² BORE PRESSURE

FIG. 72

about the longitudinal centre-line. The amount of plastic deformation, measured from the change of bore diameter was found to be quite small, and the stress system given by the removal of both pins may, except at the bridge, be taken to be that corresponding to elastic fit conditions. The absence of precise symmetry may be attributed to slight unavoidable misalignment of the pin and hole axes in the fitting process.

The values of 7.1 T/in^2 and 3.9 T/in^2 for the hoop and radial stresses at the eye-piece are the average values for the five points from the centre-line to 60° on either side. The curve is shown as a circle concentric with the hole; the dotted projections indicate the commencement of significant departure from thick cylinder conditions. It is clear that for 120° round the eye hole, the stresses are hardly affected by the conditions at the bridge-piece.

Fig. 72 shows the variation of hoop and radial stress on radial sections at the eye-piece. The values vary slightly on different sections, but the average for the 120° of eye-piece are in remarkably sound agreement with the Lamé curves drawn for a bore pressure of 4.0 T/in^2. The gauges at the inside were located about $\frac{1}{4}$" from the bore, hence the pressure is slightly higher than the value 3.9 T/in^2 recorded by the radial gauge. A table of the Lamé stress values for the locations of the strain gauges is given.

The pattern of stress round the hole is slightly different from the theoretical solution based on uniform bore pressure. Proceeding round the bore the hoop stress falls slightly, before rising rapidly to a maximum at the bridge. The ratio of this maximum value to the thick cylinder value at the eye-piece is nearly equal to the ratio given by theoretical solution. The experimental ratio is $\frac{11.0}{7.1} = 1.55$, while the theoretical ratio in the relaxation solution in Part II is $\frac{254}{167} = 1.52$. The stress concentration factor for the bridge-piece on the shear stress basis is $\frac{11.0 + 3.9}{7.1 + 3.9} = 1.35$ while that given by the theoretical work is 1.325. The principal stress difference of $11.0 + 3.9 = 14.9$ T/in^2 is exactly equal to the measured value of yield point given by the mean of the tensile tests reported in B. above.

The radial pressure distribution shows a decrease followed by an increase round the inner quarter points. It was found by Coker and Levi that the pressure was lowest at about 45° positions in the bridge-piece. The increase at 30° from the longitudinal axis shown in Fig. 71 is probably due to plastic flow at the bridge, which appears to cause a transfer of pressure away from the overstrained zone.

The stress distribution across the transverse centre-line is, apart from the slight decrease of pressure in the

middle, very similar to the distribution given theoretically, and also by Coker's photoelastic analysis. A notable discrepancy is the fact that the stress in the longitudinal direction of the web, after passing through a zero and a maximum does not return almost to zero at the outside edge. The hollow in this stress curve at the centre may indicate that overstrain has penetrated the entire zone between the pins.

The stress distribution on the longitudinal axis at BB' is quite different in shape to the theoretical distribution. The hoop stress between the pins falls gradually from 11.0 T/in^2 to 7.6 T/in^2, whereas the theoretical solution indicated a fairly sudden drop followed by a nearly constant value. The gradual fall shown here is consistent with a re-distribution of stress consequent on plastic flow at this section. The radial pressure curve is very similar in shape to that for the web B which was subjected to considerable overstrain.

2. Web.B.

In this case the stress system is quite obviously asymmetrical. A "high-spot" in the system occurs in the bridge to the left of the longitudinal centre-line, accompanied by a corresponding high-spot in the hoop stress distribution on the transverse centre-line. Increased values of hoop stress and pressure are evident on the opposite side of the hole.

This asymmetrical distribution of stress undoubtedly results from the redistribution when overstrain occurs. Local non-homegeneity or initial stress before assembly could tend to influence the progress of yield and destroy the symmetry. That such residual stresses existed before the assembly, is shown by the results of the stress relieving operation described below.

The general features of the distribution of hoop and radial stresses round the pins and at the various sections, are very similar to those in Web A . The values are, of course, different.

A significant feature is the low value of radial pressure, which falls almost to zero at the quarter points of the bridge-piece. The hoop stress is much higher than is compatible with the bore pressure on the Lamé basis, and indeed indicates a lack of equilibrium of the half-ring at the eye-piece.

The explanation is that pronounced axial friction drag is operative in this case. This complication was fully discussed with reference to the test described in Section 3. B. above in which the pins were pushed-out, but the present test presents further evidence of the type of radial distribution of the friction drag effect. Fig. 72 shows the radial and circumferential stresses at radial sections round the eye-piece. All sections show the same tendencies and the arithmetical average values may be taken as representative of the average conditions

for 120° round the eye-piece.

The Lamé curves giving the best fit for both radial and circumferential experimental points correspond to a bore pressure of 6.0 T/in^2. These thick cylinder curves indicate that the error in the value of hoop stress at the bore is nearly equal to the error in radial pressure, the errors being of the same algebraic sign, i.e., friction drag induces radial and circumferential tensile stresses almost equal in magnitude on the end faces at the bore. The correction applied in the case of test 3. B and C above was a hoop stress double the radial pressure, obtained from Love's solution for a circular area of tension on a semi-infinite solid.

An inexplicable feature is that the discrepancy does not exist only at the bore, though the magnitude is greatest there. The hoop stress shows a tendency to remain high, and the radial pressure to remain low over the entire radial section. The experimental values at positions $\frac{1}{3}$ of the eye-piece radial thickness from the bore are in best agreement with the Lamé curves.

The value of Poisson's Ratio in the two-dimensional stress-strain relationships from which the stresses were computed, was assumed to be 0.3 . Better agreement would have been obtained between hoop and radial stress values by a lower value of σ . The hoop stress at the outside, however, does not depend on Poisson's Ratio, being given by Young's Modulus only. There is

a small, but quite definite, discrepancy between the radial and circumferential stress values over the entire radial thickness, a discrepancy which apparently did not exist in Web A , though stress values in both cases were computed from strain measurements in precisely the same way.

(ii) Principal Stresses in Bridge-Piece.

The principal stress directions and magnitudes calculated from strain gauge rosettes in the vicinity of the bridge-piece, are shown in Table 14 below. Fig. 73 shows the location code and a sketch of the principal stress trajectories drawn from the tabulated values. The strain values used in the calculations were the mean of readings at symmetrical points.

It will be noted that stress directions on the centre-lines and also near the bore are mainly, but not invariably, parallel and perpendicular to these sections. The variations are generally small in magnitude and do not indicate any definite trend. Small errors in strain readings cause a relatively large rotation of the principal axes; some of the variations, particularly in the regions of the low stress magnitude may be attributed to this cause.

(iii) Length Measurements.

The measurement posts shown in Fig. 69 proved to be

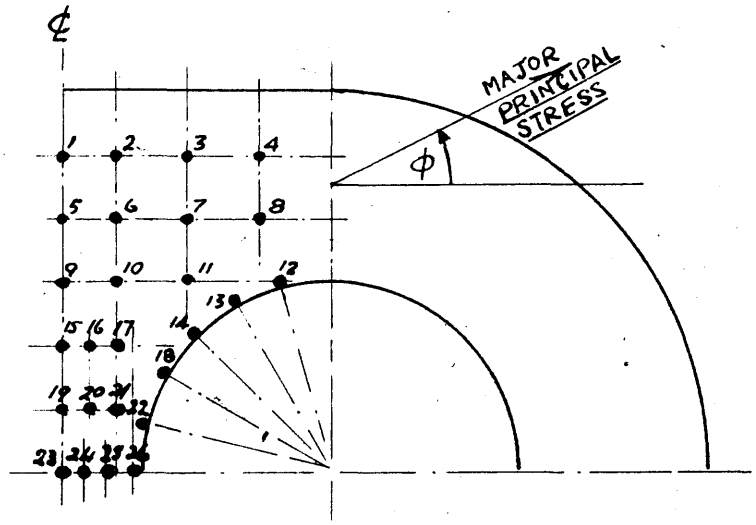

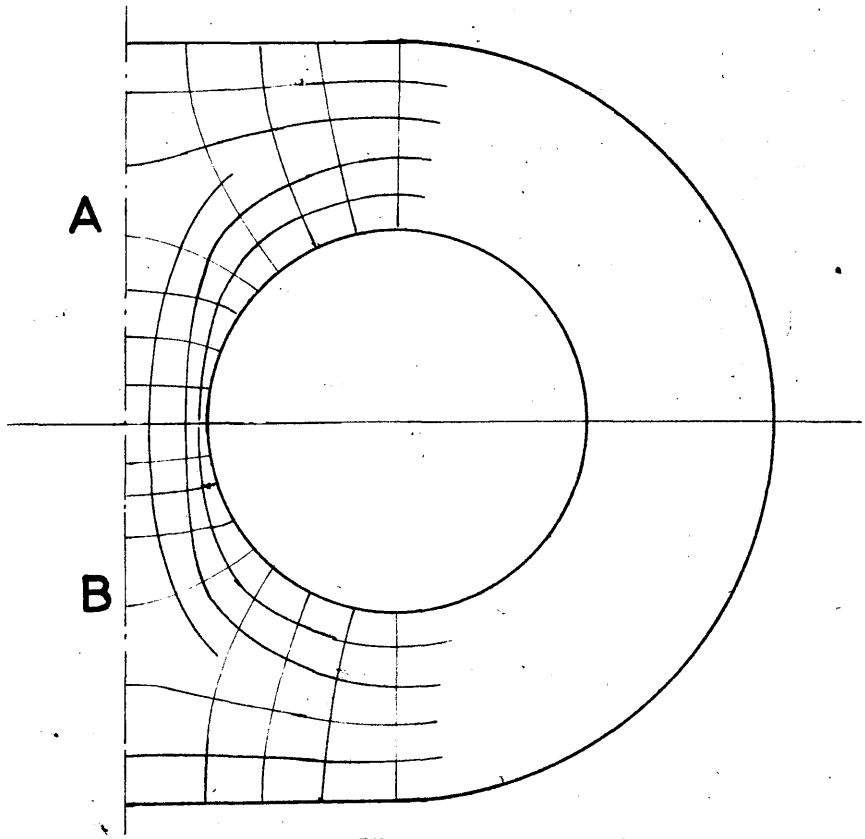

PRINCIPAL STRESS TRAJECTORIES IN BRIDGE-PIECE

FIG. 73

TABLE 14

Location No.	WEB A			WEB B		
	Direction ϕ°	Principal Stress T/in^2		Direction ϕ°	Principal Stress T/in^2	
		Major	Minor		Major	Minor
1	1	+ 2.3	+ 0.4	- 4	+ 4.6	+ 0.6
2	9	+ 2.4	+ 0.1	5	+ 4.7	+ 0.5
3	9	+ 3.0	- 0.2	3	+ 5.6	+ 0.4
4	5	+ 3.6	- 0.6	8	+ 5.1	- 1.0
5	- 12	+ 1.5	+ 0.9	20	+ 3.2	+ 0.9
6	24	+ 1.9	+ 0.2	16	+ 3.8	+ 0.6
7	22	+ 3.2	- 0.6	15	+ 5.5	- 2.4
8	11	+ 3.7	- 1.5	14	+ 6.9	- 2.4
9	103	+ 2.3	- 0.4	106	+ 3.4	- 0.2
10	57	+ 2.7	- 0.8	56	+ 2.9	- 0.7
11	33	+ 2.9	- 1.7	33	+ 6.0	- 1.5
12	45	+ 4.2	- 3.3	49	+ 8.6	- 1.4
13	34	+ 4.2	- 2.6	30	+ 9.9	- 0.2
14	15	+ 5.6	- 2.7	13	+11.9	- 2.2
15	97	+ 4.7	- 2.3	95	+ 8.7	- 6.3
16	83	+ 4.9	- 1.9	84	+ 6.3	- 4.0
17	70	+ 3.8	- 2.9	71	+ 6.3	- 4.6
18	63	+ 4.3	- 6.2	54	+ 8.6	- 4.5
19	94	+ 7.1	- 2.5	92	+ 9.8	- 4.0
20	90	+ 7.2	- 2.5	88	+ 9.8	- 4.5
21	86	+ 7.4	- 3.1	86	+10.0	- 5.3
22	82	+ 7.1	- 5.8	75	+12.9	- 4.0
23	89	+ 7.6	- 1.7	90	+10.6	- 3.1
24	88	+ 8.6	- 1.4	88	+12.0	- 2.9
25	84	+10.1	- 1.3	87	+13.1	- 2.0
26	91	+11.0	- 3.9	90	+10.6	- 4.3

very vulnerable to accidental damage. During the removal of the pin sections a few posts were dislodged, and the results of some other measurements are probably erroneous. Fig. 74 shows the results of the length measurements at the various stages of the test. When damage was discovered, additive measurements were made, and by averaging and other devices, a rough analysis is possible.

1. Changes in Bore.

The changes, in inches, due to removal of both pins are as follows:

	Web A	Web B
Diameter A	0.0129	0.0051
Diameter B	0.0128	0.0156

The values were obtained from the additive measurements in Fig. 74 by assuming equal changes in D and C (Web A) and in D , E and C , (Web B).

The value 0.0051" for Web B is apparently incorrect, and may be checked by dimension F . The change in F , less the change in thickness of the bridge, should approximately equal the change in A + E . The bridge thickness change given by the average of electrical strains is +0.0042", resulting in a value for F corresponding to the change in A + E of

$$F' = 37.6597 - 37.6301 + 0.0042" = 0.0338"$$

whereas change in A + E is equal to

$$30.7381 - 30.7351 = 0.0030"$$

FIG.74.

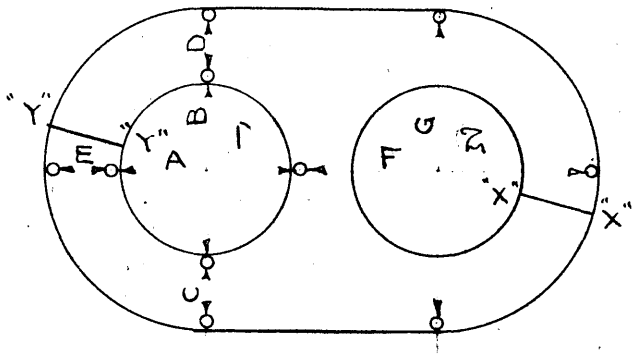

	WEB "A" [SHRINK ALLOWANCE $1{\cdot}4\times10^{-3}$ IN/INDIA]				WEB "B" [SHRINK ALLOWANCE $2{\cdot}4\times10^{-3}$ IN/INDIA]			
DIMENSION	AFTER SHRINK ASSEMBLY	DISCS DRILLED OUT	WEB CUT ON "XX"	WEB CUT ON "YY"	AFTER SHRINK ASSEMBLY	DISCS DRILLED OUT	WEB CUT ON "XX"	WEB CUT ON "YY"
A	77·0906	77·0777	77·0716	77·0547	77·0753	—	—	—
B	77·0448	—	—	—	77·1039	—	—	—
C	8·1764	8·1772	8·1770	8·1772	8·1976	8·1947	8·1945	8·1947
D	8·1177	—	—	—	8·1518	—	—	—
E	8·1864	8·1874	8·1876	8·1879	8·1678	—	—	—
F	37·5446	37·5378	37·5797	37·5305	37·6597	37·6301	37·6113	37·6119
G	39·4840	39·4734	39·4572	39·4637	39·5047	39·4893	39·4905	39·4887
A+E+0·5"	—	—	—	—	30·7381	30·7351	30·7332	30·7339
B+D+0·5"	30·6675	30·6507	30·6557	30·6495	30·7557	30·7472	30·7416	30·7389

—LENGTH MEASUREMENTS—

These two values may be averaged and the eye-piece change added giving a corrected value for change in diameter A (Web B) equal to 0.0205".

The average change in diameter of the hole at the measurement section is then

Web A 0.01285"

Web B 0.01805"

and the corresponding diametral strains are

Web A $\frac{0.01285}{22\frac{3}{4}}$ = 0.565 mils

Web B $\frac{0.01805}{22\frac{3}{4}}$ = 0.794 mils

2. Changes of Outside Diameters (at 40" diameter).

		A	B
Diameter	B + C + D	0.0110"	0.0114"
Diameter	G	0.0106"	0.0154"
	Mean	0.0108"	0.0134"
	Strains (mils)	0.270	0.335

3. Bore Pressure.

The circumferential strain at any radius y is given by

$$e_\theta = 0.90 \frac{P}{E(k^2 - 1)} \left\{ (1 - \sigma) + (1 + \sigma) \frac{k^2}{y^2} \right\}$$

Hence the bore pressures corresponding to the above strains may be evaluated, and are as follows :

	Bore Pressure T/in^2	
	Web A	Web B
From inside Diameter	4.3	6.1
From outside Diameter	4.9	6.1
Average	4.6	6.1

4. Comparison with Electrical Strains.

The electrical strain gauge readings round the bore and outside were averaged and are compared with the average measured strains below:

	Strains (mils)			
	Mechanical		Electrical	
	Web A	Web B	Web A	Web B
Inside Diameter	0.565	0.794	0.547	0.883
Outside Diameter	0.270	0.335	0.341	0.414

The agreement is fair; discrepancies show no definite trend.

(iv) Bore Measurements.

Measurements of the holes at various stages of the test are shown in Fig. 75 . The axial averages of changes in bore sizes due to fitting and removal of pins are as follows:

FIG. 75.

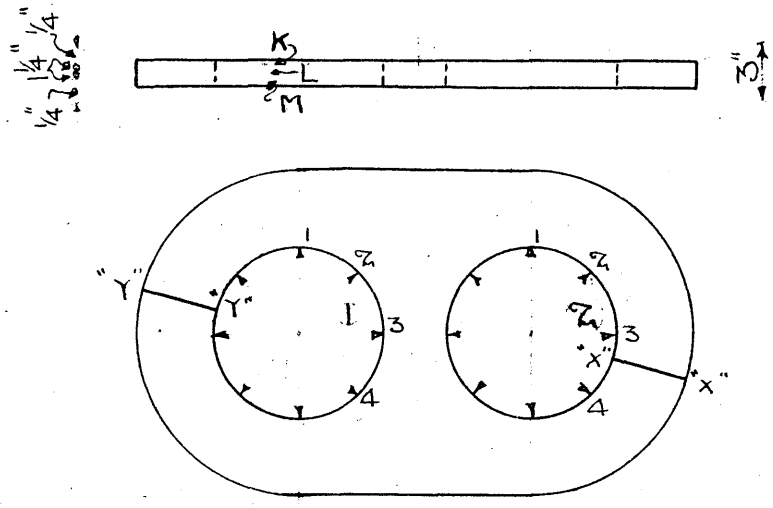

WEB "A" [SHRINK ALLOWANCE 1×10^{-3} IN./IN. DIA.]

MEASURING POSITION	MEASUREMENTS OF BORE ① BEFORE SHRINK ASSEMBLY	DISC ① DRILLED OUT	DISC ② DRILLED OUT	WEB CUT ON "XX"	WEB CUT ON "YY"	MEASUREMENTS OF BORE ② BEFORE SHRINK ASSEMBLY	DISC ① DRILLED OUT	DISC ② DRILLED OUT	WEB CUT ON "XX"	WEB CUT ON "YY"
K 1	2.1·7505	2.1·7560	2.1·7570	2.1·7577	2.1·7443	2.1·7505	—	2.1·7518	2.1·7498	2.1·7406
K 2	2.1·7498	2.1·7498	2.1·7487	2.1·7487	2.1·7348	2.1·7505	—	2.1·7518	2.1·7328	2.1·7410
K 3	2.1·7497	2.1·7481	2.1·7495	2.1·7438	2.1·7624	2.1·7503	—	2.1·7535	2.1·7438	2.1·7447
K 4	2.1·7496	2.1·7518	2.1·7501	2.1·7512	2.1·7392	2.1·7499	—	2.1·7493	2.1·7297	2.1·7351
L 1	2.1·7508	2.1·7557	2.1·7518	2.1·7577	2.1·7442	2.1·7504	—	2.1·7570	2.1·7306	2.1·7412
L 2	2.1·7497	2.1·7498	2.1·7481	2.1·7492	2.1·7352	2.1·7499	—	2.1·7570	2.1·7334	2.1·7416
L 3	2.1·7500	2.1·7485	2.1·7496	2.1·7441	2.1·7768	2.1·7500	—	2.1·7537	2.1·7438	2.1·7439
L 4	2.1·7498	2.1·7518	2.1·7504	2.1·7511	2.1·7396	2.1·7500	—	2.1·7497	2.1·7302	2.1·7359
M 1	2.1·7503	2.1·7561	2.1·7570	2.1·7580	2.1·7443	2.1·7503	—	2.1·7572	2.1·7312	2.1·7419
M 2	2.1·7499	2.1·7501	2.1·7483	2.1·7498	2.1·7362	2.1·7499	—	2.1·7572	2.1·7340	2.1·7421
M 3	2.1·7499	2.1·7491	2.1·7501	2.1·7441	2.1·7769	2.1·7500	—	2.1·7539	2.1·7438	2.1·7443
M 4	2.1·7496	2.1·7521	2.1·7507	2.1·7511	2.1·7396	2.1·7503	—	2.1·7505	2.1·7314	2.1·7368

WEB "B" [SHRINK ALLOWANCE 2×10^{-3} IN./IN. DIA.]

MEASURING POSITION	MEASUREMENTS OF BORE ① BEFORE SHRINK ASSEMBLY	DISC ① DRILLED OUT	DISC ② DRILLED OUT	WEB CUT ON "XX"	WEB CUT ON "YY"	MEASUREMENTS OF BORE ② BEFORE SHRINK ASSEMBLY	DISC ① DRILLED OUT	DISC ② DRILLED OUT	WEB CUT ON "XX"	WEB CUT ON "YY"
K 1	2.1·7510	2.1·7755	2.1·7682	—	2.1·7667	2.1·7505	—	2.1·7685	—	2.1·7687
K 2	2.1·7508	2.1·7612	2.1·7643	—	2.1·7611	2.1·7505	—	2.1·7640	—	2.1·7563
K 3	2.1·7507	2.1·7585	2.1·7620	—	2.1·7585	2.1·7509	—	2.1·7645	—	2.1·7450
K 4	2.1·7506	2.1·7622	2.1·7630	—	2.1·7579	2.1·7497	—	2.1·7613	—	2.1·7638
L 1	2.1·7510	2.1·7759	2.1·7683	—	2.1·7662	2.1·7509	—	2.1·7679	—	2.1·7675
L 2	2.1·7505	2.1·7625	2.1·7645	—	2.1·7610	2.1·7505	—	2.1·7628	—	2.1·7558
L 3	2.1·7505	2.1·7583	2.1·7623	—	2.1·7590	2.1·7505	—	2.1·7635	—	2.1·7442
L 4	2.1·7503	2.1·7630	2.1·7640	—	2.1·7572	2.1·7498	—	2.1·7614	—	2.1·7628
M 1	2.1·7510	2.1·7757	2.1·7688	—	2.1·7662	2.1·7507	—	2.1·7666	—	2.1·7660
M 2	2.1·7505	2.1·7612	2.1·7640	—	2.1·7603	2.1·7505	—	2.1·7622	—	2.1·7545
M 3	2.1·7505	2.1·7583	2.1·7621	—	2.1·7595	2.1·7505	—	2.1·7630	—	—
M 4	2.1·7503	2.1·7626	2.1·7629	—	2.1·7560	2.1·7499	—	2.1·7615	—	2.1·7618

BORE MEASUREMENTS

TABLE 15

	Web A		Web B	
	1	2	1	2
Diameter 1	+ 0.0014	+ 0.0016	+ 0.0174	+ 0.0170
Diameter 2	- 0.0016	+ 0.0019	+ 0.0137	+ 0.0125
Diameter 3	- 0.0001	+ 0.0035	+ 0.0116	+ 0.0130
Diameter 4	+ 0.0007	- 0.0002	+ 0.0129	+ 0.0116
Average	+ 0.0001	+ 0.0017	+ 0.0139	+ 0.0135
Loss of Fit (mils)	neg.	0.08	0.64	0.62
Residual Fit (mils)	1.00	0.92	1.36	1.38

Variations of diametral measurements of the order of 1.5×10^{-3} inches in Web A and of 3.5×10^{-3} inches in Web B, from the diametral average, are evident. In bore 1 of Web A the loss of fit was negligible, yet this bore also shows these considerable variations. In the axial direction variations approaching 1×10^{-3} inches are present. Furthermore, the discrepancies are apparently random. The maximum machining inaccuracies before assembly were about 0.5×10^{-3} inches; the variations therefore must be attributed to the method of heating, which produced local overstrain at certain parts of the surface, giving random distortions indicated by the above measurements, and as will be shown later, inducing an initial stress system before the assembly of the pins. The results

of the residual stress analysis discussed below indicate that this explanation is almost certainly the correct one.

Table 15 also shows the average loss of fit and residual fit. Pressures calculated from these values are as follows:

TABLE 16

Bore	Pressure T/in^2
A.1	4.3
A.2	3.9
B.1	5.8
B.2	5.9

The pressures for bores A.2 , B.2 may be compared with the results found from the stress analysis and from the length measurements, and are shown in Table 17 .

TABLE 17

	Pressure in T/in^2	
	A	B
Stress Analysis	4.0	6.0
Length Measurements	4.6	6.1
Bore Measurements	3.9	5.9

The agreement is very satisfactory in both cases.

The loss of fit in Web B shown in Table 15 is slightly greater than would be caused by the same fit allowance in a simple ring. The experiment on rings and plugs in Section 1 showed that with a fit allowance of 2 mils, the permanent set was about 0.5 mils, but the fit allowance of 2 mils in the web is equivalent to only 1.8 mils in the ring, due to the lower radial stiffness of the former. The axial grip conditions are, however, quite different, due to difference of axial length; also the stress concentration zones of the web probably allow greater premanent set to be developed, after overstrain begins. The correlation of pressure and fit allowance in the web shape with that in the simple ring would require a complete series of tests, varying the fit allowance in assemblies of both types.

(v) Residual Stress System from Cutting Eye-Piece.

After removing both pins, the eye-pieces were cut from outside to bore at XX and YY as shown in Fig. 70 . Difficulty was experienced with the drilling operation, owing to the tendency for the halves of the eye-piece to close, jamming the drill shank, although the cutting edges were ground to produce oversize holes. The jamming occurred after about half the section had been drilled. It was noticed that not only did the halves tend to close circumferentially, but a shear displacement of the two halves occurred. The amount of the closure and

displacement was about $\frac{1}{32}$" but the direction of shear was not always the same. The presence of shearing stresses on a radial section indicates a very complex and irregular stress system, which was confirmed by the strain gauge measurements.

Only the stresses adjacent to a cut section are relieved; complete analysis would require that the web be cut adjacent to every strain gauge. On this account only the stresses in the eye-piece and round bore and outside, have been calculated. The bore and outside stresses are shown in Fig. 76 , the stress or radial sections of the eye-piece are shown in Fig. 77.

In both webs the residual stress system is very complex and irregular. The circumferential variations are considerable and little purpose would be served by averaging the values for the eye-piece. Some general features stand out, however. The hoop stress round the outside is mainly compressive, though low tensile values are observed in the right hand side of Web B . The residual stress system due to overstrain of a thick cylinder by internal pressure is tensile at the outside and compressive at the bore. The stresses observed are of the opposite kind, and are quite compatible with the closing of the eye-piece with radial cutting.

The nature of the stress and its irregularities are , without reasonable doubt, due to an initial stress system existing

RESIDUAL STRESS

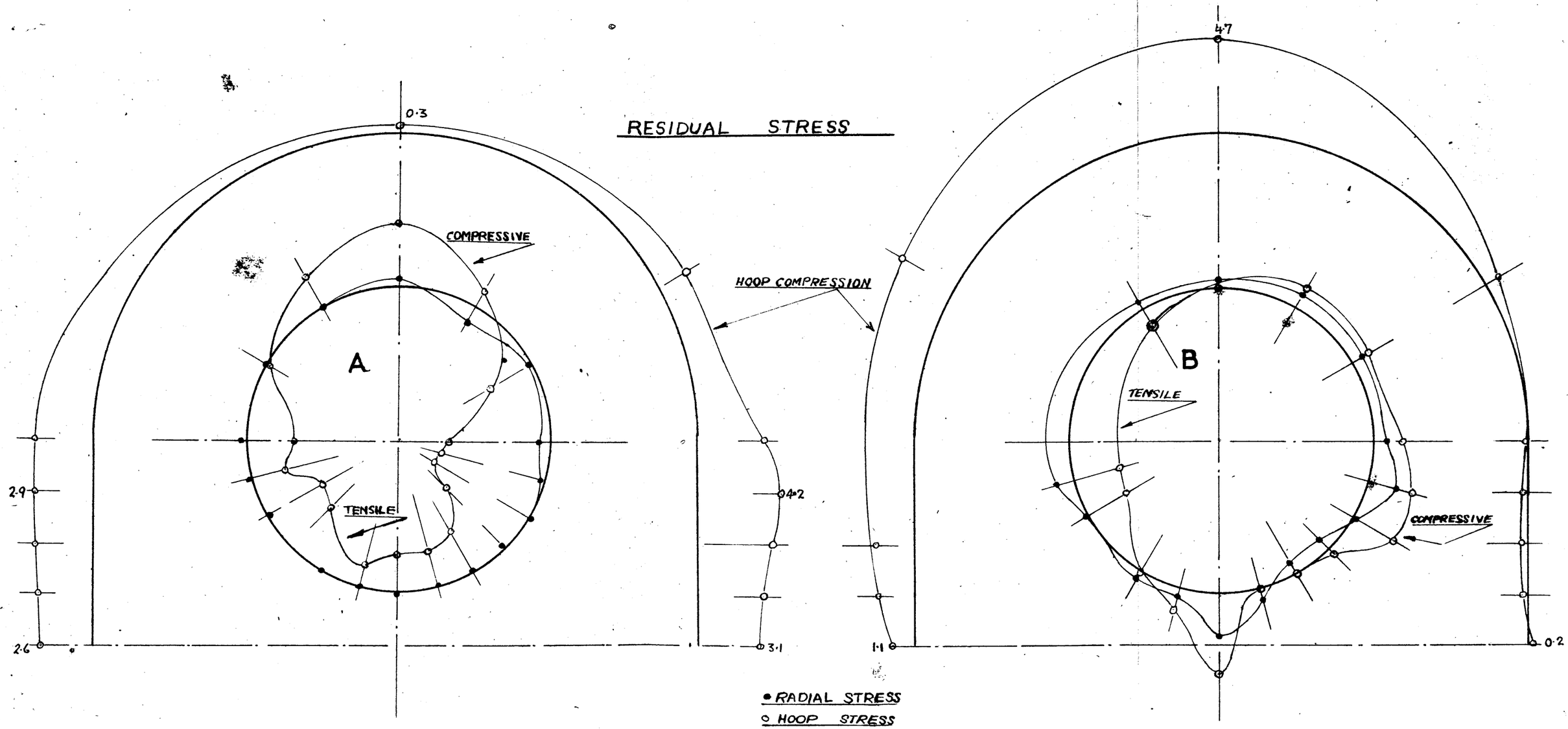

● RADIAL STRESS

○ HOOP STRESS

STRESS SCALE 1" = 5 T/IN.²

FIG. 76

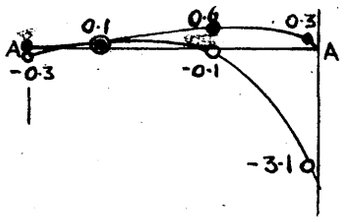

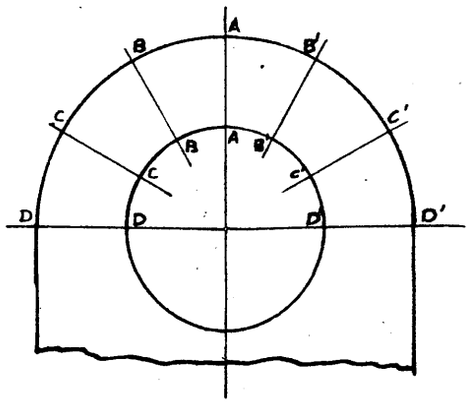

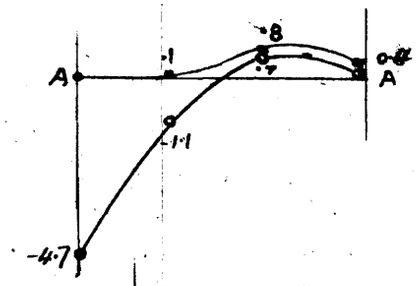

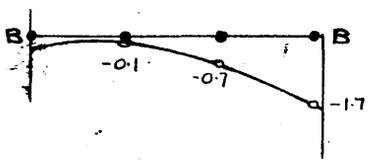

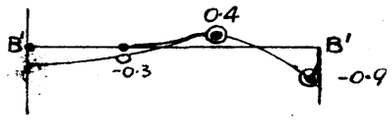

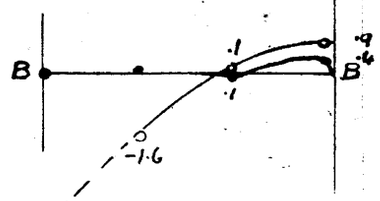

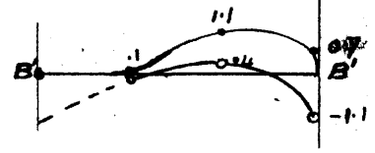

• RADIAL PRESSURE

o HOOP TENSION

STRESS SCALE: 1" = 5 T/in.²

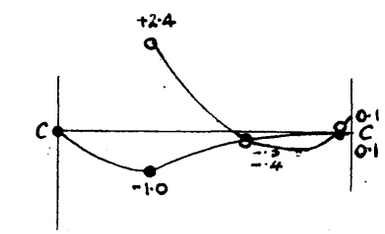

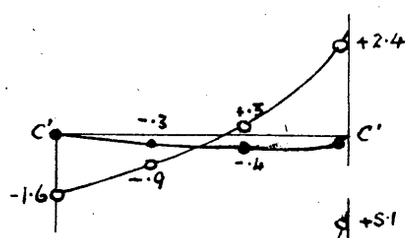

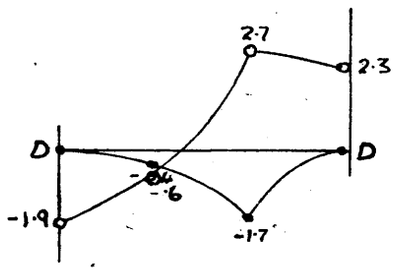

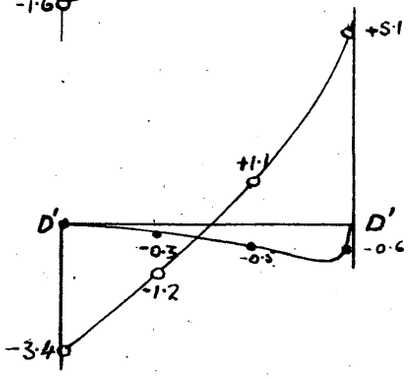

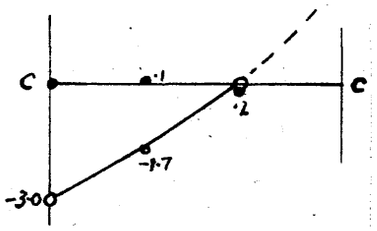

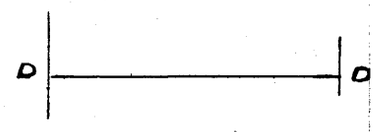

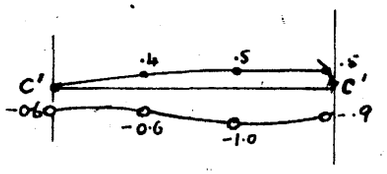

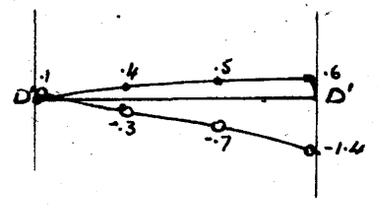

NOTE: RADIAL STRESS TENSILE — VE

RESIDUAL STRESS ON RADIAL SECTIONS

FIG.77

before assembly and resulting from plastic flow during the flame-heating of the webs. The heating was effected by a naked flame in the bores, the position of which was altered at irregular intervals to heat various parts of the circumference.

The qualitative effect of such treatment may readily be deduced by considering the affect of heating one spot on the surface of a thick plate. The spot and adjacent metal tend to expand but free expansion is prevented by the surrounding material, inducing a local compressive stress at the hot spot. With sufficient temperature gradient and taking account of the lowering of the yield stress with temperature, plastic flow by compressive stress action results. On cooling, the spot which has yielded in compression returns to a residual tensile stress, while the surrounding material is in a state of residual compression.

The spot may be associated with parts of the bores subjected to prolonged flame treatment; rotational symmetry is destroyed and compressive stresses are induced in the outside layers. By St. Venant's principal these will tend to be more uniform than the localised tensile stress at the bores. The experimental results show that this is, in fact, the case.

In Web B the residual stresses are not, in general, so high as in Web A , owing to the plastic flow inducing residual

stress of the opposite kind. It is well-known that, under pressure, the propagation of overstrain is somewhat irregular, and that plastic wedges occur with local variations of the average conditions. The spot stress 4.7 T/in^2 at the outside of section AA , Fig. 77 , indicates that the section has been comparatively little affected by the overstrain. The other sections show smaller values of residual compressive stress.

Even if the initial stress system were known precisely, it would be difficult to analyse the overstrain conditions, as existing theories of overstrained rings are based on an initial stress-free condition. Also the presence of axial shear traction at the bore complicates the flow relationships, making analysis impossible.

The residual stress system in Web A may be taken to be due to the heating effect alone, as only a small degree of overstrain was induced by fitting the pins. It is likely that this was confined to the region of the bridge-piece. The magnitude and irregular nature of this stress system cast grave doubts on the efficacy of the practice of flame heating crank webs to attain shrinking temperature.

(vi) Surface Finish.

Traces of bore finish obtained by the Tomlinson instrument are shown in Fig. 78 . The tool-feed wave length checks with records taken at the machining process. The

MAGNIFICATION:- ×1000 ←→ ×8·33

FIG.78

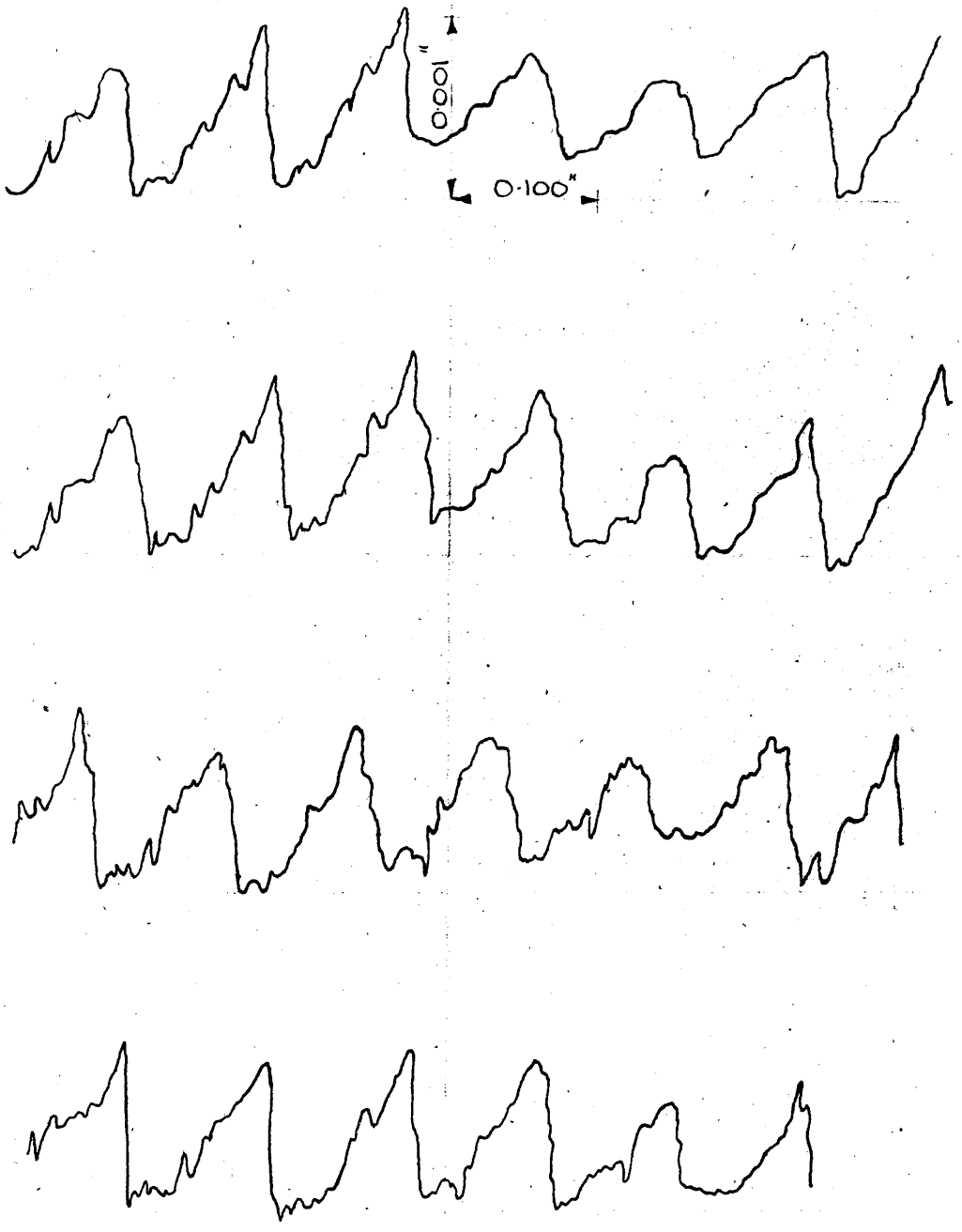

VERTICAL SCALE :- 1" = 0·001" } AFTER ×75 PROJECTION
HORIZONTAL SCALE :- 1" = 0·1320" } OF ORIGINAL RECORD

FROM RECORDS FEED OF TOOL IS 0·094" PER REVOLUTION

TOMLINSON WAVINESS RECORDS
FROM
CRANK WEB BORE
(ACROSS CUT)

amplitude of groove of about 0.001" is practically the same as that found in the used crankshaft (see Fig. 61) which had been subjected to a considerable amount of cold working. The macro finish, or waviness, is not therefore affected by the assembly and subsequent loading; the finer finishes also are not affected to any noticeable extent, as the results of tests on model webs have shown.

Measurements of bore sizes probably indicate the peak-to-peak diameters. With the tool mark the trough-to-trough diameter would be 0.002" larger. The average diameter is therefore 0.001" greater than the measured value, giving an error in the fit allowance of 0.045 mils, and a calculated interface pressure of about 0.2 T/in^2 higher than that based on the mean size. Pressures calculated from the residual fits, however, are actually slightly lower than the strain measurements indicate; it therefore seems likely that contact occurs only on the peaks of the surface. The fact that the profile is apparently unaltered by the fitting and that an appreciable quantity of oil was found in the bores of the used shaft, support this view. The oil probably penetrates the grip by capillary action, since the presence of a residual axial grip in the used shaft precludes any separation of the grip surface under running conditions.

If contact occurs only on the peaks of the tool marks

the local pressure and friction coefficients are certainly greatly in excess of the average values. Cold-welding undoubtedly occurs, causing the high initial stripping load, which is much greater than the value under sustained stripping action. The tendency for the weld to become re-established with time after stripping, has been noted earlier.

The fact that friction and pressure are invariably based on nominal area is not important, since friction values are, as yet, empirical. The writer has, however, seen examples of shrink-fitting in which no contact, even on peaks, had been made on large areas of the interface, due to machining inaccuracies of roundness and straightness. The practice of "ringing" a tail-shaft liner to indicate contact conditions is an example of this common weakness of shrink-fits. It seems doubtful whether a representative empirical friction value for the surface conditions is applicable in cases where fairly uniform area contact is lacking.

4. ELECTRICAL STRAIN GAUGE APPARATUS AND TECHNIQUE.

(a) General.

Spectacular developments in light-current electrical engineering during the past few decades have led to significant advances in many kinds of instrumentation. The convenience of electrical devices for detection, transmission, indication and recording of data, is unsurpassed. In the field of experimental stress analysis bonded wire-resistance strain gauges have contributed vast quantities of experimental data, frequently in circumstances where no alternative type of measuring device was feasible.

It is sometimes alleged that the indirection of electrical instrumentation is an objectionable feature, but strain, by definition, is essentially an inferred quantity, however measured, and the accuracy of the bonded strain gauge is likely to be as high as that of any other device of comparable gauge length. A more valid criticism is that direct calibration is often impracticable, and on this account errors of unknown magnitude are possible.

The ever-increasing number of applications of this type of gauge is, unfortunately, not commensurate with the amount of published data on the reliability and accuracy thereof. It is therefore worthwhile examining the causes of inaccuracy and

the steps which may be taken to eliminate or minimise spurious indications. A description is given below of a direct-current strain bridge with a 200-gauge capacity, designed by the writer, in which many of the more common defects of apparatus have been overcome. The technique employed for attachments, treatment and protection of large numbers of gauges is also described. The overriding consideration affecting design of apparatus and development of technique was the attainment of reasonable accuracy, with the minimum of preparatory work, in the industrial, as opposed to laboratory, conditions, in which the full-scale tests were carried out.

(b) Errors.

(i) Errors in Strain Sensitivity.

The influence of strain on electrical resistance, known as the "gauge factor" is generally assumed from a calibration of one or more gauges of a batch. Variations of the calibration may occur either by intrinsic variations of gauges or by variations in the bonding and after treatment.

The error is proportional to the strain measured. It can be minimised by quality control in the manufacture of gauges and by a satisfactory technique for the installation and treatment of gauges.

(ii) Errors in Resistance Measurement.

These errors arise from a number of widely varying causes and may be either a function of the resistance change, or entirely random.

In addition to the precautions in (i) above to ensure constancy of gauge factor, attention must be paid to the design of apparatus. A list of, and comment on, the more common sources of error is as follows:

1. Temperature Compensation.

Wires of the nickel- chromium alloys commonly used for resistance gauges, are quite sensitive to relatively small changes in ambient temperature. This disadvantage is readily overcome by a temperature compensating gauge, placed in the vicinity of the active gauge, but not subjected to strain. The principle relies upon the compensator remaining always at the same temperature as the active gauge, but appreciable errors due to time lag in conditions of rapidly changing temperature, or due to draughts, may easily occur. It is not generally realised how sensitive are the gauges to minute changes of temperature, and how great are the normal diurnal variations. The only possible precautions against such errors are to provide adequate thermal insulation, and to locate the compensator close to the active gauge.

2. Spurious Electrical Phenomena.

Precision measurements of resistance are invariably made with a bridge type of network, the simplest example of which is the Wheatstone Bridge shown in Fig. 79 . Random changes of resistance may occur in any of the loops of the network, which includes electrical leads, and minute thermal e.m.f.s. are always present. These effects can be minimised by suitable circuit and apparatus.

3. Apparatus Calibration.

Resistance changes of the strain gauge appear as changes in potential between modes in the network. The potential may be amplified before operating an indicator or reoorder, or used directly in conjunction with a precision galvanometer. In some cases the network potential changes are annulled by changing a calibrated loop of the network. Errors in calibration of the instruments or network directly affect the strain measurement.

4. Variation of Gauge Resistance.

The guage resistance may change for reasons other than strain or temperature. Three likely causes are lateral pressure, change of shunt resistance, and variations at the terminal strip to filament junction. The first of these is troublesome in pressure vessels, but unlikely in normal install-

ations. The second may be eliminated by treating the gauge with suitable preparations to exclude air. The third, however, sets the limit of accuracy which may be attained with a particular type of gauge. The filament is usually spot-welded to a fairly substantial strip tag for soldering external leads, and the welded junction is responsible for a fair number of gauge failures during tests. Furthermore the overlap of filament and strip is a non-positive connection causing random variation of resistance. This error, though quite small, limits the accuracy in gauges of this construction. The effect is less in high resistance gauges where the proportion of filament length to terminal overlap is greater.

(c) Factors Affecting Design of Apparatus.

(i) Excitation.

In static strain work gauges may be used with either a.c. or d.c. networks. The former type of excitation requires capacitance balance or phase-discrimination, but enables the network voltage to be readily amplified with standard equipment, and is invariably used in auto-recording gear. With d.c. excitation resistance only need be considered, and the network signal can be measured directly with a precision galvanometer. The equipment required is simpler, lighter, less expensive, probably more stable in calibration and considerably more attrac-

tive to mechanical engineers untrained or inexperienced in electronic applications. So far as the writer can see no advantage is gained with a.c. gear unless high amplification of the signal is necessary to operate automatic switching and recording gear. The allegation that precision galvanometers are unsuited to the robust handling inevitable in industrial conditions is quite untrue.

(ii) Deflection and Null-Point Readings.

The signal voltage which appears due change of gauge resistance may be annulled by altering the value of a calibrated resistance at another loop of the network, or measured directly by the indication of a calibrated galvanometer . The scale-spread of many galvanometers is too short to permit reasonable accuracy but this difficulty may be overcome by a combination of the two methods, a rough null-point giving the first, or first two significant figures, the remaining figures being obtained from galvo deflection. The time required for a reading is shorter by this combined system than by either method, a not unimportant advantage in multi-channel set-ups.

(iii) Zero Setting.

Adjustment for initial balance of the bridge network shown in Fig. 79 is usually provided by a small resistance between gauge and compensator, with a tapping which can be altered

to zero the signal voltage at the commencement of a test. A disadvantage is that minor variations of zero setting are likely to occur during the test, due to the non-positive sliding contact, especially if toroidally-wound potentiometers are used for zero-setting. It is better to roughly balance the bridge with cut lengths of resistance wire using soldered connections, and overcome the lack of precise balance by differencing readings taken before and after the application of strain. If a sufficiently wide range of strain calibration is available, the initial unbalance can be entirely ignored.

(iv) Cable Connections.

Soldered connections are usually necessary throughout the bridge network to avoid spurious strain indications. In large installations the wiring of gauges to apparatus is no mean undertaking, and having been carried out, the measuring apparatus is permanently connected to the component on test. The necessity for plug-and-socket type cable connectors became evident after a little experience of this type of experimental work, and the electrical circuit was re-arranged to permit the measuring apparatus to be quickly dissociated from the strain gauge installation. Experimental accuracy was not only retained but enhanced through the necessary modification to the simple bridge circuit.

(v) Flexibility of Channel Capacity.

In many tests a multi-channel strain measuring apparatus may not be worked at the full channel capacity, but use of the spare capacity on other concurrent tests is frequently impracticable. A unit type of construction allows the total capacity to be distributed, the measuring bridge being required only for the time necessary for gauge readings.

(d) Description of Strain Bridge.

(i) Gauge Connections.

In the simple bridge network of Fig. 79, network loop resistances comprise the strain gauge and temperature compensator filament resistances and also the resistance of connecting leads and terminal connections. Any resistance change in a loop other than that due to strain or temperature change, is recorded by the apparatus. It is necessary to use soldered connections at all junctions between gauges and apparatus. By modifying the simple bridge to that shown in Fig. 80, the circuit is essentially unaltered but the battery connections in which resistance variations are immaterial, are now made direct to the gauges and the other connection to the measuring apparatus is in circuit, not with the gauge, but with the measuring bridge arm, which can be of any desired resistance value. With the use of sufficiently high resistance arms, resistances of

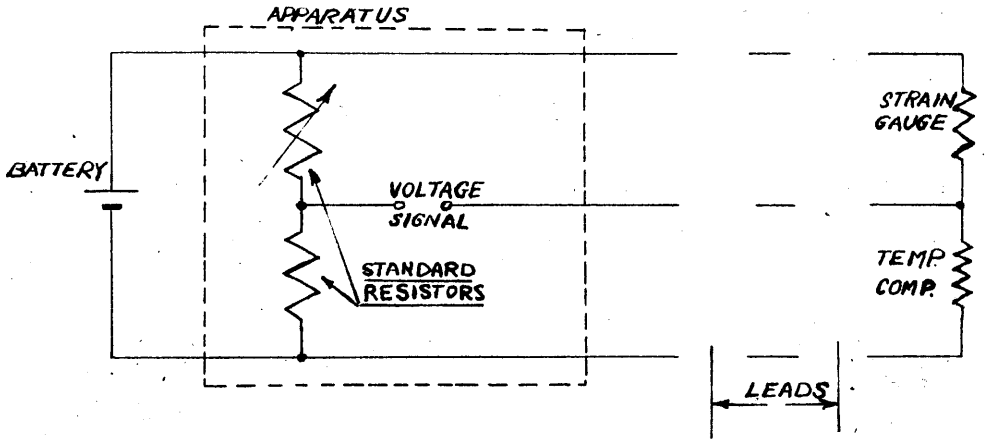
APPARATUS
BATTERY
VOLTAGE SIGNAL
STANDARD RESISTORS
STRAIN GAUGE
TEMP. COMP.
LEADS

FIG. 79

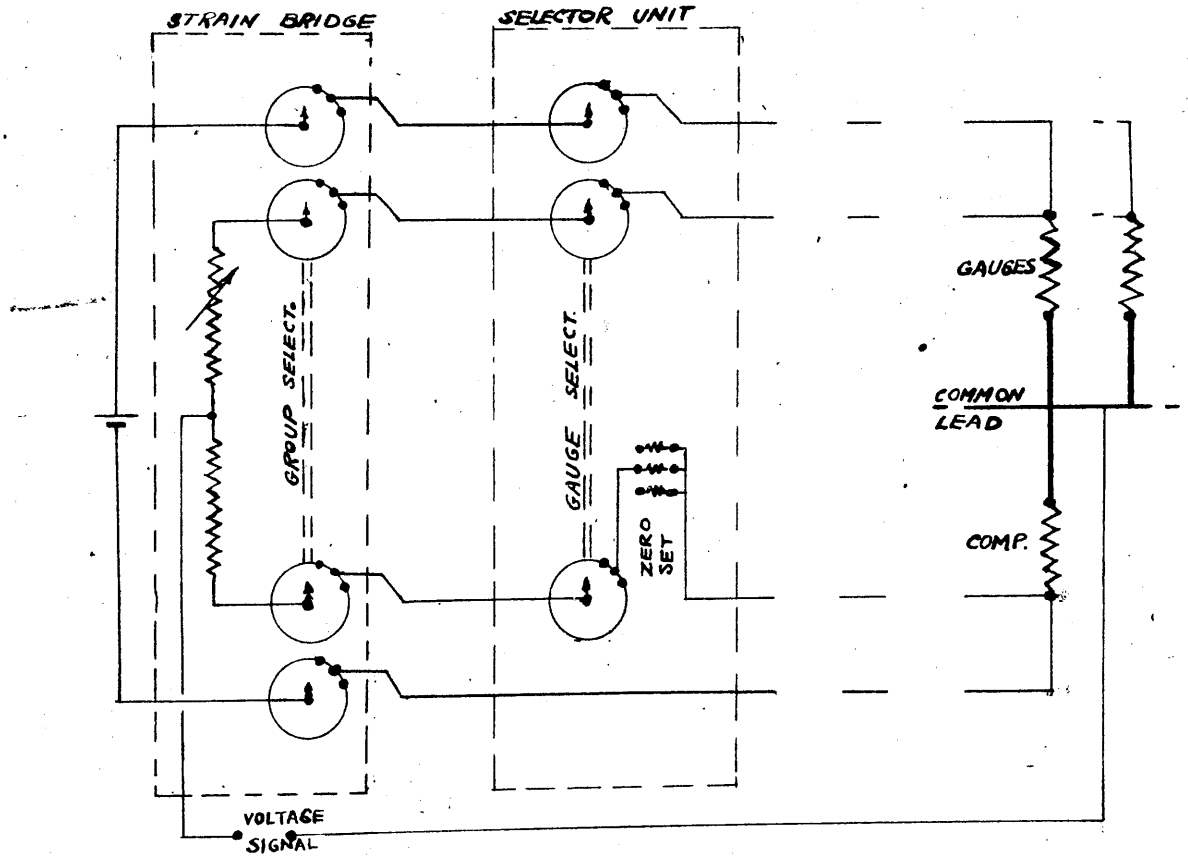
STRAIN BRIDGE
SELECTOR UNIT
GROUP SELECT.
GAUGE SELECT.
ZERO SET
GAUGES
COMMON LEAD
COMP.
VOLTAGE SIGNAL

FIG. 80

connections, switch and plug contacts etc., in the same circuit, can be disregarded.

(ii) Switching.

Several gauges may now be associated with one temperature compensator, resulting in a substantial saving both of gauges (which are expended) and of the time required for the preparation, wiring and treatment thereof. Compenaators must be located adjacent to their active gauges so a limit is set to the minimum number of compensators necessary. It was decided to construct the apparatus from standard units with a capacity of ten active gauges to which one compensator was allotted. This group of 10 + 1 gauges requires 22 connections from the apparatus, compared with the 40 required for 10 active gauges with the simple bridge.

Switching of the individual gauges of a group was effected by a 3-pole, 10-way gauge-selector switch, the current and potential leads of the gauges and the potential lead of the compensator being selected as required.

The complete apparatus comprised 20 such groups, giving a total capacity of 200 strain gauges, all of which was used in the test on the new webs. The groups were selected as required by a 4-pole, 20-way group-selector switch which connected both battery leads and both ends of the measuring resistances

to the gauge-selector.

(iii) Circuit Values.

The total number of indirect connections in either loop of the measuring arms was six (2 switch contacts and 4 cable connector ends). Tests of the ordinary commercial quality components indicated the resistance to be of the order of 0.01 ohms with a possible variation of about 50%. The maximum cumulative variation in both loops was therefore about 0.06 ohms. For an accuracy of $\pm$ 0.001% strain-resistance the minimum circuit resistance containing the variable contact resistance required to be 600 ohms. In order to depress the error to a lower significant figure, the bridge arms were fixed at 5000 ohms each.

An upper limit on the circuit resistance values is set by the loss of sensitivity, but this can be offset to some extent by using a more sensitive galvanometer. The external circuit resistance necessary for below-critical damping of a 400 ohm galvo is of the order of several thousand ohms; the high resistance bridge allows the most sensitive instruments to be used without undesirably sluggish response of heavy damping.

With a 12 volt battery giving about 30 m.A. gauge current, the sensitivity of the 400 ohm Tinsley galvanometer

was $3\frac{1}{2}$ cms. per 0.01% unbalance.

(iv) General Arrangement.

The unit group of 10 + 1 gauges is connected by short leads and soldered connections to a socket connector located adjacent to the group. Plates 9 and 10, show the completed wiring of the installation and a close-up of the bridge-piece. The G.P.O. type multi-core cables connecting the groups to the gauge-selector units can also be seen. A gauge-selector unit, comprising switch, connector sockets and zero setting terminals is shown in Plate 11. The larger cable carries 22 wires from the unit group, and the smaller 4 wires to the group-selector.

Front and back views of the complete apparatus are shown in Plates 12 and 13. The 20 gauge-selector units are contained in the two lower standard 19" panels. The top panel unit contains the group-selector switch on bottom right, the measuring resistors in a sub-unit on the top right, and various minor refinements for sensitivity, rough balance, etc. The measuring unit comprises two decade switches giving spot readings of 0.1% to 1.0% and 0.01% to 0.1% resistance change. The next decimal figure is obtained by splitting the galvanometer deflection.

(v) Accuracy.

The apparatus was tested by connecting a Tinsley

PLATE 9

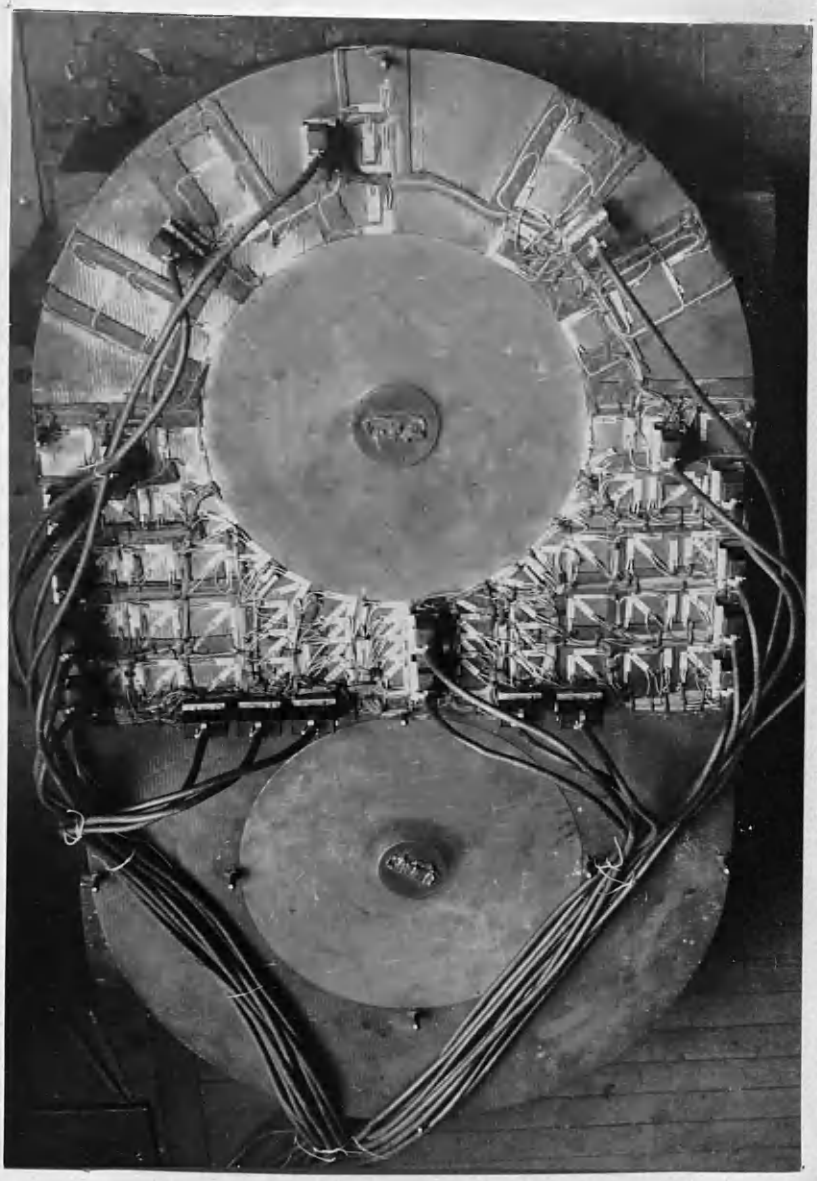

ELECTRICAL STRAIN GAUGE PATTERN

AFTER WIRING (NEW WEBS).

PLATE 10

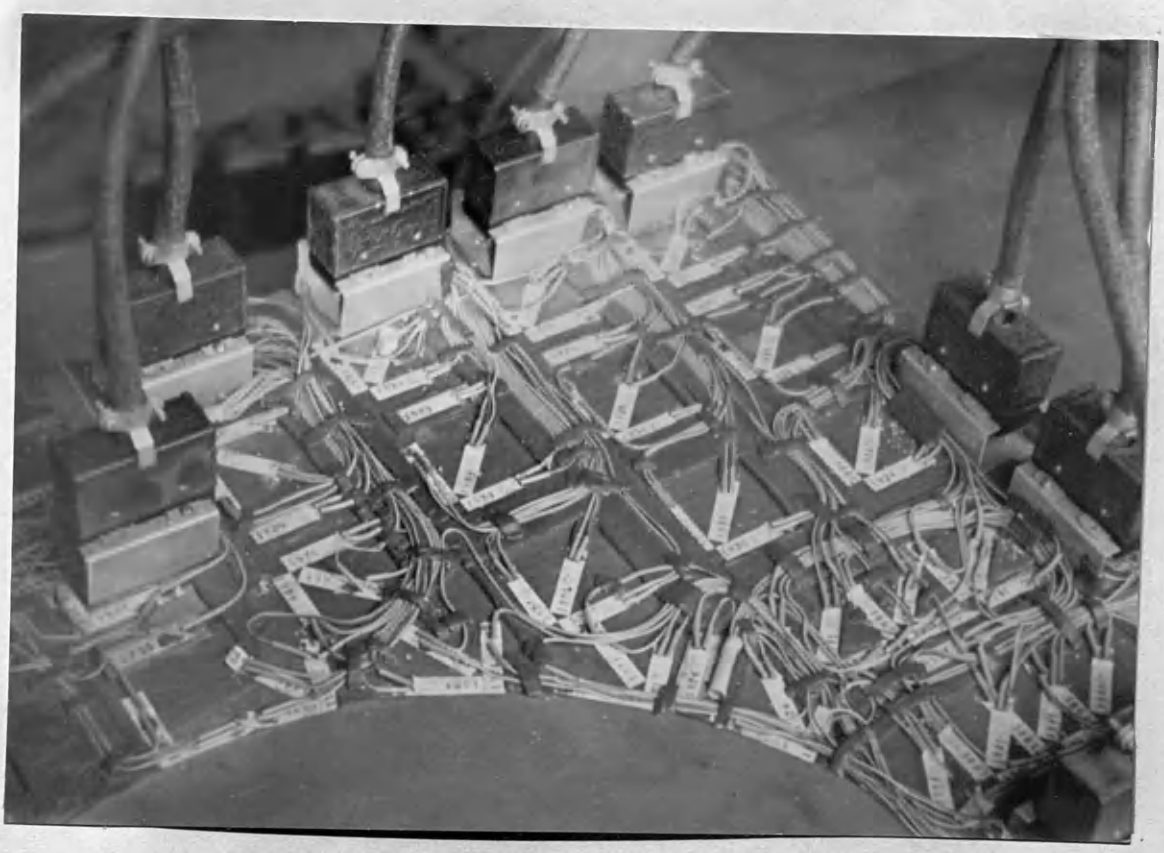

DETAIL OF WIRING AND CONNECTORS.

PLATE 11

GAUGE - SELECTOR UNIT.

PLATE 12

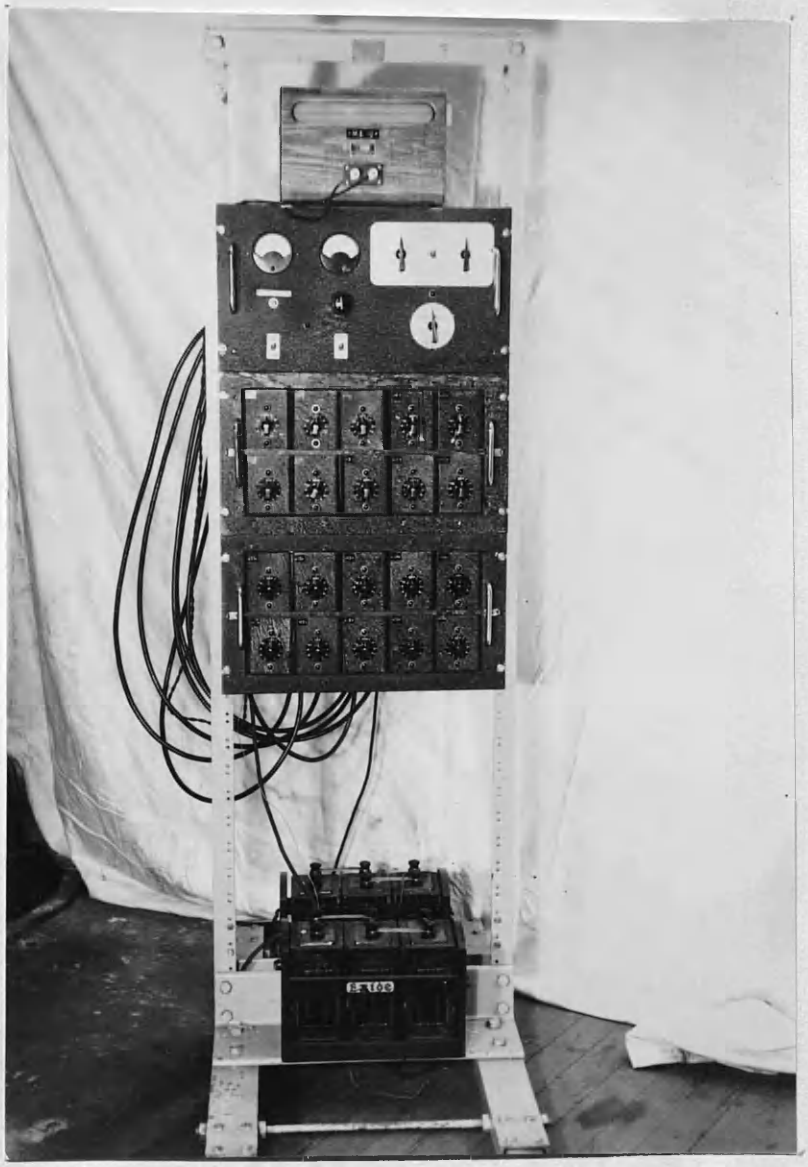

200-CHANNEL STRAIN BRIDGE - FRONT VIEW.

PLATE 13

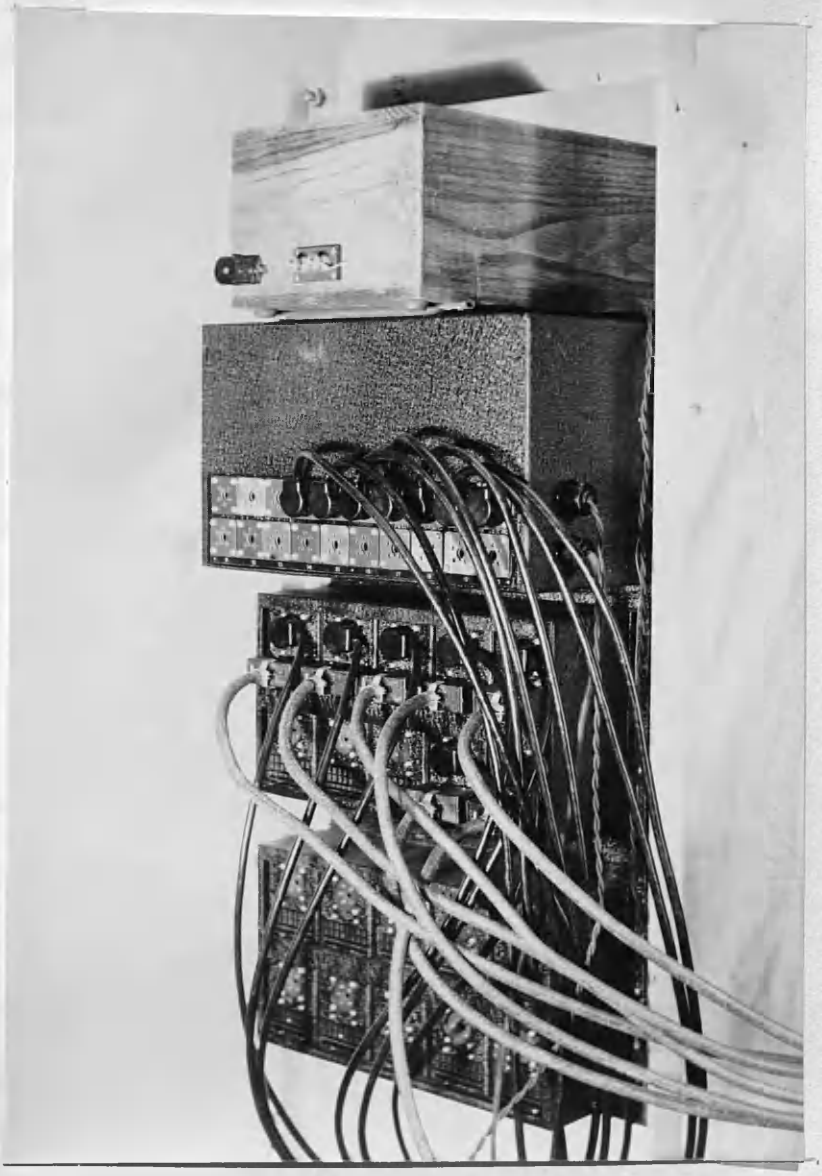

200-CHANNEL STRAIN BRIDGE - BACK VIEW.

strain bridge, consisting of two 100 ohm resistances with a centre variable slide-wire, in an exactly similar way to a strain gauge and compensator. The zero reading was not affected by undoing connectors or by switching, and remained constant over a period of several days.

When used with strain gauges, however, minor variations in strain readings could be observed. Large numbers of gauges were found to drift by amounts up to $\pm$ 0.005% resistance change. Since the drift of every gauge was practically always in the same direction it was concluded that time lag of temperature compensation was the cause. Random drift of about $\pm$0.002% was also observed. This was attributed to variations at the filament terminal overlap inside the gauge element.

In certain infrequent cases, large random variations occurred, often followed by breakdown of the gauge circuit. The cause is almost certainly bad welding at the ends of the filament.

Except for spot values which are clearly in error, the accuracy of the vast majority of strain readings is certainly better than 0.010% electrical change corresponding to about 0.005% linear strain, or in a simple stress system, $\frac{1}{3}$ T/in^2.

(e) Bonding, Wiring, Treatment and Protection of Gauges.

(i) Bonding.

The type of gauge exclusively employed was type S.E.A. 1

manufactured by the British Thermostat Co. Ltd., having a nominal resistance of 200 ohms and a $\frac{1}{2}$" gauge length. The gagues were sprayed with a cellulose cement during manufacture, and only required to be dipped in acetone and pressed on to the surfaces, which had been previously thoroughly degreased with trichlorethylene acetone, and clean cotton wool. After drying the gauges could not be removed without damage.

Compensating gauges were attached to $\frac{1"}{16}$ m.s. plates slightly larger than the gauges and located adjacent to the group.

(ii) Wiring.

Short lengths of 7/36 P.V.C. wire were soldered to the tags of the cable sockets and temporarily coded with typed brass tags. The sockets were inserted in metal holders secured by a film of Bostik 692 to the web surface, the wires run out to the appropriate gauges, cut to length, sleeved and soldered down. Some experience and practice was necessary to obtain clean wiring and good joints.

(iii) Treatment and Protection.

Wiring was started immediately the gauges were attached, but the length of time involved allowed ample drying before the gauges were covered to exclude atmosphere humidity. Towards the end of the wiring operation the webs were warmed

by any convenient method to reduce the moisture content as much as possible. A high resistivity wax, known as Di-Jell, was melted and poured over the gauges, care being taken to ensure that a complete film covering the entire gauge and ends of wires, was obtained.

The rest of the treatment was intended to afford additional protection against accidental damage, and to provide thermal insulation. A layer of 60/70 Bitumen was poured over the surface, completely sealing gauges and wires. Over the bitumen a sheet of indiarubber, sealed at the edges with Bostik 692, provided a non-tacky clean surface, resilient to accidental shock and completely waterproof.

The cable sockets were protected by metal covers against the ingress of dirt, cutting fluid and swarf. Fig. 81 shows a section through the protective covering of the gauges.

In the earlier experiments on the used webs, the gauge treatment and protection was rather more elaborate, but probably no more effective. The stages of this treatment are depicted in Plate 14.

FIG.81

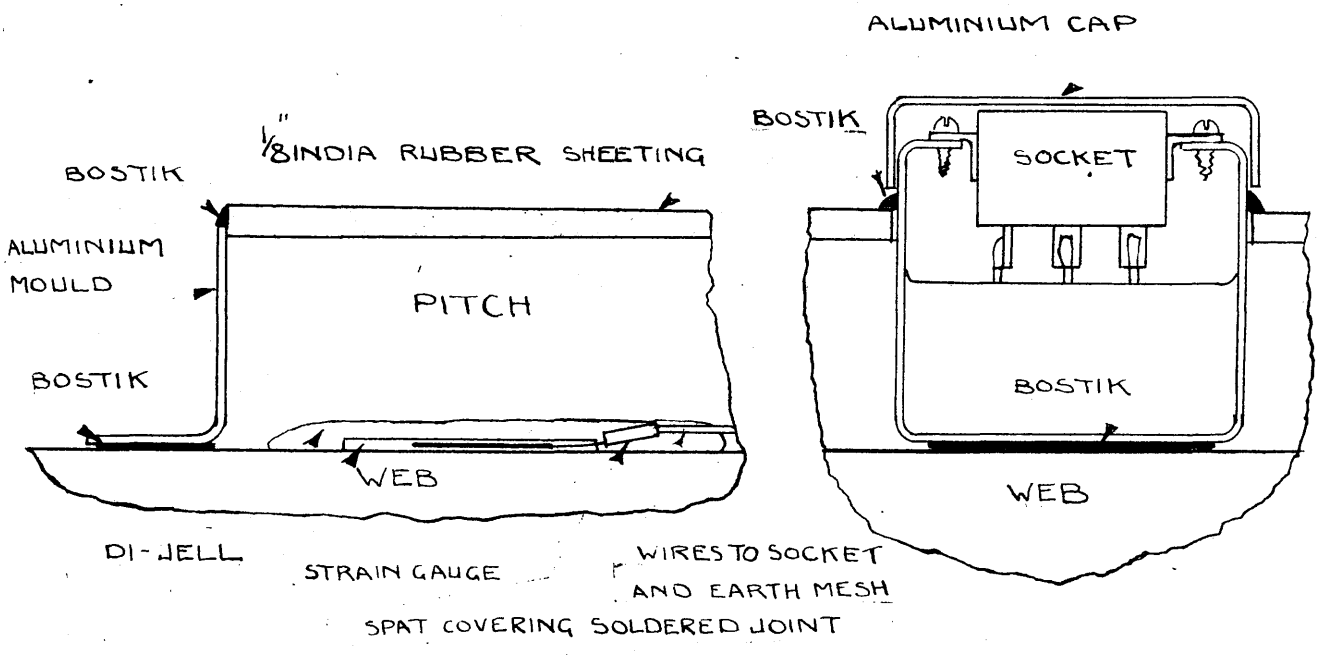

— STRAIN GAUGE PROTECTION —

PLATE 14

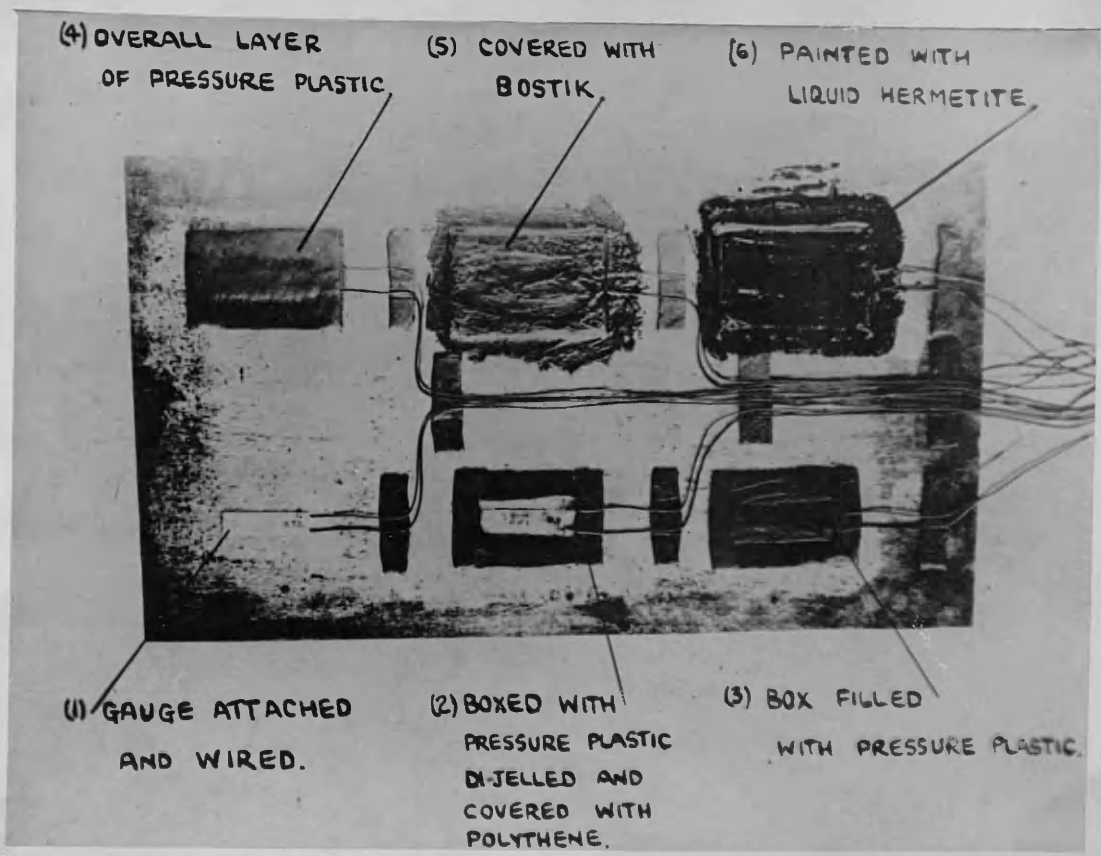

STRAIN GAUGE TREATMENT AND PROTECTION.

5. SUMMARY, CONCLUSIONS, RECOMMENDATIONS AND DESIGN DATA.

A. Ring-and-Plug Experiments.

(i) Calculated and measured deflections of the ring outside diameters with the plugs fitted, agree within the limits of experimental error. Such deflections, however, cannot indicate the presence of axial friction drag or of temperature variations of constants.

(ii) Measurements of permanent set at the bore and outside diameters after fitting and removal of plugs, suggest that axial friction drag of between $\frac{3}{4}$ and $\frac{1}{2}$ the full theoretical amount is present in this type of assembly. The trend of results indicates that correction for temperature change of elastic constants is not significant. The evidence is not conclusive, since any combination of the two effects could account for the experimental results.

(iii) Axial friction drag causes measurable warpage of the end surfaces of the ring. The axial extension of the bore layer is considerably less than the theoretical amount for no slip of the mating surfaces.

B. Model Crank Web Experiments.

(a) Friction.

(i) The grip strength of a lubricated assembly is greatly diminished by slight relative movement of the contact surfaces. The ratio of grip for recurring slip of the fitted surfaces, to the initial grip, is of the order of $\frac{3}{4}$.

(ii) The coefficient of friction corresponding to the initial grip strength is variable, but with repeated slip the friction becomes more uniform.

(iii) The effect of variations of surface finish on the grip strength is masked by experimental scatter. It may be concluded that finish of the mating surfaces is not of primary importance. The slight improvement with honed surfaces in certain cases, is probably due to improved geometry of the bore surface.

(iv) The coefficients of friction in lubricated fits are generally lower than in fits where no lubricant is used, even when the surfaces are not specially cleaned. The amount of reduction in grip varies greatly.

(v) Within the limits of experimental error, there is no evidence to show that the torsional coefficient of friction is different from the axial coefficient.

(b) Mode of Torque Failure.

(i) The deflection of a shrink-fitted assembly subjected to static torque is non-linear, due to inelastic deflection occurring at the end of the shrink-fit to which the torque is applied. Departure from linear elastic deflection occurs at a torque value approximately half the ultimate strength of the grip.

(ii) While this effect may be explained by local slipping of the grip, a more likely explanation is that plastic flow occurs due to the superposition of a stress system additional to the shrink-fit stress system.

C. Full-Scale Experiments.

(a) Fit Allowance.

(i) The residual fit allowance found after separation of the shrink-fit of a used crankshaft was between $\frac{1}{2}$ and $\frac{2}{3}$ the initial fit allowance on assembly. The bore profiles showed a considerable degree of bell-mouthing, undoubtedly due to pulsating bending of the pins under operating conditions. In these circumstances, it may be that the initial conditions are relatively unimportant and that attention should be directed to the effect of superposed cyclic force actions on

shrink-fits which actual or incipient overstrain prevails.

(ii) The maximum fit allowance for elastic conditions in the web was given in Part II as 1 mil. The test on a new assembly with this fit allowance showed that 8% loss of fit due to permanent set occurred in one bore. In this case, however, the stress system was complicated by initial stresses due to flame-heating the web.

(iii) With the overstrain fit allowance of 2 mils in a new web, the permanent set and loss of fit was slightly greater than overstrained-cylinder theory would indicate. This may be attributed to the zone of stress concentration at the bridge-piece. If a series of tests varying the fit allowance were carried out, empirical factors relating to overstrain in a web to that in a simple ring, could be found. The stress system in a crank web could then be adequately predicted by ring theory.

(b) Grip Strength.

(i) Coefficients of friction calculated from the axial stripping loads are of the same order of magnitude as those in the case of the model web experiments where the surface finish was much smoother. It may be concluded that surface finish is a relatively unimportant factor. The minimum value recorded at initial slip was 0.285 .

(ii) The surface finish is not measurably affected by assembly and separation. Apparently contact occurs only on the peaks of the surface irregularities. The presence of engine oil in the bores after separation suggests that oil enters the interstices by capillary attraction, since actual opening of the fitted surfaces could not have occurred in this case. Breathing and pumping of oil at the shrink-fits in built crankshafts is, however, not unknown.

(c) Axial Grip.

(i) Prevention of free axial shrinkage by friction drag at the bore causes warpage of the end faces; stress values recorded adjacent to the bore do not represent average conditions.

(ii) The persistance of axial drag in used crank webs demonstrates conclusively that opening of the fit or relative movement of the mating surfaces could not have occurred at any time after assembly, and that the coefficient of friction given by the initial stripping load may be used to estimate the grip strength.

(iii) The indications are that the amount of axial drag is variable and is generally not significant with fit allowances of 1 mil.

(d) Temperature Stress.

The method of flame-heating commonly employed to

bring the webs to shrinking temperature induces permanent distortion and initial stresses at the bore which are of a like kind to the stresses induced by the shrink-fit; the practice is therefore deleterious.

D. Recommendations for Built Crankshafts.

(a) Scantlings.

(i) Lloyd's Rules for the eye-piece radial thickness and for web axial thickness have apparently no theoretical basis, but probably approximate to the optimum proportions having regard to other considerations affecting marine engine design. Small variations of the eye-piece thickness have little influence on the maximum radial pressure for elastic conditions providing the appropriate fit allowance is used. An increase in axial length of fit would be beneficial, providing this could be achieved without unduly increasing the cylinder spacing and hence the overall engine length. Lengthening the grip increases the main bearing span and hence increases the bending moments on the shaft, but the arm of the couple resisting the moment at the fit is increased and also the torsional resistance to slip. The optimum length of fit is a matter of compromise, but it is felt that some effort should be made to obtain a longer grip than that given by Lloyd's proportions, in view of the bell-mouthing of the shrink-fit.

(ii) Transition fillets on the pins should be provided at the entry end of shrink-fits in order to equably distribute the applied forces over the fit surface. Present design of built crankshafts would be regarded as unsatisfactory if the component were of integral construction. It is difficult to appreciate why the re-entrant corners should be tolerated in the case of the built shaft when the stress conditions are more severe on account of the shrink-fit.

(b) Preparation of Webs.

(i) By pre-stressing the webs it would be possible to increase the fit allowance and interface pressure to a marked extent. The experiments of Russell and Shannon demonstrated the beneficial effect of cold-working in increasing the effective elastic range of the material. Macrae showed that low temperature heat treatment was necessary to stabilise the extended elastic range. The writer believes that it would not be impractical to pre-stress and stabilise marine crank webs either by a method of surface rolling or by an autofrettaging arrangement, followed by mild heat treatment.

(ii) The bore surface finish is not important, even with quite pronounced tool-mark waviness. Accurate geometry in roundness and straightness of the surfaces is, however, important in order to obtain uniform contact conditions over the entire nominal area.

(c) Grip Surface Film.

In contrast to surface finish, surface film condition is of prime importance. With a rough surface in which the tool-mark is pronounced, there is every reason to believe that engine oil will penetrate the interstices of the grip. In order to exclude this oil it is recommended that a filler substance of the setting type be applied to the surfaces during assembly. Thermosetting resins would not only fill the surface irregularities, but would provide a useful amount of bonding giving increased grip strength. The conditions of pressure and temperature in the shrink-fit are of the correct order to obtain rapid polymerisation of the resin. A little development work along this line should produce a very substantial improvement in the grip strength and complete exclusion of the lubricant.

(d) Fit Allowance.

The practice of using fit allowances which overstrain the web has no deleterious effect on the grip strength under static loading, as greater interface pressure can be obtained by exceeding the elastic limit. Tests of webs after service have shown that, with an initial fit allowance in the post-elastic range, a large loss of fit occurs due to cold-working of the bore under pulsating bending of the grip. Whether this can be avoided by maintaining entirely elastic conditions in the

initial assembly, is a matter of conjecture. Nevertheless it appears that little would be lost by reducing the allowance to that corresponding to elastic conditions, since the excess would inevitably be worked off in service; it is possible that a temporary elevation of the yield point would occur with an elastic fit under dynamic loading, inhibiting plastic flow. Furthermore, reducing the fit allowances reduces the shrinking temperature, with economies in time of heating and advantages of slower cooling rate, allowing more time for the assembly operation. The actual value of fit allowance for elastic limit conditions can be readily calculated from the data given below, in sub-section E .

(e) Shrinking Process.

The present practice of flame-heating the bores is unsound. Not all marine shops, however, have the necessary equipment for uniformly heating the webs to shrinking temperature, and an alternative (and possibly better) method would be to flame-heat the webs on the outside edge. The permanent stress set up by this, would be compressive at the bores, and thus would result in lower assembly stress. If steps were taken to reduce heat loss from the faces of the web, shrinking temperature would be attained quite quickly.

An advantage is that cleaning of the bores after heating would be unnecessary, and better film conditions would result.

(f) Cooling.

The practice of water-cooling shrink-fitted assemblies is now seldom used. Russell demonstrated the adverse effect of water cooling in his ring-and-plug experiments, and as no obvious advantage is to be gained, air cooling should be carried out.

E. Design Data.

(a) Lamé Thick Cylinder Formulae.

Hoop Stress at Bore: $$p_\theta)1 = \frac{k^2 + 1}{k^2 - 1} P$$

Hoop Stress at Exterior: $$p_\theta)k = \frac{2}{k^2 - 1} P$$

Internal Pressure: $$P = \frac{k^2 - 1}{2k^2} E\Delta$$

Elastic Limit: $$P = \frac{k^2 - 1}{k^2} s$$

and $$\Delta = \frac{2s}{E}$$

(b) Axial Grip Correction.

Interface pressure: $$P = \frac{1}{1 - m\sigma} \frac{k^2 - 1}{2k^2} E\Delta \quad , \quad 0 < m < 1$$

The value of m is a function of the diameter/length ratio and of the coefficient of friction. For long assemblies $m = 1$. In ring-and-plug tests, with length = diameter, the

experimental value was approximately $\frac{1}{2}$. A suitable value for Lloyd's proportions is probably $\frac{1}{4}$. In thin slabs the assumed value of zero resulted in no measurable discrepancy.

(c) Shape Factors.

The radial stiffness of a web with equal bridge and eye-piece thickness, is less than that of a simple ring.

Interface pressure $P = \frac{0.90}{1 - m\sigma} \frac{K^2 - 1}{2k^2} E\Delta$

The shear stress concentration factor for this web is 1.325. The elastic limit fit allowance is therefore

$$= \frac{1 - m\sigma}{0.90 \times 1.325} \frac{2s}{E}$$

$$\doteqdot 1.8 \frac{s}{E}$$

and the interface pressure at the elastic limit is

$$p_e = \frac{1}{1.325} \frac{k^2 - 1}{k^2} s$$

(d) Grip Strength.

If D = Grip diameter

L = Grip length

Limiting Torque $= \frac{1}{2}\pi D^2 L \mu P$

Present indications are that the value of μ will exceed $\frac{1}{4}$

With Lloyd's proportions, and elastic limit stress in 28 - 32 ton m.s. webs,

Limiting Torque $\doteqdot D^3$ in. tons (for D in inches)

At the elastic limit stress in the shaft

$$\text{Limiting Torque} = \frac{\pi}{16} D^3 s$$

$$\doteq 2.94\ D^3 \text{ in. tons}$$

ACKNOWLEDGMENTS

The programme of research embracing this work was planned and executed under the supervision of

Professor A.S.T. Thomson, D.Sc., Ph.D., A.R.T.C.

Head of the Department of Civil and Mechanical Engineering and Applied Mechanics, and of

Professor A.W. Scott, B.Sc., Ph.D., A.R.T.C.

Director of Research in the above Department.

Acknowledgment of generous assistance at every stage of the work is owing to

C.M. Moir, B.Sc., Ph.D., A.R.T.C.

Research Leader in charge of shrink-fit investigations.

Grateful thanks are due to

Mr. G.V. Stabler, B.Sc.

for instruction in the art and technique of fine measurement.

The writer is indebted to many other members of the Engineering Staff, of the Royal Technical College, for assistance in preparing experimental work and for checking algebraic manipulations.

.....

A great deal of the heavy machining work was carried out by Messrs David Rowan & Co. Ltd., Marine Engineers and Boilermakers, Glasgow. The careful attention given to the work by the Manager

Mr. James Brown

was much appreciated.

The possibility of successfully arriving at this stage of the investigation without the sage guidance of

Emeritus Professor William Kerr, Ph.D., A.R.T.C.

cannot be envisaged. His penetrating and constructive criticism is highly regarded by his many friends, among whom the writer hopes to be numbered.

Lastly, the writer acknowledges the assistance of the typist, whose work the reader can, but whose difficulties he cannot, appreciate.

BIBLIOGRAPHY.

1. Barton, 1931 - "Circular Cylinder with a Band of Pressure on Finite Length of Surface".

Trans. A.S.M.E., Vol. 63

2. Baugher, 1931 - "Transmission of Torque by Means of Press and Shrink Fits".

Trans. A.S.M.E., Vol.53

3. Coker & Levi, 1934 - "Force Fits and Shrinkage Fits in Crank Webs and Locomotive Driving Wheels".

Proc. I.Mech.E., Vol.127

4. Cook & Robertson, 1911 - "Strength of Thick Hollow Cylinders under Internal Pressure.

Engineering, Vol.92, P.786

5. Cook & Robertson, 1913 - "Transition from the Elastic to the Plastic State in Mild Steel".

Proc. Roy. Soc. A., Vol.88

6. Cook, 1931 - "Yield Point and Initial Stages of Plastic Strain in Mild Steel Subjected to Uniform and Non-Uniform Stress Distributions".

Phil. Trans. Roy. Soc. A., Vol.230

7. Cook, 1934 - "The Stresses in Thick-Walled Cylinders of Mild Steel Overstrained by Internal Pressure".

Proc. I.Mech.E., Vol.126

8. Cook, 1938 - "Some Factors Affecting the Yield Point in Mild Steel".

Trans. I.Eng. & Ship. Scotland, Vol.81

9. Dorey, 1931 - "Some Factors Influencing the Size of Crank-shafts for Double Acting Diesel Engines".

Trans. N.E.C.Eng. & Ship., Vol.47

10. Dorey, 1939 - "Strength of Marine Engine Shafting".

Trans. N.E.C. Eng. & Ship., Vol.55

11. Goodier, 1938 - "Frictional Effects in Shrink Fits".

Stephen Timoshenko 60th Anniv.Vol., Macmillan,N.Y.

12. Gough, 1949 - "Engineering Steels under Combined Cyclic and Static Stress".

Pres. Add. I.Mech.E.

13. Haigh, 1919 - "The Strain Energy Function and the Elastic Limit".

B.A. Report 1919

14. Hill, Lee & Tupper, 1947 - "The Theory of Combined Plastic and Elastic Deformations with Particular Reference to a Thick Tube under Internal Pressure.

Proc. Roy. Soc. A., Vol.191

15. Horger & Maulbetsch, 1936 - "Increasing the Fatigue Strength of Press-Fitted Axle Assemblies by Surface Rolling".

Trans. A.S.M.E., Vol.58

16. Horger & Nelson, 1937 - "Design of Press-and Shrink-Fitted Assemblies". - Part I.

Trans. A.S.M.E., Vol.59

17. Horger & Nelson, 1938 - "Design of Press-and Shrink-Fitted Assemblies". - Part II.

Trans. A.S.M.E., Vol.60

18. Horger & Cantley, 1946 - "Design of Crank Pins for Locomotives".

Trans. A.S.M.E., Vol.

19. Lea & Crowther, 1914 - "The Change of the Modulus of Elasticity and of other Properties of Metals with Temperature".

Engineering, Oct.16, 1914, P.487

20. Love, 1929 -

Phil. Trans. Roy. Soc. A., Vol.228

21. MacGill, 1913 - "A Record of Press Fits".

A.S.M.E. Jour., Nov.1913, P.1657

22. MacGregor & Coffin , 1947 - "Approximate Solutions for Symmetrically Loaded Thick-Walled Cylinders.

Trans. A.S.M.E., Vol. 14 No. 4.

23. MacGregor, Coffin & Fisher, 1948 - "Partially-Plastic Thick-Walled Tubes".

Jour. Franklin Inst., Vol.245

24. Macrae, 1930 - "Overstrain of Metals".

H.M. Stationary Office.

25. Morrison & Shepherd, 1949 - "An Experimental Investigation of Plastic Stress-Strain Relations".

Proc. I. Mech. E.

26. Nadai, 1931 - "Plasticity".

McGraw Hill, N.Y.

27. Peterson & Wahl, 1935 - "Fatigue of Shafts at Fitted Members with a Related Photoelastic Analysis".

Trans. A.S.M.E., Vol.57

28. Rankin, 1944 - "Shrink Fit Stress and Deformations".

Trans. A.S.M.E., Vol.66

29. Redshaw,, 1946 - "The Electrical Measurement of Strain".

Jour. Roy. Ae. Soc. Vol. 50, No.428.

30. Roberts & Northcliffe, 1947 - "Measurement of Young's Modulus at High Temperature".

Jour. Iron & Steel Inst., Nov.1947, P.345

31. Russell & Shannon, 1930 - "The Limit of Grip due to Force Fits and its Increase by Cold-working".

Jour. R.T.C. Vol.2, Pt.2

32. Russell, 1933 - "Factors Affecting the Grip in Force, Shrink and Expansion Fits".

Proc. I.Mech.E., Vol.125

33. Russell, 1935 - "Contact Film Resistance in Rail Wheel Force Fits".

Jour. R.T.C., Vol.3., Pt.3

34. Russell, 1937 - "Influence of Film and Time on Force and Shrink Fits".

Trans. I.Eng. & Ship. Scotland, Vol.80

35. Sawin, 1928 - "Research in Force Fits".

American Machinist, Vol.68, P.889

36. Sneddon, 1945 - "The Elastic Stresses Produced in a Thick Plate by the Application of Pressure to its Free Surfaces".

Proc. Camb. Phil. Soc., 42, 3

37. Sopwith, 1948 - "The Stresses and Strains in a Partly-Plastic Thick Tube under Internal Pressure and End Load".

IX Int. Cong. App. Mech.

38. Southwell, - "Relaxation Methods in Theoret. Physics". OXFORD UNIV. PRESS

Fox &
39. Southwell, 1946 - "Biharmonic Analysis Applied to Flexure and Extension of Falt Elastic Plates".

Phil. Trans. Roy. Soc. A., Vol. 240.

40. Timoshenko, 1934 - "Theory of Elasticity".

McGraw Hill, N.Y.

41. Werth, 1937 - "Austrauschbare Längspressitze".

V.D.I. Forschungshaft 383